



**Universidade do Minho**  
Escola de Ciências

Cristina Elisabete Araújo de Sousa

**Synthesis and Computational Studies of  
Iminosugars Type Products Obtained  
from D-Erythrose**

Cristina Elisabete Araújo de Sousa **Synthesis and Computational Studies  
of Iminosugars Type Products Obtained from D-Erythrose**

UMinho | 2019

novembro de 2019

# FCT

Fundação para a Ciência e a Tecnologia

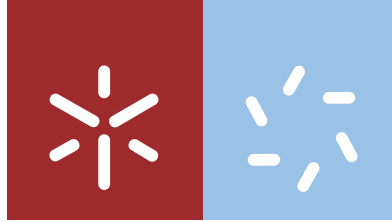
MINISTÉRIO DA CIÊNCIA, TECNOLOGIA E ENSINO SUPERIOR



GOVERNO DA REPÚBLICA  
PORTUGUESA



UNIÃO EUROPEIA  
Fundo Social Europeu



**Universidade do Minho**  
Escola de Ciências

Cristina Elisabete Araújo de Sousa

**Synthesis and Computational Studies of  
Iminosugars Type Products Obtained  
from D-Erythrose**

Tese de Doutoramento  
Doutoramento em Ciências  
Especialidade de Química

Trabalho efetuado sob a orientação da  
**Professora Doutora Maria José da Chão Alves**  
da  
**Professora Doutora Maria de Fátima Monginho Baltazar**  
e do  
**Professor Doutor Nuno Manuel Ferreira de Sousa de  
Azevedo Cerqueira**

## DIREITOS DE AUTOR E CONDIÇÕES DE UTILIZAÇÃO DO TRABALHO POR TERCEIROS

Este é um trabalho académico que pode ser utilizado por terceiros desde que respeitadas as regras e boas práticas internacionalmente aceites, no que concerne aos direitos de autor e direitos conexos.

Assim, o presente trabalho pode ser utilizado nos termos previstos na licença abaixo indicada.

Caso o utilizador necessite de permissão para poder fazer um uso do trabalho em condições não previstas no licenciamento indicado, deverá contactar o autor, através do RepositóriUM da Universidade do Minho.



Atribuição-NãoComercial-Compartilhaigual  
CC BY-NC-SA

<https://creativecommons.org/licenses/by-nc-sa/4.0/>

## Acknowledgements

---

Sou muito grata pela oportunidade de ter sido orientada pela Doutora Maria José Alves, pela sua atenção, apoio e dedicação ao trabalho, mas essencialmente pela indispensável amizade em tempos difíceis.

Ao Doutor Nuno Cerqueira por todos os ensinamentos essenciais para poder iniciar os estudos computacionais que abriram uma nova perspetiva sobre a ciência.

Também, a Doutora Maria de Fátima Monginho Baltazar pela disponibilidade embora o tempo não tenha permitido desenvolver esta área.

Aos colegas de laboratório que permitiram um ambiente saudável e pelo compartilhamento de experiências.

Dra. Elisa Pinto e Dra. Vânia pela atenção, dedicação e profissionalismo nos espectros de ressonância magnética nuclear e análise elementar, bem como como todas as pessoas do departamento de química da Universidade do Minho.

Ao grupo BIOSIM por todo o apoio nas questões em química computacional e pela boa forma como sempre me acolheram, em especial ao Doutor Sérgio Sousa.

Agradeço à Fundação para a Ciência e Tecnologia pela bolsa de Doutoramento atribuída.

Aos amigos e colegas que me ajudaram, porque na amizade a alegria é duplicada e a tristeza é dividida.

À minha família por tudo que sou e faço, especialmente aos meus filhos Pedro e André e a minha sobrinha Beatriz, que na inocência própria da idade, sempre iluminaram o meu dia.

E dedico esta tese a lutadora que me inspira pela Força, a minha Mãe.

Para todos,

Muito obrigada!

## STATEMENT OF INTEGRITY

I hereby declare having conducted this academic work with integrity. I confirm that I have not used plagiarism or any form of undue use of information or falsification of results along the process leading to its elaboration.

I further declare that I have fully acknowledged the Code of Ethical Conduct of the University of Minho.

## Resumo

---

### Síntese e Estudos Computacionais de Compostos do Tipo Iminoaçúcares Obtidos a partir da D-Eritrose

Os iminoaçúcares estão entre os inibidores de glicosidases mais potentes que existem. Como a glicosilação desempenha um papel importante na formação de tumores e de metástases, as enzimas implicadas nestes processos são hoje alvos para medicamentos promissores com potencial clínico no tratamento do cancro. Uma dessas enzimas é a Golgi  $\alpha$ -manosidase II (GM II). Com base na análise de mais de 30 compostos, esta tese incluí um modelo de farmacóforo para correlacionar estrutura com a atividade biológica na GM II. (Capítulo 2)

A síntese de iminoaçúcares desenhada nesta tese partiu da D-glucose que foi previamente transformada na 2,4-benzilideno-D-eritrose. O processo de síntese foi melhorado passando o rendimento de 54% para 95%. A partir da 2,4-benzilideno-D-eritrose obtiveram-se estruturas relacionadas com a L-prolina, estruturas híbridas de aminoácido e açúcar, de tipo swainsonina, e intermediários de síntese: a D-eritrosil  $\delta$ -lactona e as D-eritrosil N-alkiliminas.

Inicialmente foi realizado um trabalho de pesquisa bibliográfica que resultou na redação de uma revisão da literatura sobre síntese e reatividade de tetroses. (Capítulo 1) No capítulo 4 foram obtidas L-homoprolinas com excelentes rendimentos, a partir D-eritrosil N-alkiliminas. Estudos teóricos mostraram a sequência de mecanismos envolvidos nestas sínteses. No capítulo 6 foram obtidos estruturas híbridas de aminoácido e açúcar, a partir do intermediário D-eritrosil  $\delta$ -lactona, que mostrou ser um modelo altamente estéreo-seletivo em cicloadições 1,3-dipolar. (Capítulo 5) Outro intermediário, o D-eritrose-4-il-1,3-butadieno participou em cicloadições de Diels-Alder com os azodienófilos PTAD, DEAD e DBAD. As reações mostraram ser completamente estéreo-seletivas. Estudos computacionais explicaram a preferência da interação dos reagentes na face *si* do dieno com os diferentes dienófilos. (Capítulo 7)

Os diferentes produtos serão submetidos a estudos biológicos em enzimas e em células tumorais. E o conhecimento do mecanismo das reações permite no futuro facilitar as sínteses de análogos.

Palavras Chave: **D-Eritrose, Estéreo-seletividade, GM II, Iminoaçúcares, Síntese, Química Computacional**

## Abstract

---

### Synthesis and Computational Studies of Iminosugars Type Products Obtained from D-Erythrose

Iminosugars are among the most potent glycosidase inhibitors. Because glycosylation plays an important role in tumor formation and metastasis, the enzymes involved in these processes are now targets for promising drugs with clinical potential in cancer treatment. One of such enzymes is Golgi  $\alpha$ -mannosidase II (GM II). Based on the analysis of more than 30 compounds, this thesis includes a pharmacophore model to correlate structure with biological activity in GM II. (Chapter 2)

The design of the iminosugars synthesised in this thesis started from D-glucose, first transformed into 2,4-benzylidene-D-erythrose, by an improved synthetic process; the yield increased from 54% to 95%. From 2,4-benzylidene-D-erythrose were obtained L-proline-related structures, swainsonine-type compounds, amino acid-sugar hybrid structures, and intermediates in synthesis: D-erythrosyl  $\delta$ -lactone and D-erythrosyl N-alkylimines. These compounds proved to be stereoselective platforms for various reaction types.

Initially, a bibliographic research work was carried out resulting in the writing of a literature review in synthesis and reactivity of tetroses. (Chapter 1) In Chapter 4, L-homoprolines were obtained in excellent yields from D-erythrosyl N-alkylimines. Theoretical studies have shown the sequence of mechanisms involved in these syntheses. In chapters 6 were obtained hybrid amino acid and sugar structures, from the intermediate D-erythrosyl  $\delta$ -lactone, which proved to be a highly stereoselective model in 1,3-dipolar cycloadditions. (Chapter 5) Another intermediate, D-erythrose-4-yl-1,3-butadiene participated in Diels-Alder cycloadditions with the PTAD, DEAD and DBAD azodienophiles. The reactions turned out to be completely stereoselective. Computational studies explained the preference of the interaction of the reactants on *si* face the diene with different dienophiles. (Chapter 7)

The different products will be subjected to biological studies on enzymes and tumor cells. And knowledge of the mechanism of reactions allows in the future to facilitate the synthesis of analogs.

**Keywords:** Computational Chemistry, D-Erythrose, GM II, Iminosugars, Stereoselectivity, Synthesis.



# Index

ACKNOWLEDGEMENTS.....	III
RESUMO .....	V
ABSTRACT.....	VI
INDEX .....	VII
PREAMBLE.....	XI
PUBLICATIONS.....	XII
ABBREVIATIONS AND SYMBOLS .....	XIV
SECTION A: INTRODUCTION.....	1
Chapter 1	1
<b>Synthesis of Iminosugars from Tetroses</b>	1
1. Abstract.....	3
2. Introduction .....	3
3. Synthesis of D- and L-erythrose/threose and their derivatives .....	5
3.1 Carbohydrate-based synthesis.....	5
3.2 Non-carbohydrate-based synthesis .....	7
4. Synthesis of Piperidines .....	12
5. Synthesis of Pyrrolidines .....	26
6. Synthesis of Indolizidines .....	30
7. Synthesis of Pyrrolizidines.....	34
8. Conclusion .....	39
9. References .....	39
Chapter 2	45
<b>Glycosylation, the important role of Golgi <math>\alpha</math>-Mannosidase II</b>	45
1. Glycosylation .....	47
2. Golgi $\alpha$ -mannosidase II .....	50

2.1	Structure of GM II .....	50
2.2	Catalytic mechanism of GM II.....	52
2.3	Golgi Mannosidase inhibitors.....	53
1.3.1	Class A.....	54
1.3.2	Class B.....	57
1.3.3	Class C.....	59
1.3.4	Class D .....	61
1.3.5	Class E.....	62
1.3.6	Other Classes .....	64
3.	Pharmacophore model .....	65
4.	References .....	67
<b>Chapter 3</b>		<b>70</b>
<b>Computational Methods to Study Reaction Mechanisms</b>		<b>70</b>
1.	Quantum Mechanics.....	71
1.1	Schrödinger Equation.....	72
1.2	The Variational Principle.....	72
1.3	Born-Oppenheimer Approximation.....	72
1.3.1	Electronic Hamiltonian .....	73
1.3.1.1	Density Functional Theory .....	73
1.3.1.2	Basis Sets .....	75
1.3.2	Nuclear Hamiltonian .....	78
1.4	Continuum Solvation Models.....	80
1.5	Potential Energy Surface (PES).....	81
2.	References .....	83
<b>SECTION B: RESULTS AND DISCUSSION.....</b>		<b>84</b>
<b>Chapter 4</b>		<b>87</b>
<b>Synthesis of L-Homoprolines from D-Erythrose</b>		<b>87</b>
1.	Abstract.....	89
2.	Introduction .....	89
3.	Experimental Results and Discussion .....	90
4.	Computational studies .....	93
5.	Conclusion .....	101
6.	Experimental .....	102
7.	References .....	111

<b>Chapter 5</b>	<b>115</b>
<b>Synthesis of Fused Triazole, Pyrazole, and Isoxazole from Lactone</b>	<b>115</b>
1. Abstract.....	117
2. Introduction.....	117
3. Results and Discussion.....	118
3.1 Synthesis of lactone <b>1</b> .....	118
3.2 1,3-Cycloadditions of lactone <b>1</b> with 1,3-dipoles.....	119
4. Computational results.....	121
5. Conclusion.....	130
6. Experimental.....	131
7. References.....	140
<b>Chapter 6</b>	<b>143</b>
<b>Synthesis of Pyrrolidine Derivatives and Tetrahydrofuran <math>\alpha</math>-Amino Acids from D-Erythrosl Fused Triazole</b>	
<b>Lactones</b>	<b>143</b>
1. Abstract.....	145
2. Introduction.....	145
3. Results and Discussion.....	146
3.1 Synthesis of aziridines <b>4a-e</b> .....	146
3.2 Synthesis of tetrahydrofuran amino acids <b>1a-c</b> .....	147
3.3 Synthesis of pyrrolidine-2-carboxylic acids <b>7a,e</b> , and <b>8a,e</b> .....	150
3.4 Reactions's Mechanisms.....	150
4. Conclusion.....	153
5. Experimental Section.....	153
6. References.....	165
<b>Chapter 7</b>	<b>167</b>
<b>Synthesis of Indolizidines from D-Erythrosl 1,3 Butadienes</b>	<b>167</b>
1. Introduction.....	169
2. Results and Discussion.....	170
2.1 Synthesis of Cycloadducts.....	170
2.2 Functional Group Transformation of Cycloadducts <b>2</b> Leading to Aza-indolizidine <b>3</b> .....	170
3. Computational results.....	172
3.1 Diels-Alder cycloaddition mechanisms between diene <b>1</b> and PTAD.....	173
3.2 Diels-Alder cycloaddition mechanisms with DEAD or DBAD.....	176
4. Conclusion.....	179
5. Experimental.....	179

6. References .....	187
<b>SECTION C: WORK PERSPECTIVES .....</b>	<b>189</b>
<b>Chapter 8</b>	<b>189</b>
<b>Conclusion</b>	<b>189</b>
1. Final Remarks .....	190
2. Perspectives .....	191
<b>Annexes</b>	<b>192</b>
Supporting Information of chapter 5: .....	193

## Preamble

---

This thesis is composed of three major sections:

### A. Introduction

A review describing the Synthesis of Iminosugars from Tetroses is provided, in which a background of the methods found in the literature describing the synthesis of piperidine, pyrrolidine, indolizidine, and pyrrolizidine iminosugars, starting from D/L-erythrose and D/L-threose carbon chains (tetroses). (**Chapter 1**)

A brief description of Golgi  $\alpha$ -mannosidase II and its importance in glycosylation. In this chapter, it is described with detail the structure, catalytic mechanism, and the inhibitors targeting this enzyme. In the end, it is provided a pharmacophore model of tis enzyme. (**Chapter 2**) A short review of the theoretical methods used during this project is provided in **Chapter 3**.

### B. Results and Discussion

The obtained results and discussion will be present from Chapters 4 to 7.

**Chapter 4-** Synthesis of L-Homoprolines from D-Erythrose, **Chapter 5-** Synthesis of Fused Triazole, Pyrazole, and Isoxazole from Lactone, **Chapter 6-** Synthesis of Tetrahydrofuran  $\alpha$ -Amino and Pyrrolidine Derivatives from D-Erythrosyl fused Triazole Lactones.**Chapter 7-** Synthesis of Indolizidines from D-Erythrosyl 1,3 Butadienes.

### C. Work perspectives

This final chapter will present the major conclusions of this work, and the global vision of all the work that was accomplished. (**Chapter 8**)

## Publications

---

From the work presented in this dissertation 3 papers were accepted in international scientific journals with peer review, 3 papers are in process to be submitted to international scientific journals and 8 communications were published in scientific meetings.

### Papers published in international scientific journals

- Cristina E. Sousa, Raquel R. Mendes, Flora T. Costa, Vera C.M. Duarte, António G. Fortes and Maria J. Alves “Synthesis of Iminosugars from Tetroses”, *Current Organic Synthesis*, **2014**, 11, 182-203.
- Cristina E. A. Sousa, António M. P. Ribeiro, António Gil Fortes, Nuno M. F. S. A. Cerqueira, and Maria J. Alves “Total Facial Discrimination of 1,3-Dipolar Cycloadditions in a D-Erythrose 1,3-Dioxane Template: Computational Studies of a Concerted Mechanism”, *JOC*, **2017**, 82 (2), 982-991.
- David S. Freitas, Cristina E. A. Sousa, Joana Parente, Artem Droganov, A. Gil Fortes, Nuno M. F. S. A. Cerqueira, and Maria J. Alves “(3*S*,4*R*)-3,4-Dihydroxy-N-alkyl-L-homoprolines: Synthesis and Computational Mechanistic Studies”, *Organic & Biomolecular Chemistry*, **2019**, DOI: 10.1039/C9OB02141H.

### Papers in the process to be submitted to international scientific journals

- Cristina E. A. Sousa, Maria J. Alves, Nuno M. F. S. A. Cerqueira “Glycosylation, the important role of Golgi  $\alpha$ -Mannosidase II”, in submission process.
- Cristina E. A. Sousa, Maria J. Alves “A One Pot Synthesis of Tetrahydrofuran  $\alpha$ -Amino Acids and Hydroxy-Prolines from D-Erythrosyl Fused Aziridine Lactones Under Three Different Protic Acids”, *JOC*, **2019**, Manuscript ID: jo-2019-030312.
- Cristina E. A. Sousa, Daniela A. L. Salgueiro, Nuno M. F. S. A. Cerqueira and Maria J. Alves “Diels-Alder Cycloaddition of a D-Erythrose-1,3-Butadiene Azo-dienophiles. Transformation of

Cycloadducts into (3S,4S,4aS,5S,6R)-Octahydropyrrolo[1,2-b]pyridazine-3,4,5,6-tetraol. Computational Studies on Selectivity”, in submission process.

### Communications in scientific meetings

- Sousa, Cristina; Alves, M.J., Synthesize of aziridines from diazo-diazirine compounds; 4<sup>th</sup> Portuguese Young Chemists Meeting, Coimbra, April **2014**.
- Sousa, Cristina; Alves, M.J., Enantioselective Diels-Alder cycloaddition in the synthesis of Pyridazine compounds; XX Encontro Luso-Galego de Química, Porto, November **2014**.
- Noro, J.; Duarte, Vera C.M.; Silva, Paulo; Sousa, Cristina; Fortes, A. Gil; Alves, M.J., Síntese de um análogo da ceramida a partir da D-glucose como potencial inibidor de  $\beta$ -glucosidades; XX Encontro Luso-Galego de Química, Porto, November **2014**.
- Sousa, Cristina; Mendes, R.; Cerqueira, Nuno; Alves, M.J., Synthesis of *D*-glucono-1-*N*-benzyl-1,5-lactone from D-erythrose 1,3-dioxane derivative; computational mechanistic studies; 5<sup>th</sup> PYCheM 2016 e 1<sup>st</sup> EYCheM, Guimarães, May **2016**.
- Sousa, Cristina; Ribeiro, A.; Gil Fortes, A.; Cerqueira, Nuno M. F. S. A.; Alves, M.J., Total Facial Discrimination of 1,3-Dipolar Cycloadditions in a D-Erythrose 1,3-Dioxane Template. Computational Studies of Mechanism; Oral communication, XXII Encontro Luso Galego de Química, Bragança, November **2016**.
- Sousa, Cristina; Cerqueira, Nuno; Alves, M.J., Diels-Alder cycloaddition in the synthesis of Pyridazine and Swainsonine analogues; 25<sup>th</sup> Young Research Fellow Meeting, Orléans, March **2018**.
- Rocha, Juliana F.; Freitas, David S.; Noro, Jennifer; Teixeira, Carla S. Silva; Sousa, Cristina E. A.; Sousa, Sérgio F.; Alves, Maria J.; Cerqueira, Nuno M. F. S. A., Combined experimental and computational studies devoted to the synthesis of 1,4-lactones; EJIBCE, Porto, December **2018**.
- Sousa, Cristina; Ribeiro, A.; Gil Fortes, A.; Cerqueira, Nuno M. F. S. A.; Alves, M.J., Experimental and Computational Studies Addressed to 1,3-Dipolar Cycloadditions of D-Erythrose 1,3-Dioxane 1,5-Lactone with Regio- and Stereo-selectivity; EJIBCE, Porto, December **2018**.

## Abbreviations and Symbols

---

### A

Ac	acetyl group
AIBN	azobisisobutyronitrile
AMBER	assisted model building with energy refinement
aq.	aqueous
Ar	aromatic group
Arg	Arginine
Asp	Aspartate

### B

9-BBN	9-Borabicyclo[3.3.1]nonane
BJ	Becke and Johnson Functional
Bn	benzyl group
Boc	t-butylloxycarbonyl group
B3	Becke 3 Functional
B3LYP	Becke 3 and Lee, Yang and Parr Functional

### C

CAZY	Carbohydrate-Active Enzymes classification
cat.	catalyst
conc. / c	concentration
COSY	COrrrelation SpectroscopY
<sup>13</sup> C NMR	Nuclear Magnetic Resonance of Carbon

### D

DA	Diels Alder
DBU	1,8-diazabicyclo [5.4.0] undec-7-ene
DBAD	di-tert-butyl azodicarboxylate
DCM	dichloromethane
DEAD	diethyl azodicarboxylate



DET	diethyl tartrate
DFT	Density-Functional Theory
(DHQD) <sub>2</sub> -PHAL	hydroquinidine 1,4-phthalazinediyl diether
DIBALH	diisobutylaluminium hydride
DIPA	diisopropylamine
DMF	<i>N, N</i> , dimethylformamide
DMAP	4-(dimethylamino)pyridine
DMJ	1-deoxymannonojirimycin
DMSO	dimethyl sulfoxide
dr	diastereomeric ratio

## E

e.g.	<i>exempli gratia</i>
eq.	equivalent
ESI	Electrospray ionization
ER	Endoplasmic Reticulum
Et	ethyl group
exc.	excess

## F

FGT	Functional Group Transformation
FVP	Flash vacuum pyrolysis

## G

(g)	gas
GA	Golgi apparatus
GHS	Glycoside hydrolases
GH38	Glycoside hydrolases family 38
Glc	glucose
GlcNAc	<i>N</i> -acetylglucosamines
GM II	Golgi $\alpha$ -mannosidase II
Gs	Glycosidases

GTs	Glycosyltransferases
GTO	Gaussian-type orbitals
<b>H</b>	
HF	Hartree-Fock
HFT	Hartree-Fock Theory
hGM II	Human Golgi $\alpha$ -mannosidase II
His	Histidine
HIV	Human immunodeficiency viruses
HMBC	Heteronuclear Multiple Bond Correlation
HMQC	Heteronuclear Multiple Quantum Correlation
HRMS	High-Resolution Mass Spectrometry
$^1\text{H}$ NMR	Proton Nuclear Magnetic Resonance
<b>I</b>	
IC <sub>50</sub>	Half maximal inhibitory concentration
IR	infrared
<b>J</b>	
J	coupling constant (in Hertz)
<b>K</b>	
K <sub>i</sub>	Inhibition Constant
<b>L</b>	
LCAO	Linear Combination of Atomic Orbitals
LDA	Local Density Approximation
Lit.	literature
LM II	Lysosomal $\alpha$ -mannosidase II
LSDA	Local Spin-Density Approximation
LYP	Lee, Yang and Parr Functional

## M

Man	mannose
MDCK	madin-darby canine kidney cells
Me	methyl group
MOM	methoxymethyl ether group
Ms	methanesulfonyl or mesyl group
MS	molecular sieves
M.p.	melting point
M06	Minnesota 06 Functional
M06-2X	Minnesota 06-2X Functional

## N

NCS	<i>N</i> -Chlorosuccinimide
NMO	<i>N</i> -Methylmorpholine N-oxide
NOE	Nuclear Overhauser Effect

## P

PDB	Protein Data Bank
PES	Potential Energy Surface
Ph	phenyl group
ppm	parts per million
Pro	Proline
PTAD	4-phenyl-1,2,4-triazoline-3,5-dione
<i>p</i> -TsOH	<i>p</i> -Toluenesulfonic acid

## Q

QM	Quantum Mechanics
----	-------------------

## R

rt.	room temperature
RNA	Ribonucleic acid

## S

SAA	sugar amino acids
sat.	saturated
SCF	Self-consistent field
Ser	Serine
STO	Slater-type orbitals
SWA	Swainsonine

## T

TBAF	tetrabutylammonium fluoride
TBAI	tetrabutylammonium iodide
TBS	<i>tert</i> -butyldimethylsilyl group
TFA	trifluoroacetic acid
THF	tetrahydrofuran
TMS	trimethylsilyl group
Trp	Tryptophan
TS	Transition state
Tyr	Tyrosine

## V

VDW	Van der Waals representation
-----	------------------------------

## Z

Zn	Zinc
----	------

## Symbols

$\delta$	chemical drift (expressed in ppm)
$\Delta$	heating
$\nu_{\text{m\ddot{a}x}}$	maximum wave frequency (expressed in $\text{cm}^{-1}$ )

# Section **A**: Introduction

**1**

Synthesis of Iminosugars from Tetroses

*This chapter is in this publication:*

**Synthesis of Iminosugars from Tetroses**

Cristina E. Sousa, Raquel R. Mendes, Flora T. Costa, Vera C.M. Duarte, António G. Fortes, and  
Maria J. Alves,

*Current Organic Synthesis*, **2014**, 11, 182-203.

## 1. Abstract

Iminosugars continue receiving a great deal of attention from chemists and biochemists for their potential as pharmaceuticals. This is a comprehensive review of the methods found in the literature for the synthesis of piperidine, pyrrolidine, indolizidine, and pyrrolizidine iminosugars, starting from D/L-erythrose and D/L-threose carbon chains (tetroses). This review shows the crescent popularity of small molecules to build up iminosugar molecules. Methodologies described herein utilize inexpensive commercial materials. The synthesis of the four tetroses is included referring old and modern methodologies.

## 2. Introduction

Iminosugars or azasugars are mono- or bicyclic polyhydroxylated alkaloids. Their structures resemble carbohydrates, in which the endocyclic oxygen has been substituted by a nitrogen atom. These compounds have been divided into five classes: piperidines, pyrrolidines, indolizidines, pyrrolizidines and nortropenes. An example of each class is represented in **Figure 1**. D/L-Erythrose/threose or derivatives have been used in the synthesis of these types of iminosugars, except nortropenes.

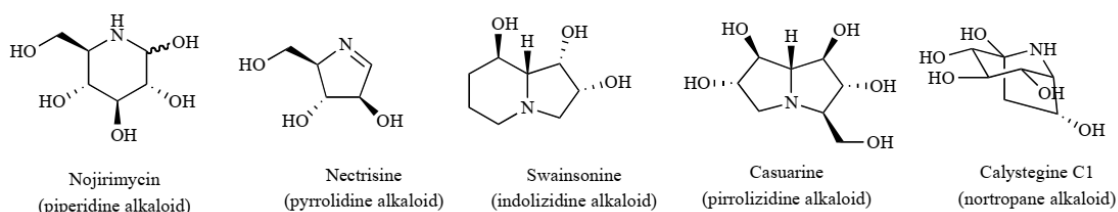


**Figure 1**– The five types of iminosugar structures.

Although the first iminosugar alkaloid discovered, nojirimycin, (**Figure 1**) was isolated by the fermentation broth of a species of *Streptomyces* [1], only a limited number of bacteria (mainly *Actinomycetes*) have subsequently been found to produce polyhydroxylated alkaloids. Iminosugars are, on the other hand, found in large scale in plants [2].

The deoxy derivative of nojirimycin, 1-deoxynojirimycin was obtained by reduction of the anomeric hydroxyl group [3] and was later isolated from plants and bacteria cultures [4,5]. Both, nojirimycin and 1-deoxynojirimycin are antibiotics and inhibit various glycosidases, including processing glucosidases of glycoprotein synthesis [6].

Nowadays there are two iminosugars therapeutically used: *Miglitol*, Gliset® **1** [7] and *Miglustat*, Zavesca® **2** [8] (**Figure 2**). *Miglitol* (*N*-2-hydroxyethyl-1-deoxynojirimycin), **1**, is an  $\alpha$ -glucosidase inhibitor to treat type II diabetes, that restrains the ability of cells to break down complex carbohydrates into glucose. *Miglustat* (*N*-butyl-1-deoxynojirimycin), **2**, acts as an inhibitor of the ceramide-specific glucosyltransferase in Gaucher's disease, the most common glycosphingolipid lysosomal disorder and the first illness to be treated by enzymatic replacement therapy [9].

Many other iminosugars have been tested *in vitro* and *in vivo*, and some of them almost reached the therapeutic level but, for different reasons caused by unwanted side effects, failed the trial. That was the case of 6-*O*-butanoylcastanospermine (**3**) (**Figure 2**), and D-swainsonine (in **Figure 1**).

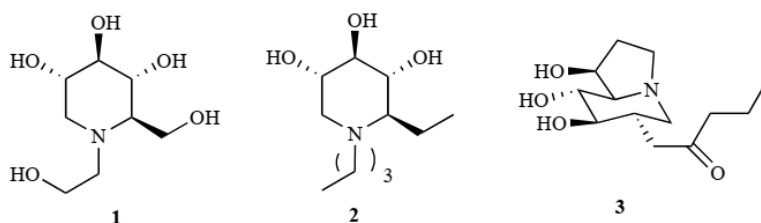


**Figure 2** – Structures of Miglitol (**1**), and Miglustat (**2**) and 6-*O*-butanoylcastanospermine (**3**).

In 1988, *N*-butyl-1-deoxynojirimycin (**2**), and 6-*O*-butanoylcastanospermine (**3**), two  $\alpha$ -glucosidase inhibitors, had shown to avoid HIV replication *in vitro* [10]. The key infection step is the interaction of glycosylated viral envelopes to CD4 receptor of T-lymphocyte glycoprotein membrane. In the presence of an  $\alpha$ -glucosidase inhibitor the glycosidase patterns of the viral coat changes making them non-infectious [9]. However, the crucial concentration needed to inhibit *in vivo* HIV replication caused significant unwanted effects [11].

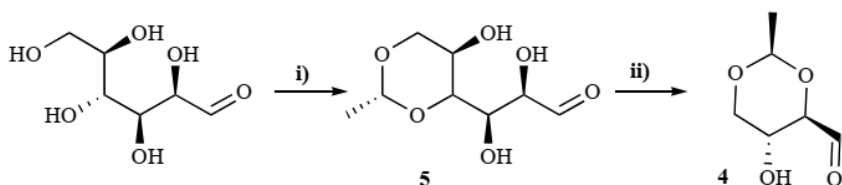
D-Swainsonine (in **Figure 1**) was isolated originally from fungus *Rhizoctonia leguminicola* (*Basidiomycetes*) and was the first iminosugar selected for clinical tests as an anticancer drug. This alkaloid revealed to be an excellent  $\alpha$ -mannosidase II inhibitor in cell Golgi's complex. Glycosidase inhibitors can play the anticancer role because tumor cells possess a higher proportion of glycosidases than normal cells. However, due to the co-inhibition of lysosomal mannosidase, swainsonine caused the accumulation of high mannose oligosaccharides in tissues, inducing mannosidosis. This unwanted side-effect avoided its commercial introduction in the pharmaceutical market as an anti-cancer drug [9].



### 3. Synthesis of D- and L-erythrose/threose and their derivatives

#### 3.1 Carbohydrate-based synthesis

Common monosaccharides have extensively been employed as starting materials in syntheses of iminosugars. Disadvantages of using the sugar chiral pool are connected with the protective, deprotective multistep manipulations and the need of enantiomerically different starting materials to cross over the enantiomeric domains. A rational way of facing the synthesis of multiple stereogenic center molecules consists in building it up from small chiral synthons [12]. Erythrose/threose or their derivatives, either L- or D- stereochemistry, are in this context interesting versatile fragments in syntheses. This review shows the crescent popularity of these small molecules in the synthesis of iminosugars. In some cases, erythrose/threose goes on being synthesized by older methods and they are summarized in **Schemes 1, 2** and **3**. **Scheme 1** shows the synthesis of 2,4-*O*-ethylidene-D-erythrose (**4**) obtained from D-glucose in two steps: formation of acetal **5** in the presence of paraldehyde under sulphuric acid catalysis followed by oxidative cleavage with sodium periodate [13].



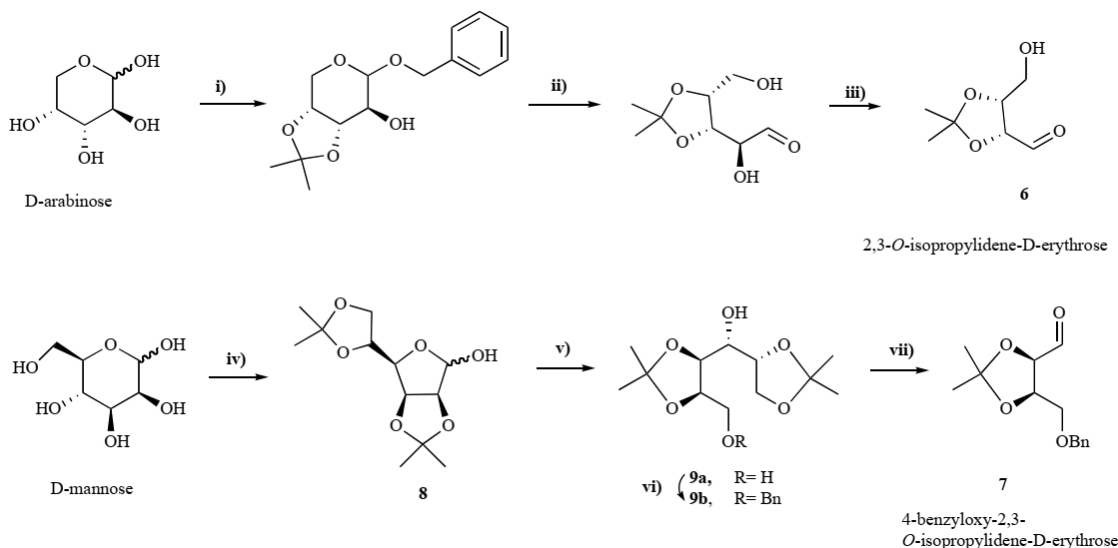
**Scheme 1**- Synthesis of 1,3-ethylidene D-erythrose (**4**) from D-glucose.

**Reaction conditions:** i) (MeCHO)<sub>3</sub>, H<sub>2</sub>SO<sub>4</sub> (cat.); ii) NaIO<sub>4</sub>, NaHCO<sub>3</sub> aq.

In **Scheme 2** is summarized the synthesis of 2,3-*O*-isopropylidene-D-erythrose **6** from D-arabinose [14] and of 4-benzyloxy-2,3-*O*-isopropylidene-D-erythrose **7** from D-mannose [15,16].

D-Arabinose was converted to benzyl β-D-arabinose, which was in turn acetonated to benzyl 3,4-*O*-isopropylidene-β-D-arabinoside. Hydrogenolysis of the latter removed the benzyl group to give 3,4-*O*-isopropylidene-D-arabinose, which could be reduced with sodium borohydride to 3,4-*O*-isopropylidene-D-arabitol. On cleavage with periodate, the latter yielded 2,3-*O*-isopropylidene-D-erythrose (**6**). D-Erythrose derivative **7** was obtained from dry D-mannose in four steps, 55% overall yield. Compound **8** was first obtained, treated with sodium borohydride to reduce the hidden aldehyde leading to compound **9a** [15]. In the third step, the primary alcohol was benzylated with

benzyl bromide in the presence of silver oxide/tetrabutylammonium iodide to give **9b**. Finally, oxidative cleavage of **9b** took place with a mixture of sodium periodate and a catalytic amount of orthoperiodic acid to afford 4-benzyloxy-2,3-*O*-isopropylidene-D-erythrose (**7**) [16].



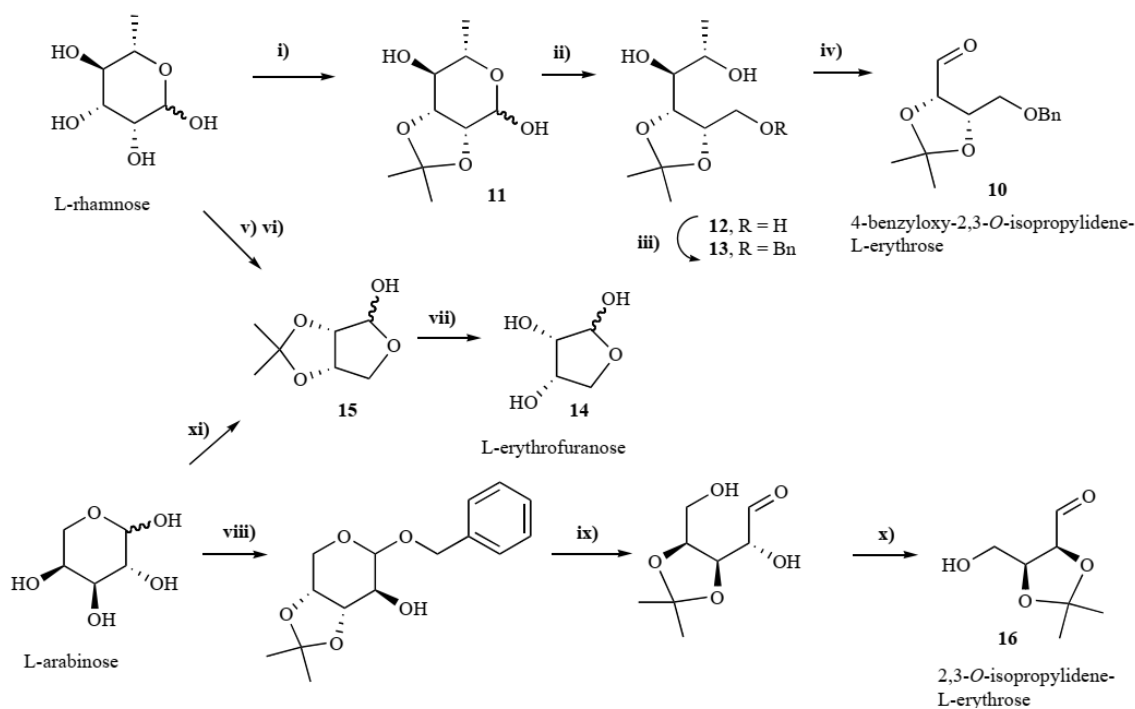
**Scheme 2** - Synthesis of 2,3-*O*-isopropylidene-D-erythrose (**6**) and its derivative **7** from D-arabinose and D-mannose respectively.

**Reaction conditions:** **i)** a) BnOH, HCl (g), rt., overnight, 91 %; b) CuSO<sub>4</sub>, H<sub>2</sub>SO<sub>4</sub>, acetone, rt., 18h; c) NH<sub>3</sub> (g), 79 %; **ii)** H<sub>2</sub>, Pd/C, 50 %; **iii)** a) NaBH<sub>4</sub>, EtOH, 2h; b) NaIO<sub>4</sub>, H<sub>2</sub>O, 77%; **iv)** a) H<sub>2</sub>SO<sub>4</sub> (conc.), acetone; b) Na<sub>2</sub>CO<sub>3</sub>, 90%; **v)** NaBH<sub>4</sub>, EtOH, 97%; **vi)** BnBr, Ag<sub>2</sub>O, Bu<sub>4</sub>N<sup>+</sup>I<sup>-</sup>, 78%; **vii)** NaIO<sub>4</sub>, H<sub>2</sub>O<sub>2</sub> (cat.), Et<sub>2</sub>O, 80%.

L-Erythrose or its derivatives were obtained from L-rhamnose according to **Scheme 3**. For instance, 4-benzyloxy-2,3-*O*-isopropylidene-L-erythrose (**10**) was obtained in 35% overall yield by reaction of L-rhamnose with 2-methoxypropene under acidic catalysis to yield acetal **11**, its reduction was accomplished in the presence of sodium borohydride in water to form compound **12**; the primary alcohol was then benzylated with benzylbromide /sodium hydride to yield compound **13**. An oxidative cleavage of the vicinal diol with sodium periodate in silica/water led to 4-benzyloxy-2,3-*O*-isopropylidene-L-erythrose (**10**) [17]. L-Erythrofuranose **14** was also accessible from dry L-rhamnose by a similar process: L-rhamnose acetonide was obtained by reaction of L-rhamnose with acetone and acid chloride; reduced with sodium borohydride and the crude material treated with sodium periodate to give the cyclic compound **15** in 83 % yield. Removal of the acetal moiety under aqueous sulphuric acid led to the target compound **14** [18]. Alternatively, compound **15** can be synthesized according to the procedure of Kiso and Hasegawa [19] after being adapted by Thompson *et al.* [20]. The crude acetal, initially formed by reaction of L-arabinose with 2,2-dimethoxypropane, was treated with sodium periodate resulting in the cleavage of the 1,2-diol unit

followed by basic hydrolysis and subsequent ring closure to afford 2,3-*O*-isopropylidene-L-erythrose (**15**) in 57% yield ( $\alpha:\beta$ , 1:6) in two steps from arabinose [20].

**Scheme 3** also includes the synthesis of 2,3-*O*-isopropylidene-L-erythrose **16** from L-arabinose. The process follows the synthesis of 2,3-*O*-isopropylidene-D-erythrose obtained from D-arabinose in **Scheme 2**.



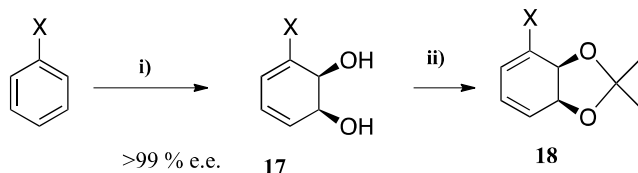
**Scheme 3** - Synthesis of 2,3-*O*-isopropylidene-L-erythrose (**16**) and its derivative **10** obtained from L-arabinose and L-rhamnose respectively.

**Reaction conditions:** **i)** 2-methoxypropane, H<sup>+</sup>, acetone, 94%; **ii)** a) NaBH<sub>4</sub>, H<sub>2</sub>O, 4h; b) HOAc, CH<sub>2</sub>Cl<sub>2</sub>, 80%; **iii)** a) NaH/DMF; b) BnBr, DMF, 60%; **iv)** NaIO<sub>4</sub>, silica, H<sub>2</sub>O, CH<sub>2</sub>Cl<sub>2</sub>, 78%; **v)** a) HCl; b) NH<sub>3</sub> (g); **vi)** a) NaBH<sub>4</sub>; b) NaIO<sub>4</sub>; **vii)** H<sub>2</sub>SO<sub>4</sub>; **viii)** a) BnOH, HCl (g), rt, overnight; b) CuSO<sub>4</sub>, H<sub>2</sub>SO<sub>4</sub>, acetone, rt., 18h; c) NH<sub>3</sub> (g); **ix)** H<sub>2</sub>, Pd/C; **x)** a) NaBH<sub>4</sub>, EtOH; b) NaIO<sub>4</sub>, H<sub>2</sub>O, 77%; **xi)** a) *p*-TsOH, dimethoxypropane, DMF; b) NaIO<sub>4</sub>, H<sub>2</sub>O then Na<sub>2</sub>CO<sub>3</sub>, 57%.

### 3.2 Non-carbohydrate-based synthesis

Modern methods are generally based on shorter chemical approaches, not based on carbohydrate starting materials, but on other sources. Some starting materials are chiral compounds as D-isoascorbic/ascorbic acids and D- /L-tartrates, others are prochiral as allylic alcohols, whereas others are even non-chiral as in the case of substituted-benzenes. Chiral cyclohexadiene-*cis*-diol metabolites **17** are generated in large scale from substituted-benzenes by

microbial oxidation in controlled enantioselective processes [21,22] (**Scheme 4**). These starting materials can be easily transformed into the chiral tetroses building blocks as it is compiled in **Schemes 4-10**.

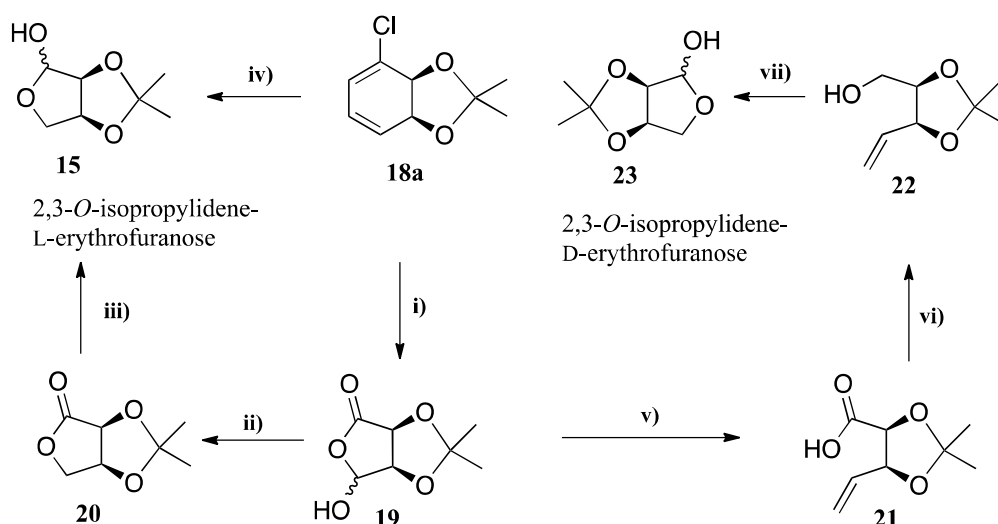


X = H, Cl, Br, I, CN, Me, etc

**Scheme 4**– Synthesis of chiral isopropylidene acetal **18** from benzenic compounds.

**Reaction conditions:** i) *Pseudomonas Putida*, a soil bacterium; ii) DMP, *p*-TsOH.

L-Erythrofuranose **15** was readily obtained by ozonolysis in one step and 54% yield from the acetonide-protected cyclohexadienediol **18a** followed by sodium borohydride workup. Or the other hand L-erythruronolactone **19** [23] could be obtained from **18** by ozonolysis followed by treatment with dimethyl sulfide. The hemiacetal reduction in compound **19** to afford lactone **20** was made by using sodium borohydride. Compound **20** after further reduction with DIBALH yielded 2,3-*O*-isopropylidene-L-erythrofuranose **15** (**Scheme 5**).

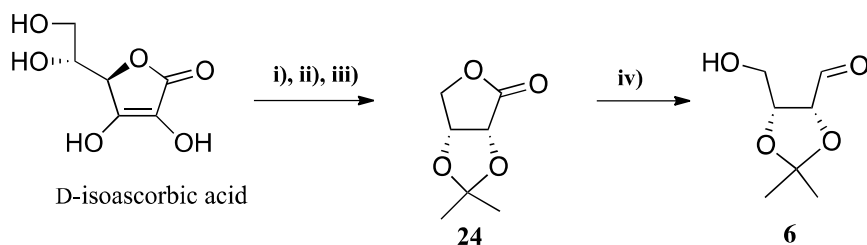


**Scheme 5**– Conversion of chiral isopropylidene **18a** to 2,3-*O*-isopropylidene-D- and L-erythrofuranose and related compounds.

**Reaction conditions:** i) a)  $\text{O}_3$ , EtOAc b) DMS, 54%; ii)  $\text{NaBH}_4$ , MeI, MeOH, 75%; iii) DIBALH,  $\text{CH}_2\text{Cl}_2$ , 82%; iv) a)  $\text{O}_3$ , EtOAc b)  $\text{NaBH}_4$ , 52%; v)  $\text{Ph}_3\text{PBrMe}$ , *n*-BuLi,  $\text{CH}_2\text{Cl}_2$ , 60%; vi)  $\text{LiAlH}_4$ , Et<sub>2</sub>O, 95%; vii) a)  $\text{O}_3$ ,  $\text{CH}_2\text{Cl}_2$ ; b) DMS, 55%.

Starting from L-erythruronolactone **19** can also be devised a D-erythro compound. First **19** was treated with triphenylmethylenephosphorane, the resulting  $\delta,\gamma$ -unsaturated acid **21** was reduced to alcohol **22** with lithium aluminium hydride. Ozonolysis of **22** was the following step to yield 2,3-*O*-isopropylidene-D-erythrofuranose **23** [24] (**Scheme 5**).

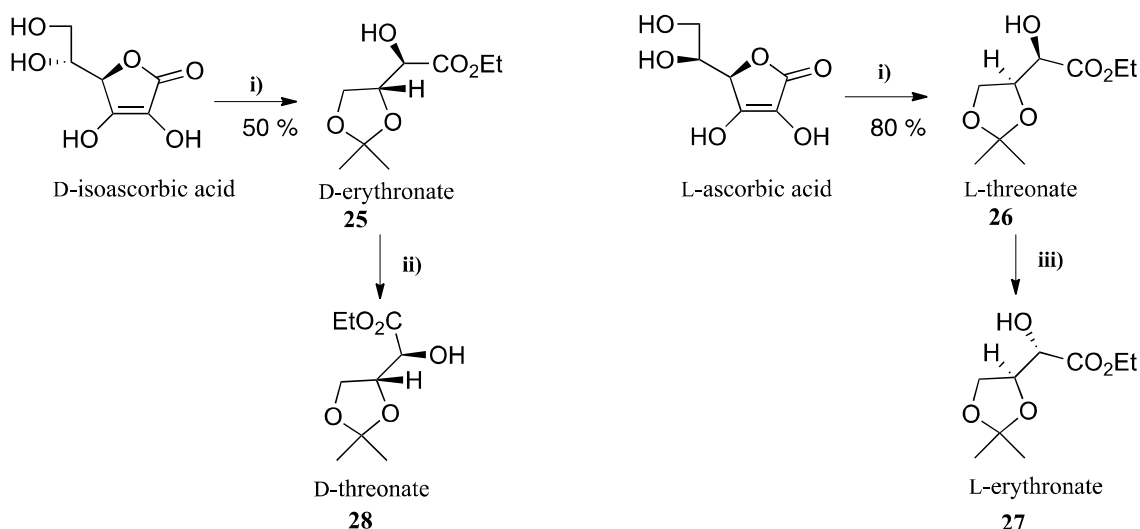
Pearson *et al.* in 1996 [25] described the preparation of 2,3-*O*-isopropylidene-D-erythronolactone **24** in three steps from D-isoascorbic acid: 1) reaction with hydrogen peroxide in the presence of sodium carbonate; 2) addition of aq. HCl; 3) reaction with 2-methoxypropane leading to acetal formation [26,27]. Compound **24** is now commercially available. Reduction of D-erythronolactone **24** with diisobutylaluminum hydride provided 2,3-*O*-isopropylidene-D-erythrose **6** (**Scheme 6**).



**Scheme 6** – Synthesis of 2,3-*O*-isopropylidene-D-erythrose (**6**) from D-ascorbic acid.

**Reaction conditions:** i) a)  $\text{H}_2\text{O}_2$ ,  $\text{Na}_2\text{CO}_3$ ; ii) HCl; iii)  $\text{Me}_2\text{C}(\text{OMe})_2$ ,  $p\text{-TsOH}\cdot\text{H}_2\text{O}$ , 74% three steps; iv) DIBALH, 84 %.

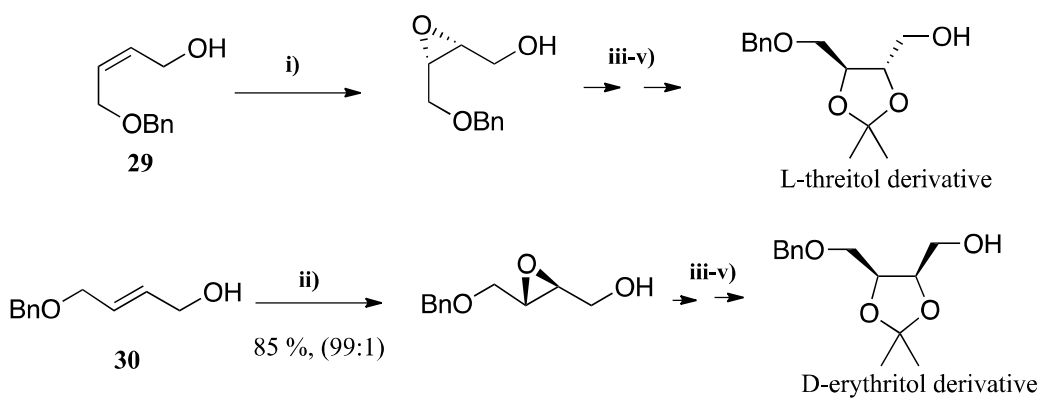
Using Abushanab's strategy [28] D-isoascorbic and L-ascorbic acids can be converted in two steps into two important intermediary synthons: ethyl D-erythronate **25** and ethyl L-threonate **26** [29] (**Scheme 7**). First isopropylidene derivatives were formed by reaction with dry acetone in presence of anhydrous copper sulfate and then subjected to oxidative cleavage with aqueous hydrogen peroxide, followed by esterification with ethyl iodide. Walden inversion at C-2 stereogenic center occurs by reaction of compounds **25** and **26** with triflic anhydride in pyridine, followed by addition of a nitrite salt leading to another two pair of diastereomeric compounds, L-erythronate **27** from **26** and D-threonate **28** from **25** in 78% and 74 %, respectively [30].



**Scheme 7** – Formation of D-erythronate/D-threonate and L-threonate/ L-erythronate respectively from D-isoascorbic and L-ascorbic acid.

**Reaction conditions:** i) a) anhydrous  $\text{CuSO}_4$ , dry acetone (exc.); b)  $\text{K}_2\text{CO}_3$ , slow addition  $\text{H}_2\text{O}_2$ ,  $\text{H}_2\text{O}$ ,  $0^\circ\text{C}$ ; c)  $\text{EtI}$ ,  $\text{CH}_3\text{CN}$ ; ii) a) 1)  $\text{Tf}_2\text{O}$ , pyridine,  $\text{CH}_2\text{Cl}_2$ ,  $-10^\circ\text{C}$  – rt.; b)  $\text{NaNO}_2$ ,  $\text{DMF}$ ; iii) a)  $\text{Tf}_2\text{O}$ , pyridine,  $\text{CH}_2\text{Cl}_2$ ,  $0^\circ\text{C}$ ; b)  $\text{Bu}_4\text{NNO}_2$ ,  $\text{CH}_2\text{Cl}_2$ ,  $40^\circ\text{C}$ .

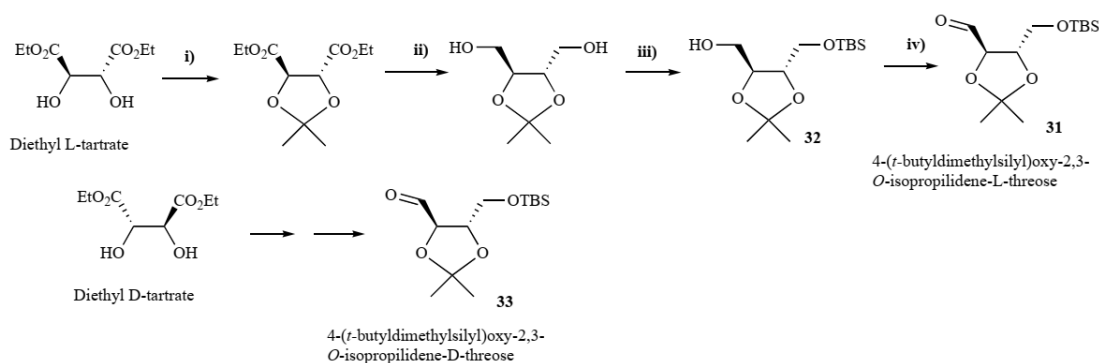
Sharpless asymmetric epoxidation of allylic alcohols introduces asymmetry into prochiral substrates, and it is able to desymmetrize *meso* substrates [31]. Along this review, various allylic alcohols were asymmetrically epoxidized as a method to obtain vicinal diols in a structure. Particular cases were depicted in **Scheme 8**: asymmetric epoxidation of prochiral allylic alcohol **29** was reported to lead to L-threitol derivative, and its stereoisomer **30** into the D-erythritol derivative [32] (**Scheme 8**).



**Scheme 8** - Sharpless asymmetric epoxidation in the synthesis of L-threitol and D-erythritol derivatives.

**Reaction conditions:** **i)** (-)-DET, TBHP, Ti(OiPr)<sub>4</sub>, CH<sub>2</sub>Cl<sub>2</sub>, 0 °C, 84 %, *dr* 96:4; **ii)** (+)-DET, TBHP, Ti(OiPr)<sub>4</sub>, CH<sub>2</sub>Cl<sub>2</sub>, 0 °C, 85 % *dr* 99:1; **iii)** PhNCO, Et<sub>3</sub>N, CH<sub>2</sub>Cl<sub>2</sub>; **iv)** 5% aqueous HClO<sub>4</sub>, MeCN; **v)** NaOH, H<sub>2</sub>O, MeOH, L-threitol 65 % from the epoxide; D-erythritol 55 % from the epoxide.

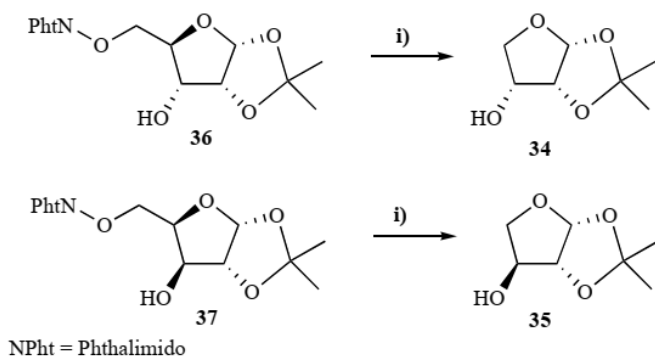
Diethyl L-tartrate was used in the sixties to achieve the synthesis of 4-*t*-butyldimethylsilyloxy-2,3-*O*-isopropylidene-L-threose **31** in 55.7 % global yield. Diethyl L-tartrate was first transformed into 2,3-*O*-isopropylidene-L-tartrate, and then reduced under lithium aluminium hydride to afford 2,3-*O*-isopropylidene-L-threitol [33]. The full synthesis of compound **31** from diethyl L-tartrate is described by Kibayashi *et al.* [34] (**Scheme 9**). 2,3-*O*-isopropylidene-L-threitol was treated with 1 eq. of *t*-butyldimethyl silyl chloride to give the monosilylated compound **32** that was then submitted to *Swern* oxidation to give the 4-substituted *O*-isopropylidene-L-threose **31**. The corresponding D-threose compound **33** was generated from diethyl D-tartrate (**Scheme 9**).



**Scheme 9** – Synthesis of 4-(*t*-butyldimethylsilyloxy)-2,3-*O*-isopropylidene-L-threose **31** from diethyl L-tartrate.

**Reaction conditions:** **i)** H<sub>2</sub>SO<sub>4</sub>, pet. ether, acetone, 83 %; **ii)** LiAlH<sub>4</sub>, Et<sub>2</sub>O, 79 %; **iii)** (Me)<sub>2</sub>CSi(Me)<sub>2</sub>Cl, NaH; 99.7% **iv)** (a) oxalyl chloride, DMSO, (b) N(Et)<sub>3</sub>, 85 %.

New methods continue to be developed aiming the synthesis of tetroses. *E.g.* compounds 1,2-*O*-isopropylidene-D-erythrose **34** and 1,2-*O*-isopropylidene-L-threose **35** have recently been obtained from primary alkoxy free radicals, readily obtained from commercial 5-*N*-phtalimido-1,2-*O*-isopropylidene-D-ribofuranose **36** and 5-*N*-phtalimido-1,2-*O*-isopropylidene-D-xylofuranose **37** in the presence of tributyltin hydride and catalytic amount of azobisisobutyronitrile. Primary alkoxy radicals derived from their corresponding xylo- and ribofuranose derivatives underwent, exclusively, an unusual  $\beta$ -fragmentation to afford L-threose and D-erythrose derivatives **34** and **35** in 89 % and 91 % yield, respectively [35] (**Scheme 10**).



**Scheme 10** – Synthesis of 1,2-*O*-isopropylidene-D-erythrose **34** and 1,2-*O*-isopropylidene-L-threose **35** respectively from ribose and xylose containing *N*-phthalimido at position 5.

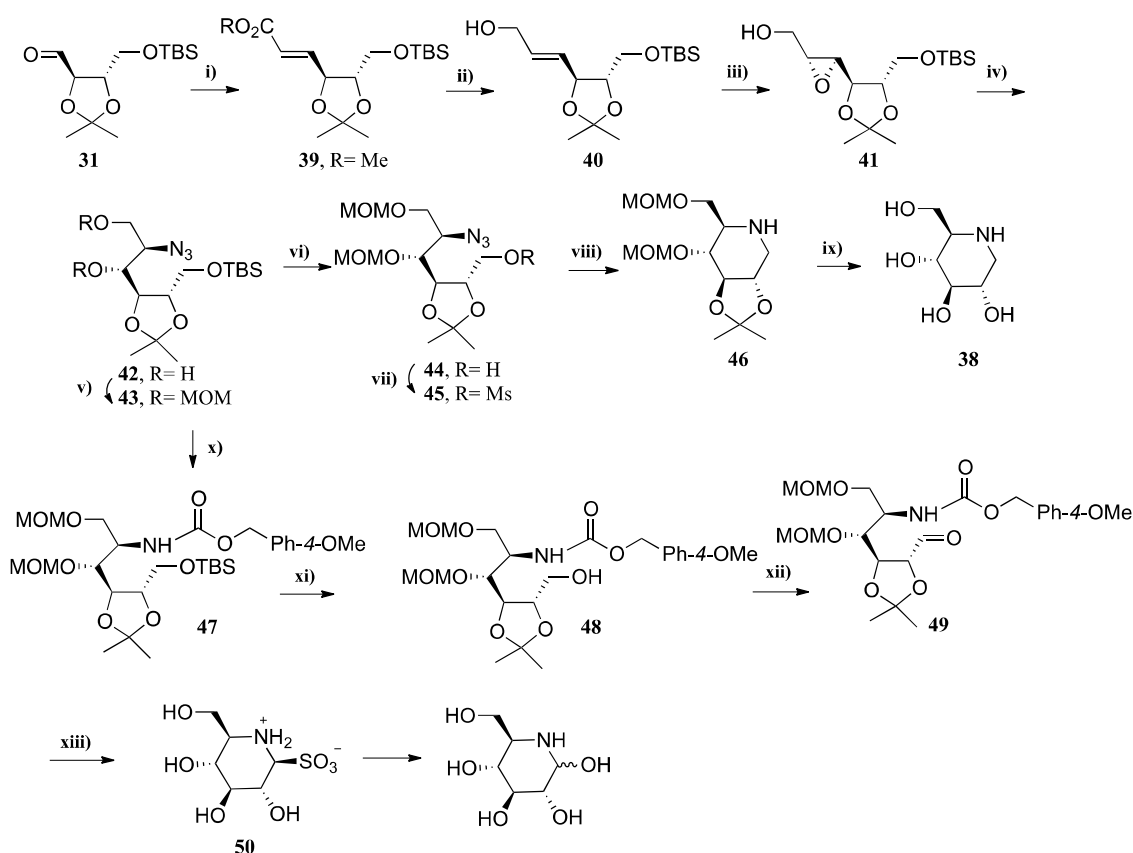
**Reaction conditions:** i) Bu<sub>3</sub>SnH/AIBN, benzene, reflux.

#### 4. Synthesis of Piperidines

Kibayashi reported an efficient convergent total synthesis of (+)-1-deoxynojirimycin **38** and (+)-nojirimycin from L-threose derivative **31**, obtained from diethyl L-tartrate [34] (**Scheme 11**). Horner-Emmons condensation of the aldehyde function with trimethyl phosphonoacetate gave exclusively the *E* isomer **39** in 95 % yield. Diisobutylaluminium hydride reduction of the ester furnished the allylic alcohol **40** (81 % yield), which was further submitted to Sharpless epoxidation using L-tartrate as chiral inductor to afford the *syn* epoxide **41** in 78 % yield. Treatment of compound **41** with sodium azide and ammonium chloride gave the azide **42** in high *regio*- and *stereo*-selectivity (75 % yield). Full protection of the alcohol functions with methyl chloride methyl ether in the presence of *N,N*-diisopropylethylamine yielded compound **43** in 91 %. Using tetrabutylammonium fluoride in tetrahydrofuran the primary alcohol of structure **43** was deprotected, and compound **44** was thus obtained and subsequently activated with the mesyl group to affording compound **45** in 92 % overall yield in the two steps. Reduction of the azide group under Pd/C in methanol yield after reflux in methanol /triethylamine a 6-membered ring compound **46** (92%). The protective groups were removed by hydrolysis with HCl to afford (+)-1-deoxynojirimycin **38** in 90% yield. (+)-Nojiromycin (**1**) was also prepared. Accordingly, **43** was subjected to hydrogenolysis to afford the corresponding amine, which underwent *N*-[*p*-(methoxybenzyl)oxy]carbonylation in the presence of *p*-(methoxybenzyl *S*-(4,6-dimethylpyrimidin-2-yl)thiocarbonate to provide compound **47**. Desilylation of the primary alcohol with tetrabutylammonium fluoride gave **48** in 76% overall yield from **41**. Under Swern conditions the alcohol **48** was oxidized to the aldehyde **49** (82 % yield). Exposure of compound **49** to aqueous sulphurous acid smoothly removes acetal group affording 1-



deoxynojirimycin-1-sulfonic acid **50** in 63% yield. In the last step (+)-nojirimycin (**1**) was obtained in 92% yield after treatment with Dowex-OH resin.

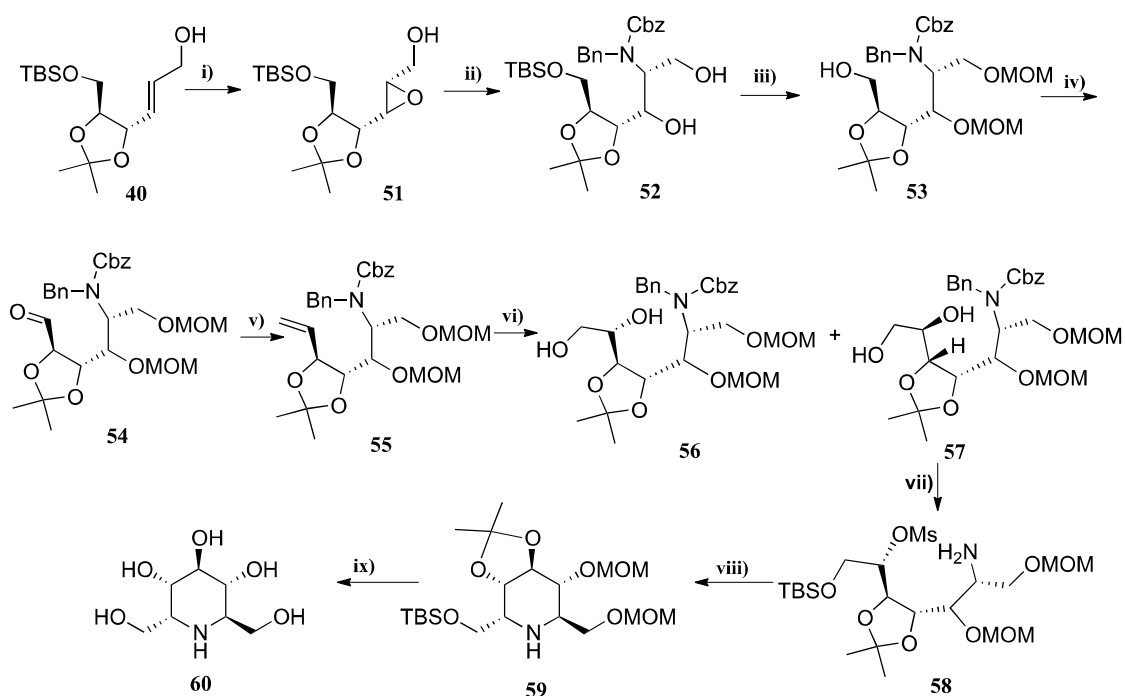


**Scheme 11** – Total synthesis of nojirimycin from L-threose derivative **31**.

**Reaction conditions:** **i)** NaH, trimethyl phosphonoacetate, benzene; **ii)** DIBALH 1M in toluene, Bu<sub>4</sub>F, THF, rt., 14 h; **iii)** Ti(*O**i*Pr)<sub>4</sub>, diethyl L-tartrate, MS 4Å, *t*-BuO<sub>2</sub>H; **iv)** NaN<sub>3</sub>, NH<sub>4</sub>Cl, 1,2-MeOCH<sub>2</sub>CH<sub>2</sub>OMe/OMeCH<sub>2</sub>CH<sub>2</sub>OH, reflux, 6 h; **v)** DIPA, MeOCH<sub>2</sub>Cl, CHCl<sub>3</sub>, reflux, 3 h; **vi)** TBAF, THF, rt, 30 min; **vii)** MsCl, NEt<sub>3</sub>, 0°C, 10 min; **viii)** a) Pd/C, H<sub>2</sub>, MeOH, 2h; b) Et<sub>3</sub>N, MeOH, reflux, 2h; **ix)** HCl-MeOH, reflux, 1 h; **x)** a) Pd/C, H<sub>2</sub>, MeOH; b) NEt<sub>3</sub>, *p*-methoxybenzyl *S*-(4,6-dimethylpyridin-2-yl)thiocarbonate, dioxane; **xi)** Bu<sub>4</sub>F, THF; **xii)** oxalyl chloride, NEt<sub>3</sub>, DMSO; **xiii)** H<sub>2</sub>SO<sub>4</sub> (aq.); **xiv)** Dowex 1x2 (OH) resin.

In 1990, Kibayasi *et al.* performed an enantioselective total synthesis of homonojirimycin starting from 2,3-*O*-isopropylidene-L-threose derivative **40** [36] (**Scheme 12**). In the first step compound **40** was epoxidized by Sharpless methodology to yield **51** [37]. The epoxide opening occurred with total *regio*- and *stereo*-selectivity, via diethylaluminium benzylamine according to Overman's method [38] to give an  $\alpha$ -amino-alcohol formed in 70 % yield. The amino group was selectively protected with benzyl chloroformate to yield the respective carbamate **52** in 98% yield. Finally, methoxymethylation of the free alcohol functions with chloromethyl methyl ether and ethyl

di-isopropylamine followed by removal of the silyl protection of the primary alcohol with tetrabutylammonium fluoride furnished **53** in 86 % overall yield from the  $\alpha$ -amino-alcohol. Swern oxidation gave the aldehyde **54** in 98 % yield, which was elongated under Wittig conditions with methyl phosphonium bromide/butyl lithium, forming the alkene **55**. Dihydroxylation with osmium tetroxide / *N*-methylmorpholine oxide in aqueous acetone, originated two diastereomers **56** and **57** in a 1:2.5 ratio respectively (90 % total yield). The alcohol functions of the major diastereomer **57** possessed the required stereochemistry to achieve the target homonojirimycine. It was protected in its primary alcohol with *t*-butyldimethyl silyl group, and in the secondary alcohol with mesyl group. Treatment with H<sub>2</sub> / palladium hydroxide released the amine function, giving compound **58** with a 77 % overall yield. The closure of a six-membered ring occurred by refluxing compound **58** in ethanol in the presence of triethylamine yielding compound **59** in 81 % yield. Full deprotection of **59** with concentrated chloridric acid gave homonojirimycine **60**.

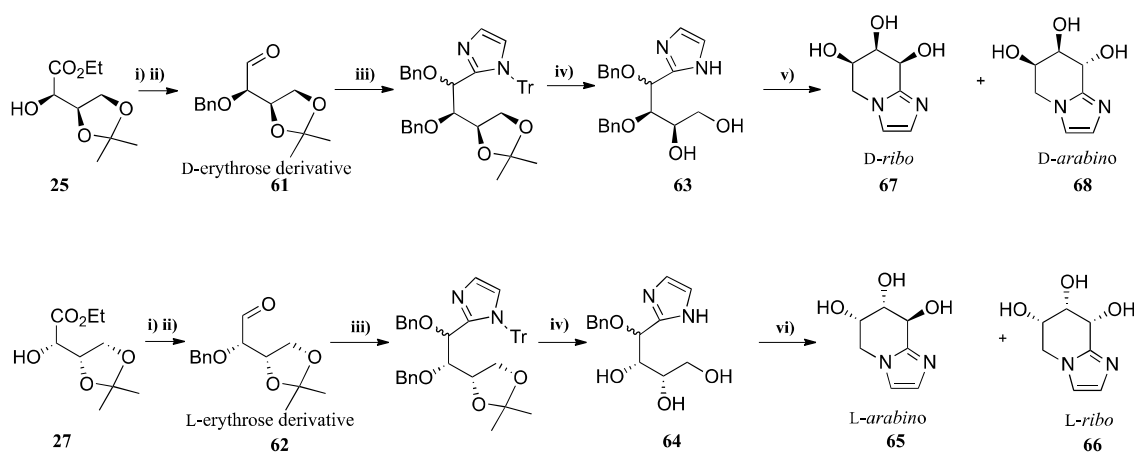


**Scheme 12** - Total synthesis of homonojirimycin from 2,3-*O*-isopropylidene-L-threose derivative **40**.

**Reaction conditions:** **i)** (+)-DET, Ti(*O*-Pr)<sub>4</sub>, TBHP; **ii)** a) Et<sub>3</sub>AlNHCH<sub>2</sub>Ph, CH<sub>2</sub>Cl<sub>2</sub>; b) PhCH<sub>2</sub>OCOCl, Na<sub>2</sub>CO<sub>3</sub> (aq.), CH<sub>2</sub>Cl<sub>2</sub>; **iii)** a) CH<sub>3</sub>OCH<sub>2</sub>Cl, (*i*-Pr)<sub>2</sub>NEt, CHCl<sub>3</sub>; b) TBAF, THF; **iv)** (COCl)<sub>2</sub>, NEt<sub>3</sub>, DMSO, CH<sub>2</sub>Cl<sub>2</sub>, -78° C; **v)** Ph<sub>3</sub>PCH<sub>2</sub>Br, *n*-BuLi, THF; **vi)** NMO, OsO<sub>4</sub>, acetone (aq); **vii)** a) TBSCl, imidazole, MsCl, NEt<sub>3</sub>, DMF, CH<sub>2</sub>Cl<sub>2</sub>; b) H<sub>2</sub>, Pd(OH)<sub>2</sub>, MeOH; **viii)** NEt<sub>3</sub>, MeOH, reflux; **ix)** HCl conc., MeOH, reflux.

Streith et al. described an enantioselective route for the synthesis of imidazole-

piperidinopentoses (**65-68**), starting from D- and L-erythrose derivatives **61** [28] and **62**, respectively [30] (**Scheme 13**). These compounds strongly resemble the natural product nagstatine, a potent inhibitor of N-acetyl-b-D-glucosaminidase. D-/L-Erythrose derivatives **61** and **62** were reacted with lithiated N-tritylimidazole at C-2, under argon, giving in each case two diastereomers, as it is represented in **Scheme 13** [35]. The new hydroxyl groups thus obtained were protected by benzylation to give the following compounds: D-*arabino* configuration with 19 % overall yield, and D-*ribo* configuration with 48 % overall yield from **61**; and L-*arabino* form with 16 % overall yield, and L-*ribo* form with 48% overall yield from compound **62**. Cleavage of the acetal and trityl groups both occurred in the presence of an acid resin yielding enantiomeric pure compounds: **63-*arabino*** form (69 %), **63-*ribo*** form (55 %), **64-*arabino*** form (83 %), and **64-*ribo*** form (87 %). Intramolecular cyclizations of the linear sugar-imidazol derivatives were *N,O*-ditosylated, then slowly dissolved in NaOH/MeOH to afford the piperidino derivatives at room temperature. The D-*ribo*-structure was obtained in 46 % yield, the D-*arabino*-structure in 45 % yield, the L-*ribo* and L-*arabino* in 95 % and 68 % yields respectively. Hydrogenolysis of the benzyl groups under Pd/C in methanol at 30 bar yielded the final products **65** (45 %), **66** (69 %), Hydrogenolysis of the L-series required Palladium hydroxide on charcoal in acetic acid. Compounds **67** and **68** were obtained in 63 and 68 % yield, respectively.

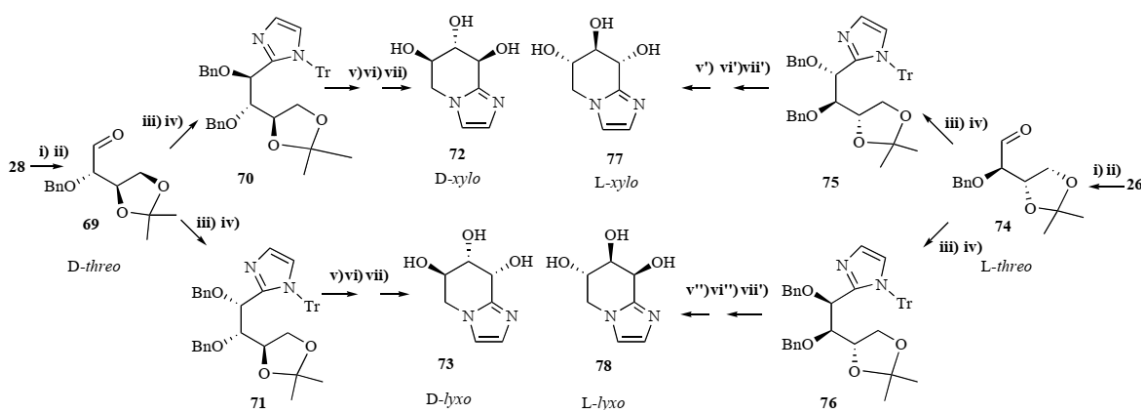


**Scheme 13** – Synthesis of imidazole-piperidinopentoses from D-/L-erythrose derivatives **61** and **62**, respectively.

**Reaction conditions:** **i)** BnBr, KI, Ag<sub>2</sub>O, MS (4 Å), toluene, reflux; **ii)** DIBALH, toluene, -78 °C; **iii)** a) *N*-trityl-imidazole in THF, *n*-BuLi, -5 °C; b) **61** or **62** in THF, -5 °C; c) magnetic stirring, 0 °C; d) H<sub>2</sub>O; **iv)** NaH, BnBr, *n*-Bu<sub>4</sub>NI (cat.), THF, 40 °C; **v)** a) Dowex®50WX8, EtOH/H<sub>2</sub>O, 60 °C; **vi)** a) TsCl, NEt<sub>3</sub>, DMAP (cat.), CH<sub>2</sub>Cl<sub>2</sub>, 0 °C; b) 2 M NaOH/MeOH, rt; **vii)** H<sub>2</sub>, Pd(OH)<sub>2</sub>/C, AcOH; **vii')** H<sub>2</sub>, Pd/C, 30 bar, MeOH.

Streith *et al.* extended the work in the same paper to D-/L-*threo* compounds **28** and **26** respectively to form the same type of compounds **72,73,77,78** [30] (**Scheme 14**). After benzylation, substituted D-threose **69** was reacted with lithiated *N*-trityl-imidazole at C-2 to give two diastereomeric adducts: **70**, the D-*xylo* configuration as the minor compound, and the D-*lyxo* configuration, **71** as the major compound in 14 % and 18 % overall yield. Intramolecular cyclization was obtained as described in **Scheme 13** for the D- and L-forms. The overall yield of bicyclic D-*xylo* form **72** was obtained in 52 % and the bicyclic D-*lyxo* form **73** in 59 %. C-2 Lithiation of L-*threo* derivative **74** occurred under similar reaction conditions and once more two diastereomeric adducts were formed: the L-*xylo* configuration compound **75** as the minor product and the D-*lyxo* configuration compound **76** as the major product in 25 % and 43 % overall yield after benzylation. Final products L-*xylo* derivative **77** and L-*lyxo* form **78** were obtained in 28 %, and 32 % overall yields, respectively.

The L-*arabino* compound **65** showed to be a potent inhibitor of both  $\beta$ -glucosidase and  $\beta$ -galactosidase with  $K_i=1 \mu\text{M}$  in each case. The D-*ribo*-**67** and D-*xylo*-**72** stereomers are a  $\beta$ -glucosidase inhibitor of similar magnitude respectively  $K_i=20 \mu\text{M}$  and  $17 \mu\text{M}$ ; the other stereomers are either modest, poor or do not show any inhibition at all [30].

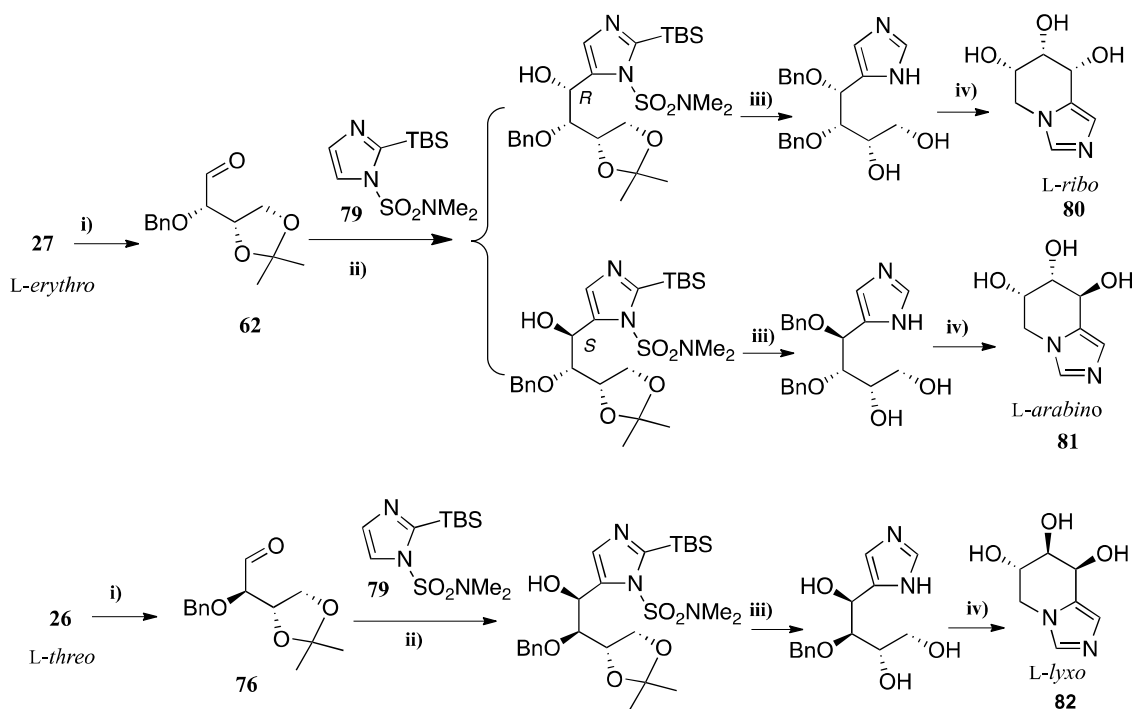


**Scheme 14** – Synthesis of D-/L-xylo and D-/L-lyxo imidazole-piperidinopentoses from D-/L-threose derivatives **69/74**.

**Reaction conditions:** **i)** BnBr, KI, Ag<sub>2</sub>O, MS (4 Å), toluene, reflux; **ii)** DIBALH, toluene, -78 °C; **iii)** a) *n*-BuLi, *N*-trityl-imidazole in THF, -5 °C; b) + **16** or **21** in THF, -5 °C, then magnetic stirring, 0 °C; **iv)** NaH, BnBr, *n*-Bu<sub>4</sub>NI (cat.), THF, 40 °C; **v)** 4M, HCl, reflux; **v')** 2M, HCl, reflux; **v'')** Dowex® 50WX8, EtOH/H<sub>2</sub>O, 60 °C; **vi)** a) NEt<sub>3</sub>, Bu<sub>2</sub>SnO, CH<sub>2</sub>Cl<sub>2</sub>, TsCl; b) 2M NaOH/MeOH; **vi')** a) NEt<sub>3</sub>, DMAP, CH<sub>2</sub>Cl<sub>2</sub>, TsCl, 0 °C; b) 2M NaOH/MeOH; **vi'')** a) NEt<sub>3</sub>, Bu<sub>2</sub>SnO, CH<sub>2</sub>Cl<sub>2</sub>, TsCl; b) 2M NaOH/MeOH; **vii)** H<sub>2</sub>, Pd(OH)<sub>2</sub>/C, EtOH/AcOH; **vii')** H<sub>2</sub>, Pd/C, MeOH 20-30 bar.

Other types of imidazolo-piperidinopentoses (**80,81,82**) have been obtained from tetroses (L-

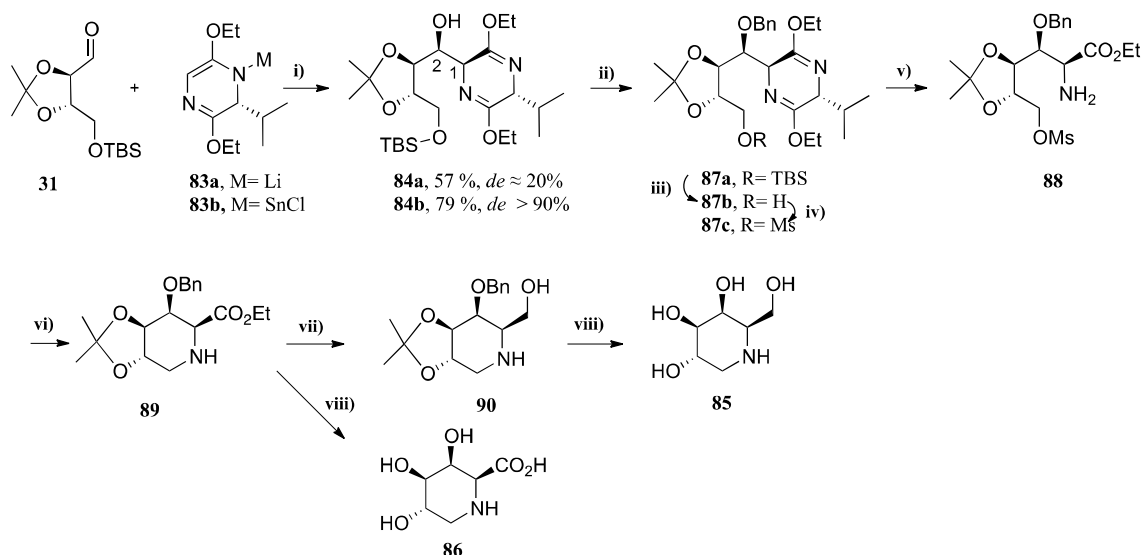
*erythro*, *D-erythro*, and *D-threo* forms) and 5-lithiated imidazole **79** [39] (**Scheme 15**). L-Erythronate **27** was submitted to *O*-benzylation with benzyl bromide in the presence of silver oxide and potassium iodide giving the fully protected ester (88%), which upon reduction with diisobutylaluminium hydride yielded L-erythrose derivative **62** quantitatively. The known lithiated imidazole derivative **79** [40, 41] was combined to the aldehyde **62** leading to a mixture of two diastereomers in 73:27 ratio and 77% yield. The major isomer corresponds to the *L-ribo* configuration (1*R*), and a minor to the *L-arabino* configuration (1*S*). Both isomers were separately submitted, to a sequence of reactions to yield the imidazo-piperidinoses: 1) *O*-benzylation of the secondary alcohol; 2) cleavage of both the silyl and the sulfonamide groups by treatment with hydrochloric acid 6M in tetrahydrofuran; 3) *N* and *O*-tosylation with tosyl chloride, triethylamine and in the presence of dimethylamino pyridine; 4) *N,O*-ditosyl crude compounds were dissolved in sodium hydroxide at 60 °C to yield the bicyclic compounds, having respectively *L-ribo* and *L-arabino* configurations; 5) hydrogenolysis of the bicyclic compounds under palladium hydroxide gave compounds **80** and **81** obtained in 25 % overall yield from the respective imidazole adducts. L-threonate **26** was first benzylated, and then converted to aldehyde **76** in 88 % overall yield. *L-lyxo* product **82** was obtained from **76** with 18 % overall yield by following the same sequence of reactions referred before for compounds **80** and **81**.



**Scheme 15** – Synthesis of L-ribo, L-arabino-, and L-lyxo imidazole-piperidinopentoses from L-erythronate **27** and L-threonate **26**, respectively.

**Reaction conditions:** i) a) BnBr, KI, Ag<sub>2</sub>O, MS (4 Å), toluene, reflux; b) DIBALH, toluene, -78 °C; ii) a) *n*-BuLi, **79** in THF, -78 °C; b) aldehyde in THF, -65 °C-rt; iii) BnBr, NaH, Bu<sub>4</sub>NI, THF, 40 °C; iv) a) HCl, 6 M, 45 °C; b) TsCl (2.3 eq.), NEt<sub>3</sub>, DMAP, CH<sub>2</sub>Cl<sub>2</sub>, 0 °C; c) NaOH (1 M) / acetone, rt; d) H<sub>2</sub>, Pd/(OH)<sub>2</sub>/C, MeOH.

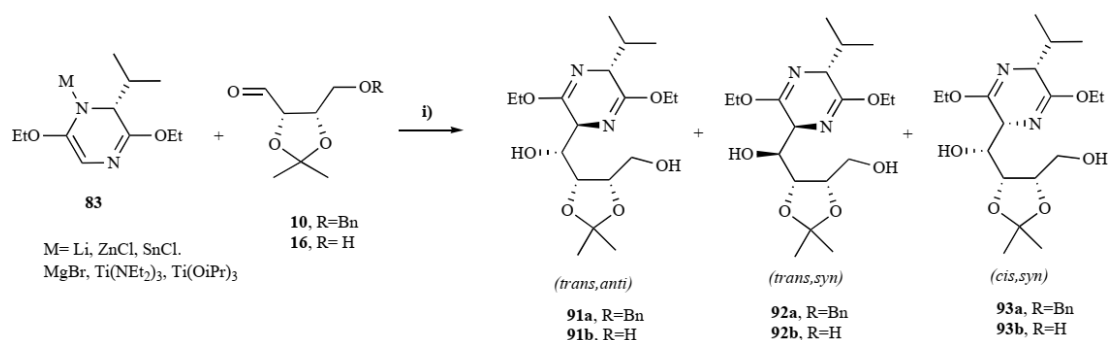
Azaenolate **83**, also known as Schöllkopf's bislactim ethers, is a homochiral glycine equivalent, obtained from glycine and D-valine [42]. Compound **83** and 4-substituted-2,3-*O*-isopropylidene-L-threose **31** form a matched reactive pair in aldol-type reactions leading to double asymmetric induction for which a high *syn* selectivity is predicted [43]. Having this in mind, Ruiz *et al.* [44] combined these reagents for the synthesis of 1-deoxygalactostatin and (2*S*,3*S*,4*R*,5*S*)-trihydroxypipelic acid, interesting for their potential in clinic. L-Threose derivative **31** reacted with lithium salt **83a** (1.2 eq) in THF at -78 °C affording a 3:1:1 mixture of isomers in 57 % combined yield. The major isomer corresponded to the expected adduct **84a**. Selective formation of the major isomer could be increased by cation exchange using a tin(II) azaenolate, obtained by addition of SnCl<sub>2</sub> 1 h prior to the addition of the aldehyde **31** raising the yield of compound **84a** to 79 % yield and *de* > 90 %. Functional group transformation for this adduct led in several steps to 1-deoxygalactostatin **85** and to (2*S*,3*S*,4*R*,5*S*)-trihydroxypipelic acid **86** [44] (**Scheme 16**). To avoid furanosyl competitive cyclization, the free secondary hydroxide was protected with benzyl bromide in the presence of catalytic amount of tetrabutylammonium iodide, with a previous activation of the hydroxyl group with sodium hydride. Compound **87a** was formed in 75 % yield. *t*-Butylsilyl group was removed from the primary alcohol with tetrabutylammonium fluoride giving **87b**, which was subsequently activated in the mesyl form by reaction with mesyl chloride, triethylamine, and dimethylaminopyridine to give **87c** in 71 % overall yield from **84b**. Selective hydrolysis of the dihydropyrazino moiety occurred in HCl / ethanol 1:2 giving the amino ester **88** in 65 % yield. Slow conversion of **88** to piperidine **89** occurred by just standing a solution of **88** at room temperature. To increase the rate of the cyclization process compound **88** was heated at 70 °C in DMSO in the presence of triethylamine. Reduction of compound **89** was produced under lithium triethyl borohydride yielding compound **90** in 84 %. Catalytic hydrogenation under Pd/C in HCl/THF followed by purification by ion-exchange resin Dowex-H<sup>+</sup> gave 1-deoxygalactostatin (**85**) in 90 %. The amino acid **86** was obtained from **89** by the same methodology in 88 % yield by the same methodology.



**Scheme 16** – Synthesis of 1-deoxygalactostatin **85** and (2*S*,3*S*,4*R*,5*S*)-trihydroxypipercolic acid **86** from L-threose **31** and azaenolate **83**.

**Reaction conditions:** **i**) a) THF, -78 °C, 1h; b) NH<sub>4</sub>Cl (aq.); **ii**) NaH, BnBr, NBU<sub>4</sub>l, rt, 24h; **iii**) NBU<sub>4</sub>F, THF, rt, 4h; **iv**) MsCl, Et<sub>3</sub>N, DMAP, CH<sub>2</sub>Cl<sub>2</sub>, rt, 1h; **v**) 0.25M HCl:EtOH 1:2, 9h; **vi**) Et<sub>3</sub>N, DMSO, 70 °C, 2h; **vii**) LiEt<sub>3</sub>BH, THF, rt, 2h; **viii**) a) 0.25M HCl/THF 1:1, H<sub>2</sub>, Pd/C, rt, 9h; b) Dowex-50x8-200, H<sup>+</sup>.

Considering the addition of metalated bis-lactim ethers with mismatched aldehydes like  $\alpha,\beta$ -*syn*-dihydroxy aldehyde [45,46] had shown an almost complete facial control, affording *syn*-adducts with excellent diastereoselectivity. This knowledge led to examine the reaction of metalated Schöllkopf's bis-lactim ethers to mismatched erythrose derivatives [47,48]. This would extend the application of the same methodology to the synthesis of iminosugars of the gluo series [49,50]. The reaction of metalated bis-lactim ether **83** with L-erythrose derivative **10** to 1 eq. of azaenolates with different metal cations [Li<sup>+</sup>, ZnCl<sup>+</sup>, SnCl<sup>+</sup>, MgBr<sup>+</sup>, Ti(NEt<sub>2</sub>)<sub>3</sub><sup>+</sup>, Ti(O*Pr*)<sub>3</sub><sup>+</sup>] at -78 °C in THF, afforded mixtures of adducts **91a/92a/93a** in good yields except for one case [49] (**Scheme 17**, **Table 1**) but with low selectivity, being compound **91a** the major diastereomer (*trans, anti*) in every cases.



**Scheme 17** – Adducts from reaction of metalated Schöllkopf's bis-lactim ethers **83** to L-erythrose derivatives **10**

**Reaction conditions:** i) a) THF, -78°C, 2h for **10**; THF, -78°C – 0 °C, 12h for **16**; b) NH<sub>4</sub>Cl or phosphate buffer; c) H<sub>2</sub>, Pd/C, THF, rt, 6 h for **10**.

**Table 1** – Selectivity and yields of aldol reactions of aldehyde **10** to lithium bis-lactams **83**.

Additive	Eq.	Yield (%)	91a:92a:93a
–	–	60	4.7:3.7:1.6
ZnCl <sub>2</sub>	2.0	14	4.6:2.6:2.5
SnCl <sub>2</sub>	1.0	65	5.7:3.8:0.5
SnCl <sub>2</sub>	2.0	65	6.5:3.1:0.3
MgBr <sub>2</sub> .OEt <sub>2</sub>	2.0	60	6.4:2.2:1.4
Ti(NEt <sub>2</sub> ) <sub>3</sub> Cl	1.0	60	6.4:2.7:0.9

By comparison of these results obtained with those reported by Kobayashi, (*syn* addition) [45-46] it appears that the *anti* diastereofacial preference with **10** it is forced by the *cis*-substituents in the aldehyde, thus reversing the selectivity. Despite the moderate substrate control the chiral azaenolate still determines the *trans* configuration dihydropyrazine moieties in the two major diastereomers formed, compounds **91a** and **92a**.

The unexpected change of stereochemical control from azaenolate to the aldehyde in the previous reactions, led to explore the potential of such mismatched situations for the selective construction of (*trans, anti*)-aminodiol fragments. Lactol-aldehyde **16** was the choice for this study since it is known to be highly stereoselective in reactions with organometallic reagents [25,51]. Adduct **91b** was the major diastereomer in most cases and as expected, Ti(II) azaenolate reacted with higher diastereoselectivity and better yield than the lithium azaenolate. (**Table 2**) Using a large excess of SnCl<sub>2</sub>, compound **91b** was formed with *d.e.* > 80% and 81% yield. Surprisingly the selectivity predominance with Mg (II) is different, giving adduct **93b** (*cis, syn*) as the major product. Addition of Ti(IV) can modulate the selectivity of the addition by using different Ti additives: Ti(Et)<sub>3</sub>Cl yields adduct-(*trans, syn*) **92b**, while Ti(*O*Pr)<sub>3</sub>Cl gave adduct-(*trans, anti*) **91b** (**Scheme 17, Table 2**).



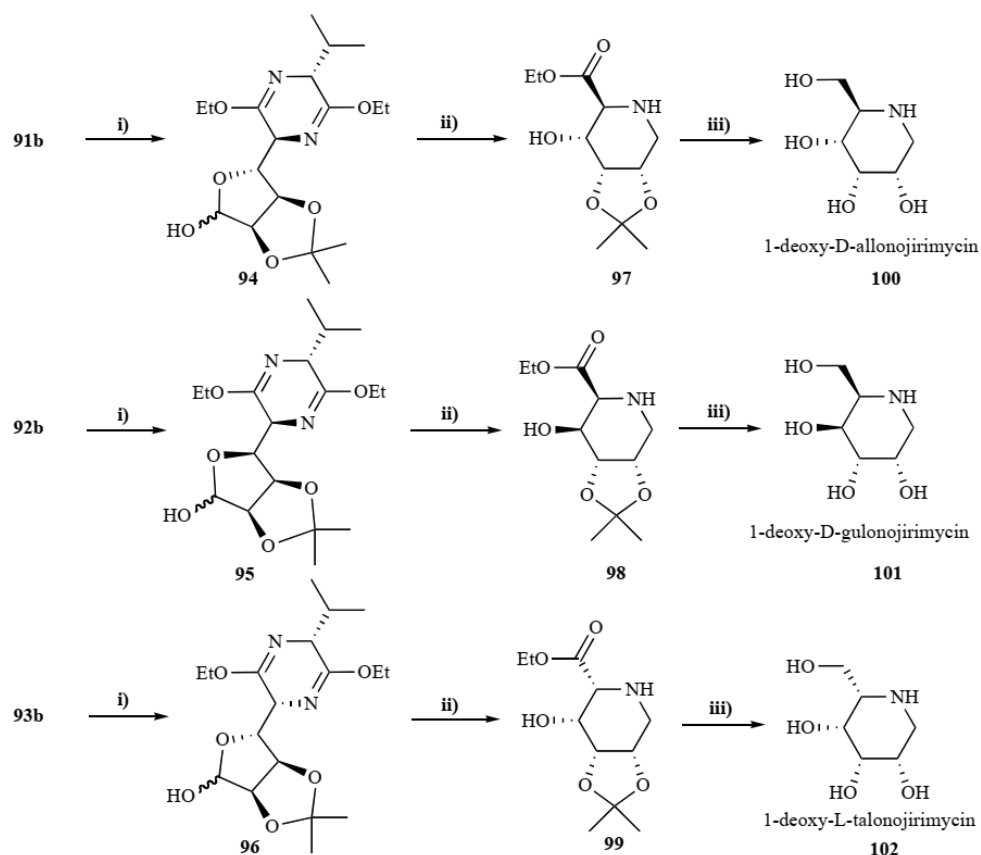
**Table 2** – Selectivity and yields of aldol reactions of aldehyde **16** to lithium bis-lactims **83**.

Additive	Eq.	Yield (%)	91b:92b:93b
–	–	52	6.2:3.8:0.0
ZnCl <sub>2</sub>	6.0	–	–
SnCl <sub>2</sub>	3.0	78	7.7:0.3:2.0
SnCl <sub>2</sub>	6.0	89	9.1:0.9:0.0
MgBr <sub>2</sub> .OEt <sub>2</sub>	3.0	70	3.3:0.6:6.1
Ti(NEt <sub>2</sub> ) <sub>3</sub> Cl	3.0	70	3.0:7.0:0.0
Ti(O <sup><i>i</i></sup> Pr) <sub>3</sub> Cl	3.0	78	6.6:3.3:1.0

pag

Conversion of adducts **91b**, **92b** and **93b** into 1-deoxy-D-allonojirimycin, 1-deoxy-D-gulonojirimycin and 1-deoxy-L-talonojirimycin involved oxidation of the primary hydroxyl group with a solution of *o*-iodoxybenzoic acid to generate furanoses intermediates **94,95,96** in 82 %, 89 %, and 86 % respectively [49] (**Scheme 18**). Selective hydrolysis of the bis-lactim moiety and reductive amination led to the six-membered ring compounds. The two reactions occurred in one pot in hydrochloric acid /ethanol in the presence of H<sub>2</sub> under palladium catalysis forming piperidines **97**, **98** and **99** in 51%, 75 % and 67 % respectively. Reduction of the ester functions with superhydride and deprotection of the acetal with Dowex-H<sup>+</sup> resin yielded 1-deoxy-D-allonojirimycine **100** (98 %), 1-deoxy-D-gulonojirimycine **101** (93 %), and 1-deoxy-L-talonojirimycine **102** (95%).

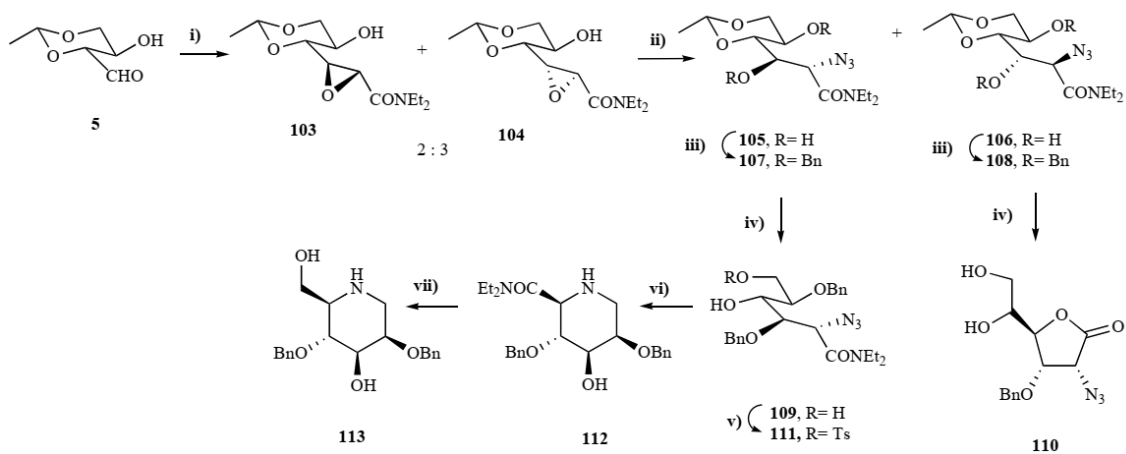
Pino-González and coworkers [52] obtained 2,4-di-*O*-benzyl-1deoxymano-jirimycine starting from ethylidene D-erythrose **5** [53] and sulphur ylides generated *in situ* in the presence of sodium hydroxide (**Scheme 19**). An isomeric mixture of epoxides, **103** and **104** was obtained in a 2:3 ratio respectively and in 85% yield. The inseparable epoxide mixture was reacted further with sodium azide in *N,N*-dimethylformamide with catalytic amount of acetic acid. The reaction was *regio*-selective, with the azide ion attacking the carboxamide  $\alpha$ -carbon, but was not *stereo*-selective. The two diastereomers **105** (38 %) and **106** (34 %) formed were separated, and the hydroxyl groups protected by benzylation, to afford compounds **107** and **108** in 65 % and 75 % respectively. The hydrolysis of the acetal group in the two isomers was carried out separately in methanol in the presence of Amberlite 15 at 40-60 °C, originating two products: an opened chain structure **109**, and a lactone **110** with *allo* configuration. The opened chain compound was tosylated in its primary alcohol to give **111**, the azide group was reduced with H<sub>2</sub> under Pd/C at 60 psi, giving a six-membered ring with D-*manno* configuration **112**.



**Scheme 18** – Conversion of adducts **91b**, **92b** and **93b** into 1-deoxy-D-allo-, 1-deoxy-D-gulo- and 1-deoxy-L-talonojirimycines.

**Reaction conditions:** i) IBX, DMSO/THF (1:1), 8 °C, 24 h; ii) 0.25 M HCl/ EtOH (1:2), H<sub>2</sub>, Pd/ C, t.a. 3 h; iii) a) LiBEt<sub>3</sub>H, THF, rt., 5 h; b) Dowex-H.

Finally, the amide group was reduced under super-H in THF to give 2,4-di-*O*-benzyl-1-deoxymannojirimycin (**113**) in 50 % overall yield from compound **105**. Lactone **110** was obtained in 53 % yield from **106**.

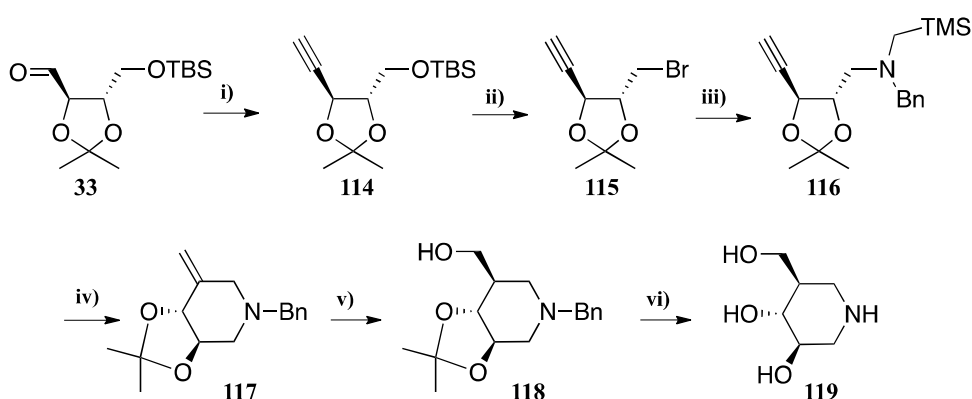


**Scheme 19** – Total synthesis of 2,4-di-*O*-benzyl-1-deoxymannojirimycin starting from ethylidene D-erythrose **5**.

**Reaction conditions:** i)  $\text{Me}_2\text{SCH}_2\text{CONEt}_2\text{Cl}$ , 50% aq. NaOH; ii)  $\text{NaN}_3$ , AcOH, DMF,  $\Delta$ ; iii) BnBr, TBAI, NaH; iv) Amberlite 15, MeOH, 40-60 °C; v) TsCl, pyridine,  $\text{CH}_2\text{Cl}_2$ ; vi)  $\text{H}_2$ , Pd/C, MeOH, 60 psi; vii) Super-H 1M, THF.

G. Pandey prepared both enantiomers of isofagomine, a potent glycosidase inhibitor of 1-*N*-aminosugar type by photoinduced electron transfer (PET) as a key step, generated from  $\alpha$ -trimethylsilylmethylamine radical cation tethered to a  $\pi$  functionality [54] (**Scheme 20**).

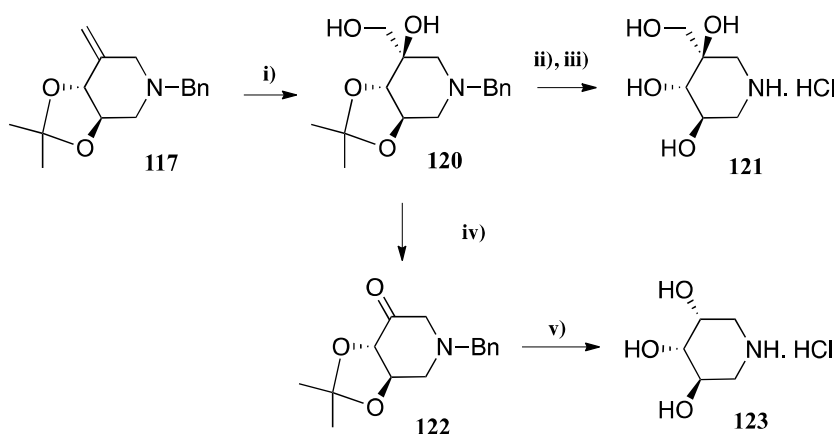
The strategy starts from the aldehyde **33**, which is transformed into **114** using Corey's protocol [55]. Compound **114** was then converted into the corresponding bromo derivative **115** using simple reaction protocols, as shown in **Scheme 20**. Compound **116** was obtained in 65% yield by refluxing a mixture of **115** with  $\alpha$ -trimethylsilylmethylbenzylamine in dry acetonitrile in the presence of  $\text{K}_2\text{CO}_3$ . PET cyclization of **116** involved irradiation with medium pressure lamp in the presence of dicyanonaphthalene (DCN) and took advantage of a three centered amine radical cation species, formed between the nitrogen and the silicon atom, due to the vertical overlap of the filled C-Si-orbital and the half vacant nitrogen orbital [56]. The intramolecular addition process occurred with simultaneous elimination of TMS cation, followed by quenching the radical by H-abstraction from 2-propanol, used as solvent. The cyclized product **117** was obtained in 60 % yield. Hydroboration of cyclic **117** with 9-BBN afforded **118** as a single isomer. Removal of the acetonide and *N*-benzyl moieties yielded (+)-isofagomine **119**. The opposite optical rotation (-)-isofagomine product was obtained from the enantiomer of **31**, that reports back to L(-)-tartaric acid [34].



**Scheme 20** - Total synthesis of (+)-isofagomine **119** from D-threose derivative **33**.

**Reaction conditions:** i) a)  $\text{CBr}_4$ ,  $\text{Ph}_3\text{P}$ , DCM, 0 °C, 2 h, 65 %; b) *n*-BuLi, THF, -78 °C, 1 h, 90 %; ii) a) TBAF, THF, 0 °C  $\rightarrow$  rt, 4 h, 85 %; b)  $\text{CBr}_4$ ,  $\text{Ph}_3\text{P}$ , DCM, 0 °C  $\rightarrow$  rt, 1 h, 80 %; iii)  $\text{PhCH}_2\text{NHCH}_2\text{TMS}$ ,  $\text{K}_2\text{CO}_3$ ,  $\text{CH}_3\text{CN}$ , reflux, 96 h, 65 %; iv) hv, DCN, 2-PrOH, 90 min, 60%; v) 9-BBN, THF, 0 °C  $\rightarrow$  rt, 20 h, then NaOH,  $\text{H}_2\text{O}_2$ , 0 °C  $\rightarrow$  rt, 4 h, 45%; vi) a) HCl, MeOH, rt, 1 h, then  $\text{NH}_4\text{OH}$ , 100 %; b)  $\text{Pd}(\text{OH})_2/\text{C}$ ,  $\text{H}_2$ , 75 psi, EtOH, 10 h, 95 %.

Pandey *et al.* used compound **117** as a general synthon to the synthesis of a series of other polyhydroxy piperidines [57,58] (**Scheme 21-23, Figure 3**). Dihydroxylation of the double bond with osmium tetroxide afforded compound **120** as a single diastereomer. The free amino compound was obtained in a two-step sequence: *N*-debenzylation, followed by acetonide deprotection, leading to **121** in a pure state. The diol **120** upon periodate oxidation afforded compound **122**, which was subjected to sodium borohydride reduction resulting in the formation of the respective alcohol in 85% yield. Acetonide deprotection and *N*-debenzylation led to triol **123** in 88% yield.

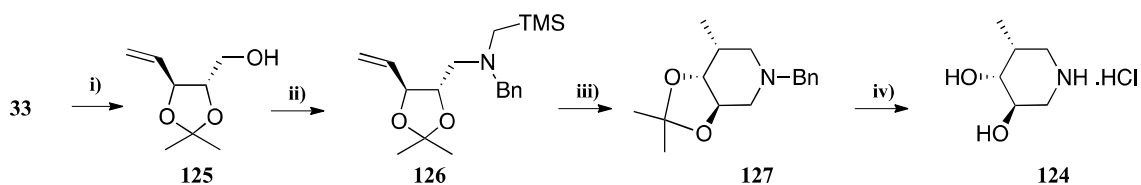


**Scheme 21** - Synthesis of two isofagomine type compounds (**121**, **123**) from intermediate **117**.

**Reaction conditions:** **i**) OsO<sub>4</sub>, *N*-methyl morpholine, pyridine, acetone-water (9:1), 0° C → rt, 24 h, 95 %; **ii**) Pd(OH)<sub>2</sub>, H<sub>2</sub>, EtOH, 65 psi, 6 h, 90 %; **iii**) HCl, MeOH, rt, 4h, quant.; **iv**) NaBH<sub>4</sub>, MeOH, rt, 40 h, then sat. NaCl, rt, 24h, 85 %; **v**) Pd(OH)<sub>2</sub>/C, HCl, MeOH, H<sub>2</sub>, 1 atm, rt, 36 h, 88 %.

The synthesis of 5'-deoxy-5-*epi*isofagomine (**124**) was better accomplished from compound **31** than from **33**.

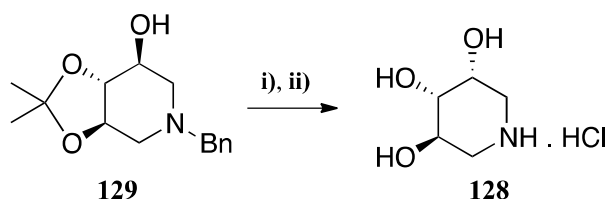
Wittig olefination of the aldehyde **33** followed by TBS removal afforded compound **125**. Nucleophilic displacement of the corresponding tosylate using  $\alpha$ -trimethylsilylmethylbenzylamine, afforded **126**. The formed amine, when irradiated under PET cyclization conditions, yielded product **127** almost as a single diastereomer d.r. >97 %. The protecting groups were removed to afford compound **124**, which was isolated in its hydrochloric acid form, in quantitative yield.



**Scheme 22** – Synthesis of isofagmine, fucose type, from D-threose derivative **33**.

**Reaction conditions:** i) a)  $\text{PPh}_3$ ,  $n\text{-BuLi}$ , THF,  $-15\text{ }^\circ\text{C} \rightarrow \text{rt}$ , 16 h, 60 %; b) TBAF, THF, rt, 4h, 90 %; ii) a) TsCl, pyridine,  $\text{CH}_2\text{CH}_2$ , rt, 24 h, 95 %; b)  $\text{PhCH}_2\text{NHCH}_2\text{TMS}$ ,  $\text{Cs}_2\text{CO}_3$ , TBAI,  $\text{CH}_3\text{CN}$ , reflux, 72 h, 58 %; iii) DCN, 2-PrOH, 2H, 55 %; iv)  $\text{Pd}(\text{OH})_2/\text{C}$ , HCl, MeOH,  $\text{H}_2$ , 1 atm, 28 h, quant.

The synthesis of *meso*-des(hydroxymethyl)-deoxynojirimycin (**128**) was accessed by inverting the stereochemistry of the free hydroxyl group either in **129** or *ent*-**129**. Mitsunobu esterification [14] of **129** followed by the cleavage of the *p*-nitrobenzoate and acetonide deprotection as well as *N*-debenzylation afforded **128**, isolated as its hydrochloride salt (**Scheme 23**) [58].



**Scheme 23** – Synthesis of *meso*-des(hydroxymethyl)-deoxynojirimycin (**128**) by inversion of the alcohol function in compound **129**.

**Reagents and conditions:** i) a) diisopropyl azodicarboxylate,  $\text{PPh}_3$ , *p*-nitrobenzoic acid, THF, rt, overnight; b) LiOH, MeOH, 60 % over two steps; ii)  $\text{Pd}(\text{OH})_2/\text{C}$ , HCl, MeOH,  $\text{H}_2$ , 1 atm, rt, 20 h, 90 %.

Using the same methodology to that described earlier, from the L-threo precursor, **31** the enantiomeric azasugars, **130** (*ent*-**121**), **131** (*ent*-**124**) and des(hydroxymethyl)-deoxygalactonojirimycin (**132**) were prepared. Many other structures of isofagmine, difficult to obtain by other methods can still be generated through Pandey' protocol (**Figure 3**) [58].

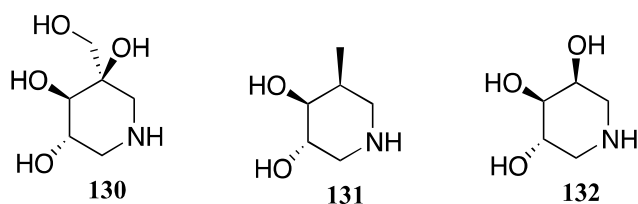
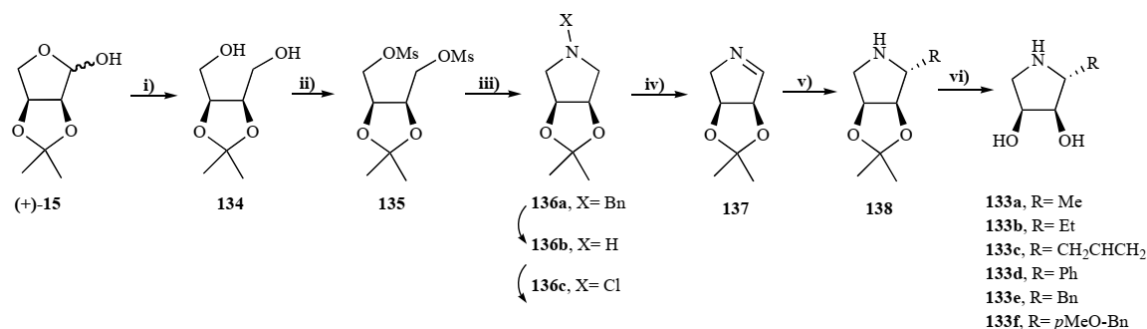


**Figure 3** - Three azasugars obtained from L-threo precursor **31**.

## 5. Synthesis of Pyrrolidines

Davis synthesized erythritol polyhydroxylated pyrrolidines (**133**) starting from 2,3-*O*-isopropylidene L-erythrose **15** [59] (Scheme 24). Starting from **15** a reduction occurs first to give a diol **134** that was dimesylated with mesyl chloride in the presence of triethylamine forming **135** in 72 % yield. Heating **135** with benzylamine (65 °C) a five-membered ring iminosugar **136a** formed in 76 % yield. Hydrogenation of **136a** under Pd(OH)<sub>2</sub>/C catalysis followed by reaction of pyrrolidine **136b** with *N*-chlorosuccinimide yielded *N*-chloramine **136c** (85% from **136a**). The key imine **137** was formed in the presence of DBU. Erythritol cyclic imine **137** was then ready for introduction of a hydrophobic aglycon by nucleophilic attack of an array of Grignard reagents (5 eq.). The best yields were obtained by slow addition of the imine to the Grignard reagents. Numerous analogues of compound **138** were obtained in generally good yields and very high diastereoselectivities. Finally, the acetal was removed with acid resin to give the iminosugar **133**. (Scheme 24) Analogues of anisomycin, a natural product to which several synthetic methods have been devoted, had also been obtained by the methodology expressed above. The erythritol adduct analog **133f** was obtained in good yield (62%) and excellent diastereoselectivity (> 98% *d.e.*) from **137**. The diastereoselectivity of the Grignard reagents is excellent since the acetonide reinforces the rigid butterfly conformation leaving one face open to the attack.



**Scheme 24** – Synthesis of erythritol polyhydroxylated pyrrolidines (**133**) from L-erythrose derivative **5**.

**Reaction conditions:** **i)** NaBH<sub>4</sub>, MeOH; **ii)** MsCl, Et<sub>3</sub>N, CH<sub>2</sub>Cl<sub>2</sub>; **iii)** a) BnNH<sub>2</sub>, 65 °C; b) H<sub>2</sub>, Pd(OH)<sub>2</sub>/C, MeOH; c) NCS, Et<sub>3</sub>O; **iv)** DBU, Et<sub>3</sub>O; **v)** RMgBr (5 eq., R= Me, Et, CH<sub>2</sub>CHCH<sub>2</sub>, Ph, Bn, or *p*-MeO-Bn; **vi)** 25% TFA (aq.), THF, Dowex H<sup>+</sup> (NH<sub>4</sub>OH (aq.)).

The obtained pyrrolidine scaffold with systematic variations in hydrophobic substituent and stereochemistry were screened against a panel of 12 carbohydrate-processing enzymes. These

compounds proved to be relatively potent to  $\alpha$ -L-fucosidase and  $\alpha$ -D-galactosidase inhibition, with  $K_i$  values in the range 250nM - 9.0  $\mu$ M [54].

Ruiz and Ojea developed a methodology for the synthesis of piperidine iminosugars, which involves the aldol reaction between metalated bislactim ethers and tetrose acetonides as the key step [49, 60]. This strategy has also been applied to the synthesis of pyrrolidine homoazasugars and their related 2,5-dideoxy-2,5-iminoglyconic acids (**139-142**) [61,62] (**Figure 4**). In particular, this novel route had been opened to the synthesis of 2,5-dideoxy-2,5-iminogalactitol (**139**) and 2,5-dideoxy-2,5-imino-L-gulonic acid (**140**) and the previously unknown 2,5-dideoxy-2,5-imino-L-galactonic acid (**141**). Some of these compounds are potent glycosidase inhibitors; 2,5-dideoxy-2,5-D-glucitol (**142**) and its epimer 2,5-dideoxy-2,5-iminogalactitol (**139**) are very active inhibitors against galactosidases and glucosidases, and consequently a significant effort has been dedicated to their synthesis. Polyhydroxylated pyrrolidine imino acids are key constituents of natural bioactive molecules, useful building blocks for the construction of peptide-mimetics with improved pharmacological profile [63-66].

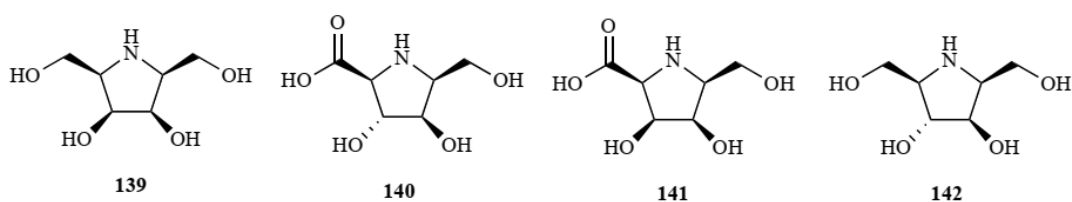
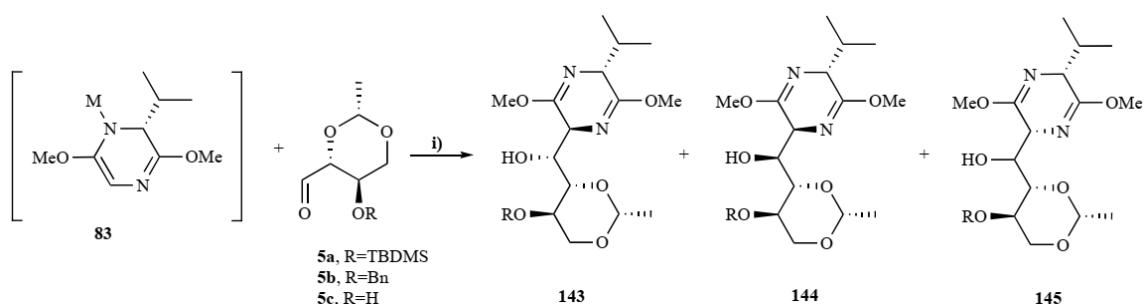


**Figure 4** – Some polyhydroxylated pyrrolidine compounds.

Starting from 2,4-*O*-ethylidene-D-erythroses (**5a-c**) and metalated bislactim ether **83** had been studied the stereoselectivity origin of the aldol reactions involved, and its dependence on the metal and the nature of  $\beta$ -alkoxy protecting group to the aldehyde function. 2,4-Alkylidene-tetroses have been commonly used in stereoselective synthesis [67], and their reactions with different nucleophilic reagents were reported to afford moderate to high *anti*-selectivity [52, 68, 69]. In contrast, it was recently found that tin(II)-mediated aldol reaction between bislactim ether **83** and matched 3-*O*-silylated-D-erythrose ethylidene **5** occurred with an unusual stereochemical course and high selectivity, affording adduct **143** with 3,1'-*anti*:1',2'-*syn* configurations [70] (**Scheme 25**, **Table 3**). Choosing a different R group, the benzyl group, it was found that stereoselective aldol additions of metalated azaenolates **83** occurred, in an analogous fashion to that previously reported for the 3-*O*-butyldiphenylsilyl derivative, but with a lower selectivity (Table 3). To further explore the effect of the  $\beta$  protective group on the stereochemical outcome of the aldol addition, the erythrose

was reacted unprotected at its hydroxyl group. An initial deprotonation by the azaenolate **83** would occur leading to an oxyanion at the  $\beta$  position, which should coordinate with the metal cation to form a temporary ring that could enhance 1',2'-*anti*-selectivity in aldol addition. Addition of aldehyde to a mixture **83** with SnCl<sub>2</sub> (3.8 equiv) gave a 6:94 ratio of adducts, respectively **143** and **144**, evidencing a reverse selectivity for this reaction. Compound **144** (3,1'-*syn*-1',2'-*anti*) formed in 83 % yield and *d.e.*>98 %.



**Scheme 25** – Stereochemical outcome of the aldol additions of 2,4-*O*-ethylidene-D-erythroses to metalated bislactim ether **83**.

**Reaction conditions:** i) a) THF, -78 – 0 °C; b) NH<sub>4</sub>Cl or NaHCO<sub>3</sub>

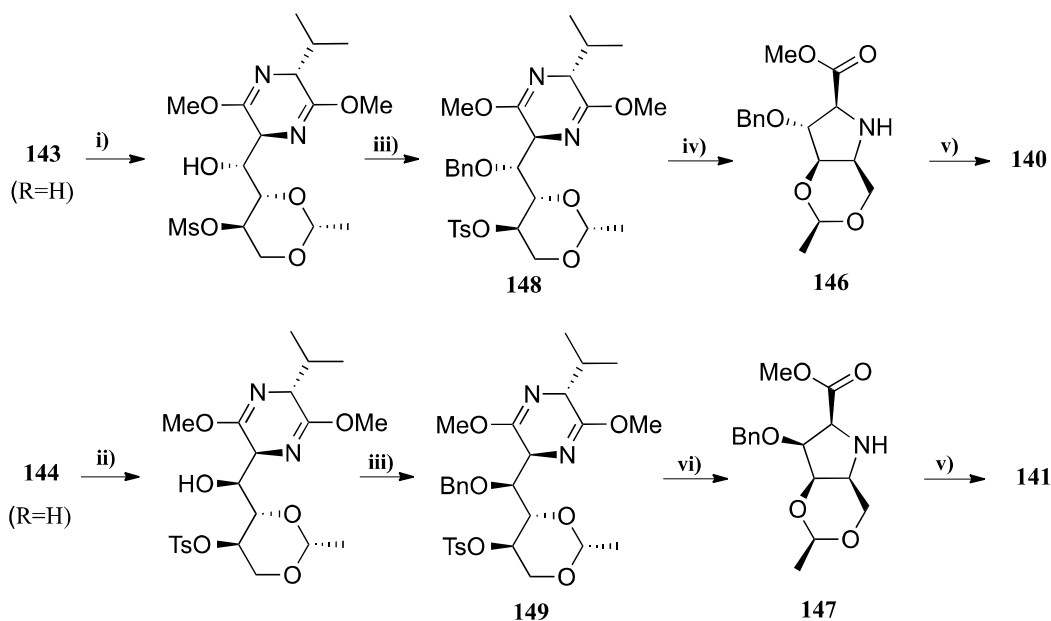
**Table 3** shows how the metal switch in the azaenolate (lithium or tin(II) to zinc(II) or titanium(IV)) changed the stereochemical outcome of aldol addition. Using Ti(O*i*Pr)<sub>2</sub>Cl<sub>2</sub> the reaction afforded a mixture of adducts **143/144/145** in 10:66:24 ratio, with 81% yield. Neither the selectivity nor the yield could be significantly changed when this reaction was performed with a larger excess of Ti(O*i*Pr)<sub>2</sub>Cl<sub>2</sub>.

**Table 3** - Aldol additions of metalated bislactim ether **83** to D-erythrose ethylidenes.

D-erythrose ethylidenes (R)	Eq.	Additive (eq.)	Yield (%)	Ratio 133:134:135
<b>5a</b> (TBDMS)	1.2	SnCl <sub>2</sub> (1.5)	80	92:-:8
<b>5b</b> (Bn)	1.5	–	75	50:37:13
<b>5b</b> (Bn)	1.5	SnCl <sub>2</sub> (1.9)	86	72:28:-
<b>5b</b> (Bn)	1.5	SnCl <sub>2</sub> (3.8)	73	69:31:-
<b>5b</b> (Bn)	1.5	Ti(O <i>i</i> Pr) <sub>2</sub> Cl <sub>2</sub> (1.9)	81	10:66:24
<b>5b</b> (Bn)	1.5	Ti(O <i>i</i> Pr) <sub>2</sub> Cl <sub>2</sub> (3.8)	83	10:65:25
<b>5b</b> (Bn)	1.5	ZnCl <sub>2</sub> (1.9)	8	36:64:-
<b>5c</b> (H)	3.2	SnCl <sub>2</sub> (3.8)	88	6:94



Conversion of the aldol adducts **143** and **144** into the targeted polyhydroxylated proline derivatives **140** and **141** required the removal of the chiral auxiliary, and selective activation of the hydroxyl group at C-3' in order to enable intramolecular cyclization [65] (**Scheme 26**). The alcohol protective group was first removed, in case of benzyl group by hydrogenolysis under heating ammonium formate and palladium catalyst in MeOH. The unprotected compounds were obtained in high yields. These compounds were efficiently transformed into gulonate **146** and galactonate **147** from diols **143** and **144**. Compound **143** was treated with MsCl, Et<sub>3</sub>N and a catalytic amount of dimethylaminopyridine leading to the *regio*-selective mesylation of the equatorial hydroxyl group at position 3', affording the mesylate in good yield. Treatment of diol **144** in the same conditions gave some dimesylated derivative; but, reaction with tosyl chloride, silver dioxide and a catalytic amount of potassium iodide in toluene introduced exclusively the tosyl group at the equatorial hydroxyl group giving the tosylated product in 91% yield. Treatment of these compounds with sodium hydride and benzyl bromide in the presence of a catalytic amount of tetrabutylammonium iodide led to the corresponding benzyl ethers **148** and **149** in good yields. Selective hydrolysis of bislactim ether ring was achieved with 0.25 M HCl in MeOH without cleaving the acetal. Under these conditions, a cyclization occurred to give compound **146** in 87 % yield. Cyclization of the amino tosylate to galactonate **147** needs heating in dimethyl sulfoxide and triethylamine giving **147** in 60 % yield. Finally, deprotection of **146** and **147** by catalytic hydrogenation and hydrolysis gave the 2,5-dideoxy-2,5-imino-L-gulonic acid **140** and 2,5-dideoxy-2,5-imino-L-galactonic acid **141** in 96 % and 87 % respectively. Pyrrolidine homoazasugars **139** and **142** were readily accessible from the gulonate **146** and galactonate **147**, respectively. Reduction of the ester group in **146** and **147** by treatment with lithium triethylborohydride followed by cleavage of the acetal and benzyl groups led to **139** in 78 % and to **142** in 86 % overall yield from compound **147** and **146**, respectively [65] (**Figure 4**).

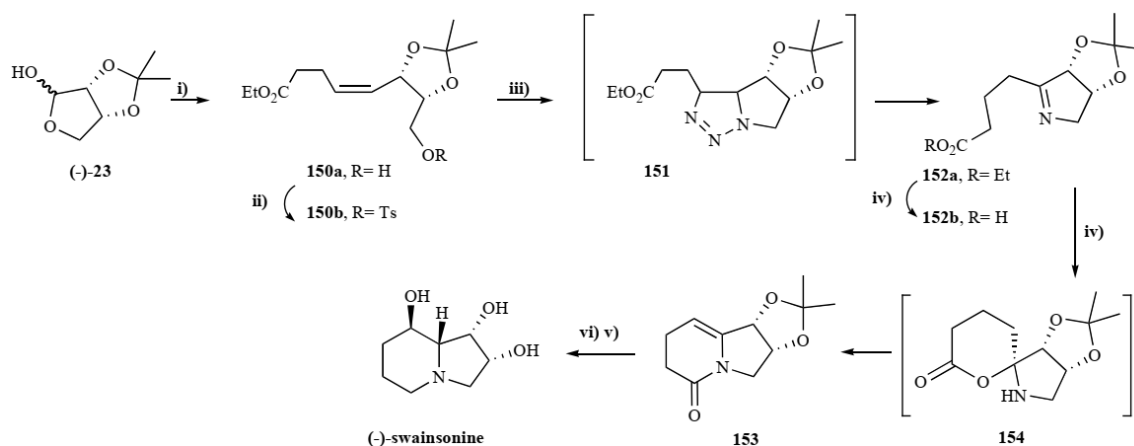


**Scheme 26** - Conversion of the aldol adducts **143** and **144** into polyhydroxylated proline derivatives.

**Reaction conditions:** **i)** MsCl, Et<sub>3</sub>N, DMAP; **ii)** TsCl, Ag<sub>2</sub>O, KI (cat.), toluene, rt; **iii)** NaH, BnBr, Bu<sub>3</sub>NI, THF, (**148**, 70 % from **143**; **149**, 91 % from **144**); **iv)** 0.25 M HCl in MeOH, rt, 82 %; **v)** a) 0.25 M HCl/THF 1:1, H<sub>2</sub>, Pd/C, rt; b) 1 M HCl, Δ, **140**, 96 %; **141**, 87 %; **vi)** a) 0.25 M HCl /MeOH 1:3, rt, b) Et<sub>3</sub>N, DMSO, Δ, 60 %.

## 6. Synthesis of Indolizidines

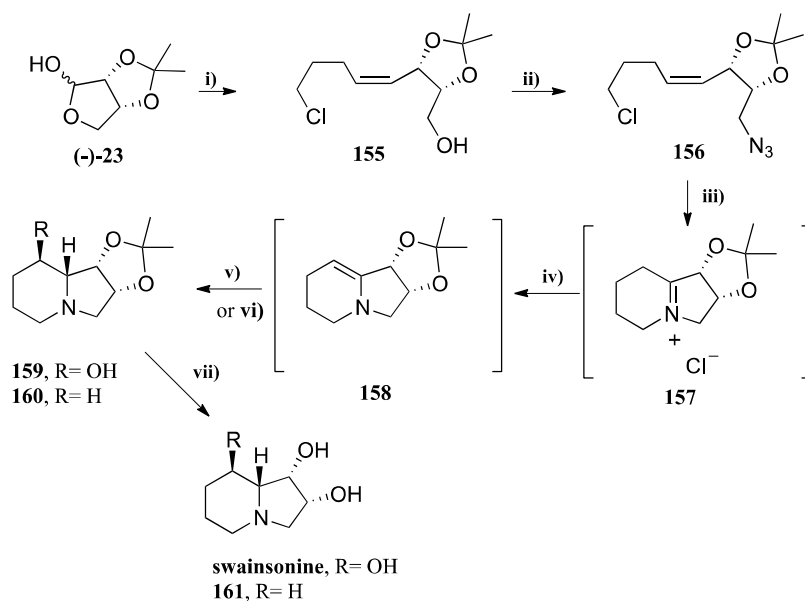
Bennet [71] has prepared (–)-swainsonine in 7 steps from 2,3-*O*-isopropylidene-D-erythrose (–)-**23** [66, 67] (**Scheme 27**). The key step involves the construction of the bicyclic imine by an intramolecular 1,3-dipolar cycloaddition with an azide. Compound **23** underwent a Wittig reaction with (3-carbethoxypropyl)triphenylphosphonium bromide in the presence of potassium bis(trimethylsilyl)amide to give the carbon chain elongation compound **150a** in 58 % yield. The alcohol function was protected with tosyl chloride and triethylamine furnishing compound **150b** in 85 %. Addition of NaN<sub>3</sub> in dimethylformamide at 70-100 °C led to a 1,3 dipolar cycloaddition with concomitant elimination of the tosyl group. Triazoline **151** was assumed to be an intermediate that readily undergoes decomposition to give imine **152** in 81 % yield overall yield. Mild hydrolysis of the ester **152a** under potassium carbonate in aqueous methanol yields the acid **152b** in 74 %. Reflux of the acid in toluene in a Dean-Stark trap generated the lactone **153** in 87% yield through the spiro compound **154**. Compound **153** was treated with diborane in tetrahydrofuran to afford the swainsonine acetonide, which was hydrolysed under 6M hydrochloric acid in tetrahydrofuran to give (–)-swainsonine in 67 % overall yield in two last steps.



**Scheme 27** – Total synthesis of (-)-swainsonine from 2,3-*O*-isopropylidene-D-erythrose (-)-23.

**Reaction conditions:** **i)**  $\text{EtO}_2\text{C}(\text{CH}_2)_3\text{P}(\text{Ph})_2\text{Br}$ ,  $\text{KN}(\text{TMS})_2$ , THF,  $-78 - 0^\circ\text{C}$ ; **ii)**  $p\text{-TsCl}$ ,  $\text{NEt}_3$ ,  $\text{CH}_2\text{Cl}_2$ ; **iii)**  $\text{NaN}_3$ , DMF,  $70 - 100^\circ\text{C}$ ; **iv)** a)  $\text{K}_2\text{CO}_3$ , MeOH (aq.), rt., 12 h; b) toluene, reflux, 30 h; **v)**  $\text{BH}_3$ , THF,  $0^\circ\text{C} - \text{rt}$ , 15 h;  $\text{H}_2\text{O}_2$ , NaOH, EtOH, reflux, 2 h; **vi)**  $\text{HCl}$  6 N, THF, rt, 15 h.

Pearson used a similar synthetic strategy to the one described by Bennet for the synthesis of (-)-swainsonine, obtained in 39% overall yield [72] (**Scheme 28**). Compound (-)-23 was first elongated by Wittig reaction to afford the alcohol 155. Under Mitsunobu conditions, azide phosphonate generated the azide 156 from 155. The cyclization of compound 156 was obtained by reflux in benzene furnishing the ionic bicyclic compound 157, that isomerized to the enamine 158 under *tert*-butyl amine and potassium bis(trimethylsilyl)amide. Hydroboration of the olefinic moiety with borane gave compound 159 as the major compound. Reduction of the salt 157 with sodium borohydride led to another indolizidine acetal, compound 160 [25]. Acid hydrolysis of acetals carried out under strong acidic conditions afforded swainsonine and (1*S*,2*R*,8*aR*)-1,2-dihydroxyindolizidine 161.

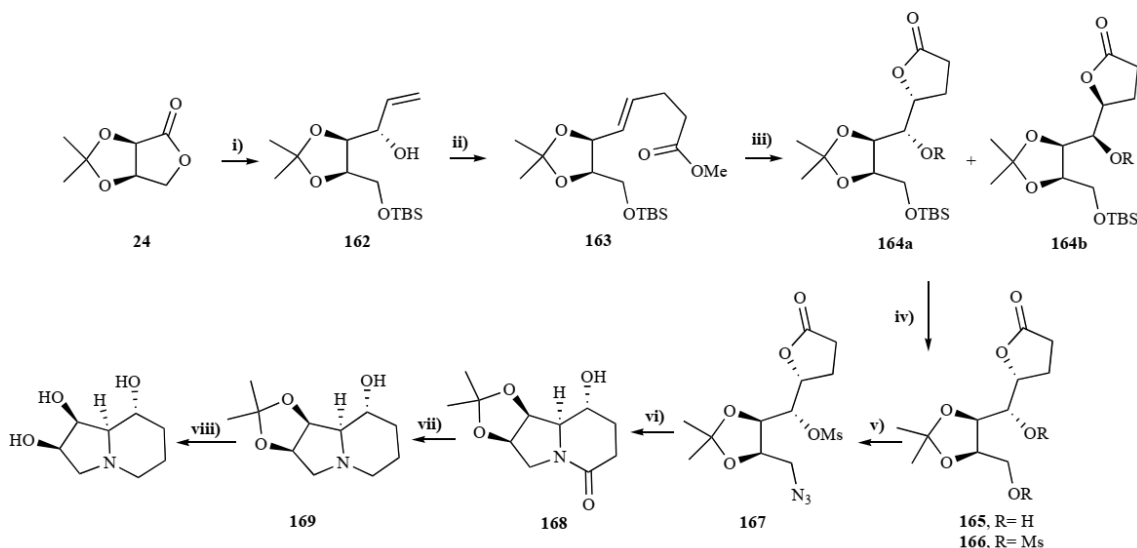


**Scheme 28** – Total synthesis of (–)-swainsonine from 2,3-*O*-isopropylidene-D-erythrose (–)-23.

**Reaction conditions:** i)  $\text{Cl}(\text{CH}_2)_4\text{P-Ph}_3\text{-Br}$ ,  $\text{KN}(\text{TMS})_2$ , THF,  $-78$  to  $23$  °C, 2 h; ii)  $(\text{PhO})_2\text{P}(\text{O})\text{N}_3$ ,  $\text{PPh}_3$ , DEAD, THF,  $23$  °C, 1 h; iii) benzene, reflux, 26 h; iv)  $t\text{-BuNH}_2$ ,  $\text{KN}(\text{TMS})_2$ ; v) a)  $\text{BH}_3$ , THF,  $23$  °C, 10 h; b)  $\text{NaOAc}$ , MeOH,  $\text{H}_2\text{O}_2$ ,  $23$  °C, 12 h; vi)  $\text{NaBH}_4$ , MeOH,  $0$  °C, 1 h; vii)  $\text{HCl}$  6 N, THF,  $23$  °C, 12 h.

Pearson synthesized (–)-swainsonine from commercially available 2,3-*O*-isopropylidene-D-erythronolactone (**24**) in 20% overall yield, in a multigram process [25] (**Scheme 29**). Besides not being the shortest route it involves simple, reproducible steps that work well on a substantial scale without requiring many separations. First, reduction of **24** with diisobutylaluminum hydride provided 2,3-*O*-isopropylidene-D-erythrose. Then the addition of vinylmagnesium bromide to **24** followed by selective monoprotection of the primary alcohol with *tert*-butyldimethylsilyl chloride in the presence of imidazole afforded allylic alcohols **162** in 97:3 ratio *anti:syn* respectively, and 73 % global yield from **24**. Both alcohols **162** yield the same *E*-unsaturated ester **163** (99 %) when subjected to Johnson orthoester Claisen rearrangement conditions [73]. Submitting crude **163** to Sharpless dihydroxylation in a biphasic mixture of *n*-butanol/water with potassium ferricyanide, potassium osmate dehydrate, hydroquinine 1,4-phthalazinediyl diether, and methanesulfonamide yielded lactones  $5\alpha$  **164a** and  $5\beta$  **164b** in 70% and 9%, respectively. The removal of the silyl protecting group from **164a** with *tetra*-butylammonium fluoride gave the diol **165**, which was smoothly converted into dimesylate **166** by reaction with mesyl chloride and dimethylamino pyridine in pyridine. Compound **166** was obtained in 76 % from **164a**. Selective displacement of the less hindered mesylate of **166** with sodium azide afforded **167** in 65 % yield. Palladium catalyzed hydrogenolysis of **167** generated the respective amine that after treatment with sodium

methoxide gave the fused six-membered lactam **168** obtained in 75% yield. Reduction of **168** with borane-methyl sulfide complex gave crystalline solid **169** in 94% yield. This was hydrolyzed to swainsonine in 96 % yield.



**Scheme 29** – Total synthesis of (-)-swainsonine from 2,3-*O*-isopropylidene-D-erythronolactone (**24**)

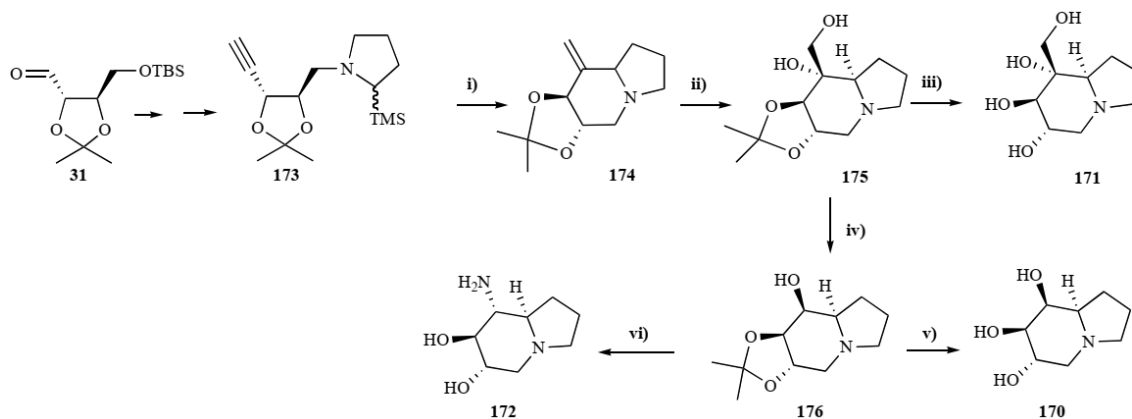
**Reaction conditions:** i) a) DIBALH; b) vinylmagnesium bromide; c) TBDMSCl, imidazole; ii) MeC(OMe)<sub>3</sub>, EtCO<sub>2</sub>H, reflux; iii) *t*-BuOH/H<sub>2</sub>O; K<sub>3</sub>[Fe(CN)<sub>6</sub>], K<sub>2</sub>CO<sub>3</sub>, K<sub>2</sub>O<sub>8</sub>·H<sub>2</sub>O, (DHQD)<sub>2</sub>-PHAL; iv) a) Bu<sub>4</sub>NF; b) MsCl, DMAP; v) NaN<sub>3</sub>, DMSO, 80 °C; vi) H<sub>2</sub>, Pd(OH)<sub>2</sub>/C, MeOH; vii) BH<sub>3</sub>·SMe<sub>2</sub>; viii) 6N HCl, Dowex 1 x 8 200 OH.

Castanospermine was found to cause osmotic diarrhoea [74] and for that fact attempts have been intensified to synthesize functional analogues of this molecule to overcome the problem.

Photoinduced electron transfer's Pandey strategy was applied to the synthesis of 1-deoxy-8-*epi*-castanospermine (**170**) and related compounds **171**, **172** [75, 76] (**Scheme 30**). Starting from L-threitol derivative **31** it was obtained the opened chain compound **173**, which was submitted to PET cyclization to give **174**. After structural manipulations as follows: 1) osmilation of **174** to give **175**; 2) cleavage of the acetal moiety in **175**, 1-azabicyclo[4.3.0]nonane alkaloid **171** was obtained. Treatment of compound **175** under C-C oxidation cleavage with sodium periodate furnished **176**, which led to 1-deoxy-8-*epi*-castanospermine (**170**).

The corresponding amino analog **172** was also synthesized from **176** as depicted in (**Scheme 30**). Glycosidase inhibitory activities for compounds **170**, **171**, **172**, were tested with different enzymes. Disappointingly all compounds turned out to be inactive against  $\alpha$ -glucosidase and  $\alpha$ -/ $\beta$ -mannosidases. 1-Deoxy-8-*epi*-castanospermine **170** showed nonspecific mild inhibition against  $\alpha$ -

galactosidase ( $K_i / \mu\text{M} = 71$ ,  $\alpha$ -galactosidase),  $\beta$ -galactosidase ( $K_i / \mu\text{M} = 73$ ,  $\beta$ -galactosidase) and  $\beta$ -glucosidase ( $K_i / \mu\text{M} = 33$ ,  $\beta$ -glucosidase).



**Scheme 30** – Synthesis of castanospermine type compounds by Pandey's protocol.

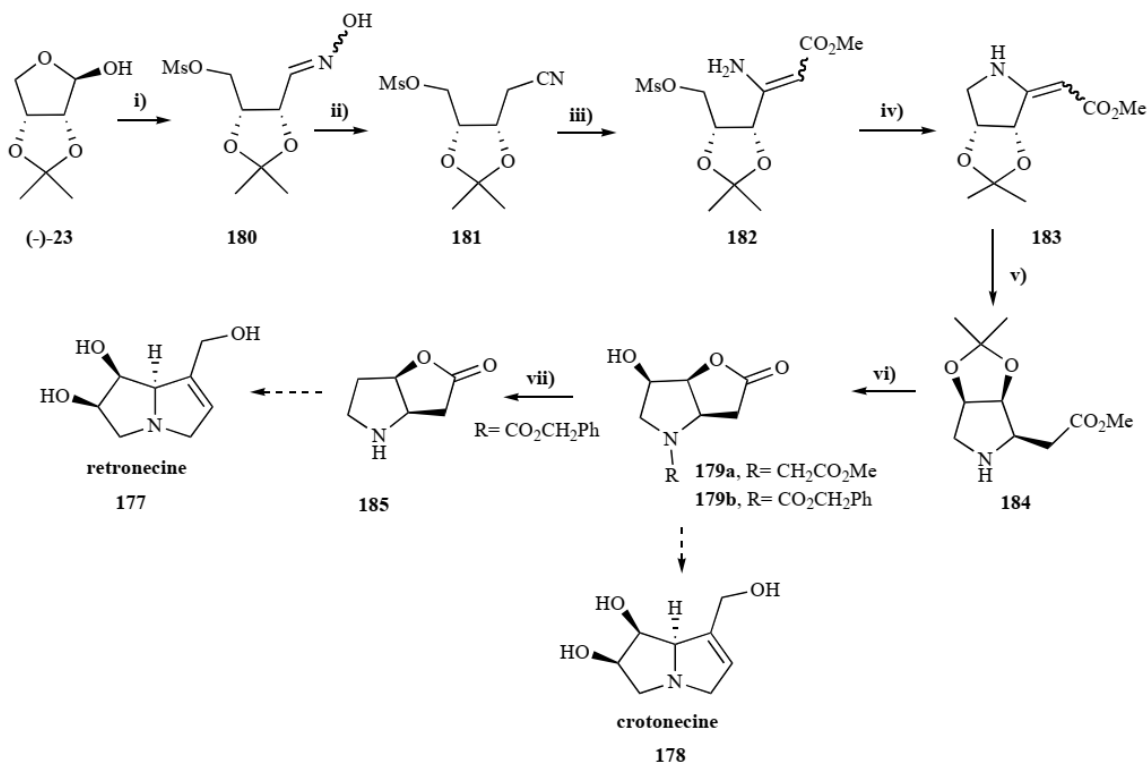
**Reaction conditions:** **i)** a)  $h\nu$ , DCN, isopropanol, 30 min; **ii)**  $\text{OsO}_4$ ,  $\text{K}_3\text{Fe}(\text{CN})_6$ ,  $\text{K}_2\text{CO}_3$ ,  $t\text{-BuOH-H}_2\text{O}$  (1:1), 12 h, rt; **iii)** 1 M HCl, MeOH, 3 h; **iv)** a)  $\text{NaIO}_4$ , silica gel,  $\text{CH}_2\text{Cl}_2$ , 10 min; b)  $\text{NaBH}_4$ , MeOH, rt, 6 h; **v)** 1 M HCl, MeOH, 3 h; **vi)** a)  $\text{MsCl}$ , Py, rt, 4 h; b)  $\text{LiN}_3$ , DMF,  $110^\circ\text{C}$ , 16 h; c)  $\text{H}_2$ , Pd-C, atm, MeOH, 7 h; d) 1 M HCl, MeOH, 4 h.

## 7. Synthesis of Pyrrolizidines

The synthesis of natural pyrrolizidines has been achieved by at least four different routes by Buchanan [53], Bennett [54] and Hudlicky [55] using 2,3-*O*-isopropylidene L-/D-erythrose (+)-**15**/(-)-**23** as starting materials.

Buchanan had used an enantiospecific strategy to prepare precursors of dextrarotatory pyrrolizidine alkaloids: (+)-retronecine **177** and (+)-crotonecine **178** and other alkaloids from 2,3-*O*-isopropylidene-D-erythrose (-)-**23** through a common precursor, lactone **179** [77] (**Scheme 31**). Compound **23** was first converted into its oxime **180** by reaction with hydroxylamine hydrate in pyridine, then in nitrilemesylester **181** by elimination of a water molecule with methanesulphonyl chloride in 95% overall yield. Reaction of compound **181** with ethyl  $\alpha$ -bromoacetate in the presence of activated zinc produced two enamino esters stereoisomers **182** in *ca.* 30% (*Z*): 1(*E*), 80% yield. Both stereoisomers could be separated and cyclized giving, after treatment with 1,8-diazabicyclo[5.4.0]undec-7-ene (DBU), another set of *Z/E* pyrrolidines isomers **183**. Both compounds yielded the same product **184** by reduction with sodium cyanoborohydride in acidified methanol in 80%. Alkylation of the nitrogen atom with ethyl bromoacetate in the presence of triethylamine gave a diester, which was further cyclized under acidic hydrolysis into  $\gamma$ -lactone **179**.

Compound **179** after a few steps as referred in literature will afford crotonecine (**178**) [56, 78, 79] (**Scheme 31**). Alcohol **179b** was subjected to deoxygenation by formation of a thiocarbonylimidazolidine followed by reduction with tri-*n*-butylstannane [80] to yield the lactone **186** in 85% overall yield from **184**. Since lactone **186** can be converted *via* Dieckmann cyclization into (+)-retronecine **177** [28, 81, 82] and other pyrrolizidine alkaloids [81-83], this work constitutes an enantiospecific route to these compounds.

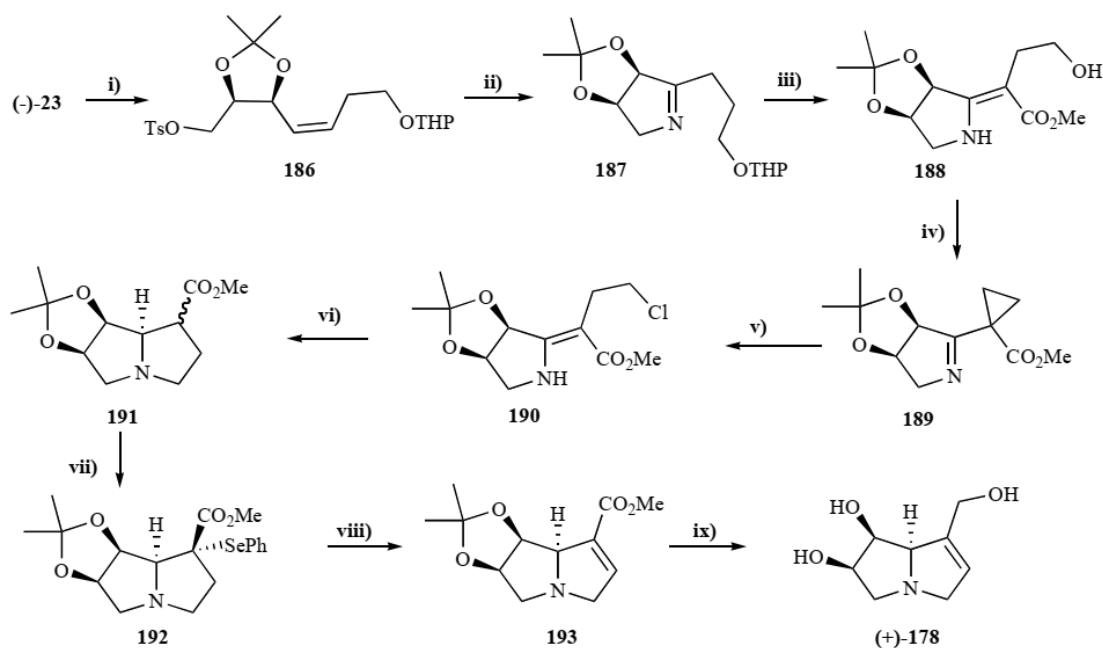


**Scheme 31** – Total synthesis of (+)-crotonecine **178** and retronecine **177** from 2,3-*O*-isopropylidene-D-erythrose (**-**)-**23**.

**Reaction conditions i)** (a)  $\text{NH}_2\text{OH}\cdot\text{HCl}$  (10 eq.), pyridine, rt.; **ii)**  $\text{MsCl}$  (12 eq.), pyridine,  $-23\text{ }^\circ\text{C}$ ; **iii)** activated Zn,  $\text{BrCH}_2\text{CO}_2\text{CH}_3$  (5 eq.), THF, reflux; **iv)** DBU (3 eq.),  $\text{CH}_2\text{Cl}_2$ , rt., 24 h; **v)**  $\text{NaBH}_3\text{CN}$ , MeOH, HCl, 2 h; **vi)** for **180a**,  $\text{BrCH}_2\text{CO}_2\text{Et}$ ,  $\text{NEt}_3$ , THF; for **180b**,  $\text{PhCH}_2\text{CO}_2\text{Cl}$ ,  $\text{Et}_3\text{N}$ ,  $\text{CH}_2\text{Cl}_2$ ,  $0\text{ }^\circ\text{C}$  – rt; **vii)** a) 1,1'-thiocarbonyldi-imidazole, pyridine, THF, reflux; b)  $\text{Bu}_3\text{SnH}$  (2.2 eq.), benzene, reflux.

Bennet developed another synthetic strategy for the synthesis of (+)-crotonecine (+)-**178** using the D-erythrose derivative (**-**)-**23** as starting material [54] (**Scheme 32**). Chain elongation of (**-**)-**23** was obtained by reaction of (3 tetrahydropyranyloxypropyl)triphenylphosphonium bromide and potassium bis(trimethylsilyl)amide, followed by tosylation of the formed hydroxyl group to afford compound **186**. Displacement of the tosyl group with sodium azide followed by a 1,3-dipolar cycloaddition generated a 1,2,3-triazolidine that spontaneously eliminate  $\text{N}_2$  and rearranged to give

imine **187** in 65% overall yield. The imine was converted to enamine **188** by sequential treatment with lithium aluminium hydride and methyl cyanofornate [82, 84] or methyl chlorofornate followed by removal of the tetrahydropyranoyl group with pyridinium *p*-toluenesulfonate (PPTs) in methanol in 73 % yield. Cyclopropylimine **189** was then readily prepared by Crossland mesylation procedure [82, 85]. The cyclopropyl group was opened with HCl in dichloromethane to afford compound **190**, which was reduced with sodium cyanoborohydride in acidic methanol to give a diastereomeric mixture of azabicyclic compounds **191**. Subsequent reaction with lithium aluminium hydride followed by addition of diphenyl selenium gave the  $\alpha$ -selenoester **192** in 56 % yield. After protonation of the nitrogen amine with sulphuric acid, the selenium underwent oxidation with *m*-chloroperbenzoic acid, becoming a good leaving group. The unsaturated compound **193** was then obtained by thermal elimination. The synthesis of (+)-crotanecine **178** was accomplished in 76 % overall yield after reduction of the ester group in **193** with di-isobutylaluminium hydride, followed by acetal hydrolysis with HCl in tetrahydrofuran.



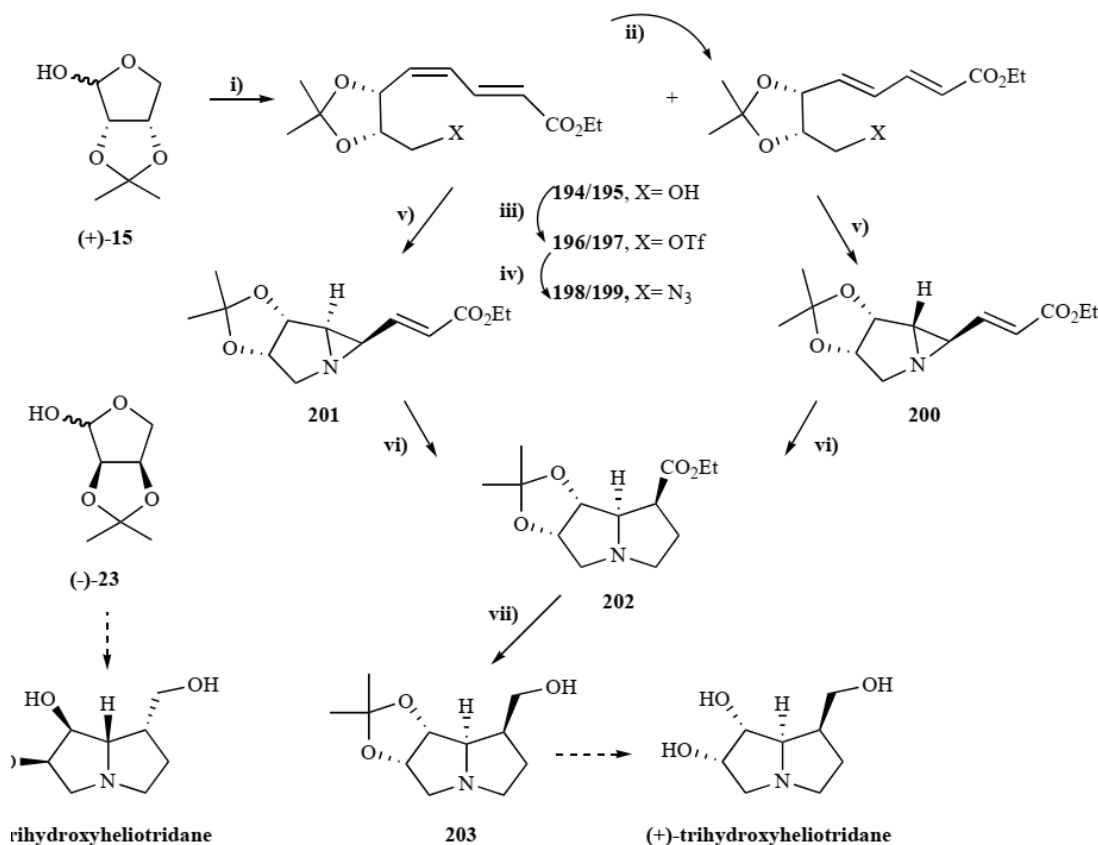
**Scheme 32** – Total synthesis of (+)-crotanecine **178** from 2,3-*O*-isopropylidene-D-erythrose (-)-**23**.

**Reaction conditions:** **i)** a) THPOCH<sub>2</sub>CH<sub>2</sub>CH=PPh<sub>3</sub>; b) *p*-TsCl, NEt<sub>3</sub>, CH<sub>2</sub>Cl<sub>2</sub>; **ii)** NaN<sub>3</sub>, DMF; **iii)** a) LDA, CNCO<sub>2</sub>CH<sub>3</sub> or ClCO<sub>2</sub>CH<sub>3</sub>, -78 °C; b) PPTs, MeOH; **iv)** MsCl, NEt<sub>3</sub>, DMAP, CH<sub>2</sub>Cl<sub>2</sub>; **v)** HCl (aq.), CH<sub>2</sub>Cl<sub>2</sub>; **vi)** a) NaBH<sub>3</sub>CN, HCl, MeOH; b) pH=9; **vii)** LDA, PhSeSePh, THF, -78 °C; **viii)** a) H<sub>2</sub>SO<sub>4</sub>; b) *m*-CPBA, CCl<sub>4</sub>, reflux; **ix)** a) DIBALH; b) HCl 1M, THF.

Hudlicky prepared both enantiomers of the pyrrolizidine alkaloid trihydroxyheliotridane by a stereocontrolled fashion from chlorobenzene through L/D-erythrose derivatives (+)-**15**/(-)-**23**. The



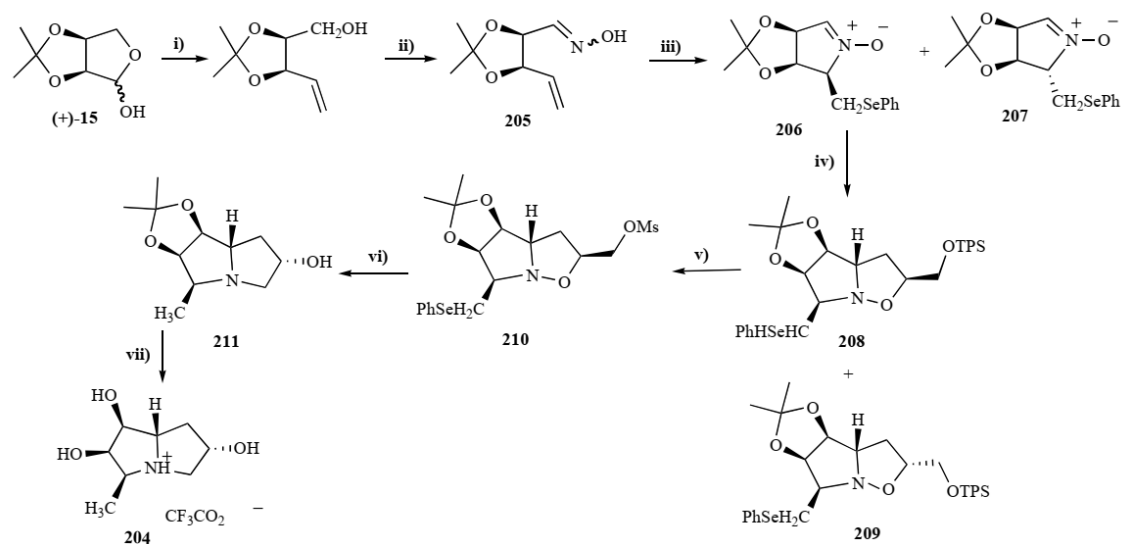
entire process is applicable to both enantiomers and the absolute stereochemistry of the final compounds depends exclusively on the starting materials [86] (**Scheme 33**). Wittig olefination of L-erythrofuranoose (+)-**15** with ethyl 4-(triphenylphosphoranylidene)but-2-enoate gave a mixture of dienol isomers **194-Z,E(5)/195-E,E(1)** in 84 % yield. Isomer **194** could be converted into the more stable *E,E*-**195** (94 %) by heating a solution of **194** in dichloromethane in the presence of iodine. Both isomers were treated separately with triflic anhydride in pyridine giving the respective triflates (**196/197**), which were further treated with sodium azide to afford the respective azides **198/199** in 69 % yield for both steps in each case. An intramolecular 1,3-dipolar cycloaddition between the ene and the azide moieties was obtained by reflux in benzene to give *cis*- and *trans*-aziridines **200** and **201**. Pyrolysis of either vinyl aziridine furnished a 2,3-dehydro compound as single isomers. This unstable enamine was hydrogenated immediately under Palladium/charcoal to afford **202**. Subsequent reduction with lithium aluminum hydride afforded (+)-trihydroxyheliotridane **203** as the protected acetonide.



**Scheme 33** –Total synthesis of (+)- (-)-trihydroxyheliotridane from L- and D-erythrofuranoose derivatives (+)-**15** and (-)-**23** respectively.

**Reaction conditions:** i) Ph<sub>3</sub>P=CHCH=CHCO<sub>2</sub>Et, CH<sub>2</sub>Cl<sub>2</sub>; ii) I<sub>2</sub>, CH<sub>2</sub>Cl<sub>2</sub>; iii) Tf<sub>2</sub>O, pyridine, CH<sub>2</sub>Cl<sub>2</sub>; iv) NaN<sub>3</sub>, 18-C-6, CH<sub>2</sub>Cl<sub>2</sub>; v) benzene, reflux; vi) (a) flash vacuum pyrolysis, 520 °C, ca. 10<sup>-4</sup> Torr; (b) H<sub>2</sub>, Pd/C, MeOH; vii) LiAlH<sub>4</sub>, THF.

Pyrrolizidine **204** was obtained from a sequence of reactions starting with 2,3-*O*-isopropylidene-L-erythrofurano-*s*-(+)-**15** having as the key intermediate  $\Delta^1$ -pyrroline-*N*-oxide [87] (**Scheme 34**). First, compound **15** was treated with methylene triphenylphosphorane to yield the respective alkene. The primary alcohol function in this compound was oxidized under Swern methodology, and the volatile aldehyde trapped with hydroxylamine to give the oxime **205** in 80 % yield, as 5:2 *E/Z* mixture of isomers. Treatment of **205** with phenylselenenyl bromide followed by neutralization with potassium carbonate promoted cyclization [88] to afford the isomeric nitrones **206** and **207** in moderate yield (45 %) and *c.a.* 1:1 ratio. The *cis* nitron **206** was reacted with the electron rich dipolarophile allyl *t*-butyldiphenylsilyl ether to yield the isoxazolidine **208** as the major product (72 %) together with its epimer, **209** (8 %). Cycloaddition occur mainly by the more accessible face of the nitron *via* an *exo*-transition state to give isoxazolidine **208**. Compound **209** is formed by an *endo*-transition state. Conventional desilylation with tetrabutylammonium fluoride in tetrahydrofuran, followed by mesylation of the obtained primary alcohol yield **210** in 92 % yield. Hydrogenolysis of **210** with Raney nickel led to cleavage of *N*-*O* bond and to phenylselenium cleavage [89, 90] with formation of pyrrolizidine **211** in 65 % yield. Removal of the isopropylidene moiety was effected under aqueous trifluoroacetic acid to furnish the free pyrrolizidine **204** as the trifluoroacetic acid salt.



**Scheme 34** - Total synthesis of pyrrolizidine **204** from 2,3-*O*-isopropylidene-L-erythrofurano-*s*-(+)-**15**

**Reaction conditions:** **i)**  $\text{Ph}_3\text{PCH}_2\text{Br}$ , BuLi, THF; **ii)** a)  $\text{COCl}_2$ , DMSO,  $\text{CH}_2\text{Cl}_2$ , -60 °C; b) Et<sub>3</sub>N; **iii)** a) PhSeBr,  $\text{CH}_2\text{Cl}_2$ , K<sub>2</sub>CO<sub>3</sub>; **iv)** allyl *t*-butyldiphenylsilyl chloride, Et<sub>3</sub>N, toluene, reflux, 2h; **v)** a) Bu<sub>4</sub>NF, THF, b) MsCl, Et<sub>3</sub>N; **vi)** H<sub>2</sub>, Raney nickel, ethanol; **vii)** aq. CF<sub>3</sub>CO<sub>2</sub>H.

## 8. Conclusion

This review summarizes the methods referred in literature for the synthesis of the four tetroses (L-/D-erythroses and derivatives, and L-/D-threoses and derivatives) and the relevance of these small molecules in the syntheses of four out of the five structure types of iminosugars known. Concise methods have been developed having these chiral synthons as building blocks of a number of D-/L-piperidine alkaloids including nagstatine analogues, pyrrolidine iminosugars, indolizidines, mainly (+)- and (-)-swainsonines, and a number of pyrrolizidines. In many cases these methodologies are open to the synthesis of other analogues/ derivatives lending an easy and general introduction to other stereochemistries/substituents to the iminosugar scaffold, enlarging the potential of iminosugars as specific enzyme inhibitors.

## 9. References

1. Inouye, S.; Tsurouka, T.; Niida, T., The structure of nojirimycin, a piperidinose sugar antibiotic. *J. Antibiot. Serv. A* **1966**, *19* (6), 288-292.
2. Watson, A. A.; Fleet, G. W. J.; Asano, N.; Molyneux, R. J.; Nash, R. J., Polyhydroxylated alkaloids — natural occurrence and therapeutic applications. *Phytochemistry* **2001**, *56* (3), 265-295.
3. Inouye, S.; Tsurouka, T.; Ito, T.; Niida, T., Structure and synthesis of nojirimycin. *Tetrahedron* **1968**, *24* (5), 2125-2144.
4. Yagi, M.; Kouno, T.; Aoyagi, Y.; Murai, H., The Structure of Moranoline, a Piperidine Alkaloid from Morus Species. *Nippon Nogeikagaku Kaishi* **1976**, *50* (11), 571-572.
5. Murao, S.; Miyata, S., Isolation and characterization of a new trehalase inhibitor, S-GI. *Agric. Biol. Chem.* **1980**, *44* (1), 219-221.
6. Peyrieras, N.; Bause, E.; Legler, G.; Vasilov, R.; Claesson, L.; Peterson, P.; Ploegh, H., Effects of the glucosidase inhibitors nojirimycin and deoxynojirimycin on the biosynthesis of membrane and secretory glycoproteins. *EMBO J.* **1983**, *2* (6), 823-832.
7. Scott, L. J.; Spencer, C. M., Miglitol: a review of its therapeutic potential in type 2 diabetes mellitus. *Drugs* **2000**, *59* (3), 521-549.
8. Yu, Z.; Sawkar, A. K.; Whalen, L. J.; Wong, C. H.; Kelly, J. W. J., Isofagomine- and 2,5-Anhydro-2,5-imino-d-glucitol-Based Glucocerebrosidase Pharmacological Chaperones for Gaucher Disease Intervention. *Med. Chem.* **2007**, *50* (1), 94-100.
9. K. Afarinkia, A. B. T., Recent advances in the chemistry of azapyranose sugars. *Tetrahedron: Asymmetry* **2005**, *16* (7), 1239-1287.
10. Karpas, A.; Fleet, G. W. J.; Dwek, R. A.; Fellows, L. E.; Tyms, A. S.; Petursson, S.; Namgoong, S. K.; Ramsden, N. G.; Smith, P. W.; Son, J. C.; Wilson, F.; Witty, D. R.; Jacob, G. S.; Rademacher, T. W., Inhibition of HIV replication by amino-sugar derivatives. *FEBS Lett.* **1988**, *237*, 128-132.

11. Khan, K. N.; Snook, S. S.; Semler, D. E.; Baron, D. A.; Alden, C. L., Pathology of Perbutylated-*N*-Butyl-1-Deoxyojiromycin (An  $\alpha$ -Glucosidase-1 Inhibitor) in Sprague-Dawley Rats. *Toxicol. Pathol.* **1996**, *24*, 531-538.
12. Casiraghi, G.; Zanardi, F.; Rassu, G.; Spanu, P., Stereoselective Approaches to Bioactive Carbohydrates and Alkaloids-With a Focus on Recent Syntheses Drawing from the Chiral Pool. *Chem. Rev.* **1995**, *95* (6), 1677-1716.
13. Barker, R.; MacDonald, D. L., Some Oxidation and Reduction Products of 2,4-*O*-Ethylidene-D-erythrose. *J. Am. Chem. Soc.* **1960**, *82* (9), 2301-2303.
14. Clinton, E. B., A New Synthesis of D-Erythrose Derivatives from D-Arabinose. *J. Am. Chem. Soc.* **1957**, *79* (1), 165-166.
15. Lee, J. B.; Nolan, T. J., Sugars with potential antiviral activity—I : A new method for the preparation of glycorufanoyl chlorides and the synthesis of a mannosyl nucleoside *Tetrahedron* **1967**, *23* (6), 2789-2794.
16. Shen, X.; Wu, Y.-I.; Wu, Y., Enantioselective Synthesis of Ethyl 4,5,7,8,9-Penta-*O*-acetyl-2,6-anhydro- 3-deoxy-D-erythro-L-gluca-nononate: a 2-Monodeoxygenated Derivative of ' 2-Keto-3-deoxy-D-glycero-D-galacto-nononic Acid'. *Helvetica Chimica Acta* **2000**, *83* (5), 943-953.
17. Munier, P.; Krusinski, A.; Picq, D.; Ankar, D., Stéréosélectivité comparée de la réduction de trifluorométhylcétone et des méthylcétone correspondantes: nouvelles voies d'accès à des dérivés trifluorométhylés de pentoses *Tetrahedron* **1995**, *51* (4), 1229-1244.
18. Baxter, J. N.; Perlin, A. S., 2,3-*O*-isopropylidene-L-erythrotetruronic acid and -L-erythrose, and the methyl D-erythro- and D-threo-tetrofuranosides. *Can. J. Chem.* **1960**, *38* (11), 2217-2225.
19. Kiso, M.; Hasegawa, A., Acetonation of some pentoses with 2,2-dimethoxypropane-*N,N*-dimethylformamide-*p*-toluenesulfonic acid. *Carbohydr. Res.* **1976**, *52* (1), 95-101.
20. Thompson, D. K.; Hubert, C. N.; Wightman, R. H., Hydroxylated pyrrolidines. Synthesis of 1,4-dideoxy-1,4-imino-L-lyxitol, 1,4,5-trideoxy-1,4-imino-D- and -L-lyxo-hexitol, 2,3,6-trideoxy-3,6-imino-D-glycero-L-altr- and -D-glycero-L-galacto-octitols, and of a chiral potential precursor of carbapenem systems *Tetrahedron* **1993**, *49* (18), 3827-3840.
21. Gibson, D. T.; Koch, J. R.; Kallio, R. E., Oxidative degradation of aromatic hydrocarbons by microorganisms. I. Enzymic formation of catechol from benzene. *Biochemistry* **1968**, *7* (7), 2653-2662.
22. Gibson, D. T.; Koch, J. R.; Schuld, C. L.; Kallio, R. E., Oxidative degradation of aromatic hydrocarbons by microorganisms. II. Metabolism of halogenated aromatic hydrocarbons. *Biochemistry* **1968**, *7* (11), 3795-3802.
23. Mandel, M.; Hudlicky, T.; Kwart, L. D.; Whited, G. M., From Chlorobenzene to a Carbohydrate in Two Steps. A New Chemoenzymatic Synthesis of 2,3-*O*-Isopropylidene-D-erythruronalactone. *Collect. Czech. Chem. Commun.* **1993**, *58* (10), 2517-2522.
24. Hudlicky, T.; Luna, H.; Price, J. D.; Rulin, F., An enantiodivergent approach to D- and L-erythrose via microbial oxidation of chlorobenzene. *Tetrahedron Lett.* **1989**, *30* (31), 4053-4054.
25. Pearson, W. H.; Hembre, E. J., A Practical Synthesis of (-)-Swainsonine *J. Org. Chem.* **1996**, *61* (20), 7217-7221.
26. Cohen, N.; Banner, B. L.; Laurenzano, A. J.; Carozza, L., 3-*O*-Isopropylidene-D-erythruronalactone. In *Org. Synth*, Wiley & Sons: New York, 1990; Vol. Collect.VII, pp 297-301.

27. Dunigan, J.; Weigel, L. O., Synthesis of alkyl (2*S*,3*R*)-4-hydroxy-2,3-epoxybutyrates from sodium erythorbate. *J. Org. Chem.* **1991**, *56* (21), 6225-6227.
28. Abushanab, E.; Vemishetti, P.; Leiby, R. W.; Singh, H. K.; Mikkilineni, A. B.; Wu, D. C. J.; Saibaba, R.; Panzica, R. P., The chemistry of L-ascorbic and D-isoascorbic acids. 1. The preparation of chiral butanetriols and -tetrols. *J. Org. Chem.* **1988**, *53* (11), 2598-2602.
29. André, C.; Bolte, J.; Demuynck, C., Syntheses of L-threose and D-erythrose analogues modified at position 2. *Tetrahedron: Asymmetry* **1998**, *9* (8), 1359-1367.
30. Streith, J.; Tschamber, T.; Gessier, F.; Tarnus, C.; Neuburger, M.; Huber, W., Synthesis of Imidazolo-Piperidinopentoses as Nagstatine Analogues. *Eur. J. Org. Chem.* **2001**, (21), 4111-4125.
31. Hudlicky, T.; Entwistle, D. a.; Pitzer, K. K.; Thorpe, A. J., Modern Methods of Monosaccharide Synthesis from Non-Carbohydrate Sources. *Chem. Rev.* **1996**, *96* (3), 1195-1220.
32. Katsuki, T.; Lee, A. W. M.; Ma, P.; Martin, V. S.; Masamune, S.; Sharpless, K. B.; Tuddenham, D.; Walker, F. J., Synthesis of saccharides and related polyhydroxylated natural products. 1. Simple alditols. *J. Org. Chem.* **1982**, *47* (7), 1373-1378.
33. Feit, P. W., 1,4-Bismethanesulfonates of the Stereoisomeric Butanetetraols and Related Compounds. *J. Med. Chem.* **1964**, *7* (1), 14-17.
34. Iida, H.; Yamazaki, N.; Kibayashi, C., Total Synthesis of (+)-Nojirimycin and (+)-1-Deoxynojirimycin. *J. Org. Chem.* **1987**, *52* (15), 3337-3342.
35. Hernández-García, L.; Quintero, L.; Sánchez, M.; Sartillo-Piscil, F., Beneficial effect of internal hydrogen bonding interactions on the beta-fragmentation of primary alkoxyl radicals. Two-step conversion of D-xylo- and D-ribofuranoses into L-threose and D-erythrose, respectively. *J. Org. Chem.* **2007**, *72* (22), 8196-8201.
36. Aoyagi, S.; Fujimaki, S.; Kibayashi, C., Total synthesis of (+)- $\alpha$ -homonojirimycin. *J. Chem. Soc., Chem. Commun* **1990**, 1457-1459.
37. Katsuki, T.; K., S., The first practical method for asymmetric epoxidation. *J. Am. Chem. Soc.* **1980**, *102* (18), 5974-5976.
38. Overman, L. E.; Flippin, L. A., Facile aminolysis of epoxides with diethylaluminum amides *Tetrahedron Lett.* **1981**, *22* (3), 195-198.
39. Tschamber, T.; Siendt, H.; Boiron, A.; Gessier, F.; Deredas, D.; Frankowski, A.; Picasso, S.; Steiner, H.; Aubertin, A.-M.; Streith, J., Stereoisomeric Imidazolo-Pentoses – Synthesis, Chiroptical Properties, and Evaluation as Glycosidase Inhibitors. *J. Org. Chem.* **2001**, (7), 1335-1347.
40. Harusawa, S.; Imazu, T.; Takashima, S.; Araki, L.; Ohishi, H.; Kurihara, T.; Sakamoto, Y.; Yamatodani, A., Synthesis of 4(5)-[5-(Aminomethyl)tetrahydrofuran-2-yl- or 5-(Aminomethyl)-2,5-dihydrofuran-2-yl]imidazoles by Efficient Use of a PhSe Group: Application to Novel Histamine H3-Ligands. *J. Org. Chem.* **1999**, *64* (23), 8608-8615.
41. Kudzma, L. V.; Tumbull, S. P., Expedient Synthesis of 4(5)-[1-(2,3-Dimethylphenyl)ethyl]-1H-imidazole, the  $\alpha$ 2-Adrenergic Agonist Medetomidine. *Synthesis* **1991**, (11), 1021-1022.
42. Rose, J. E.; D., L. P.; Gani, D., Stereospecific synthesis of  $\alpha$ -deuteriated  $\alpha$ -amino acids: regiospecific deuteration of chiral 3-isopropyl-2,5-dimethoxy-3,6-dihydropyrazines. *J. Chem. Soc. Perkin Trans 1* **1995**, 157-165.

43. Grauert, M.; Schöllkopf, U., Asymmetric Syntheses via Heterocyclic Intermediates, XXVII. Reactions of Metallated Bislactim Ethers of cyclo-(L-Val-Gly-) with (*R*)- and (*S*)-Glyceraldehyde and with (*S*)-Lactaldehyde. *Liebigs Ann. Chem* **1985**, (9), 1817-1824.
44. Ruiz, M.; Ruanova, T. M.; Ojea, V.; Quintela, J. M., Amino and Hydroxy Acid Based Diastereoselective Synthesis of 1-Deoxygalactostatin and its Imino Acid Derivative. *Tetrahedron Lett.* **1999**, 40 (10), 2021-2024.
45. Kobayashi, S.; Furuta, T.; Hayashi, T.; Nishijima, M.; Hanada, K., Catalytic Asymmetric Syntheses of Antifungal Sphingofungins and Their Biological Activity as Potent Inhibitors of Serine Palmitoyltransferase (SPT). *J. Am. Chem. Soc.* **1998**, 120 (5), 908-919.
46. Kobayashi, S.; Furuta, T., Use of heterocycles as chiral ligands and auxiliaries in asymmetric syntheses of sphingosine, sphingofungins B and F *Tetrahedron* **1998**, 54 (35), 10275-10294.
47. Evans, D. A.; Yang, M. G.; Dart, M. J.; Duffy, J. L., Double stereodifferentiating aldol reactions of (*E*) and (*Z*) lithium enolates. Model reactions for polypropionate assemblage. *Tetrahedron Lett.* **1996**, 37 (12), 1957-1960.
48. Evans, D. A.; Dart, M. J.; Duffy, J. L.; Rieger, D. L., Double Stereodifferentiating Aldol Reactions. The Documentation of "Partially Matched" Aldol Bond Constructions in the Assemblage of Polypropionate Systems. *J. Am. Chem. Soc.* **1995**, 117 (35), 9073-9074.
49. Ojea, V.; Ruanova, T. M.; Quintela, M., Access to iminosugars by aldol additions of metalated bis-lactim ethers to L-erythrose derivatives. *Tetrahedron: Asymmetry* **2002**, 13 (8), 795-799.
50. Ruiz, M.; Ojea, V.; Quintela, J. M., Diastereoselective Synthesis of 1-Deoxytalonojirimycin. *Synlett* **1999**, 2, 204-206.
51. Lehmann, T. E.; Berkessel, A., Stereoselective Synthesis of 4'-Benzophenone-Substituted Nucleoside Analogs: Photoactive Models for Ribonucleotide Reductases. *J. Org. Chem.* **1997**, 62 (2), 302-309.
52. Pino-González, M. S.; Oña, N., Synthesis of intermediates in the formation of hydroxy piperidines and 2-azido lactones from D-erythrose. *Tetrahedron: Asymmetry* **2008**, 19 (6), 721-729.
53. Perlin, A. S., D-Erythrose. *Methods Carbohydr. Chem.* **1962**, 1, 64-70.
54. Pandey, G.; Kapur, M., A general strategy towards the synthesis of 1-*N*-iminosugar type glycosidase inhibitors: demonstration by the synthesis of d- as well as l-glucose type iminosugars (isofagomines). *Tetrahedron Letters* **2000**, 41 (45), 8821-8824.
55. Corey, E. J.; Fuchs, P. L., A synthetic method for formyl→ethynyl conversion (RCHO→RCCH or RCCR'). *Tetrahedron Letters* **1972**, 13 (36), 3769-3772.
56. Yoshida, J.; Maekawa, T.; Murata, T.; Matsunaga, S.; Isoe, S., Electrochemical oxidation of organosilicon compounds. Part 7. The origin of .beta.-silicon effect in electron-transfer reactions of silicon-substituted heteroatom compounds. Electrochemical and theoretical studies. *Journal of the American Chemical Society* **1990**, 112 (5), 1962-1970.
57. Pandey, G.; Kapur, M., Design and Development of a Common Synthetic Strategy for a Variety of 1-*N*-Iminosugars. *Organic Letters* **2002**, 4 (22), 3883-3886.
58. Pandey, G.; Kapur, M.; Islam, K., M.; Gaikwad, S., M., A new access to polyhydroxy piperidines of the azasugar class: synthesis and glycosidase inhibition studies. *Organic & biomolecular chemistry* **2003**, 1 (19), 3321-3326.

59. Chapman, T. M.; Courtney, S. M.; Hay, P.; Davis, B. G., Highly diastereoselective additions to polyhydroxylated pyrrolidine cyclic imines: ready elaboration of aza-sugar scaffolds to create diverse carbohydrate-processing enzyme probes. *Chemistry* **2003**, *9* (14), 3397-3414.
60. Ruiz, M.; Ruanova, T. M.; Blanco, O.; Núñez, F.; Pato, C.; Ojea, V., Diastereoselective synthesis of piperidine imino sugars using aldol additions of metalated bislactim ethers to threose and erythrose acetonides. *J. Org. Chem.* **2008**, *73* (6), 2240-2255.
61. Asano, N.; Yamauchi, T.; Kagamifuchi, K.; Shimizu, N.; Takahashi, S.; Takatsuka, H.; Ikeda, K.; Kizu, H.; Chuakul, W.; Kettawan, A., Iminosugar-Producing Thai Medicinal Plants. *J. Nat. Prod.* **2005**, *68* (8), 1238-1242.
62. Blanco, O.; Pato, C.; Ruiz, M.; Ojea, V., Synthesis of pyrrolidine homoazasugars and 3,4-dihydroxy-5-hydroxymethylprolines using aldol additions of metalated bislactim ethers to 2,4-*O*-ethylidene-D-erythroses. *Org. Biomol. Chem.* **2009**, *7* (11), 2310-2321.
63. Chandler, C. L.; List, B., Catalytic, Asymmetric Transannular Aldolizations: Total Synthesis of (+)-Hirsutene. *J. Am. Chem. Soc.* **2008**, *130* (21), 6737-6739.
64. Xie, X.; Chen, Y.; Ma, D., Enantioselective Arylation of 2-Methylacetoacetates Catalyzed by CuI/trans-4-Hydroxy-L-proline at Low Reaction Temperatures. *J. Am. Chem. Soc.* **2006**, *128* (50), 16050-16051.
65. Chapman, T. M.; Davies, I. G.; Gu, B.; Block, T. M.; Scopes, D. I. C.; Hay, P. A.; Courtney, S. M.; McNeill, L. A.; Schofield, C. J.; Davis, B. G., Glyco- and Peptidomimetics from Three-Component Joulie-Ugi Coupling Show Selective Antiviral Activity. *J. Am. Chem. Soc.* **2005**, *127* (2), 506-507.
66. Kotsuki, H.; Ikishima, H.; Okuyama, A., Organocatalytic Asymmetric Synthesis Using Proline and Related Molecules. Part 1. *Heterocycles* **2008**, *75* (3), 493-529.
67. Veith, F. M.; Schwardt, O.; Kautz, U.; Kramer, B.; Jager, V., (1'*R*)-(-)-2,4-*O*-Ethylidene-D-erythrose and ethyl (*E*)-(-)-4,6-*O*-ethylidene-(4*S*,5*R*,1'*R*)-4,5,6-trihydroxy-2-hexenoate. *Org. Synth.* **2004**, *Coll. Vol. 10*, 405-410.
68. Adibekian, A.; Timmer, M. S. M.; Stallforth, P.; Rijn, J.; Werz, D. B.; Seeberger, P. H., Stereocontrolled synthesis of fully functionalized D-glucosamine monosaccharides via a domino nitro-Michael/Henry reaction. *Chem. Commun.* **2008**, 3549-3551.
69. Wu, W. L.; Yao, Z. J.; Li, Y. L.; Li, J. C.; Xia, Y.; Wu, Y. L., Diastereoselective Propargylation of  $\alpha$ -Alkoxy Aldehydes with Propargyl Bromide and Zinc. A Versatile and Efficient Method for the Synthesis of Chiral Oxygenated Acyclic Natural Products. *J. Org. Chem.* **1995**, *60* (10), 3257-3259.
70. Blanco, O.; Pato, C.; Ruiz, M.; Ojea, V., Access to pyrrolidine imino sugars via tin(II)-mediated aldol reactions of bislactim ethers: synthesis of 2,5-dideoxy-2,5-imino-D-glucitol. *Org. Biomol. Chem.* **2008**, *6*, 3967-3969.
71. Bennett, R. B., III; Choi, J. R.; Montgomery, W. D.; Cha, J. K., A short, enantioselective synthesis of (-)-swainsonine. *J. Am. Chem. Soc.* **1989**, *111* (7), 2580-2582.
72. Pearson, W. H.; Lin, K. C., The intramolecular cycloaddition of azides with  $\omega$ -chloroalkenes. A facile route to ( $\pm$ )-swainsonine and other indolizidine alkaloids. *Tetrahedron Lett.* **1990**, *31* (52), 7571-7574.
73. Johnson, W. S.; Werthemann, L.; Bartlett, W. R.; Brocksom, T. J.; Li, T.; Faulkner, D. J.; Petersen, M. R., Simple stereoselective version of the Claisen rearrangement leading to trans-trisubstituted olefinic bonds. Synthesis of squalene. *J. Am. Chem. Soc.* **1970**, *92* (3), 741-743.
74. Robinson, K. M.; Dumbre, S. P.; Ducep, J.-B.; Danzin, C., Intestinal disaccharidase inhibitors. *Drugs Fut.* **1992**, *17* (8), 705-720.

75. Pandey, G.; Dumbre, S. G.; Pal, S.; Khan, M. I.; Shabab, M., Synthesis and evaluation of 1-deoxy-8-epi-castanospermine, 1-deoxy-8-hydroxymethyl castanospermine, and (6*S*,7*S*,8*R*,8*aR*)-8-amino-octahydroindolizine-6,7-diol. *Tetrahedron* **2007**, *63* (22), 4756-4761.
76. Pandey, G.; Dey, D.; Gadre, S., R., Alfa-Trimethylsilylmethylamine Radical Cation in the Synthesis of Cyclic Amines and Beyond. *CHIMIA International Journal for Chemistry* **2013**, *67* (1), 30-38.
77. Buchanan, J. G.; Jigajinni, V. B.; Singh, G.; Wightman, R. H., Enantiospecific Synthesis of (+)-Retronecine, (+)-Crotonecine, and Related Alkaloids. *J. Chem. Soc., Perkin Trans 1* **1987**, 2377-2384.
78. Yadav, V. K.; Rueger, H.; Benn, M., An Enantioselective Synthesis of (+)-Crotanecine. *Heterocycles* **1984**, *22* (12), 2735-2738.
79. Atal, C. K.; Kapur, K. K.; Culvenor, C. C. J.; L. W. Smith, A new pyrrolizidine aminoalcohol in alkaloids from crotalaria species. *Tetrahedron Lett.* **1966**, *7* (6), 537-544.
80. Carney, R. E.; McAlpine, J. B.; Jackson, M.; Stanaszek, R. S.; Washburn, W. H.; Cirovic, M.; Mueller, S. L., Modification of seldomycin factor 5 at C-3'. *J. Antibiot.* **1978**, *31* (5), 441-450.
81. Rueger, H.; Benn, M., A Synthesis of (+)-2-Oxa-6-azabicyclo[3.3.0]octan-3-one (The Geissman-Waiss Lactone): A Synthone for Some Necines. *Heterocycles* **1982**, *19* (1), 23-25.
82. Rueger, H.; Benn, M., The enantioselective synthesis of (+)-retronecine, (-)-platynecine, and (+)-croalbinecine and its C-1 epimer. *Heterocycles* **1983**, *20* (7), 1331-1334.
83. Glinskil, J. A.; Zalkow, L. H., The synthesis of heliotridine and related alkaloids. *Tetrahedron Lett.* **1985**, *26* (24), 2857-2860.
84. Mander, L. N.; Sethi, S. P., Regioselective synthesis of  $\beta$ -ketoesters from lithium enolates and methyl cyanoformate. *Tetrahedron Lett.* **1983**, *24* (48), 5425-5428.
85. Crossland, R. K.; Servis, K. L., Facile synthesis of methanesulfonate esters. *J. Org. Chem.* **1970**, *35* (9), 3195-3196.
86. Hudlicky, T.; Luna, H.; Price, J. D.; Rulin, F., Microbial oxidation of chloroaromatics in the enantiodivergent synthesis of pyrrolizidine alkaloids: trihydroxyheliotridanes. *J. Org. Chem.* **1990**, *55* (15), 4683-4687.
87. Hall, A.; Meldrum, K. P.; Therond, P. R.; Wightman, R. H., Synthesis of Hydroxylated Pyrrolizidines Related to Alexine using Cycloaddition Reactions of Functionalized Cyclic Nitrones. *Synlett* **1997**, (1), 123-125.
88. Grigg, R.; Hadjisoteriou, M.; Kennewell, P.; Markandu, J., Phenylselenyl halide induced formation of cyclic nitrones from alkenyl oximes. *J. Chem. Soc., Chem. Comm.* **1992**, 1537-1538.
89. Curran, D. P., Reduction of  $\Delta^2$ -isoxazolines: a conceptually different approach to the formation of aldol adduct. *J. Am. Chem. Soc.* **1982**, *104* (14), 4024-4026.
90. Clive, D. L. J.; Chittattu, G. J.; Farina, V.; Kiel, W. A.; Menchen, S. M.; Russell, C. G.; Singh, A.; Wong, C. K.; Curtis, N. J., Organic tellurium and selenium chemistry. Reduction of tellurides, selenides, and selenoacetals with triphenyltin hydride. *J. Am. Chem. Soc.* **1980**, *102* (13), 4438-4447.



# 2

Glycosylation, the important role of Golgi  $\alpha$ -  
Mannosidase II

*This chapter will be submitted for publication as a review article.*

## 1. Glycosylation

Glycosylation is thought to be the most complex post-translational modification in the cell. Almost 50% of the human proteome is glycosylated as glycosylation plays a vital role in various biological functions such as antigen's recognition, cell-cell communication, expression of genes and protein folding [1]. All these processes take place in the endoplasmic reticulum (ER) and in the Golgi apparatus (GA), through the action of glycosyltransferases (GTs) and glycosidases (Gs). Each GT is specific to linking a particular sugar from a donor (sugar nucleotide or dolichol) to a substrate (protein or lipid) and acts independently of other GTs. The Gs hydrolyze specific glycan linkages.

The glycosylation process starts on the ER membrane where the transfer of the initial sugar(s) to the glycoproteins takes place. Subsequently, the addition/cleavage of many different sugars occurs in the Golgi apparatus and from which results the formation of mature glycans (**Figure 1**).

The full glycosylation process can be classified into six types taking into account how the glycosylation process begins, as it is illustrated in **Figure 1**. It can involve i) N-linked glycosylation, ii) O-linked glycosylation, iii) C-linked glycosylation, iv) Phospho-glycosylation, v) glypiation and vi) S-linked glycosylation [2]. The most common process in the cell involves the O-linked and the N-linked glycosylation. The first process involves the transfer of a sugar molecule to the O-terminal of the protein sequence, whereas the second process involves the transfer of a sugar molecule of the N-terminal of the protein sequence. Typical examples include the O-glycosylated proteins with acetylgalactosamine, fucose, galactose, or mannose. The N-linked glycosylation includes in proteins the precursor  $(\text{Glc})_3(\text{Man})_9(\text{GlcNAc})_2$ , three glucoses, nine mannoses, and two N-acetylglucosamines, which undergo new cycles of removal and addition of glucose over the maturation of N-glycan [3].

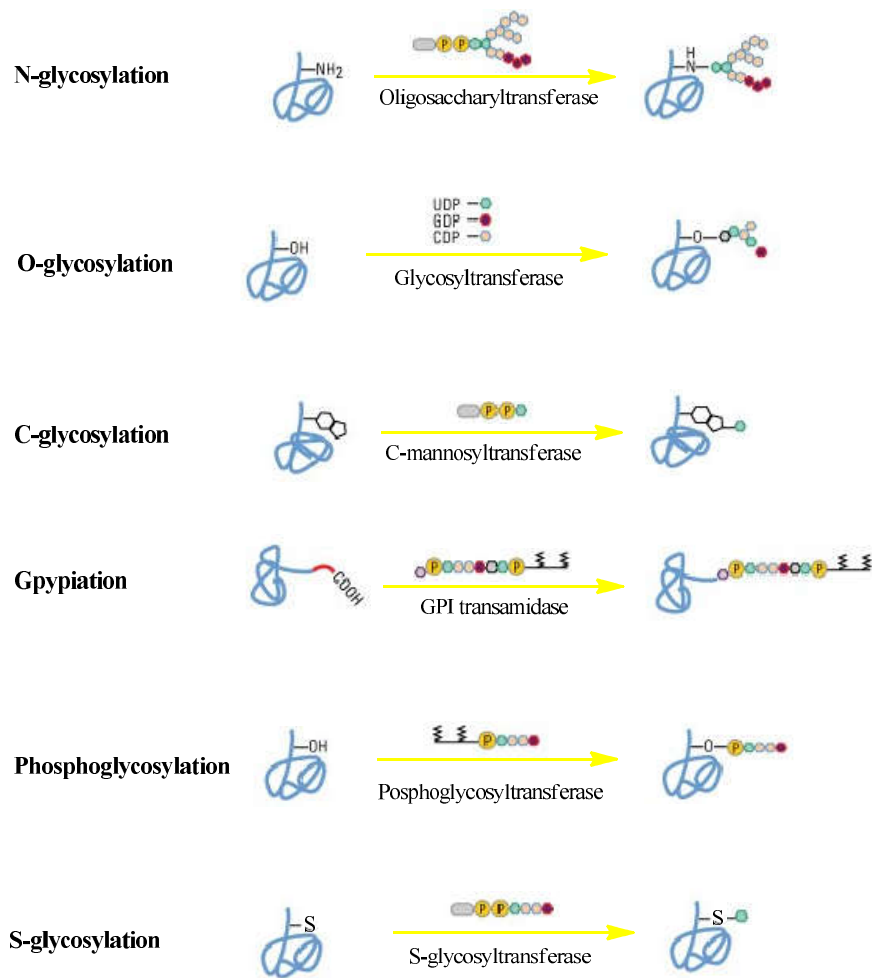


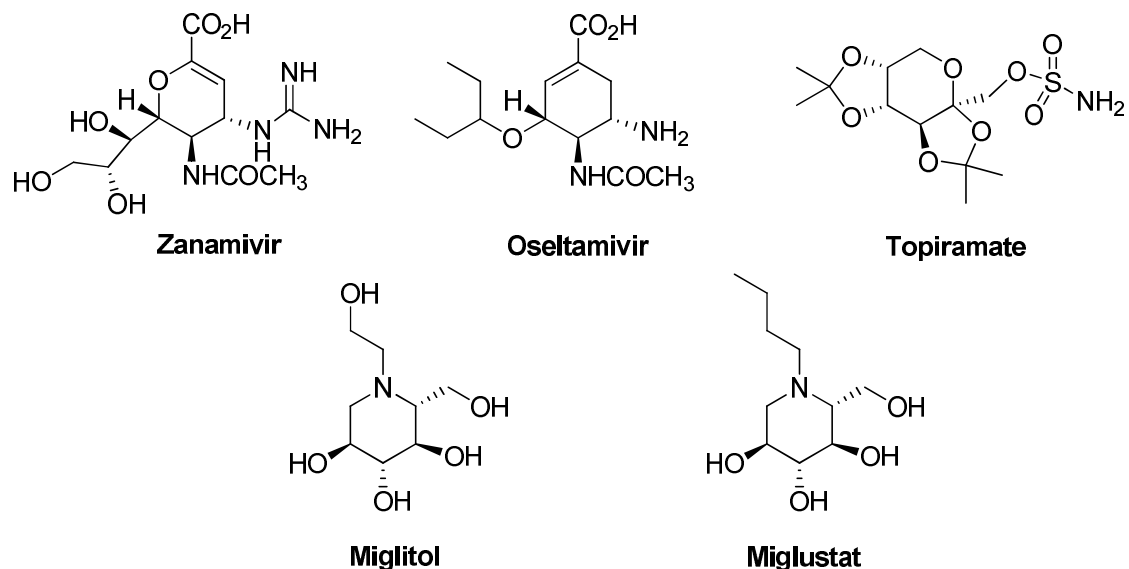
**Figure 1** - Types of protein glycosylation

After this process, further modifications can occur to the glycosylated proteins. These reactions generate a wide diversity of glycans that differ in the number and type of monosaccharide in their composition, including anomeric state, glycosidic linkage, branching, the presence of non-carbohydrate components (phosphorylation, sulfation, acetylation, etc.), and linkage to their aglycones (peptide, lipid, etc.) [4]. Such diversity leads the action control of several proteins in numerous essential biological functions, such as maturation, transport, secretion of glycoconjugates, and cell-cell or cell-virus recognition processes [5].

### 1.1 Glycosylation and diseases

Over 40 disorders have been reported in humans, where glycosylated proteins are implicated.

Therefore, glycosidase inhibitors can be the key to treat a variety of metabolic disorders and human diseases such as viral infections [6], type II diabetes [7], Gaucher disease [8], cancers [9], and asthma [10]. Popular examples are the commercial glycomimetic drugs: zanamivir (Relenza), and oseltamivir (Tamiflu) that are potent influenza virus inhibitors, miglustat (Zavesca) to treat Gaucher disease, miglitol (Glyset) is used in the treatment of diabetes, topiramate (Topamax) an anti-convulsant drug [11-13] (**Figure 2**), etc.

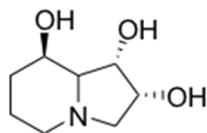


**Figure 2** - Glycomimetic drugs currently available in the market.

In what cancer disease concerns, several examples turn evident the key role that glycosylation plays in tumor formation and metastasis [14]. Specific examples include breast, colon, and skin cancer [15, 16]. Glycan's altered distribution has been associated with abnormalities in the *N*-glycosylation process. So, the respective enzymes are today promising drug targets with clinical potential in cancer treatment [17, 18]. One of these enzymes is Golgi  $\alpha$ -mannosidase II (GM II).

GM II is a key enzyme in the maturation of N-glycans and it is the first glycoside hydrolase in the Golgi pathway. For this reason, this enzyme is used as a target to treat many types of tumors [19].

Swainsonine (SWA), an indolizidine occurring naturally in several plants in Australia and North America, and was the first compound (1978) that demonstrated potential as anti-cancer with GM II as target [18, 20-23].

**Swainsonine**

Despite the success of this compound, it presented several secondary effects and toxicity that precluded its generalized use in cancer treatment. Taking this into account, during the last two decades many efforts have been conducted to synthesize new compounds based on SWA that could maintain their pharmacological potency, but at the same time decrease its associated toxicity.

In the following sections, it will be reviewed the structure of GM II enzyme, its catalytic mechanism, and discussed the different classes of compounds associated with the inhibitory activity of the enzyme. This will be done through an extensive analysis of the co-crystallized X-ray structures that are available in the Protein Databank (PDB) and the reported biological activities available in the literature.

## 2. Golgi $\alpha$ -mannosidase II

### 2.1 Structure of GM II

GM II is a Type II transmembrane protein, ~125 kDa in size (monomer), composed of a short *N*-terminal cytoplasmic tail, a single-span transmembrane domain connected by a stalk segment to a large luminal *C*-terminal catalytic portion [23-25].

According to Carbohydrate-Active Enzymes classification (CAZY), GM II is included as glycoside hydrolases family 38 (GH38). GH38 classification is based in the structure of the catalytic site and in the carbohydrate-binding modules (functional domains) [26-30].

Due to the involvement of human GM II in several diseases, and in particular in cancer, a great interest has been put in deciphering the X-ray structure of human GM II (hGM II). However, it has not been possible yet. Currently, only the X-ray structure of *Drosophila* GM II is available [24, 31]. This structure has a high similarity sequence to hGM II (41% identity, 61% similarity), comparable substrate specificity and kinetic properties, and the same inhibitor sensitivity. For this reason, this

enzyme has been used as a model of the hGM II, and throughout the manuscript discussions are referred to the *Drosophila* GM II enzyme.

GM II is a single compact entity composed of an *N*-terminal  $\alpha/\beta$ -domain, a three-helical bundle and a *C*-terminal three-helix bundle that are interconnected by five internal disulfide bonds. (**Figure 3**) The active site is located in a small cavity in the *N*-terminal  $\alpha/\beta$ -domain, formed primarily by acidic highly conserved amino acids in the neighborhood of zinc cation [24].

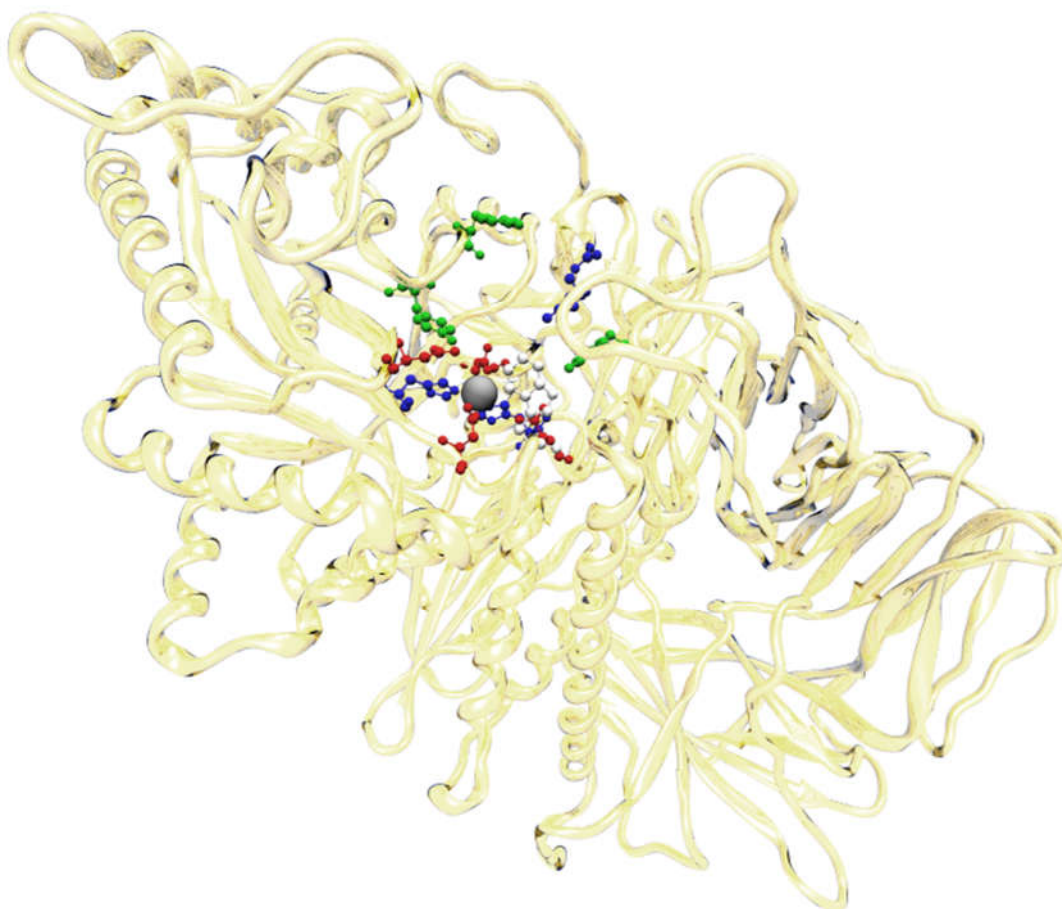


**Figure 3** - The three-dimension structure of GM II. The residues of the active site are highlighted in ball in stick representation.

The active site of GM II can be divided into three main regions: region A, B and C. (**Figure 4**) Region A is defined as the “Anchor Site” and assists the binding and orientation of the natural substrate for the hydrolytic reaction. The residues Tyr267, Trp299, His273, and Pro298 play a relevant role in this region [32]. Region B corresponds to the catalytic site and it is composed in

five fundamental residues: Tyr269, Asp341, Asp472, Trp95, and Tyr727. Region C is where the zinc ion is located and residues that are essential for its stabilization in the binding pocket, namely: Asp204, Asp92, His471, and His90.

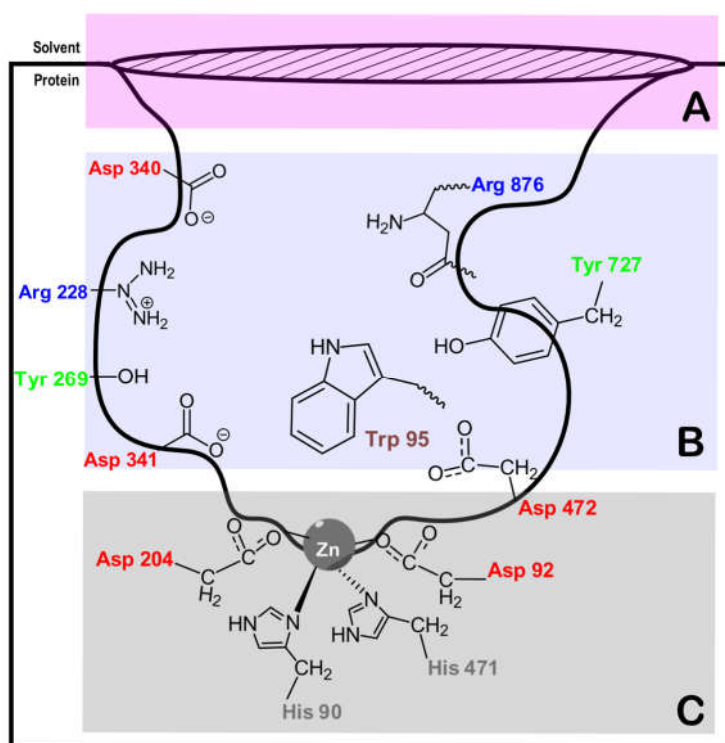


**Figure 4** - Representation of the region A, B, and C of the GM II binding pocket.

## 2.2 Catalytic mechanism of GM II

The catalytic mechanism of GM II was proposed for the first time by Kohlsland [33], in 1953. The hydrolysis of the interglycosidic bond was found to occur through a retaining type of mechanism involving the cleavage of  $\alpha(1-3)/\alpha(1-6)$ -mannoses linkages. The retaining mechanism of GH involves a covalently bound intermediate and thus retains the stereochemistry of the hydrolyzed sugar [34]. In *Drosophila melanogaster* GM II, the first step involves a proton transfer from Asp341 to the oxygen atom of the scissile glycosidic bond. Afterward, Asp204 acts as the nucleophile, attacking the carbon C1 atom to form a covalent intermediate with the protein. In the second step (deglycosylation), a water molecule attacks carbon C1 atom, breaking the covalent bond to finish the reaction and to regenerate the enzyme for the next catalytic round (**Figure 5**) [35].



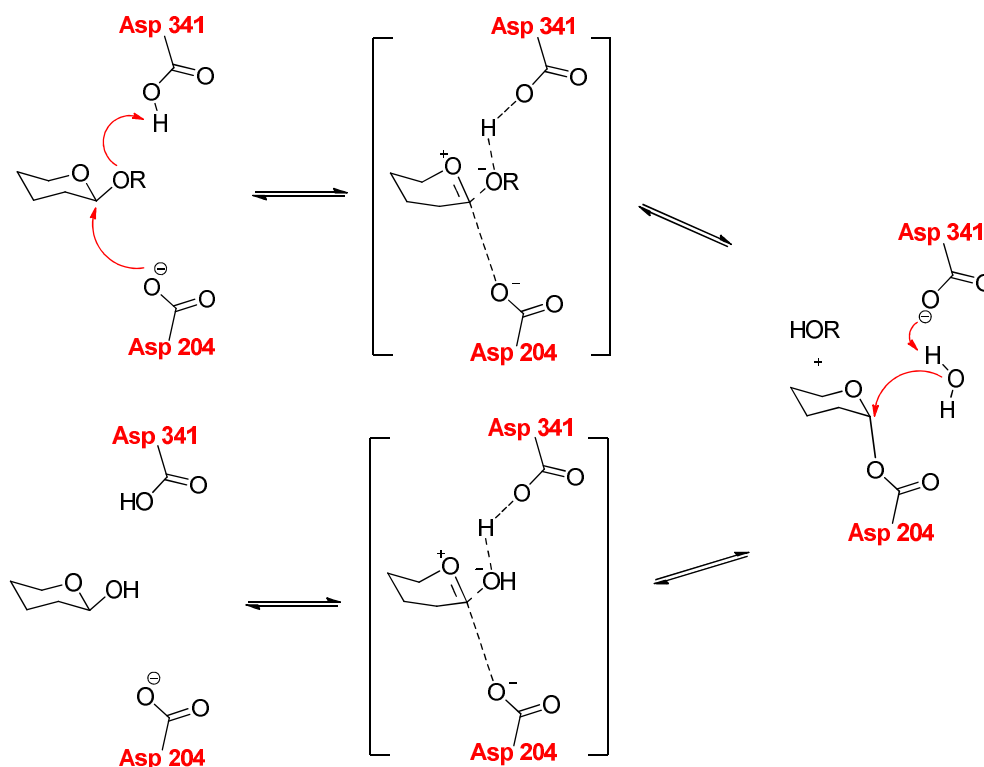


Figure 5 - Retaining mechanism of GM II

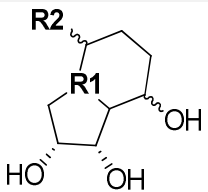
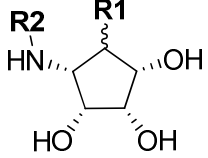
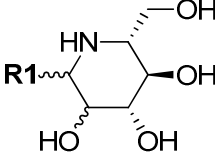
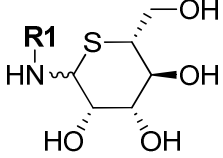
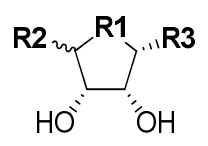
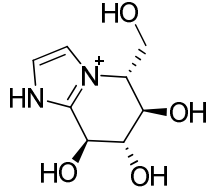
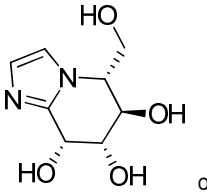
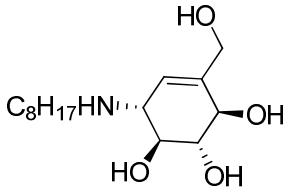
The GM II enzyme also contains a zinc cation in its binding site. The presence of the cations in the structure of GHs appears to be more common than it was initially imagined and are believed to be very important for the stabilization of the transition state's intermediates during catalysis. Several studies show that the  $Zn^{2+}$  ion in GM II is fundamental to coordinate the hydroxyl groups of the substrates, which stabilize the transition state entity, and so reduces the overall activation energy required for the reaction. It was also shown by computational studies that the zinc cation has a key role in lowering down the activation barrier of the rate-limiting step of the full process emphasizing its importance during the catalytic process [36].

### 2.3 Golgi Mannosidase inhibitors

During the last decades, various groups have synthesized many compounds aiming to make GM II inhibitors. Taking into consideration a large number of compounds that were found and to make the discussion clear, they were divided in six classes (A, B, C, D, E, and F), based on their main chemical scaffold (Table 1).

The compounds that were analyzed are the ones whose co-crystallized X-ray structures exist, and the biological activity ( $K_i$  or  $IC_{50}$ ) had been determined.

**Table 1:** Molecular scaffold of the GM II inhibitors

Class A	Class B	Class C	Class D
			
Indolizines (7 compounds)	MSN derivatives (8 compounds)	DMJ derivatives (3 compounds)	Thiopyrans (2 compounds)
Class E	Class others		
			
Pyrrolidine derivatives (10 compounds)	(3 compounds)		

In the following sections, the binding position of each inhibitor of each different class of compounds will be discussed in detail and their inhibitory activity discussed.

### 1.3.1 Class A

The scaffold of compounds of class A is derivative from indolizines. These structures closely resemble the structure of SWA.

SWA interferes with the glycosylation pathway by binding to GM II with inhibition constants of  $K_i = 3$  nM and  $IC_{50} = 37$  nM. In preliminary clinical trials in cancer patients at late stage, the specific inhibition of GM II, by administering orally SWA, resulted in reduced tumor growth and metastasis.

However, it also inhibits lysosomal  $\alpha$ -mannosidase II (LM II) which results in neurological damage, like the  $\alpha$ -mannosidosis disease [17, 18, 22, 23].

Facing the adverse side effects that preclude the use of SWA in patients, several compounds have been developed that share the SWA scaffold, namely the stereochemistry of carbon atoms attached to the alcohol functions in the five-membered ring (**Figure 6, Table 2**).

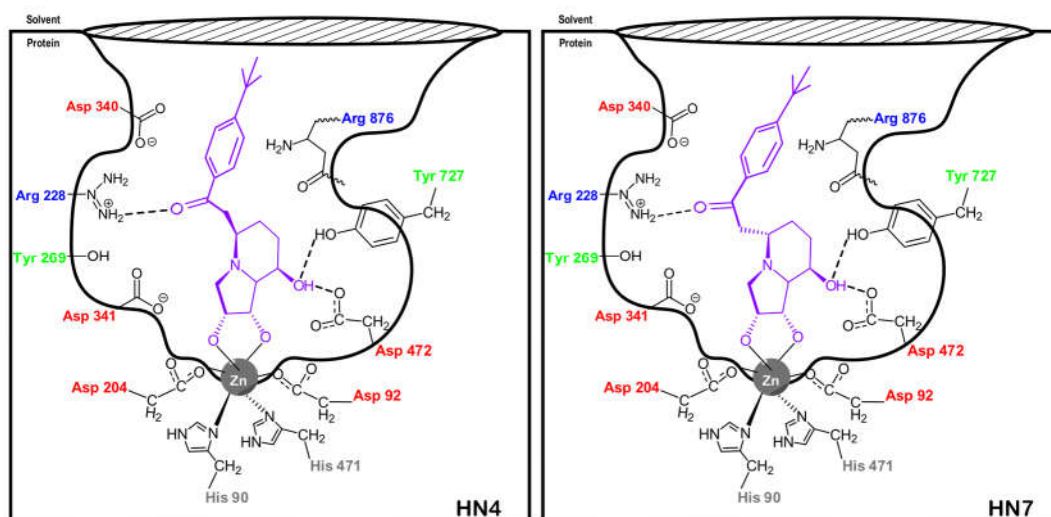


**Figure 6** - 2D Representation of the catalytic site with the inhibitor HN4 and HN7 of class A

From all the collected inhibitors, HN4 is the most promising inhibitor, and HN7 the one that showed the worst inhibitory activity.

Inhibitor NK1 is the closest structure to SWA. The only difference is the replacement of an N for S in the main scaffold. In spite of the similarities, this substitution precludes the coordination of the two hydroxyl groups to the Zn cation and changes completely the binding pose of the compound in active site with the loss of inhibitory activity.

The inhibitor activity of SWA, HN2, HN3, and HN4 are almost identical. The higher inhibitory activity seems to be related to the substituent R2 that allows an extra interaction with Arg228. The presence of bulky and hydrophobic groups at *para* position of the phenyl ring slightly improves the inhibitory activity of the HN compounds.

In compound HN5 it is observed a slight loss in the inhibitory activity (from 29nM to 44nM). This occurs due to the absence of the carbonyl group in compound HN5 missing the interaction with Arg228. The change of the stereochemistry in compound HN6 is not favored, because it loses

the interaction with Arg228, and displaces the phenyl ring to a different position in the binding pocket.

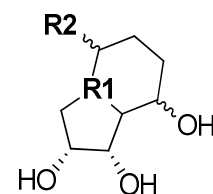


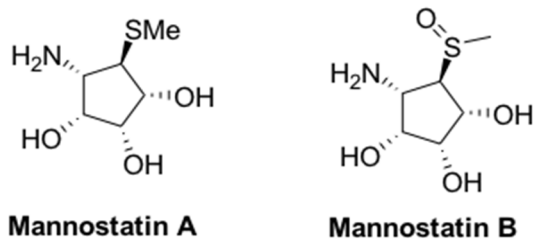
**Table 2:** Inhibitors of class A

NK1	HN2	HN3	HN4
IC <sub>50</sub> : 2.0x10 <sup>-9</sup> nM	K <sub>i</sub> : 2.8nM	K <sub>i</sub> : 2.7nM	IC <sub>50</sub> : 29nM, K <sub>i</sub> : 2.7nM
HN5	HN6	HN7	
IC <sub>50</sub> : 44nM	IC <sub>50</sub> : 250nM	IC <sub>50</sub> : 250nM	

Comparing the compound HN4 with HN7 the difference is the stereochemistry of the R2 substituent. This fact induces a very significant impact on inhibitor activity. From these results, we can conclude the stereochemistry in HN7 makes the hydrogens bonds with Asp472, Tyr727, Zn cation less efficient (1.86 Å, 1.83 Å, 2.18 Å, 2.20 Å respectively, *versus* 1.79 Å, 1.72 Å, 2.08 Å, 2.12 Å in HN4), except for Arg228 (2.27 Å *versus* 2.54 Å in HN4).

## 1.3.2 Class B

Class B contains the inhibitors that are analogues of Mannostatin A and B.



Mannostatin A and B were isolated from the soil microorganism *Streptovercillum verticillus*, during screening of culture broths for mannosidase inhibitors. They are the first non-azasugar type inhibitors to be discovered and some of the most potent inhibitors against  $\alpha$ -D-mannosidase prepared from epididymis of adult rats [37].

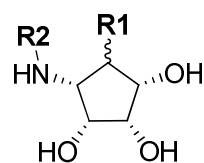
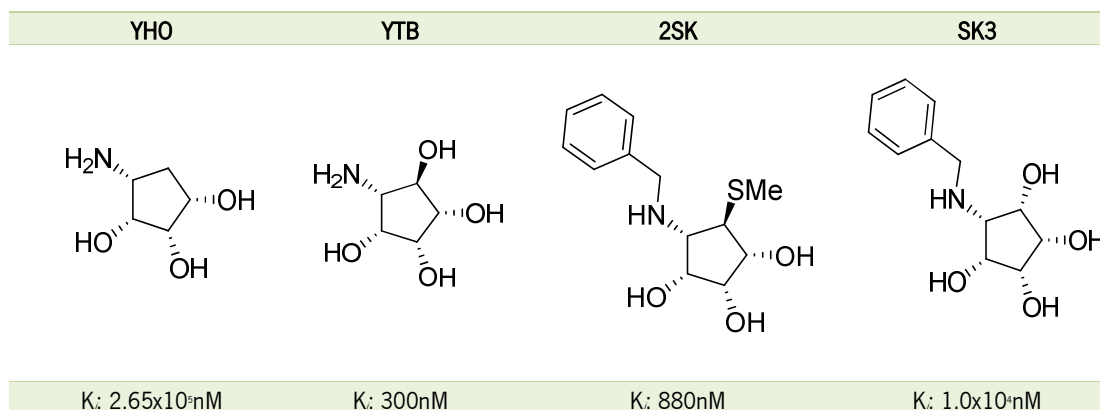


**Table 3:** Inhibitors of class B

AOL	GOO	MSN	MZB
K: 5.0x10 <sup>-10</sup> nM	K: 76nM	K: 36nM	K: 150nM



They are effective blockers of the processing of influenza viral hemagglutinin in cultured MDCK cells because they caused the accumulation of hybrid type proteins linked oligosaccharides, consistent with blocking the action of Golgi mannosidase II [38].

The binding pose of compounds from class B are very similar to each other (**Figure 7**) because they share the same stereochemistry, except in the R1 group (**Table 3**).

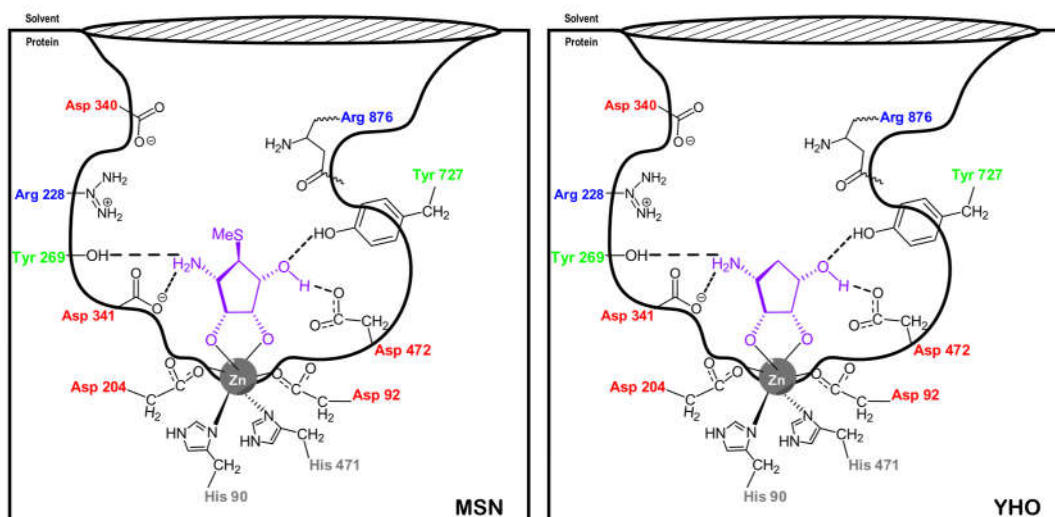


**Figure 7** - 2D Representation of the catalytic site with the inhibitors MSN and YHO of class B

All the compounds coordinate with the zinc cation through the two hydroxyl groups and interact by hydrogen bonds with Asp472, Tyr727, Asp341 and Tyr269 (around 2.23 Å, 2.18 Å, 1.76 Å, 1.88 Å, 2.77 Å, 2.23 Å, respectively).

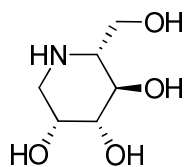
AOL and YTB structures have one difference only; that is the configuration of the carbon atom at R1. But its inhibitor activity difference is very different: AOL ( $5.0 \times 10^4$  nM), YTB (300 nM). The R1 when attached to the configuration *S*, carbon makes interactions with Asp204, but this interaction is not favorable. YTB with *R* configuration does not make such interaction and it is a much better inhibitor. In general, *R* configuration compounds do not make the unfavoured interaction with Asp204, because the substituent take a position in the center of the active site (with the exception of compound MZB).

From all the compounds that were analyzed from this class, the compound MSN (Mannostatin A) has the best inhibitor activity,  $K_i = 36$  nM. The main characteristic of this compound is the nature of R1, a thioether function. This group interacts very closely with the Phe206, Trp415, and Trp95 through hydrophobic interactions. Compounds with hydroxyl groups at this position (compounds AOL, YTB, and SK3) or hydrogen (compound YHI) are generally less potent.

Analysing the inhibitor activity power MSN *versus* 2SK compounds we can assure that the presence of a hydrophobic and bulky group at position R2 is not advantageous, because this group is facing towards a polar zone of the active site (Asp340, Ser268) and therefore a repulsive interaction follows with a substantial decreases in the inhibitory activity. Similar conclusions can also be drawn for compound SK3.

### 1.3.3 Class C

The scaffold of this class is based on 1-deoxymannojirimycin (DMJ,  $IC_{50} = 400$   $\mu$ M).



**Deoxymannojirimycin**

In 1979 [39], 1-deoxymannojirimycin (DMJ) has been isolated from *Lonchocarpus sericeus* and *L. costaricensis*. This compound has been found to be a selective inhibitor of rat liver Golgi  $\alpha$ -mannosidase I ( $IC_{50} = 1-2$   $\mu$ M), and a weak ER  $\alpha$ -mannosidase and Golgi  $\alpha$ -mannosidase II ( $IC_{50} =$

400  $\mu\text{M}$ ). To achieve Golgi  $\alpha$ -mannosidase II inhibition it is needed a high DMJ concentration [40-42] (Figure 8).

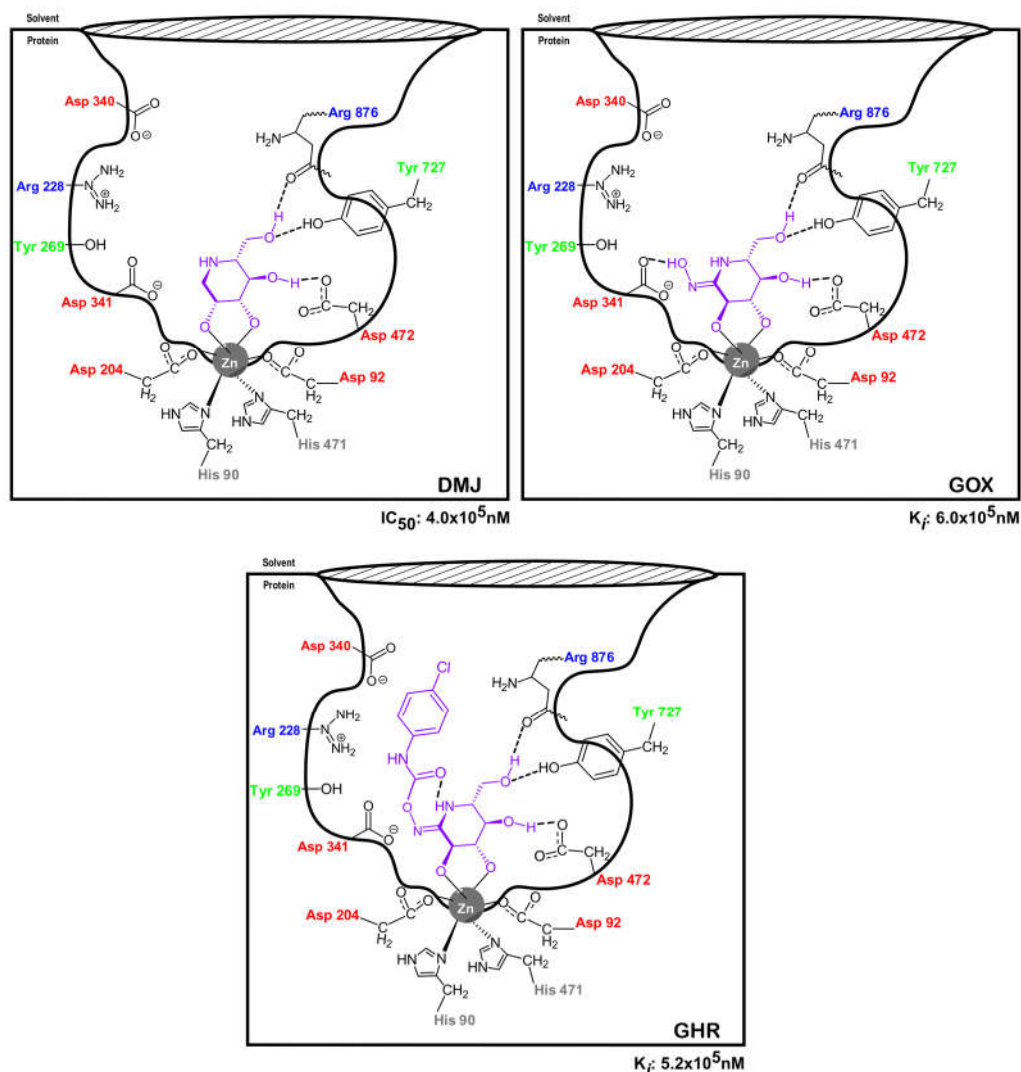


**Figure 8** - 2D Representation of the catalytic site of all inhibitors of class C, and its inhibitory activity.

All the compounds coordinate with the Zn cation through two hydroxyl groups and interact by hydrogen bonds with Arg876, Tyr727, and Asp472 (around 2.41 Å, 2.33 Å, 1.77 Å, 2.21 Å, 1.99 Å, respectively).

In general, all these compounds have low inhibitory activities. Analyzing the binding pose of DMJ and analogues represented in Figure 8, the low inhibitory activity can be correlated with the lack of interactions with the left region of the binding pocket. In the analogues, the different stereochemistry of hydroxyl groups turns the deficient the interaction to Zn cation, which is the main cause for the lack of activity (GOX and GHR). In these cases, the compound still coordinates



with the Zn cation, but the interaction is not so effective (around 2.41 Å, 2.33 Å, *versus* for example 1.79 Å, 1.72 Å, in HN4 from class A)

### 1.3.4 Class D

This class is very similar a class C. The difference is the replacement of a nitrogen atom for a sulphur atom, in the six-membered ring.

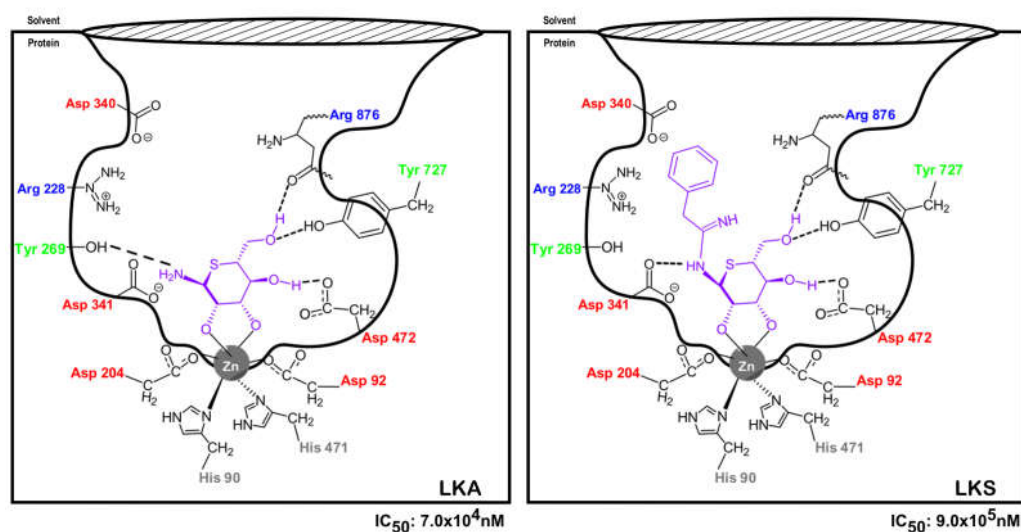


**Figure 9** - 2D Representation of the catalytic site of all inhibitors of class D, and its inhibitory activity.

Only two compounds exist in the class, but they are enough to show that the presence of the new ring does preclude an efficient coordination of the compound with the Zn cation. As occur in compounds of class A, B, C are formed two bonds with Zn cation, but the coordination is weaker in compounds of class C and D. In compounds of class D the coordination to Zn cation is around 2.23 Å, 2.22 Å *versus* for example 1.79 Å, 1.72 Å, in HN4 from class A. Are also observed interactions with Arg876, Tyr727, and Asp472, around 1.78 Å, 1.94 Å, 1.90 Å, respectively (**Figure 9**).

The better inhibitory activity of compounds LKA can be attributed to the extra hydrogen bond with Try269 (1.92Å). R1 Substituent in LKS is able to establish a hydrogen bond with the Asp341 (2.12 Å), but as the phenyl group extends to the polar region (Asp340), there is an overall negative impact.

## 1.3.5 Class E

The class E is composed of pyrrolidine derivatives, a 5-member cyclic normally with a secondary amine. In some compounds, the secondary amine was substituted by a sulphur atom, a selenium atom or by a tertiary amine (Table 6).

Table 4: Inhibitors of class E

GB1	GB2	GB3	GB6	GB7
K: $2.69 \times 10^{-9}$ nM IC <sub>50</sub> : $8.0 \times 10^{-9}$ nM	K: $2.99 \times 10^{-9}$ nM	IC <sub>50</sub> : $1.0 \times 10^{-9}$ nM	K: $2.2 \times 10^{-9}$ nM	K: $1.0 \times 10^{-9}$ nM

W72	SSD	SSE	GHA	BLT
IC <sub>50</sub> : $3.0 \times 10^{-5}$ nM	IC <sub>50</sub> : $\sim 7.5 \times 10^{-9}$ nM	IC <sub>50</sub> : $\sim 7.5 \times 10^{-9}$ nM	IC <sub>50</sub> : $\sim 7.5 \times 10^{-9}$ nM	IC <sub>50</sub> : $\sim 7.5 \times 10^{-9}$ nM

These inhibitors can be dividing into two sub-types based on the bonds they can make with the Zn cation (**Figure 10**). When compounds are capable to make two bonds with Zn cation, they establish hydrogen bonds with Asp340, Asp341, and Tyr269 (around 2.19 Å, 2.32 Å, 1.86 Å, 2.29 Å, 2.30 Å, respectively), except for GB2. The inhibitors with different stereocenter configurations in carbon attached to the hydroxyl groups establish only one bond with Zn cation and the hydrogen

bonds with Arg876, Tyr269, Tyr727 and Asp472 (around 2.15 Å, 1.84 Å, 1.72 Å, 1.74 Å, 1.69 Å, respectively).

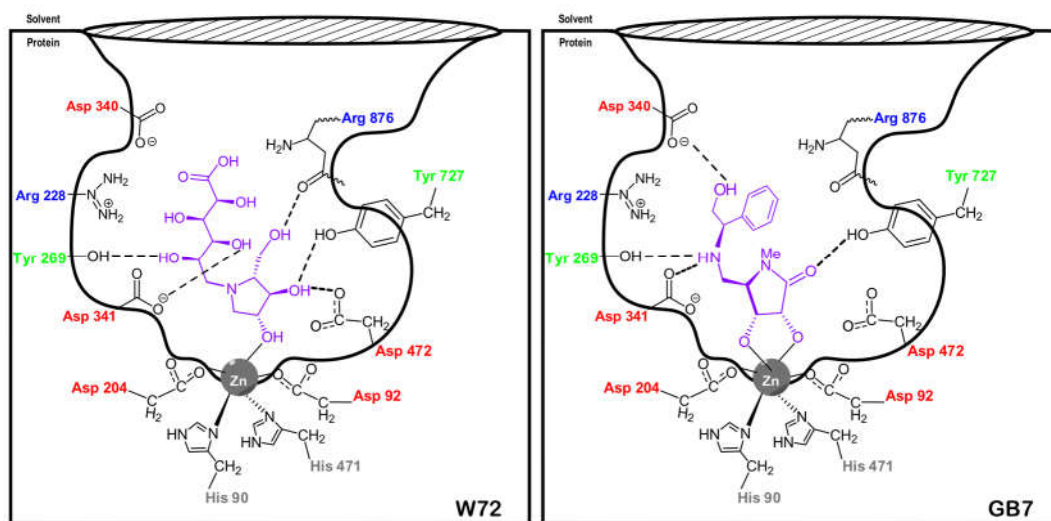


Figure 10 - 2D Representation of the catalytic site with the inhibitor W72 and GB7 of class E

The compounds that can coordinate with two bonds with the Zn cation are generally better inhibitors than the ones that only coordinate with one bond. This can be analyzed taking into account compounds W72 and GB7.

Among the compounds that can coordinate Zn cation with two bonds, the best inhibitor is GB7. Comparing with the other compounds of the same sub-class the differences in the inhibitory activity are related to the stereochemistry of the R2 group and the nature of the R1 group, and the presence/absence of a carbonyl group or methyl at position R3.

Analyzing the GB1 *versus* GB2 inhibitors, the difference in the stereocenter configuration of the secondary amino exocyclic group in R2 does not significantly impact the inhibitory activity of the compounds, although relative better inhibitory activity of GB1 can be attributed to the extra hydrogen bond that is established with Asp340.

Comparing compound GB3 with GB1 it is clear that the presence of a methyl group at R3 substantially decreases the inhibitory activity. This happens because this group becomes lodged in a polar pocket (Tyr727 and Asp472). When R3 substituent is a polar group, as the carbonyl in GB6, a hydrogen bond can be established with Tyr727 (2.00 Å), improving slightly the inhibitory activity.

The difference between GB6 and GB7 compounds is about the R1 group: NH *versus* NMe. The exchange of R1 group in GB6 (NH) for GB7 (NMe) turns the GB7 inhibitor 4.5 times more active than GB6 due to the vicinity of Phe206, Trp415, and Trp95.

The W72, SSD, GHA, SSE, and BLT compounds coordinate with only one bond with the Zn cation. All the compounds have similar inhibitory activities, except W72. The difference in the inhibitor activity between these compounds *versus* GB1 inhibitor makes clear the extreme importance of the two hydrogen bonds with zinc cation. W72 is able to make another hydrogen bond with Asp341 (2.13 Å); this justifies the improvement of inhibitory activity relatively to the others with one bond to Zn cation.

### 1.3.6 Other Classes

In this section were included all the compounds that do not fit in the previous classes. Although they have different scaffolds, they bind in the active site in a similar way. (**Figure 11**)

These compounds continue to coordinate with two bonds to the Zn cation and interact mainly with the right region of the active site, namely through hydrogen bonds with Arg876, Tyr727 and Asp472 (around 2.32 Å, 2.22 Å, 1.95 Å, 1.91 Å, 1.88 Å; respectively).

These compounds have many similarities with the ones from class C. However, these ones have better inhibitory activities. This is due to the presence of fused rings that occupy more efficiently the active site and promote closer interaction with the Zn cation (around 2.32 Å, 2.22 Å *versus* 2.41 Å, 2.33 Å in Class C).

The compounds GIM and OEV establish an extra interaction with the Asp341, nevertheless this interaction did not improve their inhibitory activity in relation to MVL. This happens because in MVL the carbon atoms bearing the hydroxyl groups have a favored stereochemistry, providing better coordination to the Zn cation. A similar effect was also observed in the compounds of class C.

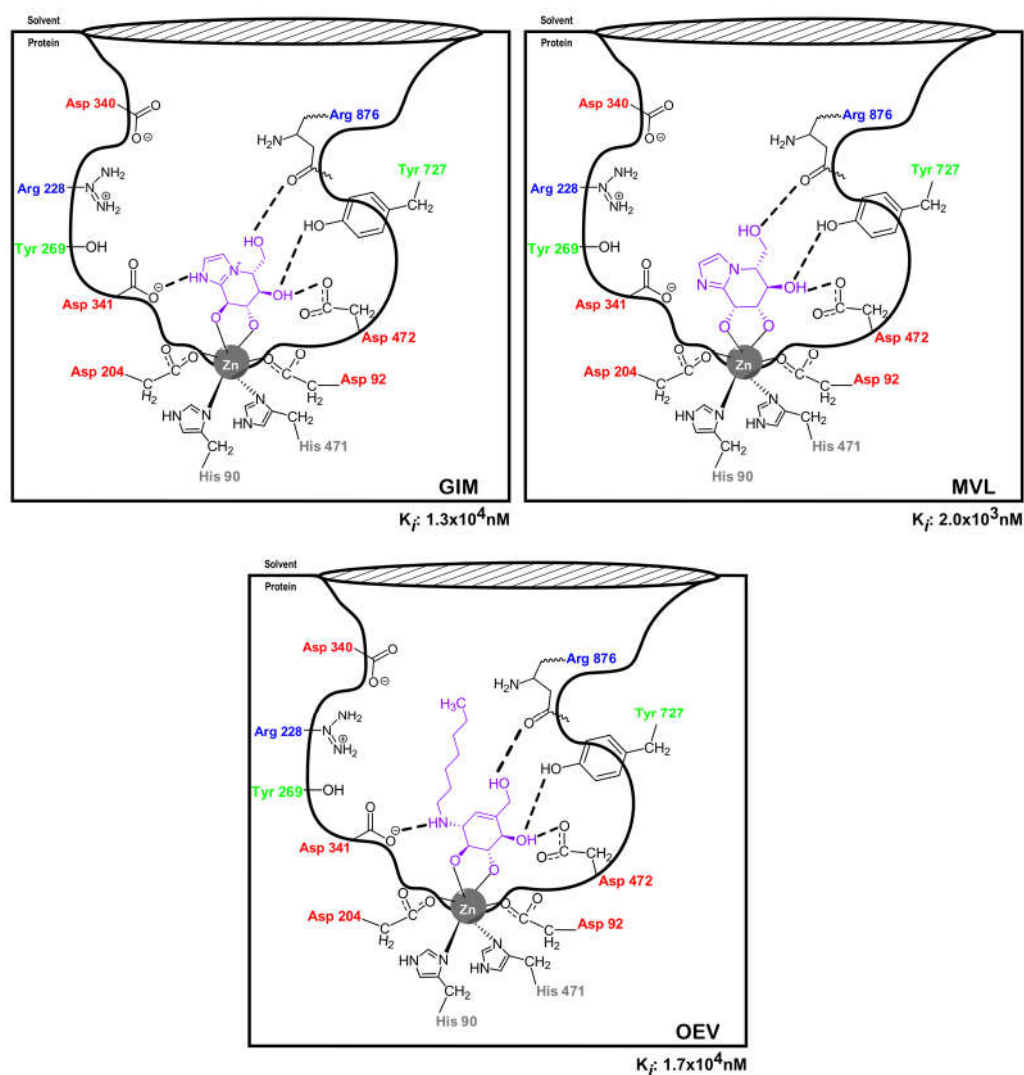


**Figure 11** - 2D Representation of the catalytic site of all inhibitors of other classes, and its inhibitory activity.

### 3. Pharmacophore model

Based on the analysis made in the previous sections involving more than 30 compounds, a pharmacophore model was set up to correlate their structure with the biological activity.

An important feature for the inhibitory activity of the compounds is the type of coordination that they establish with the Zn cation. The compounds that coordinate by two bonds with zinc are generally more potent (**Figure 12**- zone 1). This zone is part of the region C that serves as the anchor to all the inhibitors in the active site.

Region B is the one that provides the specificity and potency of the inhibitors in the active site. More interactions in this region generally improve the inhibitory activity of the compounds. From the analyzed data it is clear that the presence of fused rings that can fulfill the binding pocket tends to improve the binding affinity and therefore their inhibitory activity (Figure 12- zone 2). The compounds that interact more closely with the left side of the binding pocket (Figure 12- zone 3) are generally more active than the ones that just interact with the right region (Figure 12- zone 4).

Region A is the one that is closer to the solvent. All of the discussed inhibitors (if not the majority that are available in the literature) do not reach this region of the binding pocket. However, it is known that this region is an “Anchor Site” in the natural substrate. The natural substrate is a huge molecule allowing interactions with Try267, His273 (zone 5), Trp299 and Pro298 (zone 6) so improving the binding affinity, helping to orientate and accommodate the reactive region of the molecule in the binding site of the enzyme.

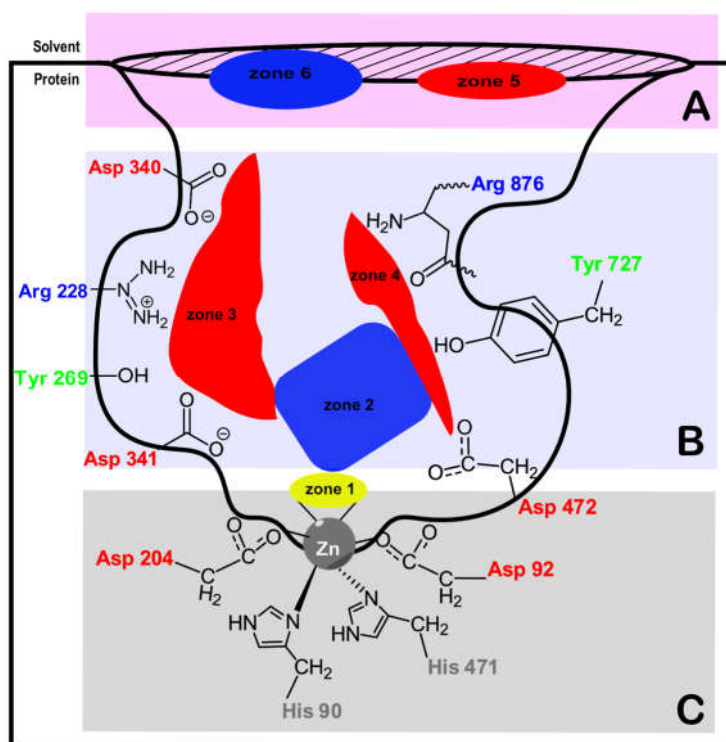


**Figure 12** - 2D Representation of the catalytic site with the essentials zones for improve the inhibitory activity.

Yellow: the Zn links region, Blue: apolar region, Red: polar region.

#### 4. References

1. Akmal, M.A.; Rasool, N.; and Khan, Y.D., Prediction of N-linked glycosylation sites using position relative features and statistical moments. *PLOS ONE*, **2017**. 12(8): p. e0181966.
2. Jayaprakash, N.G.; Surolia, A., Role of glycosylation in nucleating protein folding and stability. *Biochem J*. **2017**;474(14):2333-2347.
3. Ho, W-L.; Hsu, W-M.; Huang, M-C.; Kadomatsu, K.; Nakagawara, A., Protein glycosylation in cancers and its potential therapeutic applications in neuroblastoma. *J Hematol Oncol*. **2016**;9(1):100.
4. Werz, D.B.; Ranzinger, R.; Herget, S.; Adibekian, A.; Von der Lieth, C-W.; Seeberger, PH.; Exploring the Structural Diversity of Mammalian Carbohydrates ("Glycospace") by Statistical Databank Analysis. *ACS Chem Biol*. **2007**;2(10):685-691.
5. Varki, A., Biological roles of oligosaccharides: all of the theories are correct. *Glycobiology*. **1993**;3(2):97-130.
6. Dwek, RA., Glycobiology: Toward Understanding the Function of Sugars. *Chem Rev*. **1996**;96(2):683-720.
7. Bischoff, H., The mechanism of alpha-glucosidase inhibition in the management of diabetes. *Clin Invest Med*. **1995**;18(4):303-311.
8. Hruska, K.S.; et al., Gaucher disease: mutation and polymorphism spectrum in the glucocerebrosidase gene (GBA). *Hum Mutat*, **2008**. 29(5): p. 567-83.
9. Spearman, MA.; Ballon, BC.; Gerrard, JM.; Greenberg, AH.; Wright, JA., The inhibition of platelet aggregation of metastatic H-ras-transformed 10T12 fibroblasts with castanospermine, an N-linked glycoprotein processing inhibitor. *Cancer Lett*. **1991**;60(3):185-191.
10. Zhu, Z.; Zheng, T.; Homer, RJ.; et al., Acidic Mammalian Chitinase in Asthmatic Th2 Inflammation and IL-13 Pathway Activation. *Science (80- )*. **2004**;304(5677):1678-1682.
11. Maryanoff, B. E.; Nortey, S. O.; Gardocki, J. F.; Shank, R. P., Dodgson SP. Anticonvulsant O-alkyl sulfamates. 2,3:4,5-Bis-O-(1-methylethylidene)-beta-D-fructopyranose sulfamate and related compounds. *J Med Chem*. **1987**;30(5):880-887.
12. Nicotra, F.; Cipolla, L.; La Ferla, B.; et al., Carbohydrate scaffolds in chemical genetic studies. *J Biotechnol*. **2009**;144(3):234-241.
13. Hu, Min., Monosaccharide as a Central Scaffold Toward the Construction of Salicylate-Based Bidentate PTP1B Inhibitors via Click Chemistry. *Bulletin of the Korean Chemical Society*. **2011**; 32(3), 1000–1006.
14. Christiansen, M.N.; et al., Cell surface protein glycosylation in cancer. *Proteomics*, **2014**. 14(4-5): p. 525-46.
15. Yamashita, K.; Ohkura, T.; Tachibana, Y.; Takasaki, S.; Kobata, A., Comparative study of the oligosaccharides released from baby hamster kidney cells and their polyoma transformant by hydrazinolysis. *J Biol Chem*. **1984**;259(17):10834-10840.
16. Pierce, M.; Arango, J., Rous Sarcoma Virus-transformed Baby Hamster Kidney Cells Express Higher Levels of Asparagine-linked Tri- and Tetraantennary Glycopeptides Containing [GlcNAc-(1,6)Man- $\alpha$ (1,6)Man] and Poly-Nacetyllactosamine Sequences Than Baby Hamster Kidney Cells. *The Journal of Biological Chemistry*. **1986**;261(23):10772-10777.

17. Dennis, J. W.; Granovsky, M.; Warren, C. E., Glycoprotein glycosylation and cancer progression. *Biochim Biophys Acta*. **1999**;1473(1):21-34.
18. Goss, P. E.; Baker, M. A.; Carver, J. P.; Dennis, J. W., Inhibitors of carbohydrate processing: A new class of anticancer agents. *Clin Cancer Res*. **1995**;1(9):935-944.
19. Rose, D. R., Structure, mechanism and inhibition of Golgi  $\alpha$ -mannosidase II. *Curr Opin Struct Biol*. **2012**;22(5):558-562.
20. Dorling, P. R.; Huxtable, C. R.; Vogel, P., Lysosomal storage in swainsona spp. toxicosis: an induced mannosidosis. *Neuropathol Appl Neurobiol*. **1978**;4(4):285-295.
21. Dennis, J. W.; Laferte, S., Recognition of asparagine-linked oligosaccharides on murine tumor cells by natural killer cells. *Cancer Res*. **1985**;45(12):6034-6040.
22. Kiyohara, T.; Dennis, J. W.; Roder, J. C., Double restriction in NK cell recognition is linked to transmethylation and can be triggered by asparagine-linked oligosaccharides on tumor cells. *Cell Immunol*. **1987**;106(2):223-233.
23. Goss, P. E.; Reid, C.L.; Bailey, D.; Dennis, J. W., Phase IB clinical trial of the oligosaccharide processing inhibitor swainsonine in patients with advanced malignancies. *Clin Cancer Res*. **1997**;3(7):1077-1086.
24. Van den Elsen, J. M.; Kuntz, D. A.; Rose, D. R., Structure of Golgi alpha-mannosidase II: a target for inhibition of growth and metastasis of cancer cells. *EMBO J*. **2001**;20(12):3008-3017.
25. Moremen, K. W.; Touster, O., Biosynthesis and modification of Golgi mannosidase II in HeLa and 3T3 cells. *J Biol Chem*. **1985**;260(11):6654-6662.
26. Davies, G.; Henrissat, B., Structures and mechanisms of glycosyl hydrolases. *Structure*. **1995**;3(9):853-859.
27. Henrissat, B., A classification of glycosyl hydrolases based on amino acid sequence similarities. *Biochem J*. **1991**;280 ( Pt 2):309-316.
28. Henrissat, B.; Bairoch, A., New families in the classification of glycosyl hydrolases based on amino acid sequence similarities. *Biochem J*. **1993**;293 ( Pt 3)(Pt 3):781-788.
29. Henrissat, B.; Bairoch, A., Updating the sequence-based classification of glycosyl hydrolases. *Biochem J*. **1996**;316 ( Pt 2):695-696.
30. Henrissat, B.; Davies, G., Structural and sequence-based classification of glycoside hydrolases. *Curr Opin Struct Biol*. **1997**;7(5):637-644.
31. Rabouille, C.; Kuntz, D. A.; Lockyer, A.; et al., The Drosophila GMII gene encodes a Golgi alpha-mannosidase II. *J Cell Sci*. **1999**;112 ( Pt 19):3319-3330.
32. Shah, N.; Kuntz, D. A.; Rose, D. R., Golgi  $\alpha$ -mannosidase II cleaves two sugars sequentially in the same catalytic site. *Proc Natl Acad Sci*. **2008**;105(28):9570-9575.
33. Koshland, D. E., Stereochemistry and the mechanism of enzymatic reactions. *Biol Rev*. **1953**;28(4):416-436.
34. Venkatesan, M.; Kuntz, D. A.; Rose, D. R., Human lysosomal alpha-mannosidases exhibit different inhibition and metal binding properties. *Protein Sci*. **2009**;18(11):2242-2251.
35. Petersen, L.; Ardèvol, A.; Rovira, C.; Reilly, P. J., Molecular Mechanism of the Glycosylation Step Catalyzed by Golgi  $\alpha$ -Mannosidase II: A QM/MM Metadynamics Investigation. *J Am Chem Soc*. **2010**;132(24):8291-8300.



36. Cerqueira, N.; Brás, N.; Joo, M.; Alexandrino, P., Glycosidases – A Mechanistic Overview, Carbohydrates - Comprehensive Studies on Glycobiology and Glycotechnology. *InTechOpen*, **2012**.
37. Aoyagi, T.; Yamamoto, T.; Kojiri, K.; et al., Mannostatins A and B: new inhibitors of alpha-D-mannosidase, produced by *Streptovercillium verticillus* var. *quintum* ME3-AG3: taxonomy, production, isolation, physico-chemical properties and biological activities. *J Antibiot (Tokyo)*. **1989**;42(6):883-889.
38. Tropea, J. E.; Kaushal, G. P.; Pastuszak, I.; et al., Mannostatin A, a new glycoprotein-processing inhibitor. *Biochemistry*. **1990**;29(43):10062-10069.
39. Fellows, L. E.; Bell, E. A.; Lynn, D. G.; Pilkiewicz, F.; Miura, I.; Nakanishi, K., Isolation and structure of an unusual cyclic amino alditol from a legume. *J Chem Soc Chem Commun*. **1979**;0(22):977.
40. Bischoff, J.; Kornfeld, R., The effect of 1-deoxymannojirimycin on rat liver  $\alpha$ -mannosidases. *Biochem Biophys Res Commun*. **1984**;125(1):324-331.
41. Fuhrmann, U.; Bause, E.; Legler, G.; Ploegh, H., Novel mannosidase inhibitor blocking conversion of high mannose to complex oligosaccharides. *Nature*. **1984**;307(5953):755-758.
42. Hardick, D. J.; Hutchinson, D. W.; Trew, S. J.; Wellington, E. M. H., Glucose is a Precursor of 1-deoxynojirimycin and 1-deoxymannonojirimycin in *Streptomyces subutilus*. *Tetrahedron*. **1992**;48(30):6285-6296.

# 3

Computational Methods to Study Reaction  
Mechanisms

## 1. Quantum Mechanics

Quantum mechanics began in the early 20th century and was developed in successive stages by several physicists: Plank, Einstein, Bohr, de Broglie, Heisenberg, Schrödinger, Born, Von Neumann, Pauli, and Dirac.

This theory describes the behavior of atomic and subatomic objects (like electrons, photons, and particles in general), and this is fundamental to our understanding of all the fundamental forces of nature except gravity [1].

The fundamental postulates of quantum mechanics [2] assert that the state of a quantum mechanical system is completely specified by a wavefunction. This wavefunction is in the most general sense dependent on time and space. Like an experiment in the lab that is used to measure the value of an observable, in the quantum mechanics it is used a specific operator on the wavefunction to gather a property of a molecular system. For example, if we want to measure the energy of the system, we can use the Hamiltonian operator, from which results the time-independent Schrödinger equation that governs the time evolution of a quantum mechanical system:

$$\hat{H}\Psi(r) = E\Psi(r)$$

**Equation 1** - Time-independent Schrödinger equation

$\hat{H}$  is the Hamiltonian quantum operator;  $\Psi(r)$  is the wave function with respect to the position ( $r$ ) and  $E$  is the energy of the system.

The concept of an operator is important in quantum mechanics, and it is used to get information about system properties from the wave function. The operator application to eigenfunction results in a wave function multiplied by the correspondent eigenvalue [3]. An eigenfunction is a set of functions independent of each other that are a solution to a differential equation. An eigenvalue is defined as being the set of values of a certain parameter for a differential equation that has a nonzero solution under some known conditions. The measurable parameter in a physical system is a quantum mechanical operator, and the operator associated with the system energy is called the Hamiltonian ( $\hat{H}$ ).

## 1.1 Schrödinger Equation

The Schrödinger equation is the basis of Quantum mechanics [3]. However, the exact solutions to the Schrödinger equation is not possible to obtain due to the mathematical complexity. Therefore, several approximations and assumptions were postulated.

## 1.2 The Variational Principle

The variational principle is an approximation aiming to solve the Schrödinger equation. It uses an arbitrary wave function able to describe the electronic and nuclear coordinates appropriately.

This principle states that an approximate wave function has an energy that is above or equal to the exact energy. According to this principle, several arbitrary wave functions are tested to reveal which ones have the lowest value. The lower is the value of the variational integral and closer will be the value of the real one. Consequently, the most accurate one will be the wave function that will provide a better description of the closely “true” wave function. Taking this into account, we do not need to construct the wave function using a linear combination of orthonormal wave functions. Instead, any random wave function could be built and tested [1].

## 1.3 Born-Oppenheimer Approximation

The Born–Oppenheimer approximation assumes that the nuclei are infinitely heavier than the electrons. This approximation thus postulates that the motion of atomic nuclei and electrons can be separated into two terms that reflect two different wave functions, as illustrated in Equation 2 [1].

$$\Psi_{total} = \Psi_{nuclear} \times \Psi_{electronic}$$

**Equation 2** - General Born-Oppenheimer approximation equation

Then, we could apply this approximation in the Hamiltonian calculation and the Hamiltonian operator can be divided into electronic Hamiltonian ( $\hat{H}_{electronic}$ ) and nuclear Hamiltonian ( $\hat{H}_{nuclear}$ ). (Equation 3)

$$\hat{H}_{total} = \hat{H}_{nuclear} + \hat{H}_{electronic}$$

**Equation 3** - The Born-Oppenheimer approximation in a Hamiltonian form

### 1.3.1 Electronic Hamiltonian

The electronic Hamiltonian is calculated with nuclei positions fixed, considering kinetic energy of each electron under the nuclei force field ( $\hat{T}_e$ ), the potential energy involved in the electron's repulsion ( $\hat{V}_{ee}$ ) and the attraction between nuclei and electrons ( $\hat{V}_{ne}$ ). (Equation 4)

$$\hat{H}_{electronic} = \hat{T}_e + \hat{V}_{ee} + \hat{V}_{ne}$$

**Equation 4** - Electronic Hamiltonian following the Born-Oppenheimer approximation

Since the electronic energy is difficult to calculate, several methodologies are used to try to calculate it. There are the wave function-based methodologies, such as the Hartree Fock, semi-empirical and post-Hartree-Fock methods. Moreover, there is the Density-Functional Theory (DFT) based methods which are the ones that will be focused on this work.

#### 1.3.1.1 Density Functional Theory

The Density Functional Theory (DFT) is a theoretical approach that predicts the electronic structure, and properties of atoms and molecules, using the electronic density [3]. This approach has the advantage of being less complex than the wave function (WF) based methodologies. WF increases the complexity exponentially with the number of electrons, whereas the density of electrons has the same number of variables, but it is not so expensive.

DFT is another young methodology when compared to the wave function theory. It started to be developed in 1950, but only in the late 60s, it was only possible to use this methodology in quantum chemistry when Hohenberg and Kohn in 1964 proved two critical theorems for DFT [3].

The first theorem states that in a non-degenerated system, the ground-state energy could be

solely defined by the electron density [4]. That is, any property can be written as a functional of the electronic state density ( $\rho(r)$ ) of the fundamental state. Hohenberg and Kohn showed that it is possible to obtain the external potential (nuclei position) from the electronic density. Having knowledge of the external potential ( $v(r)$ ) and the number of electrons (which can be obtained from the derivation of the electron density), it is possible to obtain the Hamiltonian ( $\widehat{H}$ ) and consequently the wave function ( $\Psi$ ). (Equation 5)

$$\rho(r) \rightarrow v(r) \rightarrow \widehat{H} \rightarrow \Psi$$

**Equation 5** - The Hohenberg–Kohn Existence Theorem

The second theorem, the Hohenberg-Kohn variational theorem, proved that the electron density obeys a variational principle. Therefore, the density that minimizes the total energy is the exact or close to the ground state density.

However, the excellent assumptions of these two theorems doesn't predict how to achieve the system's energy calculation recurring to the density function.

In order to solve this problem, Kohn and Sham in 1965 proposed the Kohn-Sham Self-Consistent Field (SCF). It consists in using a fictitious reference system, a hypothetical system where the electrons do not interact with each other, whose Hamiltonian could be given by the sum of mono-electronic operators. So, the kinetic energy is just the sum of the individual electronic kinetic energies and the exchange-correlation term ( $E_{xc}[\rho(r)]$ ). The  $E_{xc}[\rho(r)]$  allows minimizing the difference in kinetic energy between the fictitious non-interacting system and the real system. Thus, equation 6 represents the orbital expression for the density:

$$E[\rho(r)] = \sum_{i=1}^N \left( \langle X_i | -\frac{1}{2} \nabla^2 | X_i \rangle - \langle X_i | \sum_{a=1}^M \frac{Z_k}{|r_i - r_k|} | X_i \rangle \right) + \sum_{i=1}^N \left( \langle X_i | \frac{1}{2} \int \frac{\rho(r_j)}{|r_i - r_{kj}|} dr_j | X_i \rangle \right) + E_{xc}[\rho(r)]$$

**Equation 6** - Energy calculation considering orbitals

where N is the number of electrons and M is the number of nuclei and electronic density is given by

$$\rho = \sum_{i=1}^N \langle X_i | X_i \rangle$$

To obtain a good exchange-correlation energy approximation were developed different functionals: local density approximation (LDA), approximation of local spin density (LSDA), approximation of the generalized gradient (GGA), and the hybrid methods.

The LDA is the simplest functional, and the electronic density is treated as a uniform distribution of electrons, like a uniform electron gas. This functional presents good results for systems containing metals, but it is inefficient for systems containing many different molecules because LDA requires a well-defined electronic density. Later, LSDA functional emerge and is related to LDA, but includes spin polarization. Another functional is the GGA approximation, its gradient to fulfill a maximum number of exact relations which are based on LSDA with the addition of a gradient-dependent term. The hybrid methods take advantage of the best from LDA and GGA with a Hartree-Fock exchange term.

The hybrid functional most used in computational chemistry is B3LYP, it combines Becke's three parameters functional (B3) and Lee-Yang-Parr correlation functional (LYP) with Hartree-Fock term contribution (about 20%). The exchange-correlation energy calculated through the B3LYP functional follows Equation 7.

$$E_{xc}^{B3LYP} = (1 - a)E_x^{LSDA} + aE_x^{HF} + b\Delta E_x^B + (1 - c)E_c^{LSDA} + cE_c^{LYP}$$

**Equation 7** - B3LYP exchange-correlation energy calculation

*a*, *b* and *c* are empirical parameters determined by Becke

This functional provides the best results compared to the other exchange-correlation functionals, and the free energy calculation error is about 3 kcal.mol<sup>-1</sup>.

### 1.3.1.2 Basis Sets

A basis set in theoretical and computational chemistry is a set of functions that are used to describe and characterize the electronic wave function or density-wave functional.

The more complex the basis is to describe the wave function, the more accurate the prediction is. But it has a high computational cost, so it is necessary to choose well between precision and computational cost in each case. The basis set must be able to describe the real wave function or

electron density and generate useful chemical results. Furthermore, those sets should offer a simple way to solve the exchange-correlation functionals without an excessive computational cost. There are two types of basis functions commonly used in electronic structure calculations: Slater Type Orbitals (STO) and Gaussian Type Orbitals (GTO) [1].

The STO functions depend exponentially on the distance between the nucleus and electron and accurately reflect the orbital of the hydrogen atom. However, the use of this function is only possible in small systems due to the significant computational cost.

Boys, in 1950, proposed an alternative to the use of STOs, the functions of the GTO. These functions have the advantage of being less computationally demanding but they have the disadvantage of not describing correctly the behaviour of the electrons, near the nucleus.

The GTO inaccuracies can be solved to some extent by forming STOs using a linear combination of GTO's, the contracted Gaussian functions (CGTO). The CGTO functions improve the description of the electrons near the atomic nucleus, improving the results with reduced computational cost.

There are many different contracted basis sets available in the literature or built into programs, and the average user usually only needs to select a suitable quality basis sets for the calculation [1].

Later, Pople introduced the split-valence basis concept where the core orbitals are treated under a certain scheme of Gaussian primitives, whereas the valence orbitals are treated using two or three different schemes of Gaussian contraction. A nomenclature method was also suggested to describe this method: n-abcG. n represents the number of primitives used to contract GTO of the core orbitals, and the abc represents the division and the treatment assigned to the valence orbitals. For example, a common basis set 6-31G is characterized by six primitive GTOs for the core orbitals and the valence orbitals are divided into two from which the innermost is described through three primitive GTOs and the external ones use only one.

However, CGTO functions fails in the description of molecular mechanism since they are not polarized neither have diffuse functions. To solve this issue, the CGTO functions were combined with polarization and diffusion functions to represent the intermolecular interactions.

Diffuse basis functions are extra basis functions (usually of s-type or p-type) that are added to



the basis set to represent very broad electron distributions. The use of diffuse functions in a Pople basis set is indicated by the notation + or ++. The + notation, as in 6-31+G(d), means that one set of sp-type diffuse basis functions is added to non-hydrogen atoms (4 diffuse basis functions per atom). The ++ notation, as in 6-31++G(d), means that one set of sp-type diffuse functions is added to each non-hydrogen atom and one s-type diffuse function is added to hydrogen atoms.

Another way to increase the size of the basis set in order to get closer to the exact electronic energy and wavefunction is to include polarization functions in the basis set. A polarization function is any higher angular momentum orbital used in a basis set that is not normally occupied in the separated atom. Polarization functions are not thought to be formally fully occupied in molecules. They are included solely to improve the flexibility of the basis set, particularly to better represent electron density in bonding regions [5]. The electron distribution about an atom does not remain spherically symmetric as the two atoms approach each other. One way to represent this effect is by adding a set of orbitals d denoted by \* or (d) or adding a set of orbitals to hydrogen and a set of orbitals of the heavy atoms denoted by \*\* or (d, p).

The basis functions have been optimized for the various types of atoms and therefore should be selected with concern so that correct results are obtained. In **table 1** we have the various basis sets available in gaussian 09 and the field of action of each one of them.

**Table 1:** The basis sets available by gaussian 09 [6]

Basis set	Applies to	Polarization functions	Diffuse functions
3-21G	H-Xe		+
6-21G	H-Cl	* or **	
4-31G	H-Ne	* or **	
6-31G	H-Kr	<i>through (3df,3pd)</i>	+,++
6-311G	H-Kr	<i>through (3df,3pd)</i>	+,++
D95	H-Cl <i>except Na and Mg</i>	<i>through (3df,3pd)</i>	+,++
D95V	H-Ne	(d) or (d,p)	+,++
SHC	H-Cl	*	
CEP-4G	H-Rn	* ( <i>Li-Ar only</i> )	
CEP-31G	H-Rn	* ( <i>Li-Ar only</i> )	

CEP-121G	H-Rn	<i>* (Li-Ar only)</i>	
LANL2MB	H-La, Hf-Bi		
LANL2DZ	H, Li-La, Hf-Bi		
SDD, SDDALL	<i>all but Fr and Ra</i>		
CC-PVDZ	H-Ar, Ca-Kr	<i>predefined</i>	<i>added</i> <i>via AUG- prefix (H-Ar, Sc-Kr)</i>
CC-PVTZ	H-Ar, Ca-Kr	<i>predefined</i>	<i>added</i> <i>via AUG- prefix (H-Ar, Sc-Kr)</i>
CC-PVQZ	H-Ar, Ca-Kr	<i>predefined</i>	<i>added</i> <i>via AUG- prefix (H-Ar, Sc-Kr)</i>
CC-PV5Z	H-Ar, Ca-Kr	<i>predefined</i>	<i>added</i> <i>via AUG- prefix (H-Na, Al-Ar Sc-Kr)</i>
CC-PV6Z	H, B-Ne	<i>predefined</i>	<i>added</i> <i>via AUG- prefix (H, B-O)</i>
SV	H-Kr		
SVP	H-Kr	<i>predefined</i>	
TZV AND TZVP	H-Kr	<i>predefined</i>	
QZVP AND DEF2*	H-La, Hf-Rn	<i>predefined</i>	
MIDIX	H, C-F, S-Cl, I, Br	<i>predefined</i>	
EPR-II, EPR-III	H, B, C, N, O, F	<i>predefined</i>	
UGBS	H-Cn	<b>UGBS(1,2,3)P</b>	<b>+,++,2+,2++</b>
MTSMALL	H-Ar		
DGDZVP	H-Xe		
DGDZVP2	H-F, Al-Ar, Sc-Zn		
DGTZVP	H, C-F, Al-Ar		
CBSB7	H-Kr	<i>predefined</i>	<b>+,++</b>

### 1.3.2 Nuclear Hamiltonian

Nuclear Hamiltonian is important for the calculation of free activation and free reaction energies, since even the smallest effect of the nuclear movement on global free energy can cause divergence

between experimental and theoretical data. Based on the Born-Oppenheimer approximation, the nuclear Hamiltonian can be described by:

$$\hat{H}_{nuclear} = \hat{T}_n + \hat{V}_{n-n}$$

**Equation 8** - Nuclear Hamiltonian following the Born-Oppenheimer approximation

The nuclear motion is not null, even at 0 K, and the internal energy of the system is given by the electronic energy added to the zero-point energy (ZPE). ZPE is the lowest possible energy that a physical system can have in the ground state.

The nuclear Hamiltonian can be expressed, as can be demonstrated by empirical approximations, in energy and it is often calculated classically by the sum of translational energy ( $E_{translational}$ ), rotational energy ( $E_{rotational}$ ) and vibrational energy ( $E_{vibrational}$ ) at a certain temperature and pressure. (Equation 9)

$$E_{nuclear} = E_{translational} + E_{rotational} + E_{vibrational}$$

**Equation 9** - The nuclear Hamiltonian in terms energetics

The translational part is often approximated with a particle in a box model. The rotational part can be calculated based on a rigid rotor model and the vibrational part can be written as a system of harmonic oscillators. The vibrational frequency calculations provide the magnitudes of vibrational frequencies for each vibrational mode of a molecule [7]. The analysis of the normal mode of vibrational energies gives the values of all frequencies in the system.

The TS has only one imaginary frequency, while P and R have only positive frequencies. The imaginary frequency must have the atoms that are associated with the reaction coordinate in the TS.

The frequency calculation is used to obtain the  $\Delta H$  energy based on the energy that was calculated with the electronic Hamiltonian and based on the approximation of an ideal gas model. The frequency calculations are also used to calculate the entropy of a system. This value can then be added to the enthalpy energy, that is calculated from the electronic Hamiltonian, in order to obtain the Gibbs free energy ( $\Delta G = H - TS$ ). The entropy is calculated assuming that only the fundamental electronic state is occupied and, therefore, the electronic entropy of nondegenerate

systems is zero. Then, the entropy is computed only considering the translational, rotational and vibrational contributions of the nuclei, using several approximations. Generally, the entropic contributions are only calculated at stationary points, such as reagent (R), transition state (TS), or product (P).

### 1.4 Continuum Solvation Models

It has been known for centuries that; the solvent may affect the properties of chemical substances. However, it was only in the second half of 19th century, with the rise of the atomistic theory of matter, when people started to understand how the effect of the solvent affects the chemical reactions.

Nowadays, it is known that solvent can play a relevant role and affect the structure, energies, spectra and other properties of solute. Therefore, it must be considered in Computational Chemistry when we are modeling chemical reactions.

There are several approaches in Computational Chemistry to treat the solvent: the explicit model or an implicit model.

In our case, we use the implicit continuum solvation models. This approach considers the solvent as a uniform medium characterized by some macroscopic properties, like the dielectric constant. However, in cases where the solvent is required for the reaction to occur, the solvent molecules have been put explicitly.

The Polarizable Continuum Model (PCM), originally formulated in 1981 by Miertus et al.[8], it is the most used method in implicit model calculations with the integral equation formalism variant (IEFPCM).

PCM has been implemented in three different versions, called Dielectric (D-PCM), Conductor (C-PCM) and Integral Equation Formalism (IEFPCM).

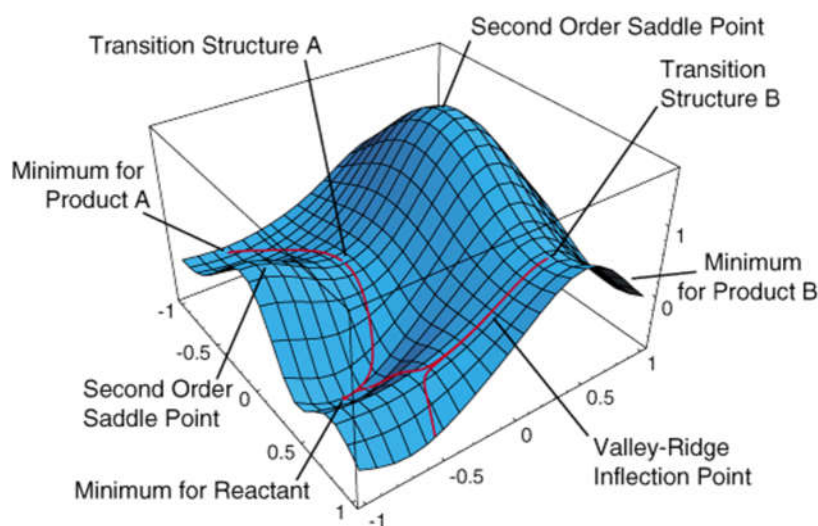
In all PCM versions, the cavity is defined as the envelope of spheres placed around atoms or atomic groups: other spheres, not centered on solute atoms, are automatically added to mimic the so-called solvent excluding surface, i.e., the surface touched by the solvent, described as a sphere

rolling on the solute. These cavities allow one to calculate solvation free energies with average errors lower than  $0.2 \text{ kcal.mol}^{-1}$  for neutral solutes and around  $1 \text{ kcal.mol}^{-1}$  for charged solutes [9].

In the variant IEFPCM, the solvent is described as a polarizable infinite dielectric and potentially extended to anisotropic liquids and ionic solutions.

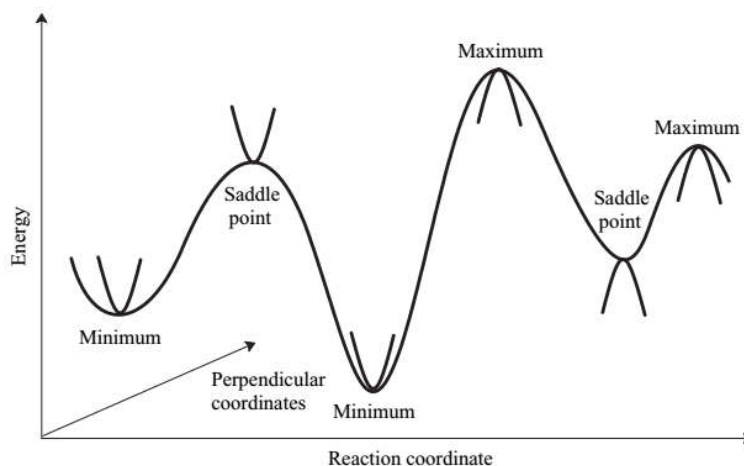
### 1.5 Potential Energy Surface (PES)

The concept of a potential energy surface (PES) is one of the most important aspects in chemistry. It plays a fundamental role in chemical kinetics, spectroscopy, and in the study of bulk properties of matter. PES provides a correlation (mathematical and graphical) between the energy of a system and its geometry. (Graphic 1)



**Graphic 1:** The energy of a system in function of two reactional coordinates, an example of 3D PES[10]

Chemical reactions and conformational changes correspond to paths between the minima of energy on PES's. The stationary points or minimum represents reactants and products or different conformation of these chemical species. The transition states are also stationary points but are represented by first-order saddle points. (Graphic 2)



**Graphic 2:** Illustrating a multidimensional energy surface [1]

The reactants and products of one reaction are easily located by current optimization techniques, with all forces (first and second derivatives equal to 0) of the energy, with respect to the spatial coordinates equal to zero. On the other hand, the localization of saddle points is usually a difficult task and constitutes the main problem in applying the transition-state theory to chemical reactions.

TS should be a maximum (point of highest energy, the negative second derivative) that connects the R and P, but still a minimum on the PES (first derivative equal to 0). So, it is good practice to identify the minima that are truly connected with the transition state, by performing the calculations along a reaction coordinate. One particular choice is the intrinsic reaction coordinate (IRC), defined as the minimum energy reaction pathway in mass-weighted cartesian coordinates between the transition state of a reaction and its reactants and products. It can be thought of as the path that the molecule takes moving down the product and reactant valleys with zero kinetic energy [7].

The study of reaction paths and transition states is of great importance because it is very difficult to study transition states by experimental methods, although they are one of the most important species in a chemical reaction [11]. It must be said that theoretical calculations, by its own cannot predict the mechanism or the most favorable pathway. The user should explore all the possibilities and draws several models of the pathways that the reaction can follow. The calculated Gibbs free energies analysis, of the studied reactions, concludes which are the most favorable ones, that is in terms of kinetically (lower barriers) and thermodynamic (more exergonic) points of view.

## 2. References

1. Jensen F., Introduction to Computational Chemistry. John Wiley & Sons; **2007**.
2. Erkoç S., Fundamentals of Quantum Mechanics. Taylor & Francis; **2007**.
3. Leach AR., Molecular Modelling : Principles and Applications. Prentice Hall; **2001**.
4. Hohenberg, P.; Kohn, W., Inhomogeneous Electron Gas. Phys Rev. **1964**;136(3B):B864-B871.
5. Standard JM. Chemistry 460 Spring 2013 Dr. Basis Set Notation.; **2013**.  
<http://erg.biophys.msu.ru/~comcon1/qmdata/basis-set-notation.pdf>
6. Basis Sets gaussian 09. <http://gaussian.com/basissets/>
7. Cerqueira, N.M.F.S.A.; Fernandes, P.A.; Ramos, M.J., Protocol for Computational Enzymatic Reactivity Based on Geometry Optimisation. ChemPhysChem. **2018**;19(6):669-689.
8. Miertuš, S.; Scrocco, E.; Tomasi, J., Electrostatic interaction of a solute with a continuum. A direct utilization of AB initio molecular potentials for the prevision of solvent effects. Chem Phys. **1981**;55(1):117-129.
9. Cossi, M.; Barone, V., Density-functional thermochemistry III. The role of exact exchange. J Chem Phys. **1998**; 109:2427.
10. Yarkony, D.R., Modern Electronic Structure Theory, Advanced Series in Physical Chemistry World Scientific Publishing Company, **1995**, 459.
11. Fernandez, G.M.; Sordo, J.A.; Sordo, T.L., Analysis of Potential Energy Surfaces the Concept of a Potential Energy Surface (PES) Is One of the Most Important in Chemical Physics. It Plays a Fundamental Role in the Stationary Points of Eq 2. Let the Gradient Be Zero. **1988**; Vol 65.

## Section **B**: Results and discussion



## Introduction

The discussion of this thesis is based on the experimental work developed from 2,4-benzylidene-D-erythrose **1** [1] mainly in the development of new iminosugars by three synthetic routes. The work is accompanied by theoretical energy calculations in order to establish the mechanism of the reactions and make them predictable for the future.

In the first synthetic route, the reaction of 2,4-benzylidene-D-erythrose **1** was used with alkylamines to afford D-erythrosyl alkylimines **2**; to the D-erythrosyl alkylimines was added 1-(tert-butyltrimethylsilyloxy)-1-methoxyethene in the presence of BF<sub>3</sub> etherate leading to a single stereoisomer, *R* configuration at the new stereogenic center. Acid treatment of these adducts triggers a reaction cascade leading to a mixture of L-homoproline **3**, and a bicyclic compound, shown to be its precursor; full conversion to L-homoproline occurs by addition of base. N-Alkyl L-homoprolines are obtained in overall excellent yields from **1**. The theoretical mechanism's studies were made and full explained the experimental results: a) an equilibrium between L-homoprolines and its bicyclic counterpart is established in acid; b) the equilibrium suffers a complete displacement towards the L-homoprolines side in basic medium. (Chapter 4)

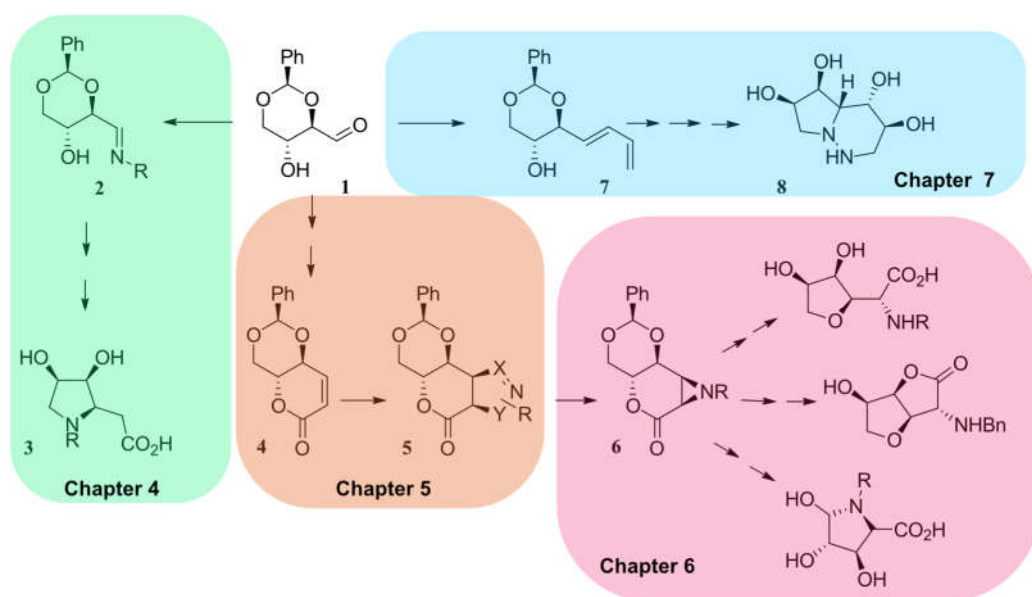
In the second synthetic route, in two steps 2,4-benzylidene-D-erythrose **1** was transformed in D-erythrosyl  $\delta$ -lactone **4**. The synthesis of **4** involves: 1) Wittig olefination of the aldehyde by reaction with methyl (triphenylphosphoranylidene)acetate, 2) intramolecular cyclization of the *Z* isomer (Chapter 5). During the synthetic process, the synthesis of 2,4-benzylidene-D-erythrose **1** could also be improved from 54% to 95% yield. (experimental section, Chapter 4)

Lactone **4** proved to be a highly stereoselective template as a dipolarophile. Different 1,3-dipoles of allenyl-type were employed, giving different regioselectivities, depending on its nature; the regioselectivity is complete with alkyl azides and phenyldiazomethane, but is nonexistent with nitrile oxides. The high selectivity displayed by template **4** towards 1,3-dipolar cycloadditions was explained by computational studies.

From  $\delta$ -lactone triazoles **5** were obtained 5-membered iminosugars in reactions with complete stereoselectivity. This synthesis process involves the transformation of the triazole unit into aziridine compounds **6** by nitrogen extrusion under photolysis. Aziridines **6** were treated under three different

acids:  $\text{BiI}_3$  /  $\text{H}_2\text{O}$ , TFA, and HCl, which resulted in the synthesis of two types of sugar amino acid compounds. (Chapter 6)

In the three-synthetic route, from 2,4-benzylidene-D-erythrose by a double Wittig reaction was obtained D-erythrose-4-yl-1,3-butadiene **7** [2]. This 1,3-butadiene was used in  $4\pi + 2\pi$  cycloadditions with azo [2], aza [3], and carba-dienophiles [4]. Reactions of diene **7** with PTAD, DEAD and DBAD led to aza-indolizidine **8**. The origin of the diastereoselectivity in these Diels-Alder cycloadditions was analyzed by computational studies in order to find the reactivity of the *si* / *re* face of the diene **7**. This study was for reaction with PTAD, DEAD, and DBAD. (Chapter 7)



**Scheme 1** – Geral scheme overall synthetic routes in the next chapters

## References

1. Barker, R.; MacDonald, D. L., Some Oxidation and Reduction Products of 2,4-*O*-Ethylidene-D-erythrose. *J. Am. Chem. Soc.* **1960**, *82* (9), 2301-2303.
2. Alves, M.J.; Duarte, V. C. M.; Faustino, H.; Gil, A., Diastereo-controlled Diels–Alder cycloadditions of erythrose benzylidene-acetal 1,3-butadienes by 4-substituted-1,2,4-triazoline-3,5-dione: Evidence for the stereoelectronic effects on the dienes. *Tetrahedron Asymmetry*, **2010**, *21*, 1817-1820
3. Duarte, V. C. M.; Faustino, H.; Alves, M. J.; Gil Fortes, A.; Micaelo, Nuno, Asymmetric Diels–Alder cycloadditions of D-erythrose 1,3-butadienes to achiral *t*-butyl 2H-azirine 3-carboxylate. *Tetrahedron-Asymmetry*, **2013**, *24*, 1063-1068.
4. Salgueiro, D.A.L.; ; Duarte, V.C.M.; Sousa, C.E.A.; Alves, M.J.; Gil Fortes, A., Asymmetric Diels–Alder cycloadditions of D-erythrose 1,3-butadienes to achiral *t*-butyl 2H-azirine 3-carboxylate. *Synlett* **2012**, *23*, 1765-1768.

# 4

Synthesis of L-Homoprolines from D-Erythrose

*The results presented in this chapter are in the publication:*

**(3*S*,4*R*)-Dihydroxy-N-Alkyl L-homoprolines: Synthesis and Computational Mechanistic Studies.**

David S. Freitas, Cristina E. A. Sousa, Joana Parente, Artem Drogalim, A. Gil Fortes, Nuno M. F. S. A. Cerqueira, and Maria J. Alves

*Organic & Biomolecular Chemistry*, **2019**, DOI: 10.1039/C9OB02141H.

My contribution to this paper was: the computational work.

## 1. Abstract

This is the first synthetic report of (3*S*,4*R*)-dihydroxy *N*-alkyl-L-homoprolines described so far. 2,4-*O*-Benzylidene-D-erythrose was obtained from D-glucose with improved yield and then transformed into the title (3*S*,4*R*)-dihydroxy-*N*-alkyl L-homoprolines, in a two-step strategy, with excellent overall yields. Hydrogenolysis of the benzyl group led to the *MH* congener. The synthesis of final products from 1,4-lactone intermediates was studied by computational means either in acidic and basic conditions. The theoretical mechanism's studies full explain the experimental results: a) an equilibrium between L-homoprolines and its bicyclic counterpart is established in acid; b) the equilibrium suffers a complete displacement towards the L-homoprolines side in basic medium.

## 2. Introduction

Carbohydrates have served as chiral starting materials for the synthesis of several amino acids [1-3]. Some of these syntheses are multi-stage, involving considerable manipulation of protecting groups. However, some elegant protocols are known for 3,4-dihydroxyprolines [4]. Three members of the L-series have been isolated from natural sources: **1**, from *Navicula pelicullosa* [5]; **2** from *Amanita virosa*[6]; and **3**, the sixth residue of the decapeptide sequence of Mefp1 (**Figure 1**), an adhesive protein, from the marine mussel *Mytilus edulis* [7]. Though, the homoproline congeners syntheses are very scarce; only two methods have been published for these compounds: one, by Davis group [8], and another from our laboratory [9]. This is as far as we know the first reported synthesis of L-3,4-dihydroxyprolines. A major feature of proline amino acid in Nature is related to the rigidity imposed into the peptide sequence in which proline is incorporated, leading to protein folding ( $\alpha$ -, $\beta$ -, $\gamma$ -turns), which is known to play important roles in: i) proteins tertiary structure, ii) molecular/cellular recognition processes, iii) interactions between substrates and receptors [10-14]. However, in the modified-peptide-backbones the conformational torsions have been successfully attained through introduction of other amino acids than L-proline;  $\beta$ -,  $\gamma$ -amino acids, amino acids of the D-series, and various types of cyclic monomers [10,15].  $\beta$ -Amino acids are between the best-studied of those compounds [16,17]. In this context, the development of asymmetric synthetic routes to the synthesis of homopropyl residues is highly desirable as new templates in the design of specific turn-mimics of biologically active molecules. The present work intends to be a contribution to the required pool of homoproline molecules. Besides, the two

hydroxyl groups at 3,4-positions of the proline ring being polar and capable of hydrogen-bonding can be easily tunable into nonpolar groups, by acetal protection. Additional importance of these compounds comes from the recent synthesis of their D-congeners, obtained by a divergent synthesis from 2,4-*O*-benzilidene-D-erythrose [9]. Knowing that a matching configuration of amino acids is crucial in shaping the outcome for the peptide secondary structure [15] the choice between D- and L-structures is preeminent in the design of new peptide foldamers.

2,4-*O*-Benzilidene-D-erythroylimines generated *in situ* from D-erythrose display a complete facial selectivity towards 1-(*tert*-butyldimethylsilyloxy)-1-methoxyethene nucleophilic addition giving the *R* configuration at the new stereogenic centre. Acid treatment of adducts followed by basic treatment triggers a reaction cascade leading to a L-homoproline in excellent overall yields. The computational results are consistent with the formation of (3*S*,4*R*)-dihydroxy L-homoprolines in two stages from the imine adducts.

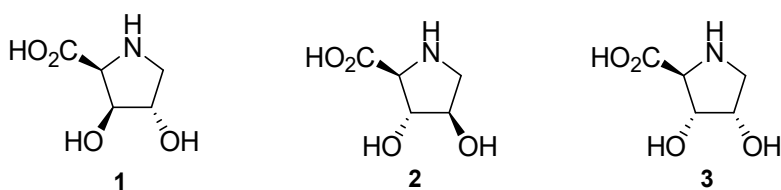
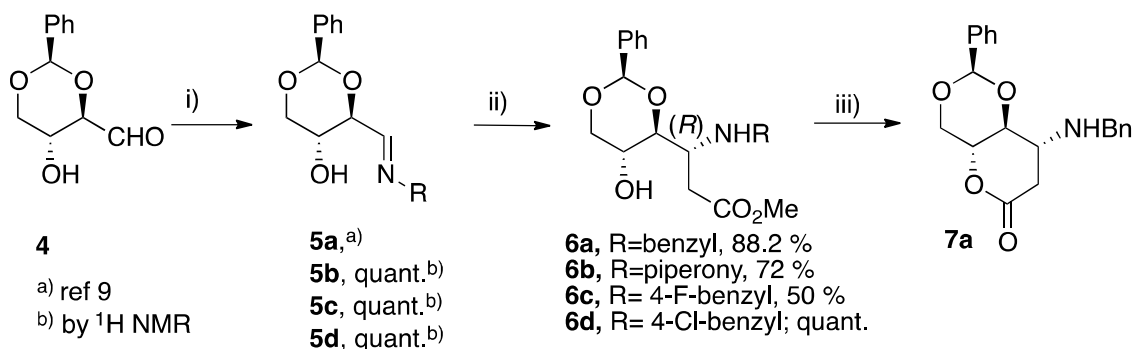


**Figure 1** - Dihydroxyprolines isolated from natural sources

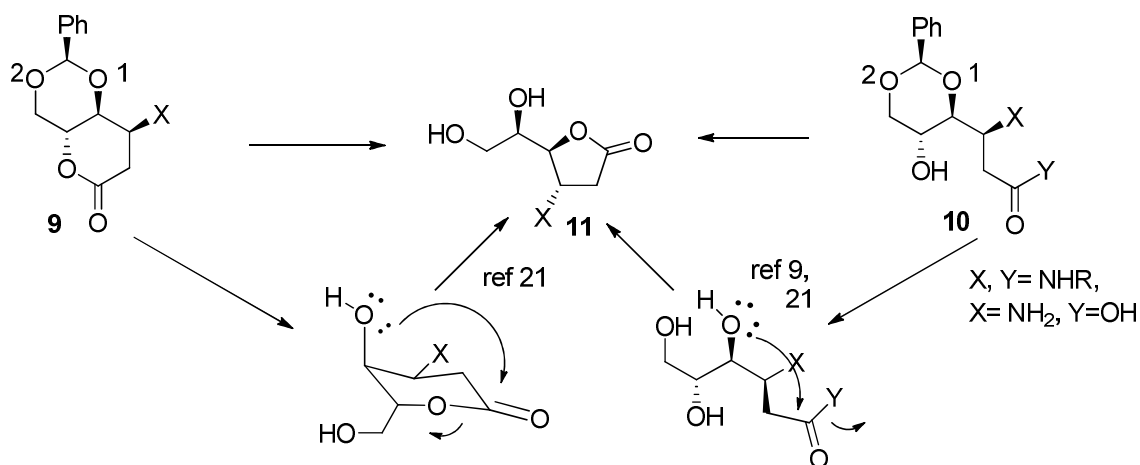
### 3. Experimental Results and Discussion

2,4-*O*-Benzilidene-D-erythrose [18] (**4**) is obtained in a 10 g scale from D-glucose, by adapting a known procedure for the synthesis of 2,4-*O*-isopropylidene-D-erythrose[19]. 2,4-*O*-Benzilidene-D-erythrose reacted with alkyl amines, as before did with aromatic amines[20] to give the respective *N*-alkylimines **5**. Imines **5** showed to be excellent chiral templates able to induce complete stereoselectivity in nucleophilic additions with 1-(*tert*-butyldimethylsilyloxy)-1-methoxyethene, furnishing single adducts **6a-d**, in high yields (**Scheme 1**). Compounds **6a-d** were purified by flash column chromatography in silica. It was found that silica promote cyclization to the six-membered lactones **7a-d** during the course of the chromatographic purification. <sup>1</sup>H NMR spectra of adducts **6a-d** showed the presence of lactones **7a-d** as contaminants. In case **a**, an enriched sample of **7a** was obtained during chromatography.



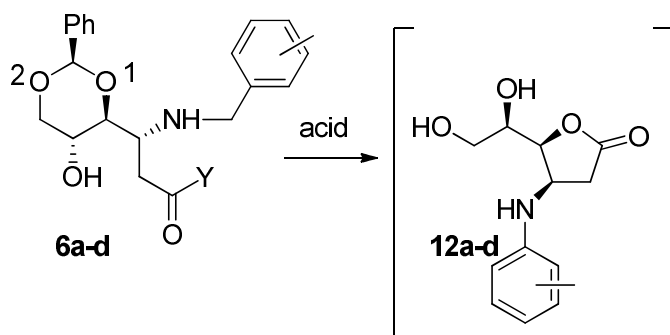
**Scheme 1** - Synthesis of D-erythrosyl alkylimines **5**, and its reactions with 1-(*tert*-butyldimethylsilyloxy)-1-methoxyethene - **i**) alkylamines 0.7 eq., THF (dry), 1 h, 35 °C, 4 Å MS, N<sub>2</sub> (g); **ii**) BF<sub>3</sub>·OEt<sub>2</sub> 0.7 eq., 1-(*tert*-butyldimethylsilyloxy)-1-methoxyethene 0.7 eq., THF (dry), 4 Å MS, N<sub>2</sub> (g), -84 °C to rt, 2 h; **iii**) ethyl acetate : pet. ether (1:1), rt., prolonging contact with silica (in chromatographic column).

In a previous work, acid treatment of compounds **9** and **10** led a 1,4-lactone **11**. **Scheme 2** resumes how the spatial proximity of O1 to the carbonyl in either compounds **9** and **10** can easily lead to 1,4-lactone **11** in both cases. Computational mechanistic studies were developed before for some of these cases [21].



**Scheme 2** - Synthetic mechanism leading to 1,4-lactone **11**, obtained by acid treatment of D-erythrose 6-carbon chain derivatives **9** and **10**.

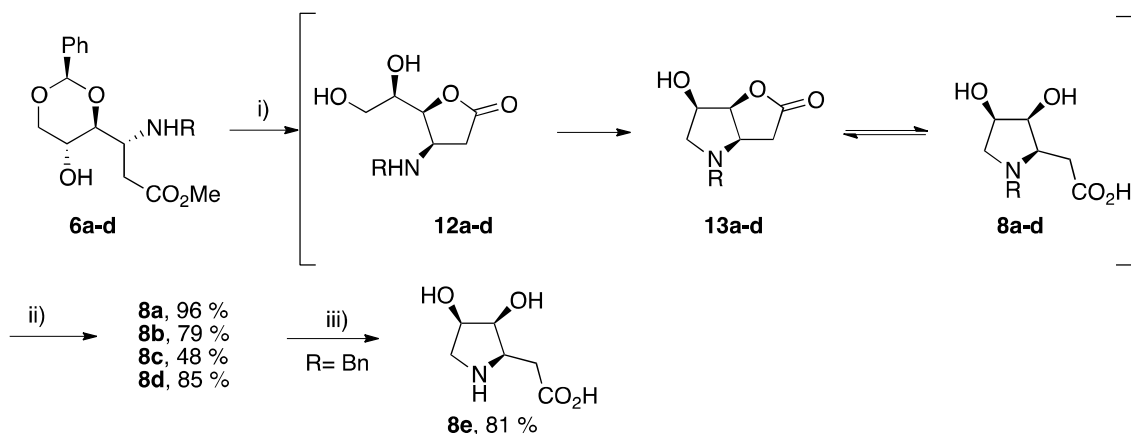
Accordingly, compounds **6a-d** (together with their contaminants **7a-d**) were subjected to strong acid conditions with the aim to generate lactones **12a-d** (**Scheme 3**).



**Scheme 3** - Synthesis of lactones **12a-d** obtained by acid treatment of compounds **6a-d**.

It is likely that the matching configuration of the amino group and the 1,2-dihydroxyethyl arm in lactone **12** turn the aminocyclization a much easier process than the aminocyclization of its epimer **11** [9]. Lactone **11** had to suffer bromination at the primary hydroxyl group in order to make cyclization occur. Theoretical calculations have confirmed that compound **12a** can be converted into **13a** under other acids besides HBr (HCl, TFA, see third section) by a relatively easy process. The treatment of compound **6a** with TFA led to an evanescent compound, tentatively assigned as compound **12a**. It was observed over the reaction period in aliquots studied by  $^1\text{H}$  NMR. After a 5 h reaction's course at room temperature, this compound was the main specie in the reaction mixture. Overtime (5 – 8 days) a dynamic equilibrium had been reached leading to a 1:3:1 mixture of three components: **13a** (major) together with **8a** and **12a** (**Scheme 4**). Any attempt to isolate compound **12a** by chromatography showed to be not possible; the mixture systematically evolve the compounds **13** and **8**. The obtained products showed to be a 2 (**13a**):1 (**8a**) ratio in reactions run in the standard HCl-dioxane; a 1:1 mixture with HBr in acetic acid; and a 3 (**13a**):1 (**8a**) with trifluoroacetic acid 6 M in dioxane. In the last case, the ratio did not change by prolonging the reaction time for a week. Full conversion of the bicyclic compounds **13** into L-homoprolines **8** occurs by basification of the reaction medium with KOH or triethylamine followed by acidic resin treatment, to adjust pH to 7. In some spectra of homoprolines **8**, vestigial amounts of the respective bicyclic compounds are always present. Compounds **8a-d** are generally formed in high yields. Debenzylation of homoproline **8a** was achieved by hydrogenation in the presence of Pd/C at room temperature (**Scheme 4**).





**Scheme 4** - Synthesis of L-homoprolines **8a-d** - **i**) HCl 6 M, dioxane: water 1:1, rt, 2 h; **ii**) **a**) KOH 6M; rt, overnight; **b**) Amberlite IR-120 (H<sup>-</sup>), pH 7, rt; **iii**) **a**) Pd/C, 10 mol %, H<sub>2</sub>, 1 atm., MeOH, 1,1,2-trichloroethane (1.1 eq.), 2 days; **b**) KOH (0.01 M) till pH 12.

When a D<sub>2</sub>O solution of the obtained compound **8a** contained in a NMR tube was treated with TFA-d<sub>8</sub> **8a** an equilibrium between **8a** and **13a** is re-established. Computational mechanistic studies clearly show how energetics favors the equilibrium back in acidic medium.

#### 4. Computational studies

Computational studies were carried out, using density functional theory, to understand the mechanism of the reactions involving the reaction of 1,4-lactones **12a** under different acidic conditions, eventually followed by basic conditions, and from which the *N*-benzyl (3*S*,4*R*)-dihydroxy L-homoprolines **8a** is obtained.

The computational results have shown that although the reaction is done experimentally in one-pot synthesis, the mechanism goes through several sequential stages and involves the formation of the intermediate **13a**, as described in the next sections.

##### Stage 1: Formation of the reaction intermediate **13a** from 1,4-lactones **12a**

An intramolecular cyclization of lactones **12a** occurs under acidic conditions at the first stage (**Figure 2**). In compound **12a**, nitrogen N1 and carbon C2 are at 3.13 Å distance from each other. The proton from HCl is stabilized by a hydrogen bond network provided by one water molecule W1 and the hydroxyl group (O2) of the lactone.

The transition state of the reaction is characterized by an imaginary frequency at  $386.33i \text{ cm}^{-1}$ . This stationary point reveals that nitrogen N1 and carbon C2 become closer to each other ( $2.26 \text{ \AA}$ ) at the same time that the bond lengths between carbon C2 and oxygen O2 become extended ( $1.87 \text{ \AA}$  versus  $1.44 \text{ \AA}$  in the reactants), enabling the simultaneous proton transfer among them, through the HCl molecule and the water molecule W1.

In the end of this stage, the intramolecular cyclization is complete. Carbon C2 and nitrogen N1 become covalently bonded to each other by a single bond ( $1.52 \text{ \AA}$ , versus  $3.13 \text{ \AA}$  in the reactants). At the same time, one proton migrates from nitrogen N1 to the water molecule W1 and from the latter one to oxygen O2 of the lactone, through HCl. This process results in the cleavage of the bond between oxygen O2 and carbon C2 ( $3.17 \text{ \AA}$ , versus  $1.44 \text{ \AA}$  in the reactants) and the formation of one water molecule (W2).

This reaction requires a free activation energy of  $19.2 \text{ kcal.mol}^{-1}$  and is exergonic in  $-21.6 \text{ kcal.mol}^{-1}$ .

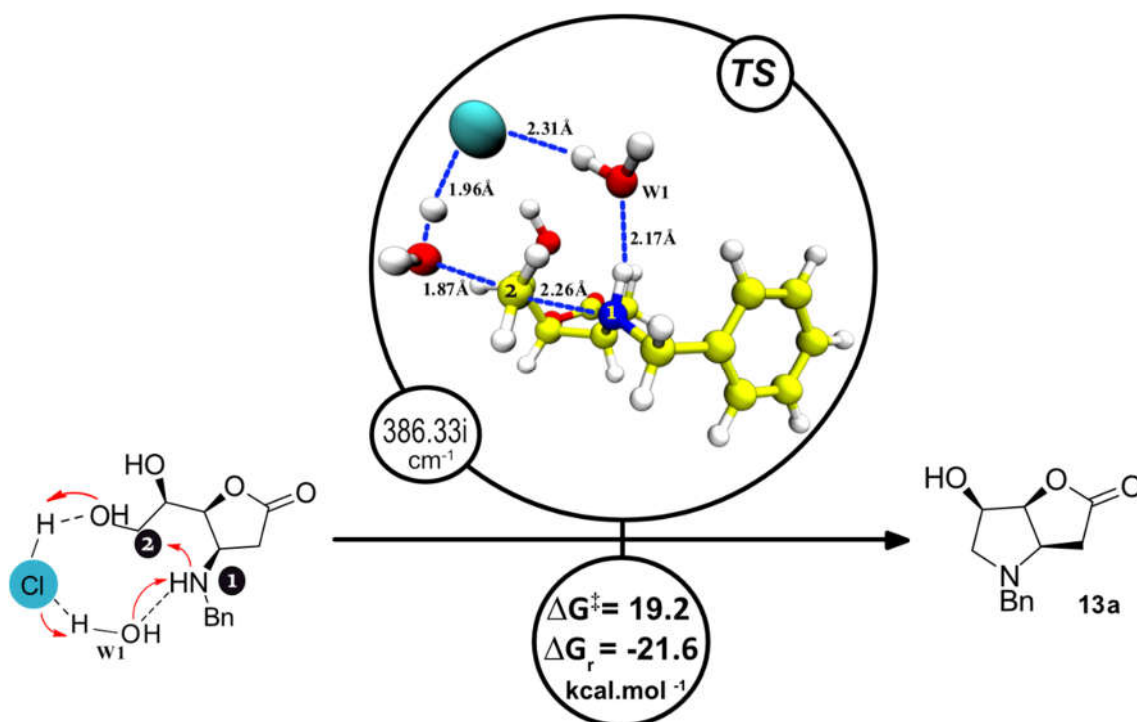


Figure 2 – Aminocyclization mechanism for the synthesis of bicyclic compound 13a, from 12a.

The intra-molecular network of hydrogen bonds plays an important role in this step since: i) it enables the correct alignment of nitrogen N1 and carbon C2 within the lactone, making them ready

for the nucleophilic attack, and ii) it enables the proton transfer from nitrogen N1 to the hydroxyl group bonded to carbon C2, through the HCl molecule. The HCl molecule behaves as a catalyst in the reaction facilitating the proton transfer through the water molecules that is determinant for the cyclization process.

Experimentally compound **12**, once formed, easily evolves to **13**. The computational results showed an free activation energy ( $\Delta G^\ddagger=19.2$  kcal.mol<sup>-1</sup>) compatible with the reaction's room temperature. As this conversion is very exergonic ( $\Delta G_r = -21.6$  kcal.mol<sup>-1</sup>) the reverse step is not possible, in accordance with experimental results.

### Stage 2: Formation of L-homoproline **8a** from bicyclic compound **13a**

The next stage of the mechanism involves the formation of the homoproline **8a** from intermediate **13a**, obtained at the end of the first stage. Experimentally, this reaction was found to diverge whenever acidic or basic conditions were employed. Under acidic conditions, it is observed an equilibrium between compounds **13a** and **8a**. However, the yields of the reactions change significantly depending on the type of acid that is employed (HCl, HBr, and TFA). Under basic conditions, the reaction is very efficient, giving solely compound **8a**.

The computational results explain the mechanistic differences, both under acid and basic conditions as described in detail below.

- **Acid catalysis**

Under acid conditions, the reaction involves the cleavage of the lactone ring in intermediate **13a**. The reaction requires the direct participation of one water molecule and an acid specie molecule, and it is completed in two sequential steps (**Figure 3**). The mechanism is very similar for the different acids that were employed (HCl, HBr or TFA).

In the first step, occurs the adduct formation. The proton from the acid species approach oxygen O1 of the reactant and establishes one hydrogen bond with it (in average 1.68 Å), and a weaker interaction with the neighbor water molecule (in average 2.43 Å).

The transition states of these additions are characterized by one imaginary frequency (*see* first step in **Figure 3**). The bond length between carbon C1 and oxygen O1 increases to around 1.33 Å (1.22 Å in the reactants), at the same time the oxygen from the water molecule (W1) becomes aligned with carbon C1 and very close to it (in average 1.69 Å *versus* 3.30 Å in the reactants), and the acid proton establishes a bond with oxygen O1.

The adduct is formed when carbon C1 - oxygen O1 bond is 1.38 Å (*versus* 1.22 Å in compound **13a**), and the hydroxyl group from the water molecule becomes covalently bonded to carbon C1 (around 1.44 Å). At the same time, the proton from the water molecule migrates to the acid.

The free activation energy of the first step is lower when HBr is used and higher when TFA and HCl are employed (**Table 1**). No significant differences are observed in the free reaction energy. In all the studies cases the reactions are endergonic and with similar values.

The second step involves the ring cleavage ring and the formation of compound **8a**.

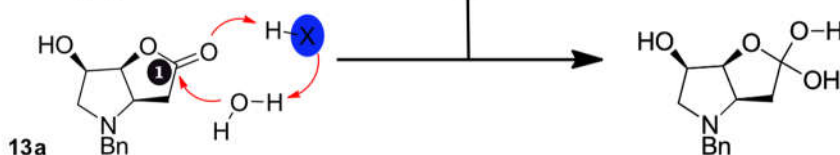
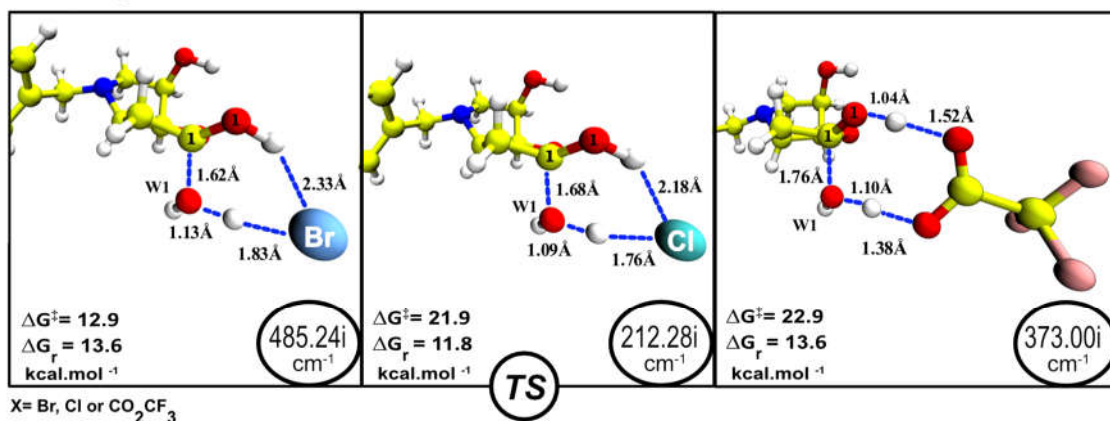
In the adduct, carbon C1 and oxygen O2 are bonded to each other by a covalent bond (1.50 Å in HBr and HCl, 1.47 Å in TFA) and the proton from the acid species is bonded to a water molecule W1(1.07 Å, except for TFA (1.54 Å)).

The transition states of the second step are characterized by one imaginary frequency (*see* second step in **Figure 3**). The bond between carbon C1 and oxygen O2 starts to elongate (in average 1.65 Å), and one hydrogen from the water molecule W1 becomes very closer to oxygen O2 (in average 1.31 Å *versus* 1.53 Å in HBr and HCl, and 1.78 Å in TFA in the adducts).

In the product, the bond between carbon C1 and oxygen O2 is cleaved (2.45 Å in HBr/ HCl, 2.72 Å in TFA), and the protic acid is on the way to be regenerated from hydroxyl group converted into carbonyl.

The free activation energy of the first step is lower when HBr and HCl are employed in the reactions (**Table 1**). No significant differences are observed in the free reaction energy. In all the studies cases the reactions are exergonic and with similar values.

## First step



## Second step

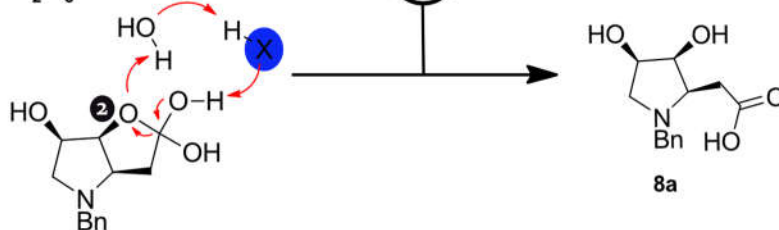
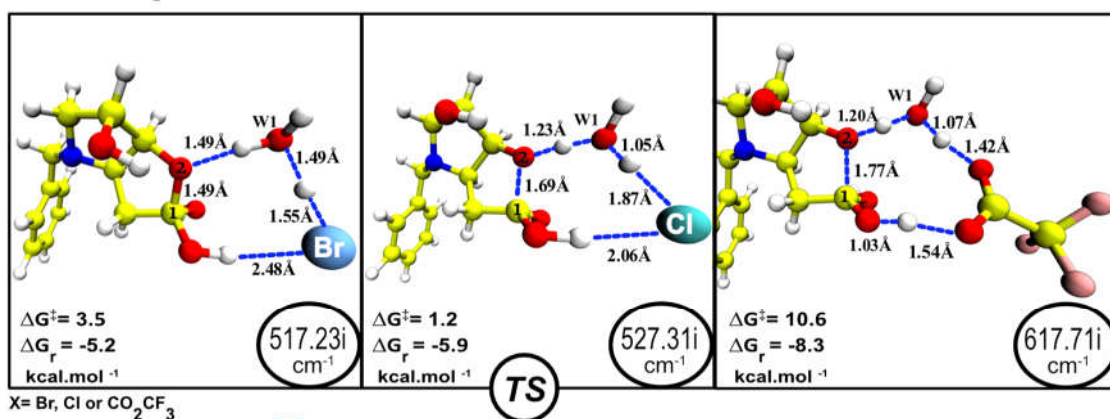


**Figure 3** - Mechanism involved in lactone cleavage in compound **13a** to form compound **8a**, under HCl, HBr, and TFA.

As an overall, the addition-elimination reaction's mechanisms do not show significant differences within the acids employed (HBr, HCl, and TFA). The calculated free energies show that the first step is the rate-limiting one in all studied reactions. The reaction with the best full energetic profile (faster kinetics) is the one where HBr is employed. This happens due to the largest atomic radius of bromine that makes the proton shuttle more efficient in HBr, especially in the first step

(see **Figure 3**). The slowest reaction is the one where TFA is employed, due to the highest activation free energies that are observed in both steps (**Table 1**).

**Table 1** - Free activation energies ( $\Delta^\ddagger$ ) and free reaction energies ( $\Delta_r$ ) for the transformation of compound **13a** into **8a**, in TFA, HCl, and HBr.

	First step		Second step		13a/8a
	$\Delta^\ddagger$ (kcal.mol <sup>-1</sup> )	$\Delta_r$ (kcal.mol <sup>-1</sup> )	$\Delta^\ddagger$ (kcal.mol <sup>-1</sup> )	$\Delta_r$ (kcal.mol <sup>-1</sup> )	
TFA	22.89	13.55	10.55	-8.28	3:1
HCl	21.91	11.80	1.25	-5.90	2:1
HBr	12.86	13.55	3.54	-5.18	1:1

The energetic profile of the theoretical calculations of hydrolysis in HBr in acetic acid showed that free activation energy of 12.9 kcal.mol<sup>-1</sup> in the first step, and 3.5 kcal.mol<sup>-1</sup> in the second step. As so, an open equilibrium with very low free activation energies to both sides should operate. The ratio between compounds **13a/8a** is nevertheless difficult to predict from the differences in activation and reaction energies.

The energetic profile of the theoretical calculations of hydrolysis in HCl showed that the first step ( $\Delta^\ddagger=21.9$  kcal.mol<sup>-1</sup>) controls the lactone hydrolysis process. At room temperature the energetic barrier is predicted to be surpassed, counting with an energy supplement released in the formation of compound **13a**. The second step showed a very low free activation energy ( $\Delta^\ddagger=1.3$  kcal.mol<sup>-1</sup>), and it is exergonic ( $\Delta_r = -5.9$  kcal.mol<sup>-1</sup>). Being so, the reversal process needs to be surmounted is only 16 kcal.mol<sup>-1</sup>. These findings go in line with the experimental equilibrium observed in the hydrolysis of the bicyclic lactone **13a** with HCl. The intermediate **13a** evolved to compound **8a** in equilibrium with **13a** in 2 (**13a**): 1 (**8a**).

In a separated experiment it was found that compound **8a** quickly sets an equilibrium back with **13a**. The experiment consisted in adding TFA-d<sub>8</sub> to a solution of **8a** in D<sub>2</sub>O contained in a NMR tube. After 30 minutes a 3 (**13a**) : 1 (**8a**) ratio was verified.

The energetic profile obtained from the theoretical calculations for this transformation is only 18 kcal.mol<sup>-1</sup> for the limiting step, which is likely to take place at room temperature. From the thermodynamic point of view compound **13** is favored over **8a** in ca. 5 kcal.mol<sup>-1</sup>. Interestingly, the

intermediate adduct for the direct/inverse processes requires similar free activation energies for both sides of the reaction (direct: 10.6 kcal.mol<sup>-1</sup>; inverse: 9.3 kcal.mol<sup>-1</sup>). The reaction point of equilibrium showed so to be dependent on the ground energy of the **8a** and **13a**.

- **Basic catalysis**

Under basic conditions, only one product is obtained at the end of the reaction, compounds **8a-d**. The mechanism requires the presence of a base, KOH, and two water molecules. The reactions are complete in two sequential steps (**Figure 4**).

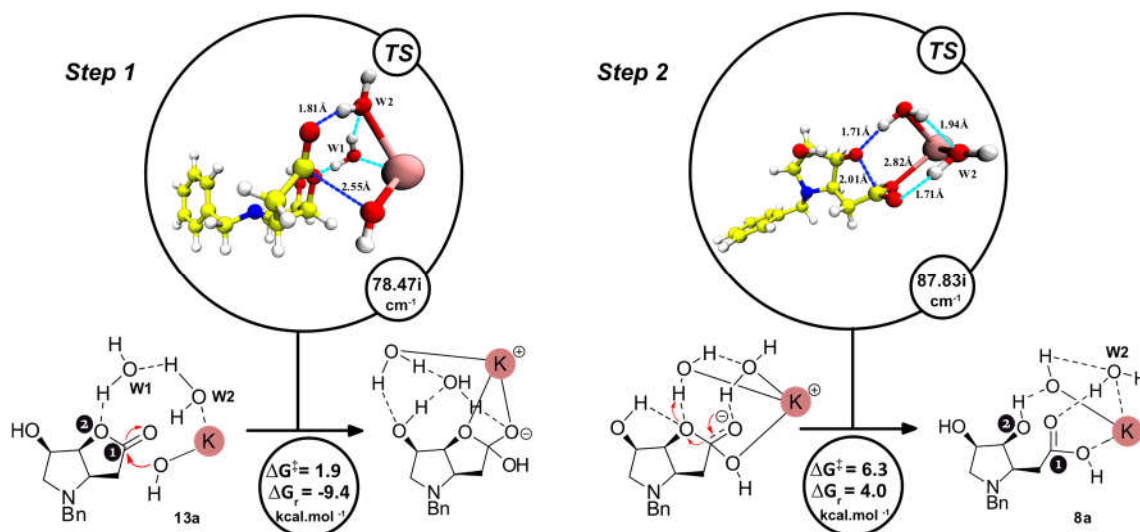


**Figure 4** - Mechanism involved in lactone unit cleavage in compound **13a** to form compound **8a**, under basic conditions.

The computational results have shown that the reaction requires two steps; the first step involves the formation of a zwitterionic reaction intermediate.

In the reagent, compound **13a**, the bond length between carbon C1 and the oxygen O of KOH is 3.05 Å. Its position is stabilized by two water molecules that are aligned with oxygen O2, through a network of hydrogen bonds (2.65 Å and 1.89 Å).

The transition state of this reaction is characterized by one imaginary frequency at 78.47i cm<sup>-1</sup>. In these structures, it becomes clear the central role played by the potassium cation on the reaction. It favors: i) the alignment of the hydroxide with carbon C1 (2.55 Å), ii) the hydrogen bond

between water molecule 2 (W2) and the carbonyl group (1.81 Å) and, iii) the hydrogen bond between water molecule 2 (W2) with the potassium (2.81 Å).

At the end of this reaction, it is obtained a stable zwitterionic reaction intermediate. Carbon C1 acquires a tetrahedral configuration, and oxygen O1 becomes negatively charged (-1.00 a.u. *versus* -0.78 a.u. in the reactants). The negative charge is stabilized by one water molecule, W2, that is now very close to the positively charge potassium. The water molecule W1 is also close to the potassium cation, but also interacts with oxygen O2 through a short hydrogen bond (1.99 Å).

This reaction is almost spontaneous requiring a very low free activation energy (1.9 kcal.mol<sup>-1</sup>) and it is exergonic in -9.4 kcal.mol<sup>-1</sup>.

The second step involves the cleavage of the zwitterionic intermediate into compounds **8a**.

The reactant of this step is very similar to the product of the last step. Carbon C1 is firmly attached to oxygen O2 by a covalent bond (1.59Å) and the potassium cation (0.94 a.u.) continues to be stabilized by the oxygen atoms provided by the two water molecules and the hydroxyl group that is now attached to carbon C1.

The transition state of the studied reaction is characterized by one imaginary frequency at 87.83i cm<sup>-1</sup>. The bond length between carbon C1 and oxygen O2 starts to elongate (2.01Å *versus* 1.59Å in the reactant) and one of the hydrogens from water molecule W1 becomes very close to oxygen O2.

In the product of this reaction, the formation of compound **8a** is complete. The bond between carbon C1 and oxygen O2 is cleaved (2.41 Å *versus* 1.59 Å in the reactant), and KOH is regenerated after the proton transfer from water molecule W2 to water molecule W1.

Similarly, to the previous step, this reaction requires a low free activation energy (6.3 kcal.mol<sup>-1</sup>), being slightly endergonic in 4.0 kcal.mol<sup>-1</sup>.

From the experimental work, it is known that the equilibrium completely shifted towards to the right giving **8a**. This is in accordance with the theoretical results obtained which display an energetically favored profile.



## 5. Conclusion

The study describes the development of a very simple, high yielding strategy for the synthesis of (3*S*,4*R*)-dihydroxy L-homoprolines from D-erythrose. Trivial reagents, cascade reactions, no purification needs, completely selective reactions, make this process highly appealing for the synthesis of (3*S*,4*R*)-dihydroxy homoprolines of L-stereochemistry. Considering the biological importance of the final products, as new molecular scaffolds of an important type, conjugated with the simplicity of the chemical process, an insight on the energetics of reactions involved became a major demand. As the cyclization mechanism of 6-carbon atom D-erythrosyl derivatives to a related type of 1,4-lactone intermediate had been previously studied, the theoretical work was now focused on the transformation of these intermediates into (3*S*,4*R*)-dihydroxy L-homoprolines.

The computational results reveal that the mechanism of the formation of the *N*-benzyl-(3*S*,4*R*)-dihydroxy L-homoprolines **8a** from 1,4-lactones **12a** diverges under acidic or basic conditions, although they share some similarities. In both, acid and basis cases, the catalysts favor the proton shuttle that is required for the cleavage of the lactones. The main difference in the mechanism is that with KOH involves the formation of a zwitterionic reaction intermediate in which K<sup>+</sup> take part. This effect favors the intramolecular hydrogen bond network between the compound and the two water molecules required for the next step. This effect is not observed in acid catalysis, which leads to a significant increase in the calculated free activation energies.

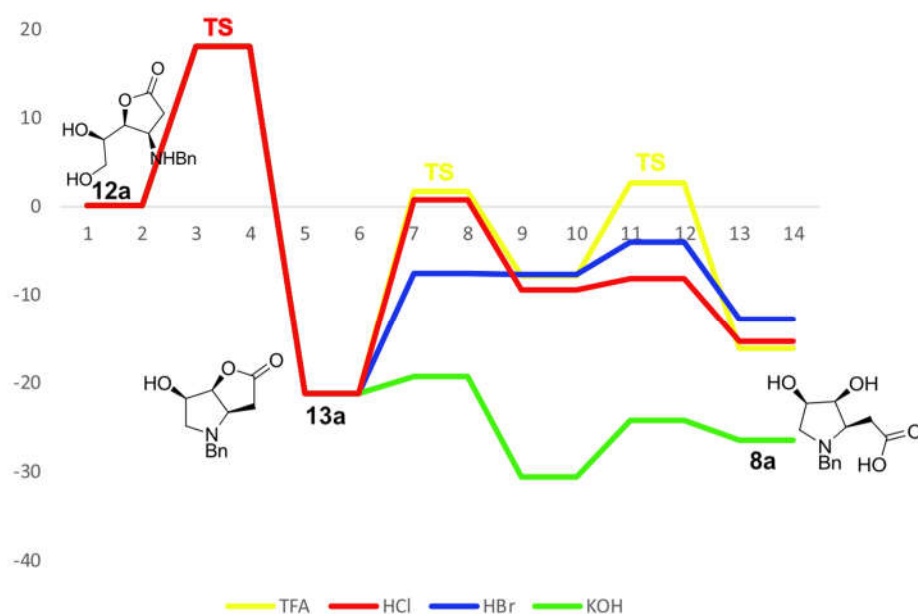


**Figure 5**– Energetic profile of all the studies reactions to yield the formation of *N*-benzyl-(3*S*,4*R*)-dihydroxy L-homoprolines **8a** under acidic and basic conditions.

## 6. Experimental

### 6.1 General

All reagents were purchased from Sigma-Aldrich, Acros, TCI or Alfa Aesar and used without further purification, except for *p*-toluenesulfonic acid monohydrate which was dried under a vacuum pistol at 120 °C, THF was dried by reflux under Na(s), and BF<sub>3</sub>·OEt<sub>2</sub> by distillation. Aldehyde **4** [18,19], and imine **6a** [9] were synthesized following the procedures described in the literature. An optimized synthesis of **4** was obtained from a synthetic description of an analog described in lit [19].

### 6.2 Optimized synthesis of 2,4-benzylidene-D-erythrose

i) Acetal protection of D-glucose to yield (2*R*,4*aR*,6*S*,7*S*,8*S*,8*aS*)-2-phenylhexahydropyrano[3,2-*d*][1,3]dioxine-6,7,8-trio [18].

ii) To a solution of NaIO<sub>4</sub> (8.2 g; 0.038 mol; 2.2 eq.) in water (62 mL), refrigerated at 0 °C, and kept at pH=4, was added dropwise a suspension of (2*R*,4*aR*,6*S*,7*S*,8*S*,8*aS*)-2-phenylhexahydropyrano[3,2-*d*][1,3]dioxine-6,7,8-triol (5 g), in water (21 mL), with permanent pH control (pH ≥4), by addition of aqueous sodium hydroxide 8 M (~ 8 mL). The temperature was kept under 10 °C until total dissolution (~ 3h). After the 3 h reaction time, the pH was adjusted to 6.5, and the stirring continued for another 2 h, at room temperature. The solution was evaporated and the residue dried in vacuum. Ethyl acetate (40 mL) is added to the residue and the flask heated for 2 min at 80 °C with stirring. The suspension formed was filtered and the solid residue washed with ethyl acetate (3 x 30 mL). The combined liquid fractions were dried over anhydrous sodium sulphate for 1 h, and concentrated in the rotary evaporator to yield 3.69 g (95 %) of 2,4-*O*-benzylidene D-erythrose [18,19].

### 6.3 Synthesis of D-erythrosyl benzylimine 5a-c

#### 6.3.1 General procedure

To a solution of aldehyde **4** (150-200 mg; 0.72-0.96 mmol) in dry THF (4-10 mL), containing activated 4 Å molecular sieves (1.0 g) was added the amine (57-84 μL; 63-110 mg; 0.50-0.67 mmol) under magnetic stirring and N<sub>2</sub> atmosphere. The reaction mixture was kept stirring for 1 h

at 35 °C. According to the  $^1\text{H}$  NMR, products are clear yellow oils, virtually pure, used in the next step without purification.

### 6.3.2 Synthesis of (2*R*,4*S*,5*R*)-4-((*E*)-(benzylimino)methyl)-2-phenyl-1,3-dioxan-5-ol (5a)

Aldehyde **4** (150 mg, 0.72 mmol); THF (4 mL); benzylamine (55  $\mu\text{L}$ , 54 mg, 0.50 mmol).

$^1\text{H}$  NMR (400 MHz,  $\text{CDCl}_3$ )  $\delta$  3.73 (t,  $J$  = 10.8 Hz, 1H, *H*6), 4.04 (ddd,  $J$  = 10.4, 8.8, 5.2 Hz, 1H, *H*5), 4.22 (dd,  $J$  = 8.8, 1.6 Hz, 1H, *H*4), 4.38 (dd,  $J$  = 10.8, 5.2 Hz, 1H, *H*6), 4.77 (s, 2H, *H*1''), 5.69 (s, 1H, *H*2), 7.36 – 7.65 (m, 10H, Ph-CH), 7.98 (d,  $J$  = 1.6 Hz, 1H, *H*1').

### 6.3.3 Synthesis of (2*R*,4*S*,5*R*)-4-((*E*)-((benzo[*d*][1,3]dioxol-4-ylmethyl)imino)methyl)-2-phenyl-1,3-dioxan-5-ol (5b)

Aldehyde **4** (150 mg; 0.72 mmol); THF (5 mL); piperonylamine (63  $\mu\text{L}$ ; 76 mg; 0.50 mmol).  $^1\text{H}$  NMR (400 MHz,  $\text{CDCl}_3$ )  $\delta$  3.73 (t,  $J$  = 10.4 Hz, 1H, *H*6), 4.02 (ddd,  $J$  = 10.4, 8.8, 5.2 Hz, 1H, *H*5), 4.20 (dd,  $J$  = 8.8, 1.6 Hz, 1H, *H*4), 4.37 (dd,  $J$  = 11.2, 5.2 Hz, 1H, *H*6), 4.55 (s, 2H, *H*1''), 5.58 (s, 1H, *H*2), 6.69-6.83 (m, 3H, *H*Ph), 7.37-7.42 (m, 3H, *H*Ph), 7.51-7.53 (m, 2H, *H*Ph), 7.92 (d,  $J$  = 1.2 Hz, 1H, *H*1').

### 6.3.4 Synthesis of (2*R*,4*S*,5*R*)-4-((*E*)-((4-fluorobenzyl)imino)methyl)-2-phenyl-1,3-dioxan-5-ol (5c)

Aldehyde **4** (150 mg, 0.72 mmol); THF (5 mL); 4-(fluoro)benzylamine (57  $\mu\text{L}$ ; 63 mg; 0.50 mmol).  $^1\text{H}$  NMR (400 MHz,  $\text{CDCl}_3$ )  $\delta$  3.73 (t,  $J$  = 10.4 Hz, 1H, *H*6), 4.03 (ddd,  $J$  = 10.4, 8.8, 5.2 Hz, 1H, *H*5), 4.22 (dd,  $J$  = 8.8, 1.6 Hz, 1H, *H*4), 4.49 (dd,  $J$  = 10.8, 5.2 Hz, 1H, *H*6), 4.62 (s, 2H, *H*1''), 5.59 (s, 1H, *H*2), 7.04 (t,  $J$  = 8.8 Hz, 2H, *H*Ph), 7.23 (dd,  $J$  = 5.2, 3.6 Hz, 2H, *H*Ph), 7.35-7.42 (m, 3H, *H*Ph), 7.52 (dd,  $J$  = 7.2, 2 Hz, 2H, *H*Ph), 7.96 (d,  $J$  = 1.2 Hz, 1H, *H*1').

### 6.3.5 Synthesis of (2*R*,4*S*,5*R*)-4-((*E*)-((4-chlorobenzyl)imino)methyl)-2-phenyl-1,3-dioxan-5-ol (5d)

Aldehyde **4** (200 mg, 0.96 mmol); THF (10 mL); 4-(chloro)benzylamine (82  $\mu\text{L}$ , 95 mg, 0.67 mmol).  $^1\text{H}$  NMR (400 MHz,  $\text{CDCl}_3$ )  $\delta$  3.72 (t,  $J$  = 10.4 Hz, 1H, *H*6), 4.03 (ddd,  $J$  = 10, 8.8, 5.2 Hz, 1H, *H*5), 4.22 (dd,  $J$  = 8.8, 1.2 Hz, 1H, *H*4), 4.38 (dd,  $J$  = 10.8, 5.2 Hz, 1H, *H*6), 4.62 (s, 1H, *H*1''),

1''), 5.59 (s, 1H, *H*2), 7.19 (d, *J* = 6.8 Hz, 2H, *H*Ph), 7.23-7.43 (m, 5H, *H*Ph), 7.52 (dd, *J* = 7.2, 2.0 Hz, 2H, *H*Ph), 7.97 (d, *J* = 1.2 Hz, 1H, *H*1').

#### 6.4 Reaction of D-erythrosylbenzylimine **5a-d** with 1-(tert-butyldimethylsilyloxy)-1-methoxyethene

##### 6.4.1 General procedure

The imine reaction mixture obtained in the precedent step (0.34-0.67 mmol) was refrigerated at -84 °C for 15 min, and BF<sub>3</sub>·OEt<sub>2</sub> (42-83 μL; 47-95 mg; 0.34-0.67 mmol) was added under magnetic stirring followed by 1-(tert-butyldimethylsilyloxy)-1-methoxyethene (79-150 μL; 63-130 mg; 0.34-0.67 mmol). The mixture was kept stirring under the conditions described for 1-2 h, and then allowed to recover room temperature. The reaction mixture was passed through a pad of Celite®, and the filtrate evaporated in the rotary evaporator to give a brownish oil, which was re-dissolved in chloroform (40 mL) and successively washed with water (3 x 20 mL), aqueous sat. NaHCO<sub>3</sub> (3 x 20 mL) followed by saturated NaCl solution (2 x 20 mL). The organic layers were combined and dried with anhydrous magnesium sulfate, filtered, and the solvent evaporated to give a yellow oil residue. The crude product was submitted to column chromatography (silica, petroleum ether: ethyl acetate).

##### 6.4.2 Synthesis of (*R*)-methyl-3-(benzylamino)-3-((2*R*,4*S*,5*R*)-5-hydroxy-2-phenyl-1,3-dioxan-4-yl)propanoate (**6a**)

##### 6.4.2 Synthesis of (*R*)-methyl-3-(benzylamino)-3-((2*R*,4*S*,5*R*)-5-hydroxy-2-phenyl-1,3-dioxan-4-yl)propanoate (**6a**)

Imine **5a** (100 mg, 0.34 mmol) obtained previously; THF (4 mL); BF<sub>3</sub>·OEt<sub>2</sub> (42 μL; 47 mg; 0.34 mmol); 1-(tert-butyldimethylsilyloxy)-1-methoxyethene (79 μL; 63 mg; 0.34 mmol); 2 h. Product: yellow oil (112 mg; 0.30 mmol)  $\eta = 88\%$ .<sup>a)</sup>  $[\alpha]_D^{17} = -13.3$  (*c* 0.6, MeOH); IR  $\nu_{\max}$  3323, 1724 cm<sup>-1</sup>; <sup>1</sup>H NMR (400 MHz, CDCl<sub>3</sub>)  $\delta$  2.57 (dd, *J* = 16.4, 10.4 Hz, 1H, *H*2'), 2.94 (dd, *J* = 16.4, 3.2 Hz, 1H, *H*2'), 3.55 (ddd, *J* = 10.4, 4.4, 3.2 Hz, 1H, *H*1'), 3.65 (s, 3H, OMe), 3.65 (t, *J* = 10.8 Hz, 1H, *H*6), 3.90 (d, *J* = 12.4 Hz, 1H, *H*1''), 3.93 (dd, *J* = 9.6, 4.4 Hz, 1H, *H*4), 4.00 (ddd, *J* = 10.4, 9.6, 5.2 Hz, 1H, *H*5), 4.03 (d, *J* = 12.4 Hz, 1H, *H*1'''), 4.35 (dd, *J* = 10.8, 5.2 Hz, 1H, *H*6), 5.54 (s, 1H, *H*2), 7.30 – 7.48 (m, 10H, *H*Ph); <sup>13</sup>C NMR (100 MHz, CDCl<sub>3</sub>)  $\delta$  33.9 (C-2'), 51.9 (OMe), 52.6 (C-1''), 56.4 (C-1'), 63.0 (C-5), 70.9 (C-6), 77.9 (C-4), 101.6 (C-2), 126.1, 127.7, 128.2, 128.5, 128.7, 129.1 (CH-Ph), 137.5, 138.4 (C-q), 172.8 (C=O); HRMS (ESI): calcd for [C<sub>21</sub>H<sub>26</sub>NO<sub>5</sub>]<sup>+</sup>: 372.1766 (M+H<sup>+</sup>); found: 372.1803.

- a) A small fraction enriched in product **7a** (3 mg) was obtained from chromatographic purification of compound **6a**.

Compound **7a**:  $^1\text{H}$  NMR (400 MHz,  $\text{CDCl}_3$ )  $\delta$  2.61 (dd,  $J = 18.0, 7.6$  Hz, 1H,  $H7$ ), 3.12 (dd,  $J = 18.0, 7.6$  Hz, 1H,  $H7$ ), 3.38 (dt,  $J = 8.8, 7.6$  Hz, 1H,  $H8$ ), 3.77 (t,  $J = 9.2$  Hz, 1H,  $H4$ ), 3.77 (d,  $J = 13.2$  Hz, 1H,  $\text{CH}_2\text{-Ph}$ ), 3.83 (t,  $J = 10.4$  Hz, 1H,  $H6$ ), 3.87 (d,  $J = 13.2$  Hz, 1H,  $\text{CH}_2\text{-Ph}$ ), 4.21 (ddd,  $J = 10.0, 9.6, 5.2$  Hz, 1H,  $H5$ ), 4.45 (dd,  $J = 10.4, 4.8$  Hz, 1H,  $H6$ ), 5.60 (s, 1H,  $H2$ ), 7.28 - 7.49 (m, 10H,  $H\text{Ph}$ );  $^{13}\text{C}$  NMR (100 MHz,  $\text{CDCl}_3$ )  $\delta$  36.2 (C-2'), 50.9 (C-7), 53.7 (C-8), 68.3 (C-6), 69.3 (C-5), 79.8 (C-4), 101.9 (C-2), 126.1, 127.3, 128.1, 128.4, 128.6, 129.4 (CH-Ph), 136.6, 139.3 (C-q), 168.4 (C=O).

#### 6.4.3 Synthesis of (R)-methyl 3-((benzo[d][1,3]dioxol-4-ylmethyl)amino)-3-((2R,4R,5R)-5-hydroxy-2-phenyl-1,3-dioxan-4-yl)propanoate (**6b**)

Imine **5b** (171 mg; 0.50 mmol); 1-(*tert*-butyldimethylsilyloxy)-1-methoxyethene (110  $\mu\text{L}$ , 95 mg, 0.50 mmol);  $\text{BF}_3 \cdot \text{OEt}_2$  (62  $\mu\text{L}$ , 71 mg, 0.50 mmol). Product: yellow oil (150 mg, 0.36 mmol);  $\eta = 72\%$ ;  $[\alpha]_D^{24} = -16.0$  ( $c$  0.9, DCM); IR (nujol):  $\nu_{\text{max}}$  3330, 1731  $\text{cm}^{-1}$ ;  $^1\text{H}$  NMR (400 MHz,  $\text{CDCl}_3$ )  $\delta$  2.56 (dd,  $J = 16.4, 10.4$  Hz, 1H,  $H2'$ ), 2.93 (dd,  $J = 16.0, 3.2$  Hz, 1H,  $H2'$ ), 3.52 (dt,  $J = 10.4, 3.6$  Hz, 1H,  $H1'$ ), 3.65 (dd,  $J = 10.4, 9.5$  Hz, 1H,  $H6$ ), 3.66 (s, 3H, OMe), 3.79 (d,  $J = 12$  Hz, 1H,  $H1''$ ), 3.93 (dd,  $J = 9.2, 4.0$  Hz, 1H,  $H4$ ), 3.94 (d,  $J = 12.4$  Hz, 1H,  $H1''$ ), 3.99 (ddd,  $J = 9.2, 5.2, 4.8$  Hz, 1H,  $H5$ ), 4.33 (dd,  $J = 10.8, 5.2$  Hz, 1H,  $H6$ ), 5.53 (s, 1H,  $H2$ ), 5.94 (d,  $J = 2$  Hz, 2H,  $H8''$ ), 6.75-6.83 (m, 3H,  $H\text{Ph}$ ), 7.27-7.41 (m, 5H,  $H\text{Ph}$ );  $^{13}\text{C}$  NMR (100 MHz,  $\text{CDCl}_3$ )  $\delta$  33.9 (C-2'), 51.9 (OMe), 52.3 (C-1''), 56.7 (C-1'), 63.1 (C-5), 70.9 (C-6), 77.9 (C-4), 101.0 (C-8''), 101.6 (C-2), 108.3, 108.8, 121.7 (C-, C-4'', C-7''), 126.1, 126.2, 128.2, 128.4, 129.1 (CH-Ph), 132.3 (C-2''), 137.5 (C-q), 147.1 (C-q), 147.9 (C-q), 172.8 (C=O). Elemental Analysis, calcd for  $\text{C}_{22}\text{H}_{25}\text{NO}_5$ : C, 63.6; H, 6.07; N, 3.37. Found C, 63.2; H, 6.10; N, 3.10.

#### 6.4.4 Synthesis of (R)-methyl 3-((4-fluorobenzyl)amino)-3-((2R,4R,5R)-5-hydroxy-2-phenyl-1,3-dioxan-4-yl)propanoate (**6c**)

Imine **5c** (158 mg; 0.50 mmol); 1-(*tert*-butyldimethylsilyloxy)-1-methoxyethene (110  $\mu\text{L}$ , 95 mg, 0.50 mmol),  $\text{BF}_3 \cdot \text{OEt}_2$  (62  $\mu\text{L}$ , 71 mg, 0.50 mmol). Product: yellow oil (96 mg, 0.25 mmol);  $\eta = 50\%$ ;  $[\alpha]_D^{24} = -27.0$  ( $c$  0.6, DCM); IR (nujol):  $\nu_{\text{max}}$  3331, 1732  $\text{cm}^{-1}$ ;  $^1\text{H}$  NMR (400 MHz,  $\text{CDCl}_3$ )  $\delta$  2.67 (dd,  $J = 16.0, 9.2$  Hz, 1H,  $H2'$ ), 2.95 (dd,  $J = 16.8, 4.1$  Hz, 1H,  $H2'$ ), 3.60 (dt,  $J = 9.6, 4.0$  Hz,

1H, *H*1'), 3.64 (dd, *J* = 10.8, 9.6 Hz, 1H, *H*6), 3.66 (s, 3H, OMe), 3.93 (d, *J* = 13.2 Hz, 1H, *H*1''), 3.94 (dd, *J* = 9.2, 3.6 Hz, 1H, *H*4), 4.00 (ddd, *J* = 10.4, 9.2, 4.8 Hz, 1H, *H*5), 4.03 (d, *J* = 12.8 Hz, 1H, *H*1''), 4.33 (dd, *J* = 10.8, 5.2 Hz, 1H, *H*6), 5.51 (s, 1H, *H*2), 7.01-7.06 (m, 2H, *H*Ph), 7.27-7.47 (m, 7H, *H*Ph); <sup>13</sup>C NMR (100 MHz, CDCl<sub>3</sub>) δ 33.4 (C-2'), 51.3 (OMe), 52.0 (C-1''), 53.7 (C-1'), 62.7 (C-5), 70.9 (C-6), 78.3 (C-4), 101.6 (C-2), 115.4 (d, *J* = 21 Hz, C-4'' or C-6''), 115.7 (d, *J* = 21 Hz, C-4'' or C-6''), 126.1, 128.3, 128.4, 129.1, 129.5 (CH-Ph), 129.8 (d, *J* = 8.0 Hz, C-3'' or C-7''), 130.5 (d, *J* = 8.0 Hz, C-3'' or C-7''), 132.7, 137.3 (C-q), 162.5 (d, *J* = 246 Hz, C-5''), 172.5 (C=O). HRMS (ESI): calcd for [C<sub>21</sub>H<sub>26</sub>FNO<sub>5</sub>]: 390.1717 (M+H<sup>+</sup>); found: 390.1717.

#### 6.4.5 Synthesis of (R)-methyl 3-((4-chlorobenzyl)amino)-3-((2R,4R,5R)-5-hydroxy-2-phenyl-1,3-dioxan-4-yl)propanoate (6d)

Imine **5d** (222 mg; 0.67 mmol); 1-(*tert*-butyldimethylsilyloxy)-1-methoxyethene (150 μL, 130 mg; 0.67 mmol); BF<sub>3</sub>·OEt<sub>2</sub> (83 μL, 95 mg, 0.67 mol). Product: yellow oil (280 mg, 0.67 mmol); η = quant.  $[\alpha]_D^{24} = -42$  (c 0.6, DCM); IR (nujol): ν<sub>max</sub> 3327, 1728 cm<sup>-1</sup>; <sup>1</sup>H NMR (400 MHz, CDCl<sub>3</sub>) δ 2.57 (dd, *J* = 16.4, 10.0 Hz, 1H, *H*2''), 2.93 (dd, *J* = 16.0, 3.2 Hz, 1H, *H*2'), 3.50 (dt, *J* = 10.0, 3.6 Hz, 1H, *H*1'), 3.64 (dd, *J* = 10.4, 9.6 Hz, 1H, *H*6), 3.65 (s, 3H, OMe), 3.87 (d, *J* = 12.4 Hz, 1H, *H*1''), 3.91 (dd, *J* = 10.0, 4.0 Hz, 1H, *H*4), 3.98 (d, *J* = 12.8 Hz, 1H, *H*1''), 3.99 (ddd, *J* = 9.6, 5.2, 4.4 Hz, 1H, *H*5), 4.33 (dd, *J* = 10.8, 5.2 Hz, 1H, *H*6), 5.53 (s, 1H, *H*2), 7.26-7.39 (m, 7H, H-Ph), 7.45-7.48 (m, 2H, H-Ph); <sup>13</sup>C NMR (100 MHz, CDCl<sub>3</sub>) δ 33.9 (C-2'), 51.8 (OMe), 51.9 (C-1''), 56.8 (C-1'), 63.1 (C-5), 70.9 (C-6), 78.0 (C-4), 101.6 (C-2), 126.1, 128.3, 128.8, 129.1, 129.7 (CH-Ph), 133.4 (C-q), 136.9 (C-q), 137.4 (C-q) 172.8 (C=O). HRMS (ESI): calcd for [C<sub>21</sub>H<sub>26</sub>ClNO<sub>5</sub>]: 406.1421/ 408.1392 (M+H<sup>+</sup>); found: 406.1420/ 408.1392.

### 6.5 Treatment of the adducts 6a-d with acids

#### 6.5.1 Hydrochloric acid

##### 6.5.1.1 General procedure

i) To a solution of the β-aminoester **6a-d** (60-111 mg; 0.15-0.27 mmol) in dioxane (2-4 mL) was added hydrochloric acid 37 % (1.5-2.8 mL) to form a 6 M solution. The reaction mixture was stirred for 2 h at room temperature, evaporated in the rotary evaporator till a solid foam or a brown oil (a mixture of compounds **13** and **8** in a 2:1 ratio). The reaction mixture was used in the next stage.

ii) To the reaction mixture obtained in i) (60-111 mg, 0.15-0.27 mmol) was added water (2.5-3.3 mL) and solid KOH (23-33 mg, 0.14-0.20 mmol). The reaction mixture was stirred overnight. An aqueous suspension of acid resin IR-120 (H<sup>-</sup>) was added until pH 7, keeping hand stirring. The resin was filtered off, and the solvent removed in the rotary evaporator to give a pasty residue. This was dissolved in ethanol (2 mL), filtered and evaporated to give light brownish oils (20-70 mg, 0.074-0.26 mmol, 48 - 96.3 % yield), as the respective L-homoprolines **8a-d**.

#### 6.5.1.2 Synthesis of 2-((2*S*,3*S*,4*R*)-*N*-benzyl-3,4-dihydroxypyrrolidin-2-yl)acetic acid (**8a**)

i)  $\beta$ -Aminoester **6a** (100 mg, 0.27 mmol); 1,4-dioxane (3 mL); HCl 37% (2.5 mL). Quantitative mixture of compounds **13a:8a** in a 2:1 ratio, by <sup>1</sup>H NMR.

Compound **13a**<sup>a)</sup>: <sup>1</sup>H NMR (400 MHz, D<sub>2</sub>O)  $\delta$  3.10 (dd,  $J = 19.2, 2.0$  Hz, 1H, *H*3), 3.30 (dd,  $J = 19.2, 8.4$  Hz, 1H, *H*3), 3.78 (dd,  $J = 12.4, 2.0$  Hz, 1H, *H*7), 3.90 (dd,  $J = 12.4, 3.6$  Hz, 1H, *H*7), 4.17 (d,  $J = 13.2$  Hz, 1H, *H*1'), 4.32 – 4.36 (m, 2H, *H*3a + *H*6), 4.44 (d,  $J = 13.2$  Hz, 1H, *H*1'), 4.87 (dd  $J = 5.6, 4.4$  Hz, 1H, *H*6a), 7.44 – 7.51 (m, 10H, *H*Ph); <sup>13</sup>C NMR (100 MHz, D<sub>2</sub>O)  $\delta$  31.5 (C-3), 49.2 (C-1'), 55.6 (C-3a), 61.1 (C-7), 68.1 (C-6), 80.8 (C-6a), 128.9 (C-2), 129.0 (C-3' or C-4' or C-5'), 129.3 (C-3' or C-4' or C-5'), 129.5 (C-3' or C-4' or C-5'), 175.3 (C=O).

a) The <sup>1</sup>H NMR and <sup>13</sup>C NMR descriptions were taken from the crude material of reaction of compound **6a** with TFA, where was isolated a 3:1 ratio of compounds **13a** (3): **8a** (1).

ii) To the mixture obtained in step i) (72.6 mg) was added water (3.0 mL) and solid KOH (30 mg, 0.18 mmol). Product **8a**: (70 mg, 0.26 mmol);  $\eta = 96.3\%$ ;  $[\alpha]_D^{24} = -20.5$  ( $c = 0.4$ , MeOH); IR (nujol):  $\nu_{\max}$  3187, 1680 cm<sup>-1</sup>; <sup>1</sup>H NMR (400 MHz, D<sub>2</sub>O)  $\delta$  2.89 (dd,  $J = 18.0, 6.0$  Hz, 1H, *CH*<sub>2</sub>CO<sub>2</sub>H), 3.95 (dd,  $J = 18.0, 6.4$  Hz, 1H, *CH*<sub>2</sub>CO<sub>2</sub>H), 3.51 (dd,  $J = 12.0, 6.4$  Hz, 1H, *H*5), 3.65 (dd,  $J = 12.0, 4.0$  Hz, 1H, *H*5), 3.80 (td,  $J = 6.8, 3.2$  Hz, 1H, *H*2), 3.86 (td,  $J = 5.6, 4.0$  Hz, 1H, *H*4), 3.91 (dd,  $J = 5.6, 3.2$  Hz, 1H, *H*3), 4.32 (d,  $J = 13.2$  Hz, 1H, *H*1'), 4.46 (d,  $J = 13.2$  Hz, 1H, *H*1'), 7.54 (s, 5H, *H*Ph); <sup>13</sup>C NMR (100 MHz, D<sub>2</sub>O)  $\delta$  30.2 (*CH*<sub>2</sub>CO<sub>2</sub>H), 46.4 (C-1'), 52.9 (C-2), 59.3 (C-5), 66.0 (C-3), 70.3 (C-4), 126.6 (C-3' or C-4' or C-5'), 127.1 (C-3' or C-4' or C-5'), 127.2 (C-3' or C-4' or C-5'), 127.8 (C-2'), 172.2 (C=O); Elemental Analysis, calcd for C<sub>13</sub>H<sub>17</sub>NO<sub>4</sub>: C, 62.14; H, 6.82; N, 5.57. Found C, 62.20; H, 6.65; N, 5.76.

#### 6.5.1.3 Synthesis of 2-((2*S*,3*S*,4*R*)-*N*-piperonyl-3,4-dihydroxypyrrolidin-2-yl)acetic acid (**8b**)

i)  $\beta$ -Aminoester **6b** (100 mg, 0.24 mmol); 1,4-dioxane (3 mL); HCl 37% (2.5 mL). Quantitative mixture of compounds **13b** : **8b** in a 2:1 ratio.

Compound **13b** was identified by  $^1\text{H}$  NMR (400 MHz,  $\text{D}_2\text{O}$ )  $\delta$  3.00 (dd,  $J=18.8, 1.6$  Hz, 1H,  $H3$ ), 3.23 (dd,  $J=18.8, 8.0$  Hz, 1H,  $H3$ ), 3.72 (dd,  $J=12.4, 2.0$  Hz, 1H,  $H7$ ), 3.84 (dd,  $J=12.0, 3.2$  Hz, 1H,  $H7$ ), 4.03 (d,  $J=13.2$  Hz, 1H,  $H1'$ ), 4.14 (d,  $J=13.6$  Hz, 1H,  $H1'$ ), 4.25-4.31 (m, 2H,  $H3a + H6$ ), 4.67 (dd,  $J=5.6, 4.8$  Hz, 1H,  $H6a$ ), 5.95 (s, 2H,  $H8'$ )<sup>a)</sup>, 6.88-6.94 (m, 3H,  $H\text{Ph}$ )<sup>a)</sup>.

a) These signals are coincident in the  $^1\text{H}$  NMR spectrum of the mixture of the two compounds **13b** and **8b**.

ii) To a mixture obtained in step i) (78 mg) was added water (3.0 mL) and solid KOH (30 mg, 0.18 mmol). Product **8b**: (56 mg, 0.19 mmol);  $\eta = 79\%$ ;  $[\alpha]_D^{24} = -25.0$  ( $c$  0.6, MeOH); IR (nujol):  $\nu_{\text{max}}$  3350, 1586  $\text{cm}^{-1}$ ;  $^1\text{H}$  NMR (400 MHz,  $\text{D}_2\text{O}$ )  $\delta$  2.40-2.70 (m, 2H,  $\text{CH}_2\text{CO}_2\text{H}$ ), 3.47-3.58 (m, 2H,  $H4 + H5$ ), 3.68 (br d,  $J=12.0$  Hz, 1H,  $H5$ ), 3.82 (br s, 2H,  $H3 + H4$ ), 4.12 (d,  $J=13.2$  Hz, 1H,  $H1'$ ), 4.24 (d,  $J=13.2$  Hz, 1H,  $H1'$ ), 5.93 (s, 1H,  $H8'$ ), 5.94 (s, 1H,  $H8'$ ), 6.85-6.94 (m, 3H,  $H\text{Ph}$ );  $^{13}\text{C}$  NMR (100 MHz,  $\text{D}_2\text{O}$ )  $\delta$  35.5 ( $\text{CH}_2\text{CO}_2\text{H}$ ), 48.8 (C-1'), 55.5 (C-2), 61.7 (C-5), 69.6 (C-3), 72.7 (C-4), 100.9 (C-8'), 108.3, 109.1, 122.9 (CH-Ph), 127.2, 146.9, 147.1 (C-q), 178.1 (C=O). HRMS (ESI): calcd for  $[\text{C}_{14}\text{H}_{20}\text{NO}_7]$ : 314.1234 (M+ $\text{H}_2\text{O}$ +H); found: 314.1233.

#### 6.5.1.4 Synthesis of 2-((2*S*,3*S*,4*R*)-*N*-(4-fluorobenzyl)-3,4-dihydropyrrolidin-2-yl)acetic acid (**8c**)

i)  $\beta$ -Aminoester **6c** (60 mg, 0.15 mmol); solvent: 1,4-dioxane (2 mL); HCl 37% (1.5 mL). Quantitative mixture of compounds **13c** : **8c** in a 2:1 ratio. Compound **13c** was identified by  $^1\text{H}$  NMR (400 MHz,  $\text{D}_2\text{O}$ )  $\delta$  2.91 (dd,  $J=19.2, 2.0$  Hz, 1H,  $H3$ ), 3.12 (dd,  $J=19.2, 8.0$  Hz, 1H,  $H3$ ), 3.59 (dd,  $J=12.4, 2.0$  Hz, 1H,  $H7$ ), 3.70 (dd,  $J=12.4, 3.2$  Hz, 1H,  $H7$ ), 3.99 (d,  $J=13.6$  Hz, 1H,  $H1'$ ), 4.10 (d,  $J=13.2$  Hz, 1H,  $H1'$ ), 4.23-4.27 (m, 2H,  $H3a + H6$ ), 4.77 (dd,  $J=6.0, 4.4$  Hz, 1H,  $H6a$ ), 7.01-7.05 (t, 2H,  $H4' + H6'$ ), 7.28-7.31 (m, 2H,  $H3' + H7'$ ).

ii) To a mixture obtained in step i) (43 mg) was added water (2.5 mL) and solid KOH (23 mg, 0.14 mmol). Product **8c**: (20 mg, 0.074 mmol);  $\eta = 48\%$ ;  $[\alpha]_D^{24} = -23.0$  ( $c$  0.6, MeOH); IR (nujol):  $\nu_{\text{max}}$  3347, 2926, 2856, 1660  $\text{cm}^{-1}$ ;  $^1\text{H}$  NMR (400 MHz,  $\text{D}_2\text{O}$ )  $\delta$  2.55 (dd,  $J=14.8, 6.8$  Hz, 1H,  $\text{CH}_2\text{CO}_2\text{H}$ ), 2.60 (dd,  $J=14.8, 6.4$  Hz, 1H,  $\text{CH}_2\text{CO}_2\text{H}$ ), 3.27 (td,  $J=6.8, 2.8$  Hz, 1H,  $H2$ ),



3.50 (dd,  $J = 12.0$  Hz, 6.0 Hz, 1H,  $H_5$ ), 3.67 (dd,  $J = 12.0$  Hz, 4.8 Hz, 1H,  $H_5$ ), 3.73 (dd,  $J = 6.0$ , 2.8 Hz, 1H,  $H_3$ ), 3.76-3.80 (m, 1H,  $H_4$ ), 3.79 (d,  $J = 12.8$  Hz, 1H,  $H_{1'}$ ), 3.96 (d,  $J = 13.2$  Hz, 1H,  $H_{1'}$ ), 7.13-7.18 (m, 2H,  $H_{Ph}$ ), 7.39-7.43 (m, 2H,  $H_{Ph}$ );  $^{13}C$  NMR (100 MHz,  $D_2O$ )  $\delta$  38.5 ( $CH_2CO_2H$ ), 49.5 (C-1'), 55.7 (C-2), 62.3 (C-5), 71.5 (C-3), 73.4 (C-4), 115.2 (d,  $J = 22.0$  Hz, C-4' or C-6'), 115.4 (d,  $J = 22.0$  Hz, C-4' or C-6'), 130.5 (d,  $J = 8.0$  Hz, C-3' or C-7'), 130.6 (d,  $J = 8.0$  Hz, C-3' or C-7'), 134.2 (C-2'), 161.9 (d,  $J = 241.0$  Hz, C-5'), 180.3 (C=O). HRMS (ESI): calcd for  $[C_{13}H_{19}FNO_5]$ : 288.1242 (M+H $_2O$ +H $^+$ ); found: 288.1242.

#### 6.5.1.5 Synthesis 2-((2*S*,3*S*,4*R*)-*N*-(4-Chlorobenzyl)-3,4-dihydropyrrolidin-2-yl)acetic acid (8d)

i)  $\beta$ -Aminoester **6d** (111 mg, 0.27 mmol); solvent: 1,4-dioxane (4 mL); HCl 37% (2.8 mL). Quantitative mixture of compounds **13d** : **8d** in a 2:1 ratio. Compound **13d** was identified by  $^1H$  NMR (400 MHz,  $D_2O$ )  $\delta$  3.02 (dd,  $J = 19.2$ , 2.0 Hz, 1H,  $H_3$ ), 3.23 (dd,  $J = 19.2$ , 8 Hz, 1H,  $H_3$ ), 3.70 (dd,  $J = 12.4$ , 2.0 Hz, 1H,  $H_7$ ), 3.83 (dd,  $J = 12.4$ , 3.6 Hz, 1H,  $H_7$ ), 4.09 (d,  $J = 13.2$  Hz, 1H,  $H_{1'}$ ), 4.22-4.29 (m, 2H,  $H_{3a} + H_6$ ), 4.35 (d,  $J = 13.2$  Hz, 1H,  $H_{1'}$ ), 4.80 (dd,  $J = 6.0$ , 4.8 Hz, 1H,  $H_{6a}$ ), 7.34-7.45 (m, 4H,  $H_{Ph}$ ).

ii) Mixture obtained in step i) (83 mg) in water (3.3 mL) was added solid KOH (33 mg, 0.20 mmol). Product **8d**: (66 mg; 0.23 mmol);  $\eta = 85.0$  %;  $[\alpha]_D^{24} = +6.0$  ( $c$  0.7, MeOH); IR (nujol):  $\nu_{max}$  3346, 1690  $cm^{-1}$ ;  $^1H$  NMR (400 MHz,  $D_2O$ )  $\delta$  2.64 (dd,  $J = 16.4$  Hz, 6.8 Hz, 1H,  $CH_2CO_2H$ ), 2.70 (dd,  $J = 16.4$  Hz, 6.4 Hz, 1H,  $CH_2CO_2H$ ), 3.52 (dd,  $J = 11.6$  Hz, 5.6 Hz, 1H,  $H_5$ ), 3.60 (td,  $J = 6.4$  Hz, 3.2 Hz, 1H,  $H_2$ ), 3.67 (dd,  $J = 12.8$  Hz, 4.4 Hz, 1H,  $H_5$ ), 3.80-3.87 (m, 2H,  $H_3 + H_4$ ), 4.16 (d,  $J = 13.2$  Hz, 1H,  $H_{1'}$ ), 4.28 (d,  $J = 13.2$  Hz, 1H,  $H_{1'}$ ), 7.44 (d,  $J = 8.4$  Hz, 2H,  $H_{Ph}$ ), 7.48 (d,  $J = 8.4$  Hz, 2H,  $H_{Ph}$ );  $^{13}C$  NMR (100 MHz,  $D_2O$ )  $\delta$  34.4 ( $CH_2CO_2H$ ), 47.8 (C-1'), 55.9 (C-2), 61.6 (C-5), 69.1 (C-3), 72.6 (C-4), 128.7, 130.7 (CH-Ph), 130.5, 134.1 (C-q), 177.4 (C=O). HRMS (ESI): calcd for  $[C_{13}H_{17}ClNO_4]$ : 286.0846 (M+H $^+$ ); found: 286.0851.

### 6.5.2 Trifluoroacetic acid

#### 6.5.2.1 Formation of a mixture of salts of trifluoroacetic acid: (3*aR*,6*R*,6*aS*)-4-benzyl-6-hydroxyhexahydro-2*H*furo[3,2-*b*]pyrrol-2-one (13a), and 2-((2*R*,3*S*,4*R*)-1-benzyl-3,4-dihydropyrrolidin-2-yl) acetic acid (8a)

To a solution of the  $\beta$ -aminoester **6a** (30 mg; 0.08 mmol) in 1,4-dioxane (1.62 mL) was added

trifluoroacetic acid till a 6 M acid solution was formed (1.38 mL). The reaction mixture was run at room temperature, under magnetic stirring for one week. The solvents were removed in the rotary evaporator, leaving a brownish oil consisting of a virtually pure mixture of compounds **13a** and **8a**, in a 3:1 ratio and quantitative yield.

### 6.5.3 Bromidic acid in acetic acid

#### 6.5.3.1 Formation of a mixture of salts of hydrobromidic acid: (3*a*,*R,R*,6*a*,*S*)-4-benzyl-6-hydroxyhexahydro-2*H*furo[3,2-*b*]pyrrol-2-one (**13a**), and 2-((2*R*,3*S*,4*R*)-1-benzyl-3,4-dihydropyrrolidin-2-yl) acetic acid (**8a**)

A solution of the  $\beta$ -aminoester **6a** (50 mg; 0.13 mmol) in 33 % bromidic acid in acetic acid (1 mL) was stirred at room temperature for 2 hours. Then was added methanol (3.6 mL), and the reaction mixture was kept under magnetic stirring for three days. The solvents were removed in the rotary evaporator, leaving a brownish oil consisting of a virtually pure mixture of compounds **13a** and **8a**, in a 1:1 ratio and quantitative yield.

#### 6.5.3.2 Cleavage of the benzyl group in compound **8a** to give **8e**

To the benzylated L-homoproline (**8a**) (20 mg, 0.075 mmol) in MeOH (4 mL) in presence of catalyst (Pd/C 10 mol%) was added 1,1,2-trichloroethane (8  $\mu$ L, 1.1 eq.). The mixture was stirred for 2 days under hydrogen atmosphere (1 atm). The mixture was filtered through glass-fiber filter. To the filtrate was added KOH 0.01 M aq. solution to till pH=12. The solvent was removed in the rotary evaporator to give an yellow oil, compound **8e** (12 mg, 0.061 mmol);  $\eta = 81\%$ ;  $[\alpha]_D^{21} = -32.3$  ( $c$  0.01, MeOH); IR (nujol):  $\nu_{\max}$  3328, 3257, 1722  $\text{cm}^{-1}$ ;  $^1\text{H}$  NMR (400 MHz,  $\text{D}_2\text{O}$ )  $\delta$  2.41 (dd,  $J = 7.6$  Hz, 15.2 Hz, 1H,  $\text{CHCO}_2\text{H}$ )<sup>a)</sup>, 2.58 (dd,  $J = 5.2$  Hz, 14.8 Hz, 1H,  $\text{CH}_2\text{CO}_2\text{H}$ ), 3.23 (q,  $J = 5.2$  Hz, 1H, *H*2), 3.63-3.68 (m, 1H, *H*4), 3.23 (t,  $J = 4.8$  Hz, 1H, *H*3), 3.76-3.84 (m, 2H, *H*5);  $^{13}\text{C}$  NMR (100 MHz,  $\text{D}_2\text{O}$ )  $\delta$  32.2( $\text{CH}_2\text{CO}_2\text{H}$ ), 61.8 (C-2), 62.4 (C-5), 71.5 (C-3), 72.6 (C-4), 179.2 (C=O);\* HRMS (ESI), calcd for  $[\text{C}_6\text{H}_{12}\text{NO}_4]$ : 162.0761 ( $\text{M}+\text{H}^+$ ); found: 162.0758.

<sup>a)</sup> contaminated with DMSO

## 6.6 Computational Calculations (Methodology)

All geometry optimizations were performed with Gaussian 09<sup>22</sup> by applying density functional theory [23] with the B3LYP functional [24-28] together with the 6-31G(d) basis set [29-32].

In all geometry optimizations, we first searched for the transition state starting from a structure like a reactant model. This was generally obtained with unidimensional scans along the particular reaction coordinate in which we were interested. Once a putative transition structure was located, it was fully optimized and characterized. Subsequently, the reactants and products associated with the calculated transition state structures were determined through intrinsic reaction coordinate (IRC) calculations that were followed by a final geometry optimization [33]. In all cases, the geometry optimizations and the stationary points were obtained with standard Gaussian convergence criteria. The transition-state structures, reactants, and products were all verified by vibrational frequency calculations. All the TS structures have only one imaginary frequency with the correct transition vector, whereas the reactant and products have all the frequencies positives.

The free final energies were calculated with density functional theory, as a sum of the electronic energies, using the all-electron 6-311++G(3df,2pd) basis set and the functional M06-2X, plus the ZPE, thermal, and entropic energies ( $T = 310.15$  K,  $P = 1$  bar), calculated with B3LYP functional but with the 6-31G(d) basis set and the dispersion corrections with the DFT-D3 methodology [34,35]. This value has also added the contribution of a conductor-like polarizable continuum model using the integral equation formalism variant (IEF-PCM) [36-38], as implemented in Gaussian 09, to simulate the different solvents employed in the experimental work. To this end, different dielectric constants were applied: water, 78.355; Acetic Acid, 6.2528 and 1,4-dioxane, 2.210.

All the activation and reaction energies provided in the text and figures refer to free energy differences calculated at the M06-2X /6-311++G(3df,2pd) level of theory.

## 7. References

1. Hannessian, S., Total Synthesis of Natural Products: The Chiron Approach. Pergamon, Oxford, **1983**.
2. Miyashita, M.; Chida, N.; Yoshikoshi, A., Synthesis and absolute configuration of the p-nitrobenzyl ester of SQ 27860. *J. Chem. Soc., Chem. Commun.*, **1984**, 195.
3. Bernotas, R.C.; Ganem, B., Synthesis of 2S-carboxy-3R,4R,5S-trihydroxypiperidine; a naturally occurring inhibitor of  $\beta$ -D-glucuronidase. *Tetrahedron Lett.*, **1985**, 26, 4981.
4. Zanardi, F.; Battistini, L.; Nespi, M.; Rassu, G.; Spanu, P.; Cornia, M.; Casiraghi, G., Total synthesis of both enantiomers of trans-2,3-cis-3,4-dihydroxyproline. *Tetrahedron: Asymmetry* **1996**, 7, 4, 1167-1180; Fujii, M.; Miura, T.; Kajimoto, T.; Ida, Y., Facile Synthesis of 3,4-Dihydroxyprolines as an Application of the L-

- Threonine Aldolase-Catalyzed Aldol Reaction. *Synlett* **2000**, 1046; Taylor, C.M.; Jones, C.E.; Bopp, K., The conversion of pentoses to 3,4-dihydroxyprolines. *Tetrahedron* **2005**, *61*, 9611–9617.
5. Nakajima, T.; Volcani, B. E., 3,4-Dihydroxyproline: A New Amino Acid in Diatom Cell Walls. *Science* **1969**, *164*, 1400–1401; Karle, I. L.; Daly, J. W.; Witkop, B., 2, 3-cis-3, 4-trans-3, 4-Dihydroxy-L-proline: Mass Spectrometry and X-ray Analysis. *Science* **1969**, *164*, 1401–1402; Karle, I. L., The structure of a new natural amino acid, 2,3-cis-3,4-trans-3,4-dihydroxy-L-proline. *Acta Crystallogr., Sect. B* **1970**, *26*, 765–770.
  6. Buku, A.; Faulstich, H.; Wieland, T.; Dabrowski, 2,3-trans-3,4-trans-3,4-Dihydroxy-L-proline: An amino acid in toxic peptides of *Amanita virosa* mushrooms. *J. Proc. Natl. Acad. Sci. U.S.A.* **1980**, *77*, 2370–2371.
  7. Faulstich, H.; Buku, A.; Bodenmueller, H.; Wieland, T., Virotoxins: actin-binding cyclic peptides of *Amanita virosa* mushrooms. *Biochemistry* **1980**, *19*, 3334–3343.
  8. Csatajov, K.; Davies, S.G.; Figuccia, A. L.A.; Fletcher, A.M.; Ford, J.G.; Lee, J.A.; Roberts, P.M.; Saward, B.G.; Song, H.; Thomson J.E., Asymmetric syntheses of polysubstituted homoprolines and homoprolinols. *Tetrahedron* **2015**, *71*, 9131-9142; Davies, S.G.; Foster, E.M.; Lee, J. A.; Roberts, P.M.; Thomson, J.E., Asymmetric syntheses of dihydroxyhomoprolines via doubly diastereoselective lithium amide conjugate addition reactions. *Tetrahedron* **2013**, *69*, 8680.
  9. Freitas, D. S.; Noro, J.; Drogalin, A.; Fernandes, M.C.S.; Baptista, A.V.M.; Parente, J.F.C.; Rodríguez-Borges, J. E.; Gil Fortes, A.; Alves, M.J., A Short Synthesis of (2S,3S,4R)-Dihydroxyhomoprolines from D-Erythrose-Derived 5,6-Dihydro-2H-pyran-2-one. *Synthesis* **2019**, *51*, 2720-272.
  10. Vass, E.; Hollósi, M.; Besson, F.; Buchet, R., Vibrational Spectroscopic Detection of Beta- and Gamma-Turns in Synthetic and Natural Peptides and Proteins. *Chem. Rev.* **2003**, *103*, 1917-1954.
  11. Smith, J. A.; Pease, L. G., Reverse Turns in Peptides and Protein. *CRC Crit. Rev. Biochem.* **1980**, *8*, 315-399.
  12. Gierasch, L. M.; Deber, C. M.; Madison, V.; Niu, C. H.; Blout, E. R., Conformations of (X-L-Pro-Y)<sub>2</sub> cyclic hexapeptides. Preferred  $\beta$ -turn conformers and implications for  $\beta$  turns in proteins. *Biochem.* **1981**, *20*, 4730-4738.
  13. Rose, G. D.; Gierasch, L. M.; Smith, J. A., Turns in Peptides and Proteins. *Adv. Protein Chem.* **1985**, *37*, 1-109.
  14. Kuntz, I. D., Protein folding. *J. Am. Chem. Soc.* **1972**, *94*, 4009-4012.
  15. Sussman, F.; Sánchez-Pedregal, V. M.; Estévez, J. C.; Balo, R.; Jiménez-Barbero, J.; Ardá, A.; Gimeno A.; Royo, M.; Villaverde, M. C.; Estévez, R.J., Factors Governing MgO(111) Faceting in the Thermal Decomposition of Oxide Precursors. *Chem: Eur J.*, **2018**, *24*, 1-6.
  16. Chung, Y. J.; Christianson, L. A.; Stanger, H. E.; Powell, D. R.; Gellman, S. H., A  $\beta$ -Peptide Reverse Turn that Promotes Hairpin Formation. *J. Am. Chem. Soc.* **1998**, *120*, 10555-10556.
  17. Schumann, F.; Müller, A.; Kocsch, M.; Müller, G.; Sewald, N., Are  $\beta$ -Amino Acids  $\gamma$ -Turn Mimetics? Exploring A New Design Principle for Bioactive Cyclopeptides. *J. Am. Chem. Soc.* **2000**, *122*, 12009-12010.
  18. Baker, S.R.; Clissold, D.W.; McKillop, A., Synthesis of leukotriene A4 methyl ester from D-glucose. *Tetrahedron Lett.* **1988**, *29*, 991–994; Zimmermann, P.; Schmidt, R.R., Synthese von erythro-Sphingosinen über die Azidoderivate. *Liebigs Ann. Chem.* **1988**, 663–667.

19. Fengler-Veith, M.; Schwardt, O.; Kautz, U.; Krämer, B.; Jäger, V., (1'R)-(-)-2,4-O-ETHYLIDENE-D-ERYTHROSE AND ETHYL (E)-(-)-4,6-O-ETHYLIDENE-(4S,5R,1'R)-4,5,6-TRIHYDROXY-2-HEXENOATE. *Org. Synth. Coll.*, **10**, **2004**, 405; *Org. Synth.* **78**, **2002**, 123.
20. Ferreira, J.; Duarte, V.C.M., Noro, J.; Gil Fortes, A.; Alves, M.J., Total facial selectivity of a D-erythrosyl aromatic imine in  $[4\pi + 2\pi]$  cycloadditions; synthesis of 2-alkylpolyol 1,2,3,4-tetrahydroquinolines. *Org. Biomol. Chem.*, **2016**, **14**, 2930 – 2937.
21. Rocha, J. F.; Freitas, D. S.; Noro, J.; Teixeira, C. S. S.; Sousa, C.E.A.; Alves, M. J.; Cerqueira N. M. F. S. A., Total Stereoselective Michael Addition of N- and S- Nucleophiles to a D-Erythrosyl 1,5-Lactone Derivative. Experimental and Theoretical Studies Devoted to the Synthesis of 2,6-Dideoxy-4-functionalized-d- ribonohexono-1,4-lactone. *J. Org. Chem.*, **2018**, **83**, 8011–8019.
22. Frisch, M. J., Trucks, G. W.; Schlegel, H. B.; Scuseria, G. E.; Robb, M. A.; Cheeseman, J. R.; Scalmani, G.; Barone, V.; Mennucci, B.; Petersson, G. A.; Nakatsuji, H.; Caricato, M.; Li, X.; Hratchian, H. P.; Izmaylov, A. F.; Bloino, J., Zheng, G.; Sonnenberg, J. L.; Hada, M.; Ehara, M.; Toyota, K.; Fukuda, R.; Hasegawa, J.; Ishida, M.; Nakajima, T.; Honda, Y.; Kitao, O.; Nakai, H.; Vreven, T.; Montgomery, J. A.; Jr, Peralta, J. E.; Ogliaro, F.; Bearpark, M. J.; Heyd, J.; Brothers, E. N.; Kudin, K. N.; Staroverov, V. N.; Kobayashi, R.; Normand, J.; Raghavachari, K.; Rendell, A. P.; Burant, J. C.; Iyengar, S. S.; Tomasi, J.; Cossi, M.; Rega, N.; Millam, N. J.; Klene, M.; Knox, J. E.; Cross, J. B.; Bakken, V.; Adamo, C.; Jaramillo, J.; Gomperts, R.; Stratmann, R. E.; Yazyev, O.; Austin, A. J.; Cammi, R.; Pomelli, C.; Ochterski, J. W.; Martin, R. L.; Morokuma, K.; Zakrzewski, V. G.; Voth, G. A.; Salvador, P.; Dannenberg, J. J.; Dapprich, S.; Daniels, A. D.; Farkas, Ö.; Foresman, J. B.; Ortiz, J. V.; Cioslowski, J.; and Fox, D. J. (2009) Gaussian 09. Gaussian, Inc., Wallingford, CT, USA.
23. Hohenberg, P.; Kohn, W., Inhomogeneous Electron Gas. *Phys. Rev.* **1964**, **136** (3b), B864.
24. Becke, A. D., A new mixing of Hartree–Fock and local density-functional theories. *J. Chem. Phys.* **1993**, **98** (2), 1372-1377.
25. Becke, A. D., Density-functional thermochemistry. III. The role of exact exchange. *J. Chem. Phys.* **1993**, **98** (7), 5648-5652.
26. Lee, C. T.; Yang, W. T.; Parr, R. G., Development of the Colle-Salvetti correlation-energy formula into a functional of the electron density. *Phys. Rev. B: Condens. Matter Mater. Phys.* **1988**, **37** (2), 785-789.
27. Vosko, S. H.; Wilk, L.; Nusair, M., Accurate spin-dependent electron liquid correlation energies for local spin density calculations: a critical analysis. *Can. J. Phys.* **1980**, **58** (8), 1200- 1211.
28. Stephens, P. J.; Devlin, F. J.; Chabalowski, C. F.; Frisch, M. J., Ab Initio Calculation of Vibrational Absorption and Circular Dichroism Spectra Using Density Functional Force Fields. *J. Phys. Chem.* **1994**, **98** (45), 11623 11627.
29. Rassolov, V. A.; Ratner, M. A.; Pople, J. A.; Redfern, P. C.; Curtiss, L., 6-31G\* basis set for third-row atoms. *J. Comput. Chem.* **2001**, **22** (9), 976-984.
30. Ditchfield, R.; Hehre, W. J.; Pople, J. A., Self-Consistent Molecular-Orbital Methods. IX. An Extended Gaussian-Type Basis for Molecular-Orbital Studies of Organic Molecules. *J. Chem. Phys.* **1971**, **54** (2), 724.
31. Hariharan, P. C.; Pople, J. A., Accuracy of AH n equilibrium geometries by single determinant molecular orbital theory. *Mol. Phys.* **1974**, **27** (1), 209-214.

32. Gordon, M. S.; The isomers of silacyclopropane. *Chem. Phys. Lett.* **1980**, 76 (1), 163-168.
33. Cerqueira, N.; Fernandes, P. A.; Ramos, M. J., Protocol for Computational Enzymatic Reactivity Based on Geometry Optimisation. *ChemPhysChem* **2018**, 19 (6), 669-689.
34. Grimme, S.; Antony, J.; Ehrlich, S.; Krieg, H., A consistent and accurate ab initio parametrization of density functional dispersion correction (DFT-D) for the 94 elements H-Pu. *J. Chem. Phys.* **2010**, 132 (15), 154104.
35. Grimme, S.; Ehrlich, S.; Goerigk, L., Effect of the damping function in dispersion corrected density functional theory. *J. Comput. Chem.* **2011**, 32 (7), 1456-65.
36. Scalmani, G.; Frisch, M. J., Continuous surface charge polarizable continuum models of solvation. I. General formalism. *J. Chem. Phys.* **2010**, 132 (11), 114110.
37. Cancès, E.; Mennucci, B.; Tomasi, J., A new integral equation formalism for the polarizable continuum model: Theoretical background and applications to isotropic and anisotropic dielectrics. *J. Chem. Phys.* **1997**, 107 (8), 3032-3041.
38. Tomasi, J.; Mennucci, B.; Cammi, R., Quantum mechanical continuum solvation models. *Chem. Rev.* **2005**, 105 (8), 2999-3093.

# 5

Synthesis of Fused Triazole, Pyrazole, and Isoxazole  
from Lactone

*The results presented in this chapter are in the publication:*

**Total Facial Discrimination of 1,3-Dipolar Cycloadditions in a D-Erythrose 1,3-Dioxane Template.  
Computational Studies of a Concerted Mechanism.**

Cristina E. A. Sousa, Antonio M. P. Ribeiro, Antonio Gil Fortes, Nuno M. F. S. A. Cerqueira, and  
Maria J. Alves

*JOC*, 2017, 82, 982–99



## 1. Abstract

A new D-erythrose 1,3-dioxane derivative was synthesized from D-glucose and found to be a highly stereoselective template as a dipolarophile. Different 1,3-dipoles of allenyl-type were employed, giving different regioselectivities, depending on its nature; the regioselectivity is complete with alkyl azides and phenyldiazomethane, but is inexistence with nitrile oxides. Computational studies were performed to understand the mechanisms of cycloadditions. All the studied cycloadditions were found to be concerted involving small free activation energies and are all exergonic. The stereoselectivity is due to a combined result of the steric effect H-8a and the hyperconjugative effect of the  $\text{C-O}$  to the incoming 1,3-dipole. The regioselectivity observed in alkyl azides and phenyldiazomethane is mostly dependent on the distortion effect during the cycloaddition process. This distortion effect is however higher in the alkyl azide compounds than in phenyldiazomethane.

## 2. Introduction

The synthesis of multiple stereogenic center molecules, can be efficiently made by adding up small chiral synthons to build larger structures [1]. Tetroses are in this context interesting versatile fragments, useful in the synthesis of iminosugars of several types [2]. 2,4-*O*-Ethylidene/benzylidene-D-erythroses are tetroses easily accessed in large scale from cheap D-glucose in two steps. In particular, the synthesis of benzylidene-D-erythrose [3,4] is a quite accessible starting material. Wittig elongation of the aldehyde function would generate  $\alpha,\beta$ -unsaturated carbonyl compounds to which many applications in syntheses can be ascribed [5]. In fact, the compounds are scarcely known in the literature. This is probably due to a poor facial selectivity of the olefinic portion in reactions, connected to its high degree of freedom. Elongation of 2,4-*O*-ethylidene D-erythrose with simultaneous functionalization of the olefinic portion was attempted before by reaction with sulphur ylides, but a 3:2 mixture of diastereomeric epoxides was obtained [6]. Reasoning that the lock of the double bond into a six-membered ring would improve the stereo-selectivity of the reactions, a  $\delta$ -lactone was obtained from the *Z*-stereoisomer. Besides, the  $\alpha,\beta$ -unsaturated lactone bearing a well-exposed electronic  $\pi$  cloud would enable a better reactivity than the open-chain precursor. This compound can be envisaged as a good 1,4-Michael acceptor, and as an electron-poor dipolarophile/dienophile.

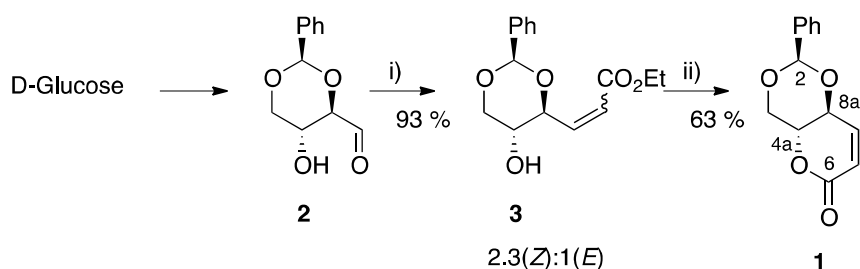
In the present work, the lactone was synthesized and reacted with alkyl azides, phenyldiazomethane, and nitrile oxides by  $[3\pi+2\pi]$  cycloaddition to afford the respective adducts. The concept of “cycloaddition” gives a formal description of the overall reaction but not a mechanistic interpretation. Unlike the Diels–Alder reaction, in the case of  $[3+2]$  cycloadditions the principal question is whether the new  $\sigma$ -bonds that are generated during the fusion of the 1,3-dipole with the dipolarophile, and from which results a five-membered ring, occurs in a concerted or stepwise way. In addition, the cycloaddition can follow different routes depending on the nature of the 1,3-dipole molecule. It can have a polar character when the reactant displays electrophile or nucleophile activities [7], a bi-radical character [8] or even a non-polar character [9].

In order to understand the mechanism of the  $[3+2]$  cycloadditions, the free energy profile of these reactions was studied by theoretical and computational means.

### 3. Results and Discussion

#### 3.1 Synthesis of lactone 1

As far as we know lactone **1** is a new compound with non-studied reactivity and selectivity. It was obtained from D-erythrose derivative **2** by Wittig olefination with methyl (triphenylphosphoranylidene)acetate. First a 2.3:1 ratio of *Z* and *E* isomers **3** was obtained. The isomeric mixture was heated in dry toluene in the presence of silica in a rotary evaporator for several hours. After consumption of the *Z* isomer, the crude was chromatographed to give lactone **1** in 63 % overall yield, from D-erythrose derivative **2** (Scheme 1).

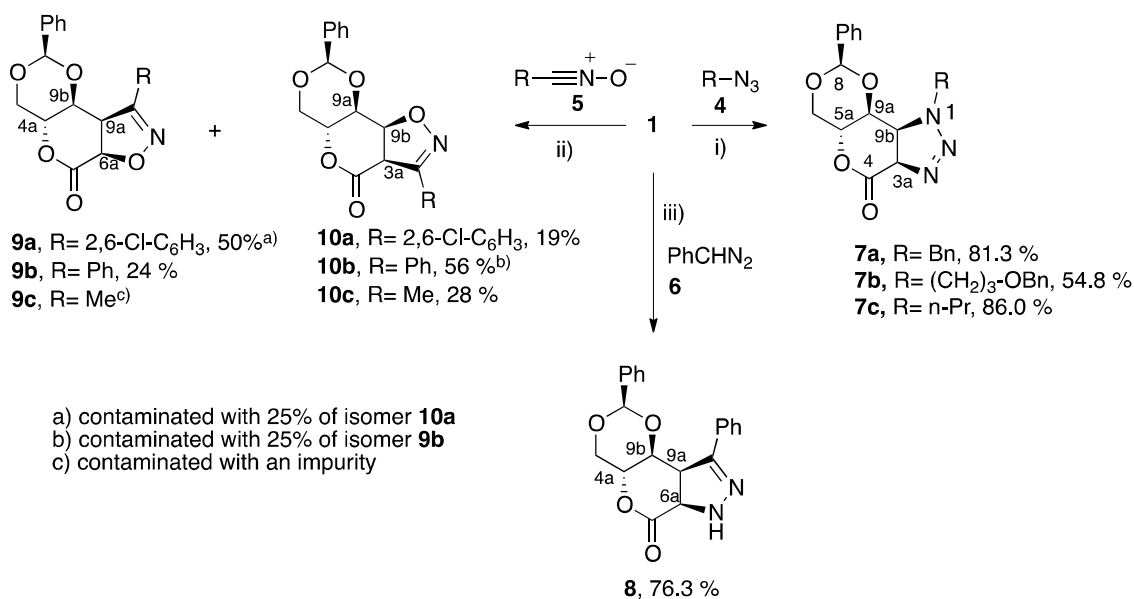


**Scheme 1** - Synthesis of lactone **1**

**i)** methyl (triphenylphosphoranylidene)acetate, *p*-TsOH (cat), dry THF, 23h, rt; **ii)** silica, dry toluene, 75 °C, vacuum.

3.2 1,3-Cycloadditions of lactone **1** with 1,3-dipoles

Lactone **1** was reacted with three types of 1,3-dipoles: alkyl azides (**4**), nitrile oxides (**5**), and a diazo compound (**6**). According to the nature of the 1,3-dipole, reactions took place within a large range of temperatures, from rt to 102 °C. In the cases of alkyl azides and the diazo compound products are isolated as single isomers, within the detection limit of  $^1\text{H}$  NMR spectroscopy. With nitrile oxides the *stereo*-selectivity of reactions continue to be effective, but the *regio*-selectivity is not (Scheme 2).



**Scheme 2** - 1,3-Dipolar cycloaddition of lactone **1** to azides, nitrile oxides and phenyldiazomethane

i) a) benzyl azide (2 eq.), HC(OMe)<sub>3</sub>, reflux, 65 h; b) (3-azidopropoxy)methyl benzene (2eq.), 95 °C, 44 h; c) *n*-propyl azide, (1 eq., every 3 hours for 30h); 95 °C; ii) a) 2,6-dichloro-*N*-hydroxybenzimidoyl chloride, dry ether, Et<sub>3</sub>N, 0° - rt, 15 h; b) *N*-hydroxybenzimidoyl chloride, dry ether, Et<sub>3</sub>N, 0° - rt, 12 h; c) NCS, acetaldehyde oxime, pyridine then Et<sub>3</sub>N in toluene, 0° - rt, 15h; iii) phenyldiazomethane, toluene, 60-70 °C, 1h15m.

Intermolecular reactions of alkenes to azides are known but not common, and require harsh conditions, due to the poor reactivity of the reactants [10]. On the other hand, intramolecular 1,3-cycloadditions are frequent, although triazolines cycloadducts are rarely isolated, and in most cases the chiral center(s) formed are destroyed in the following rearrangements. Nevertheless, reaction of tri-*O*-acetyl-D-glucal with alkyl azides occurred before at high temperature in trimethyl- or triethylorthoformate, and the respective triazolines were isolated in good yields and with complete *stereo*-selectivity [11]. Inspired by these reactions lactone **1** was combined with three alkyl azides

under reflux in trimethylorthoformate. Triazolines were obtained in high yields in two cases (**7a,c**), and in moderate yield in one case (**7b**). *Stereo*- and *regio*-selectivities are complete in every case. An ORTEP X-ray analysis of the adduct **7a** is consistent with the attack of alkyl azide on the *re* face of the lactone ring (see **Figure 1** in supporting information).

Reaction of lactone **1** with phenyldiazomethane gave a single product in 76 % yield.  $^1\text{H}$  NMR spectrum evidenced that the primary cycloadduct suffered a 1,3-H-shift rearrangement to form compound **8**. The *regio*-selectivity of the reaction was elucidated by a NOE experiment on compound **8**: irradiation of 9a-H induced an increase of 9b-H and H-aromatic signals (**Figure 1**). These observations are consistent with the *regio*-chemistry of compound **8** in **scheme 2**. NOE experiment also showed that phenyldiazomethane approaches lactone by the *re* face, since 9a-H and 9b-H protons are located on the same side of the molecule.

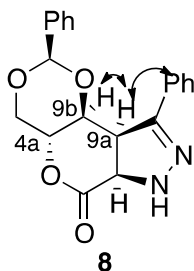


**Figure 1:** NOE interaction elucidates both the *regio*-chemistry and stereochemistry of the newly formed chiral centres.

Reactions of lactone **1** with nitrile oxides gave a pair of *regio*-isomers **9** and **10**, in approximately 1:1 ratio. The identification of isomers was conclusive after  $^1\text{H}$  MNR spectra analysis: the oxygen position in the fused-oxazole **9/10** is likely to affect the proton chemical shift attached to its neighbor carbon atom. In fact, isomers **9** showed consistently H-6a at a higher chemical shift ( $\delta$  5.33-5.10 ppm) than H-9a ( $\delta$  4.86-3.95 ppm); the opposite trend occurs in isomers **10** where H-9a appears at  $\delta$  5.37-5.09, higher than H-6a ( $\delta$  4.98-4.34 ppm). Irradiation of 6a-H's signal in compound **10b** induced a 13.9 % increase of the aromatic peak, demonstrating its neighborhood to the aromatic ring. The facial approach of the nitrile oxide to the lactone **1** was also determined by NOE experiment: irradiation of H-9b's signals in the pair **9b/10b** indicated that H-9a and H-9b are located on the same side in both isomers. As C-9b's configuration refers to the starting material, it is clear that the approach of reagents would have occurred from the *re* face of the lactone. Additionally, H-2 signals also increase by H-9b's irradiation in both isomers.

## 4. Computational results

### A. *Stereo*-specificity of the cycloadducts

The high *stereo*-selectivity of the compounds is one of the key features of the studied reactions. In all of the studied cases, the cycloaddition of the 1,3-dipoles was found to occur by the *re* face of the lactone ring, *i.e.*, in the opposite plane where the hydrogen atom covalently bonded to carbon C8a is located at. (**Figure 2A**) The transition state structures of these reactions show that the main moiety of the lactone, including the keto group, are perpendicular to the new bonds formed during the 1,3-dipoles approach in the top face of the lactone (**Figure 2B**). This process is facilitated by the small size of the 1,3-dipole molecules, allowing them to react in largely occluded areas where other reagents cannot fit due to steric bulk. Hydrogens **8a** in the lactone is very close to the reactive region and it was found to play an important role in the *stereo*-specificity of the cycloaddition process. Hydrogen **8a** located at the *si* face precludes the correct alignment of the 1,3-dipole to the lactone. This is patent on free energies calculated for the nitrile oxide, R=Ph, that requires an activation energy of 40 kcal.mol<sup>-1</sup>, and the reaction is endothermic by 15 kcal.mol<sup>-1</sup>. On the other hand, the hydrogen **4a** is located further away from the region where the reaction takes place, at the *re* face of the lactone, leading way to a more suitable approach of the 1,3-dipole at the *re* face of the lactone. Overmore the attack at the *re* face is also favored by a hyperconjugative interaction of the sigma\*C-O to the electron positively charged atom of the 1,3 dipole. So the *re* face is more favored either by steric and electronic reasons.[12] In fact, the cycloaddition process at the *re* face requires a free activation energy of 21.3 kcal.mol<sup>-1</sup> and a free reaction energy of -17.8 kcal.mol<sup>-1</sup>. The same conclusion is applied to the azides, diazo and nitrile oxide compounds.

### B. *Regio*-specificity of the compounds

The cycloaddition involving unsymmetrical 1,3-dipole and the lactone **1**, can potentially generate two *regio*-isomeric products, depending on the orientation of the 1,3-dipole molecules in relation to the lactone. When the R group of the 1,3-dipole molecule is pointing to the same side of the phenyl group of the lactone, the cycloaddition follows pathway A (**Figure 3**). Otherwise, when the R group is pointing towards the opposite direction of the phenyl group of the lactone, the cycloaddition follows pathway B (**Figure 3**). In principle, a mixture of both *regio*-isomers could be obtained in

these type of reactions, as it was observed in the reactions with the nitrile oxides **5**. However, alkyl azides **4** and diazo compound **6** gave a single *regio*-isomer cycloadduct.

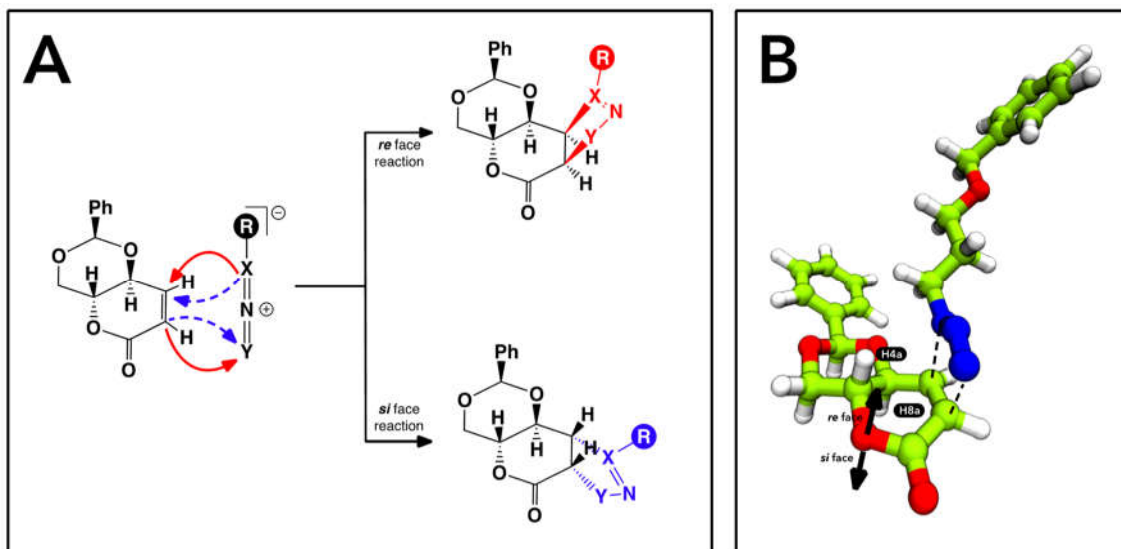


**Figure 2:** (A) *Stereo*-selectivity of the reactions of the lactone **1** with 1,3-dipole compounds. The red pathway shows the attack in the *re* (top) face of the lactone ring. The blue pathway shows the attack in the *si*/ (bottom) face of the lactone ring (do not happen). (B) Transition state structure obtained from cycloaddition of an azide compound at the *re* face of the lactone.

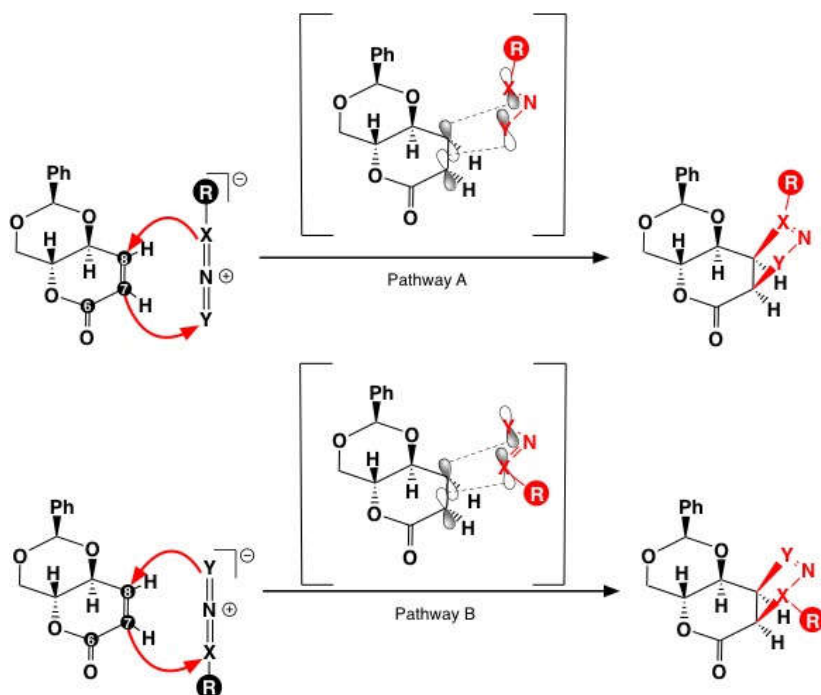


**Figure 3:** Possible catalytic mechanisms of lactone **1** with 1,3-dipoles. Y,X=N in the case of alkyl azides; X=C, Y=O in the case of nitrile oxides; X=C, Y=NH in the case of phenyldiazomethane.

The most generally satisfactory interpretation of the *regio*-chemistry of dipolar cycloadditions is based on frontier molecular orbitals (FMO) concepts. As with the Diels-Alder reaction, the most favourable orientation is the one that involves the complementary interaction between the frontier orbitals.

Generally, the 1,3-cycloadditions can be classified into three types based on the relative FMO energies between the dipole and the dipolarophile. In 1,3-cycloadditions type I, the dominant FMO interaction is that of the HOMO dipole with the LUMO's dipolarophile. For 1,3-cycloadditions type II, the similarity of the dipole and dipolarophile FMO energies implies that both HOMO-LUMO interactions are important. In 1,3-cycloadditions type III the interaction is obtained between the LUMO's dipole and the HOMO's dipolarophile.

The evaluation of the energies of the HOMO and LUMO of all the transition state structure involving the reaction of diazo, azide and nitrile oxides compounds with the lactone reveal that the diazo compounds follow a mechanism of type I and the azide and nitrile oxides compounds follow a mechanism of type II. The mechanism of type II is a characteristic of the reactions involving 1,3-dipole molecules with high nucleophilic nature, as it is the case of the nitrile oxides and alkyl azides, which turns the energy gap between the HOMO and LUMO of the dipole and dipolarophile very close to each other. (See supporting SI-2 for detailed description of the energy involved in this process)

This interpretation of the results is however not sufficient to explain the origin of the *regio*-specificity present on the studied reactions. For example, the mechanism of cycloadditions involving either nitrile oxides and alkyl azides are type II, however the energy gap between the HOMO and LUMO in the transition state cannot be use to explain why with nitrile oxides gave two *regio*-isomers and alkyl azides gave only one isomer.

A better explanation to understand the *regio*-specificity of the studied reactions was obtained analyzing the energetic profiles of the cycloaddition process.

## B1. Mechanism of the 1,3-cycloadditions

The computational results have shown that the 1,3-cycloadditions are controlled by the electronic/stereo-electronic and steric factors that require highly ordered transition states and only moderate free energies requirements.

Independently on the pathway that is followed (pathway A or B), the full process is complete in a unique step involving the concerted formation of two covalent bonds between the 1,3-dipole molecules and the lactone. This is confirmed by all the transition state structures, from all the studied reactions, that present a single imaginary frequency, and in which the 1,3-dipole molecule adopts a partially folded conformation well-aligned and in close contact to C7 and C8 carbons of the lactone. Examples of the transition state structures involved in the cycloaddition process of lactone **1** and each of the 1,3-dipole molecules are shown in **Figure 4**.

Independent on the 1,3-dipole molecule that was studied and, on the substitutions, present on these molecules, all the reactions require relative small free activation energies (below 28 kcal.mol<sup>-1</sup>) and are all exergonic (**Figure 5**). Despite these similarities, the free energetic profile of the studied reactions, whenever pathway A or B is followed, are distinct and allow to understand the origin of the *regio*-specificity of the cycloadditions of the studied 1,3-dipole molecules.

The calculated free energies involving the cycloaddition of the 1,3-dipole azides with lactone **1** reveal that pathway A is always favored either from the kinetic or thermodynamic points of views in relation to pathway B. This is more clear in the cycloaddition process involving the 1,3-dipole azides that are substituted with propyl and benzyl groups, in which pathway A is favored kinetically in more than 3.5 kcal.mol<sup>-1</sup> and thermodynamically in more than 2.3 kcal.mol<sup>-1</sup>. When the 1,3-dipole azides have a (CH<sub>2</sub>)<sub>3</sub>-OBn group, pathway A continues to be kinetically favored in 2.6 kcal.mol<sup>-1</sup> but it is only thermodynamically favoured in 1 kcal.mol<sup>-1</sup>. These results agree to what is observed experimentally, since only one isomer is observed and isolated (**Figure 5**).



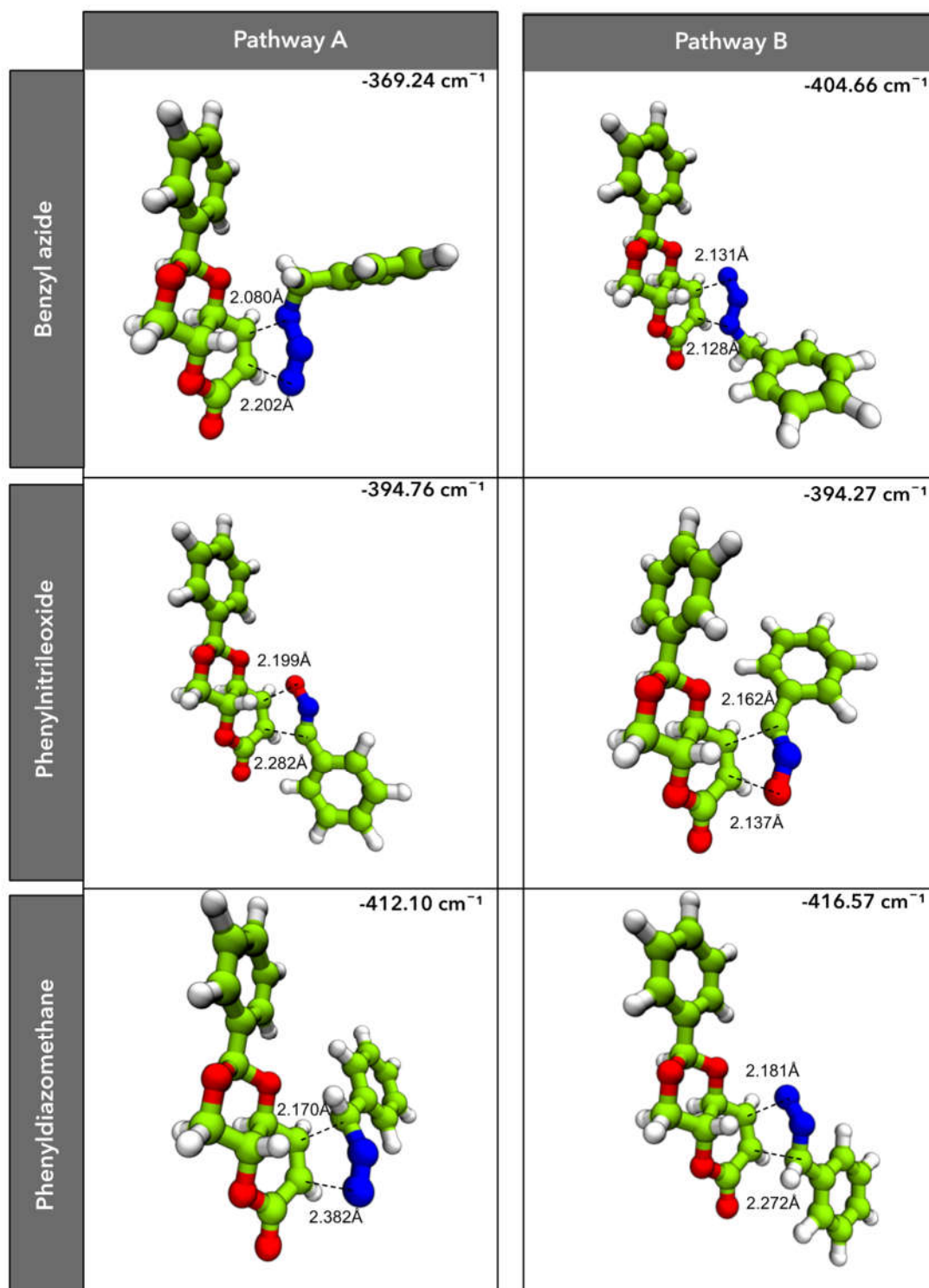


**Figure 4:** Transition state structures of the cycloaddition process of lactone **1** and benzyl azide (**7a**), phenylnitrileoxide (**9b/10b**) and the diazo compound (**8**).

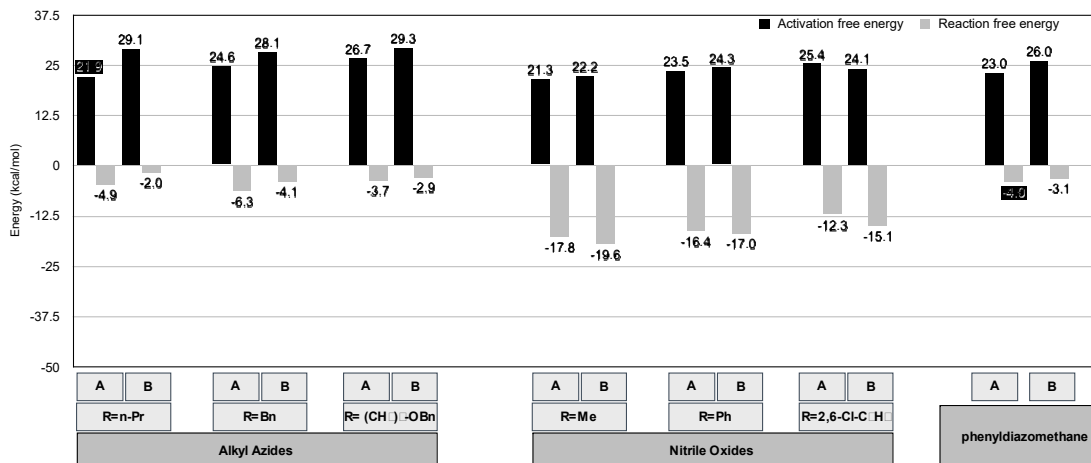


**Figure 5:** Activation and reaction free energies of the cycloaddition process involving lactone **1** and the alkyl azides, nitrile oxides and phenyldiazomethane.

The cycloaddition process of the 1,3-dipole nitrile oxides with lactone **1** produces two isomers instead of a single one, contrasting to what is observed with 1,3-dipole azides. The computational results indicate that the energetic profiles of pathways A and B for these reactions are very similar either from the kinetic (energy differences below 1.2 kcal.mol<sup>-1</sup>) and thermodynamic (energy differences below 2.8 kcal.mol<sup>-1</sup>) points of views, indicating that both pathways should be competitive. These results go in line with what is observed experimentally since, a mixture of two isomers are obtained (**Figure 5**). For example in the case of compounds **9b** and **10b**, compound **9b** is obtained in 24% yield and compound **10b** in 56%. However, as compound **10b** is contaminated with 25% of compound **9b**, the ratio between the yields is near 1:1, in agreement with the computational results.

The cycloaddition of lactone **1** with the 1,3-dipole phenyldiazomethane was also studied through pathways A and B. However, and contrarily to what was found with nitrile oxides and the alkyl azides, the formation of compound **8** requires two steps instead of one. First occurs the cycloaddition process. Afterwards takes place the 1,3-H shift.

The calculated free energy profiles for pathway A (E<sub>a</sub>=23.0 kcal.mol<sup>-1</sup> and E<sub>r</sub>=-4.0 kcal.mol<sup>-1</sup>) and pathway B (E<sub>a</sub>=26.0 kcal.mol<sup>-1</sup> and E<sub>r</sub>=-3.1 kcal.mol<sup>-1</sup>) indicate that pathway A is from the kinetic and thermodynamic points of views favored in relation to pathway B (**Figure 5**). These results go in line with the experimental observations in which only one isomer is isolated from this reaction.

The second step of the reaction involves the 1,3-H shift. Since pathway A was the most favored one, this reaction was only studied for the product of this reaction. The 1,3-H shift requires the participation of two water molecules that form a hydrogen bond network allowing the proton exchange between the carbon and nitrogen atoms from the cycloaddition product obtained in pathway A. The transition state of this reaction is characterized by an imaginary frequency at  $-944.57\text{ cm}^{-1}$  and the full process requires a free activation energy of  $38.14\text{ kcal}\cdot\text{mol}^{-1}$  and it is exergonic in  $-8.03\text{ kcal}\cdot\text{mol}^{-1}$ .

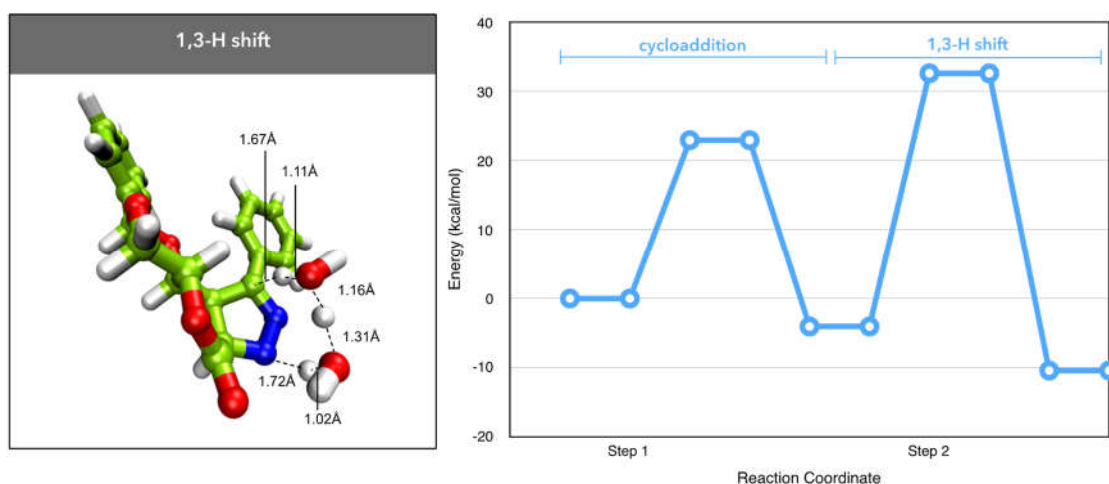


**Figure 6:** Left: Transition state structure of the 1,3-H shift mechanism. Right: Free energetic profile for the formation of compound **8**.

The full energetic profile obtained for the formation of compound **8** is depicted in **figure 6**. The computational results reveal that the 1,3-H shift mechanism is the rate-limiting step in the formation of compound **8**.

## B2. Origin of the *regio*-specificity of the cycloadditions

In order to evaluate the origin of the *regio*-specificity of the alkyl azides and phenyldiazomethane in relation to the nitrile oxide compounds we have decomposed the free activation energies in different energetic terms: the distortion energy, interaction energy, entropic contribution, and solvent effects.

The distortion energy was calculated summing up the energy difference between the geometry of lactone and 1,3-dipole *per se* and for each reagent in the transition state. The interaction energy

was calculated based on the energy difference between the energies of the 1,3-dipole and the lactone molecules together and alone in the transition state and reactants of all the studied reactions. The entropic contributions and the solvent effect on each reaction were obtained directly from the calculations. The results from these analyses are displayed in **figure 9**.

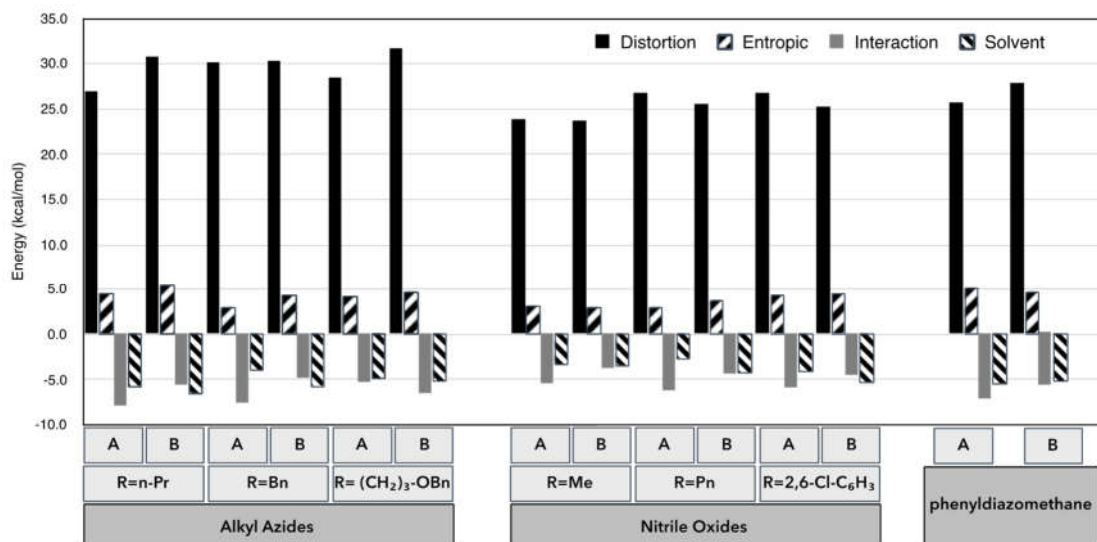


**Figure 7:** Decomposition of the activation energies of the cycloaddition process involving lactone **1** and the alkyl azides, nitrile oxides and the diazo compound.

The results indicate that the main contributor for all the calculated activation energies is the distortion energy, i.e. the energy that is required to move the 1,3-dipole molecules and the lactone in a proper way to endorse the concerted cycloaddition process. From these two molecules, the 1,3-dipoles are the ones that suffer the highest distortion effect. The calculations also reveal that

the distortion of these molecules accounts in average 70% of the total distortion energy (see supporting information SI-3). The other negative contributor for the activation energies of all the studied reactions is the entropy. This is expected since the cyclization process is from the entropic point of view unfavourable. However, its contribution is very small (below 5 kcal.mol<sup>-1</sup>) when compared to the distortion energy. The calculated interaction energy and solvent effects have a positive contribution to the calculated activation energies; in average they decrease the activation energies in -5.9 kcal.mol<sup>-1</sup> and -4.2 kcal.mol<sup>-1</sup> respectively. The interaction energy is the one that makes the cycloaddition process possible. The solvent effect was introduced in the calculations with the inclusion of a dielectric constant. This was found to be important for the stabilization of zwitterionic species particularly during the distortion of these molecules nearby the transition state.

From all the studied reactions, the cycloaddition of alkyl azides with lactone **1** are the ones that require higher activation energies. The results shown that this is proportional to the higher distortion effect that is observed in the 1,3-dipole molecules. These results also shown that the distortion effect of alkyl azides in pathway B is higher than in pathway A and justify why these reactions are *regio*-selectives (pathway A).

In the case of nitrile oxides, a similar contribution of the energetic terms that were calculated is observed on pathways A and B, justifying why in this case two isomers are obtained.

The energy decomposition of the cycloaddition of phenyldiazomethane with lactone **1** reveal that the energetic profile is similar to the one observed with nitrile oxides. However, in this case the distortion energy is smaller in pathway A than in pathway B turning this reaction *regio*-selective for pathway A, similarly to what happens in the mechanism of alkyl azides.

### C. The effect on the substituents of the 1,3-dipoles on the calculated free energies.

The cycloaddition of the lactone with the 1,3-dipoles, nitrile oxides and alkyl azides, having different substituents, were also carried out in order to understand the effect of such substituents on the free energies of the reactions and so in the obtained yields (**Figure 5**). With the alkyl azides bearing propyl, and benzyl groups pathway A is favoured either from the kinetic and thermodynamic points of view relatively to pathway B. The computational results with (propoxymethyl)benzene showed to be less favourable than in the other two cycloadditions, which go in line with the

experimental results; compound **7b** was obtained with a lower yield (55 %) than the others. The computational results indicate that the energetic profile of pathway A is less favoured because of the volume of the (propoxymethyl)benzene that creates a steric hindrance either with the Ph group of the lactone in pathway A and with the carbonyl group in pathway B.

The cycloaddition of the nitrile oxides was also investigated with the methyl, phenyl and dichlorophenyl groups. The computational results reveal that in all of the three reactions, pathway A and pathway B present similar energetic profiles. For each compound the activation free energies for each pathway differ only in 1 kcal.mol<sup>-1</sup>, and the reaction free energies are below 3 kcal.mol<sup>-1</sup>. This indicates that the cycloadditions of the nitrile oxides with the two different orientations are competitive and therefore a mixture of both isomers should be obtained in the end. This is in accordance with the experimental results where both isomers were obtained in similar amounts in the three reactions.

## 5. Conclusion

A new D-erythrose 1,3-dioxane derivative, lactone **1**, has been synthesized and found to be a highly selective template in 1,3-dipolar cycloadditions. Alkyl azides, nitrile oxides and diazoalkanes were reacted as models. The computational results showed the *stereo*-selectivity is due to the steric effect of the hydrogen atom (H8a). The activation and reaction free energies calculated for the cycloadditions allow to explain the origin of the *regio*-selectivity observed with alkyl azides and diazo compounds in relation to the nitrile oxides.

The cycloaddition processes can occur with two different orientations of the 1,3-dipole molecule in relation to the lactone (pathway A and B). In the nitrile oxides cases, pathways A and B are competitive and both isomers are obtained. However, in the cases of the alkyl azides and diazo compounds only one isomer is favored from kinetic and thermodynamic points of view. The detailed analysis about energies involved in the cycloaddition process indicate that pathway A is favored because it requires a lower distortion of the 1,3-dipole molecules during the reaction.

## 6. Experimental

### 6.1 General

Solvents were used as purchased except: dichlorometane and methanol, dried under  $\text{CaH}_2$  and  $\text{Mg/I}_2$ , respectively; tetrahydrofurane, and ether, dried under Na-benzophenone, and DMF and toluene distilled with elimination of the head distillation fractions. Petroleum ether 40-60 °C used in chromatography was submitted to distillation. D-erythrose benzylidene acetal was obtained according to lit. [3,4] Alkylazides were obtained from the respective alkyl bromides, by reaction with sodium azide under standard conditions [13]. Benzyloxypropyl azide was prepared from 3-bromopropanol by reaction with sodium azide followed by protection of the hydroxyl group with benzyl bromide [14]. Nitrile oxides were obtained *in situ* from  $\alpha$ -chlorobenzaldoximes in the presence of triethylamine [15]. Phenyl diazomethane was obtained from the aldehyde and tosylhydrazone according to lit. [16].

All other reagents were purchased and used without further purification. Glassware was dried prior to use. Compounds were purified by dry flash chromatography using silica 60, <0.063 mm and water pump vacuum or by flash-chromatography using silica 60Å 230–400 mesh as stationary phases. TLC plates (silica gel 60 F<sub>254</sub>) were visualized either at a UV lamp or in I<sub>2</sub> chamber.

### 6.2 Synthesis of Lactone 1

#### i) Synthesis of methyl 3-((2'*R*,4'*S*,5'*R*)-5'-hydroxy-2'-phenyl-1',3'-dioxan-4'-yl)acrylate

To a solution of aldehyde **2** (1.0 g, 4.8 mmol) in dry THF (20 mL), stirred under nitrogen in the presence of a catalytic amount of *p*-toluene sulfonic acid (5 mg) was added a solution of methyl (triphenylphosphoranylidene)acetate (1.6 g, 4.8 mmol) in dry THF (10 mL). The solvent was evaporated till dryness after 23 h, and the crude subjected to column chromatography (ethyl acetate / petroleum ether 1:1). A mixture of *Z/E* isomers were obtained in a 2.3: 1 ratio (1.18 g, 4.5 mmol, 92.8%). The mixture was submitted to the next step without further purification. Some <sup>1</sup>H NMR peaks of the *Z* isomer in the spectrum of the crude product are: <sup>1</sup>H NMR (300 MHz, CDCl<sub>3</sub>)  $\delta$  3.80 (s, 3H, OMe), 5.21 (td,  $J = 9.0, 1.2$  Hz, 1H, 4'-*H*), 5.57 (s, 1H, 2'-*H*), 6.19 (dd,  $J = 11.8, 1.4$  Hz, 1H, 2'-*H*), 6.36 (dd,  $J = 11.8, 7.7$  Hz, 1H, 3'-*H*).

## ii) Synthesis of (2*R*,4*aR*,8*aS*)-2-phenyl-4,4*a*-dihydropyrano[3,2-*d*][1,3]dioxin-6(8*aH*)-one (1)

To a solution of the crude material obtained in i) (0.80 g, 3.03 mmol) in ethyl acetate (70 mL) was added silica (*ca.* 40 g). The mixture was heated at 75 ° C for 10 h in a rotary evaporator under water pump vacuum. Successive portions of dry toluene (5 x 100 mL) were added to the flask to avoid dryness. The residue was purified by column chromatography (ethyl acetate: petroleum ether 1: 1), giving a white solid (0.03 g, 1.29 mmol, 63.0 %), identified as lactone **1**. M.p. = 135.9 – 136.8 °C;  $[\alpha]_D^{25} = +17.6$  (c 0.5%, DCM); IR (nujol):  $\nu_{\max}$  3070, 3054, 1753  $\text{cm}^{-1}$ ;  $^1\text{H}$  NMR (400 MHz,  $\text{CDCl}_3$ )  $\delta$  4.02 (t,  $J = 10.0$  Hz, 1H, 4-*H*), 4.40 (dd,  $J = 10.4, 4.8$  Hz, 1H, 4*a*-*H*), 4.69 (dd,  $J = 10.4, 4.8$  Hz, 1H, 4-*H*), 4.89 (ddd,  $J = 10.0, 2.4, 1.6$  Hz, 1H, 8*a*-*H*), 5.65 (s, 1H, 2-*H*), 6.04 (dd,  $J = 10.0, 2.8$  Hz, 1H, 7-*H*), 7.03 (dm,  $J = 10.0$  Hz, 1H, 8-*H*), 7.42-7.40 (m, 3H, 3'-*H* + 4'-*H*), 7.51-7.50 (m, 2H, 2'-*H*),  $^{13}\text{C}$  NMR (100.6 MHz,  $\text{CDCl}_3$ )  $\delta$  68.2 (4-C), 72.7 (4*a*-C), 73.9 (8*a*-C), 102.4 (2-C), 120.7 (7-C), 126.1 (CH), 128.5 (CH), 129.6 (CH), 136.3 (Cq), 146.9 (8-C), 161.8 (6-C); HRMS (ESI-TOF) found for  $\text{C}_{13}\text{H}_{12}\text{O}_4\text{Na}$ : 255.0621; calcd: 255.0628.

## 6.3 Synthesis of 1,3-Dipoles

### 6.3.1 Nitrile oxides 5

A solution of 2,6-dichlorobenzaldehyde / benzaldehyde oximes (0.104-0.143 g) in dry DMF (10 mL) was pre-heated at 40-43 °C. A solution of *N*-chlorosuccinimide (NCS) (0.100 g; 0.75 mmol) in dry DMF (5 mL) was added dropwise, under magnetic stirring and  $\text{N}_2$  atmosphere. The reaction mixture was kept for 3 h, followed by another 15-19h period at rt. The reaction was quenched in ice/water (*ca.* 30 mL) and extracted with ether (4 x 20 mL). The ethereal solution was washed with sat. aq. sol. NaCl (2 x 10 mL) and water (2 x 10 mL). The organic phases were combined and dried over  $\text{MgSO}_4$ . The solvent was removed in the rotary evaporator to give the respective chloro oximes ( $\eta = 77\% - 89\%$ ).

#### 6.3.1.1 2,6-Dichloro-*N*-hydroxybenzimidoyl chloride

2,6-dichlorobenzaldehyde oxime (0.143 g; 0.75 mmol); 43 °C; 15h rt.; beige solid (0.130 g; 0.58 mmol;  $\eta = 77\%$ );  $^1\text{H}$  NMR:  $\delta$  (300 MHz,  $\text{CDCl}_3$ ) 7.20-7.40 (3H, m, Ar); 10.11 (1H, sl, OH).



### 6.3.1.2 *N*-hydroxybenzimidoyl chloride

benzaldehyde oxime (0.104 g; 0.86 mmol); 40 °C; 19h rt.; brownish oil (0.123 g; 0.790 mmol);  $\eta = 89\%$ ;  $^1\text{H NMR}$ : (300 MHz,  $\text{CDCl}_3$ )  $\delta$  7.32-7.41 (3H, m, Ar), 7.80-7.88 (2H, m, Ar); 10.9 (1H, br s, OH).

### 6.3.1.3 *N*-hydroxymethylimidoyl chloride

*N*-hydroxymethylimidoyl chloride, was generated "*in situ*" by a similar methodology described to the synthesis of previous chloro oximes, and used immediately in the 1,3-dipolar cycloaddition.

## 6.4 1,3-Dipolar cycloadditions

### 6.4.1 with alkyl azides **4**

To a solution of lactone **1** (0.10-0.360 g; 0.431 mmol - 1.55 mmol) in methyl orthoformate (20-25 mL) was added the alkyl azide **4** (2 - 20 eq.). The reaction mixture was heated under nitrogen atmosphere for 30 to 65 h. The solvent was evaporated and the resulting solid residue recrystallized from ethanol. The title compound was obtained as white solid (38.3 - 86 %).

#### 6.4.1.1 Synthesis of (3*aS*,5*aR*,9*aS*,9*bA*)-1-benzyl-8-phenyl-(5*a*,6,9*a*,9*b*)-tetrahydro-1*H*-[1,3]dioxino(4',5':5,6)pyrano[3,4-*d*][1,2,3]triazol-4(3*aH*)-one (**7a**)

Lactone **1** (0.36 g, 1.55 mmol); methyl orthoformate (25 mL); benzyl azide (2 eq., 387  $\mu\text{L}$ , 3.10 mmol); reflux; 65 h; obtained product (0.46 g, 1.26 mmol, 81.3%); M.p. = 177.4 – 178.1 °C;  $[\alpha]_{\text{D}}^{25} = -438.0^\circ$  (c 2.7%, DCM); UV-Vis: 267.1 nm; IR (nujol):  $\nu_{\text{max}}$  1753  $\text{cm}^{-1}$ ;  $^1\text{H NMR}$  (400 MHz,  $\text{CDCl}_3$ )  $\delta$  3.85-3.78 (m, 1H, 6-H), 3.83 (dd,  $J = 13.2, 4.0$  Hz, 1H, 9b-H), 4.10 (dd,  $J = 9.6, 4.0$  Hz, 1H, 9a-H), 4.39 (dd,  $J = 10.0, 5.6$  Hz, 1H, 5a-H), 4.49 (dd,  $J = 10.8, 5.6$  Hz, 1H, 6-H), 4.69 (d,  $J = 14.8$  Hz, 1H, CH), 5.31 (d,  $J = 13.2$  Hz, 1H, 3a-H), 5.43 (d,  $J = 14.8$  Hz, 1H, CH), 5.60 (s, 1H, 8-H), 7.18-7.16 (m, 2H, Ar), 7.53-7.32 (m, 8H, Ar);  $^{13}\text{C NMR}$  (100.6 MHz,  $\text{CDCl}_3$ )  $\delta$  52.7 (9b-C), 54.2 (CH), 65.8 (5a-C), 67.8 (6-C), 76.1 (9a-C), 80.8 (3a-C), 102.3 (8-C), 128.2 (CH, Ph), 128.5 (CH, Ph), 128.8 (CH, Ph), 128.9 (CH, Ph), 134.8 (Cq, Ph), 136.3 (Cq, Ph), 161.6 (4-C);

*Crystallography*. Formula: C<sub>23</sub>H<sub>26</sub>N<sub>3</sub>O<sub>5</sub>. Molecular weight: 365.38; Temperature: 100(2) K; a (Å) = 5.6268(11); b (Å) = 17.614(3); c (Å) = 9.1708(17); β (°) = 105.330(2); GoF: 1.064; R = 0.0390.

#### 6.4.1.2 Synthesis of (3*a**S*,5*a**R*,9*a**S*,9*b**R*)-1-(propyl-3'-benzyloxy)-8-phenyl-(5*a*,6,9*a*,9*b*)-tetrahydro-1*H*[1,3]dioxino(4',5':5,6)pyrano[3,4-*d*][1,2,3]triazol-4(3*a**H*)-one (7*b*)

Lactone **1** (0.10 g, 0.431 mmol); methyl orthoformate (20 mL); (3-azidopropoxy)methyl benzene (2 eq., 166 mg, 0.862 mmol; 100 °C; 44 h; obtained product (70 mg, 0.165 mmol, 38.3 %); M.p. = 110.3 – 110.5 °C; [α]<sub>D</sub><sup>25</sup> = - 235.6 (c 2.4%, CH<sub>2</sub>Cl<sub>2</sub>); IR (nujol): ν<sub>max</sub> 2097, 1772 cm<sup>-1</sup>; <sup>1</sup>H NMR (400 MHz, CDCl<sub>3</sub>) δ 2.05-2.02 (m, 2H, 2'-*H*), 3.50 (dt, *J* = 6.4, 3.6 Hz, 2H, 3'-*H*), 3.78 (t, *J* = 10.8 Hz, 1H, 6-*H*), 3.82 (t, *J* = 6.4 Hz, 1H, 1'-*H*), 4.07-4.05 (m, 3H, 9*b*-*H*+9*a*-*H* +1'-*H*), 4.22 (dt, *J* = 9.6, 5.6 Hz, 1H, 5*a*-*H*), 4.43 (dd, *J* = 10.8, 5.6 Hz, 1H, 6-*H*), 4.43 (s, 2H, 4'-*H*), 5.25 (d, *J* = 12.8 Hz, 1H, 3*a*-*H*), 5.56 (s, 1H, 8-*H*), 7.39-7.27 (m, 8H, Ph), 7.47-7.46 (m, 2H, Ph); <sup>13</sup>C NMR (100.6 MHz, CDCl<sub>3</sub>) δ 28.2 (2'-C), 48.1 (1'-C), 54.7 (9*b*-C), 65.6 (5*a*-C), 67.6 (3'-C), 67.8 (6-C), 73.0 (4'-C), 76.0 (9*a*-C), 80.2 (3*a*-C), 102.1 (8-C), 125.9 (CH, Ph), 127.6 (CH, Ph), 127.7 (CH, Ph), 128.3 (CH, Ph), 128.4 (CH, Ph), 129.4 (CH, Ph), 136.2 (Cq, Ph), 138.0 (Cq, Ph), 162.0 (4-C); HRMS (ESI-TOF), found for C<sub>23</sub>H<sub>26</sub>N<sub>3</sub>O<sub>5</sub>: 424.1860, calcd: 424.1867.

#### 6.4.1.3 Synthesis of (3*a**S*,5*a**R*,9*a**S*,9*b**R*)-1-propyl-8-phenyl-(5*a*,6,9*a*,9*b*)-tetrahydro-1*H*[1,3]dioxino(4',5':5,6)pyrano[3,4-*d*][1,2,3]triazol-4(3*a**H*)-one (7*c*)

Lactone **1** (0.20 g, 0.86 mmol); methyl orthoformate (20 mL); propyl azide (2 eq., every 3 h); 95 °C; 30 hours; obtained product (0.25 g, 0.754 mmol, 86%). M.p. = 125.4 – 126.3 °C; [α]<sub>D</sub><sup>25</sup> = - 279.1 (c 3.2%, CH<sub>2</sub>Cl<sub>2</sub>); IR (nujol): ν<sub>max</sub> 1774 cm<sup>-1</sup>; <sup>1</sup>H NMR (400 MHz, CDCl<sub>3</sub>) δ 0.91 (t, *J* = 7.4 Hz, 3H, 3'-*H*), 1.78 (m, 1H, 2'-*H*), 3.65 (ddd, *J* = 13.6, 8.0, 5.6 Hz, 1H, 1'-*H*), 3.80 (t, *J* = 10.4 Hz, 1H, 6-*H*), 3.87-3.80 (m, 1H, 1'-*H*), 4.13-4.08 (m, 2H, 9*b*-*H*+9*a*-*H*), 4.27 (dt, *J* = 9.4, 5.4 Hz, 1H, 5*a*-*H*), 4.47 (dd, *J* = 11.0, 5.4 Hz, 1H, 6-*H*), 5.41 (d, *J* = 13.2 Hz, 1H, 3*a*-*H*), 5.57 (s, 1H, 8-*H*), 7.46-7.27 (m, 5H, H-Ar); <sup>13</sup>C NMR (100.6 MHz, CDCl<sub>3</sub>) δ 11.2 (3'-C), 21.4 (2'-C), 52.1 (1'-C), 54.8 (9*b*-C), 65.6 (5*a*-C), 67.9 (6-C), 76.2 (9*a*-C), 80.1 (3*a*-C), 102.3 (8-C), 126.0 (CH, Ph), 128.4 (CH, Ph), 129.6 (CH, Ph), 136.3 (Cq, Ph), 162.0 (4-C); HRMS (ESI-TOF), found for C<sub>16</sub>H<sub>20</sub>N<sub>3</sub>O<sub>4</sub>: 318.1455; calcd: 318.1448.

### 6.4.2 with diazomethyl benzene (6)

Diazomethyl benzene (6) [12] (3 eq.; 0.35 g; 2.99 mmol) recently obtained, and contained in a round bottom flask was added a solution of lactone **1** (0.212 g; 0.999 mmol) in dry toluene (18 mL). The reaction mixture was kept under nitrogen, stirring and submitted to heat in a pre-heated oil bath 60°C - 70°C. After some time a light pink colour develops and fades away after 1h 25 min. The reaction mixture was refrigerated in an ice/water bath. A solid precipitated out, was removed by filtration, and the mother-liquid evaporated to a residue. A white solid (0.210 g; 0.598 mmol;  $\eta = 76.3\%$ ) was recrystallized from ethanol giving compound **8**.

#### 6.4.2.1 Synthesis of (4*aR*,6*aR*,9*aR*,9*bS*)-2,9-diphenyl-6*a*,7,9*a*,9*b*-tetrahydro-4*H*[1,3]dioxino[4',5':5,6]pyrano[3,4-*c*]pyrazol-6(4*aH*)-one (8)

M.p. = 159.5 – 160.7 (dec.);  $[\alpha]_{D}^{25} = -116$  (c 0.7 %, CH<sub>2</sub>Cl<sub>2</sub>); IR (nujol):  $\nu_{\max}$  3337, 1750, 1586 cm<sup>-1</sup>. <sup>1</sup>H NMR (400 MHz, CDCl<sub>3</sub>):  $\delta$  3.79 (1H, dd,  $J = 9.0, 15.2$  Hz, *H*9*a*); 3.98 (1H, dd,  $J = 9.6, 10.4$  Hz, *H*4*ax*); 4.28-4.37 (2H, m, *H*4*a* + *H*9*b*); 4.59 (1H, dd,  $J = 4.8, 10.4$  Hz, *H*4*eq*); 4.44 (1H, d,  $J = 15.2$  Hz, *H*6*a*); 5.57 (1H, s, *H*2); 6.56 (1H, br s, *H*7); 7.32-7.35 (3H, m, Ph); 7.40-7.42 (5H, m, Ph); 7.50-7.54 (2H, m, Ph); <sup>13</sup>C NMR  $\delta$  100.6 MHz, CDCl<sub>3</sub> 50.1 (C-9*a*); 68.0 (C-4); 69.5 (C-4*a*); 73.2 (C-6*a*); 75.2 (C-9*b*); 101.1 (C-2); 125.9 (CH, Ph); 128.0 (CH, Ph); 128.2 (CH, Ph); 128.5 (CH, Ph); 128.6 (CH, Ph); 129.2 (CH, Ph); 136.4 (Cq, Ph); 137.8 (Cq, Ph); 140.7 (C-9); 161.0 (C-6). Elem. Anal. Found: C, 68.48 %; H, 5.05 %; N, 7.72 %; calcd for C<sub>20</sub>H<sub>18</sub>N<sub>2</sub>O<sub>4</sub> C, 68.56 %; H, 5.18 %; N, 8.00 %.

### 6.4.3 with nitrile oxides

#### Method A

A solution of 2,6-dichloro-*N*-hydroxybenzimidoyl chloride / *N*-hydroxybenzimidoyl chloride (0.11 - 0.130 g; 0.58 - 0.70 mmol) in dry ether (3-5 mL) was added to lactone **1** (0.084-0.091 g; 0.40 mmol - 0.43 mmol) contained in a round bottom flask kept under nitrogen and in an ice/water bath. To the previous mixture was added dropwise triethylamine (51-55 mL; 0.037 - 0.040 g; 0.37 - 0.39 mmol) recently distilled, in dry ether (6 mL) during 30 - 40 min. The reaction mixture was stirred at rt for 12-15 h. The volatiles were removed in the rotary evaporator, and the residue re-

dissolved in dichloromethane (10 mL) and passed through a pad of celite. The filtrate was evaporated to give solids, as mixtures of isomers **9a,b** and **10a,b**.

**6.4.3.1 Synthesis of (2*R*,4*aR*,6*aR*,9*aR*,9*bS*)-9-(2,6-dichlorophenyl)-2-phenyl-4,4*a*,9*a*,9*b*-tetrahydro-[1,3]dioxino[4',5':5,6]pyrano[4,3-*d*]isoxazol-6(6*aH*)-one (9*a*) and (5*aR*,8*R*,9*aR*,9*bR*)-3-(2,6-dichlorophenyl)-8-phenyl-5*a*,6,9*a*,9*b*-tetrahydro-[1,3]dioxino[4',5':5,6]pyrano[3,4-*d*]isoxazol-4(3*aH*)-one (10*a*)**

2,6-dichloro-*N*-hydroxybenzimidoyl chloride (0.130 g; 0.58 mmol); ether (5 mL); lactone **1** (0.084 g; 0.40 mmol); triethylamine (55 mL; 0.040 g; 0.39 mmol); rt; 15h; white-greenish solid (0.172 g; 0.409 mmol;  $\eta$ = quant.)<sup>a)</sup> recrystallized from ethanol, giving two fractions: the first fraction contained isomer **10a** as white solid (0.031 g; 0.074 mmol; 19 %); the second fraction contained a 3 (**9a**): 1(**10a**) mixture of isomers (0.083 g; 0.198 mmol; 50 %).

a) The <sup>1</sup>H NMR spectrum showed a 1.25(**9a**):1 (**10a**) mixture of isomers.

**Isomer 9a**<sup>a)</sup> <sup>1</sup>H NMR (400 MHz, CDCl<sub>3</sub>)  $\delta$  3.79 (1H, dd,  $J$  = 10.4, 10.8 Hz, *H*4<sub>ax</sub>); 4.07 (1H, dd,  $J$  = 7.2, 9.6 Hz, *H*9b); 4.54 (1H, dd,  $J$  = 5.6, 10.8 Hz, *H*4<sub>eq</sub>); 4.83 (1H, dt,  $J$  = 5.6, 10.0 Hz, *H*4a); 4.86 (1H, dd,  $J$  = 7.2, 10.8 Hz, *H*9a); 5.33 (1H, d,  $J$  = 10.4 Hz, *H*6a); 5.41 (1H, s, *H*2); 6.94-6.98 (2H, m, Ar) 7.15-7.46 (6H, m, Ar); <sup>13</sup>C NMR  $\delta$  (100.6 MHz, CDCl<sub>3</sub>) 51.5 (C-9a); 66.6 (C-4a); 67.9 (C-4); 74.8 (C-9b); 80.4 (C-6a); 101.5 (C-2); 125.6 (CH, Ar); 127.8 (CH, Ar); 128.9 (CH, Ar); 130.7 (Cq, Ar); 135.7 (Cq, Ar); 153.4 (C-9); 163.1 (C-6).

a) contaminated with 25 % of isomer **10a**

**Isomer 10a** M.p. = 209.5-211.0 (dec.);  $[\alpha]_D^{25} = + 86.7$  (c 0.3 %, CH<sub>2</sub>Cl<sub>2</sub>); IR (nujol):  $\nu_{\max}$  1749 cm<sup>-1</sup>; <sup>1</sup>H NMR (400 MHz, CDCl<sub>3</sub>)  $\delta$  3.87 (1H, t,  $J$  = 10.4 Hz, *H*4<sub>ax</sub>); 4.17 (1H, dd,  $J$  = 3.6, 10.0 Hz, *H*9b); 4.58 (1H, dd,  $J$  = 5.2, 10.8 Hz, *H*4<sub>eq</sub>); 4.90 (1H, m, *H*4a); 4.91 (1H, d,  $J$  = 10.8 Hz, *H*6a); 5.37 (1H, dd,  $J$  = 3.2, 11.2 Hz, *H*9a); 5.68 (1H, s, *H*2); 7.34-7.45 (6H, m, *H*-Ar); 7.55-7.59 (2H, m, *H*-Ar); <sup>13</sup>C NMR  $\delta$  (100.6 MHz, CDCl<sub>3</sub>) 56.6 (C-6a); 65.2 (C-4a); 68.0 (C-4); 75.1 (C-9b); 77.9 (C-9a); 102.6 (C-2); 125.5 (CH, Ar); 126.4 (CH, Ar); 128.2 (CH, Ar); 128.4 (CH, Ar); 129.6 (CH, Ar);

132.0 (Cq, Ar); 135.1 (Cq, Ar); 136.1 (Cq, Ar); 149.6 (C-9); 161.4 (C-6). HRMS<sup>a</sup> (ESI-TOF), found for C<sub>20</sub>H<sub>15</sub>Cl<sub>2</sub>NO<sub>5</sub>: 420.0397; calcd 420.0400.

#### 6.4.3.2 Synthesis of (2*R*,4*aR*,6*aR*,9*aR*,9*bS*)-2,9-diphenyl-4,4*a*,9*a*,9*b*-tetrahydro[1,3]dioxino[4',5':5,6]pyrano[4,3-*d*]isoxazol-6(6*aH*)-one (9*b*) and (3*aR*,5*aR*,8*R*,9*aR*,9*bS*)-3,8-diphenyl-5*a*,6,9*a*,9*b*-tetrahydro-[1,3]dioxino[4',5':5,6]pyrano[3,4-*d*]isoxazol-4(3*aH*)-one (10*b*)

*N*-hydroxybenzimidoyl chloride (0.11 g; 0.70 mmol); dry ether (3 mL); lactone **1** (0.091 g; 0.43 mmol); triethylamine (51 mL; 0.037 g; 0.37 mmol); 12h; white solid (0.132 g; 0.38 mmol;  $\mu$ = 87.6 %) constituted by a mixture 1 (**9b**) :1.25 (**10b**). Isomer **9b** was obtained from dichloromethane (0.036 g; 0.102 mmol; 24 %). Isomer **10b** recrystallized from dichloromethane (0.085 g; 0.24 mmol; 56 %), contaminated with 25 % of isomer **9b**.

**Isomer 9b** M.p. = 296.0 – 298.0 °C (dec.);  $[\alpha]_{D}^{25} = -93.6$  (c 0.25%; CH<sub>3</sub>CN); IR (nujol):  $\nu_{\max}$  1758 cm<sup>-1</sup>; <sup>1</sup>H NMR (400 MHz, CDCl<sub>3</sub>)  $\delta$  3.80 (1H, dd,  $J = 10.2, 10.8$  Hz, *H*4<sub>ax</sub>); 4.18 (1H, dd,  $J = 7.4, 9.8$  Hz, *H*9*b*); 4.46 (1H, dd,  $J = 5.2, 10.2$  Hz, *H*4<sub>eq</sub>); 4.58 (1H, dt,  $J = 5.6, 10$  Hz, *H*4*a*), 4.60 (1H, dd,  $J = 7.2, 9.2$  Hz, *H*9*a*); 5.20 (1H, d,  $J = 9.6$  Hz, *H*6*a*); 5.46 (1H, s, *H*2); 6.71-6.76 (2H, m, Ph); 7.07-7.13 (2H, m, Ph); 7.20-7.26 (1H, m, Ph); 7.36-7.49 (3H, m, Ph); 7.75-7.80 (2H, m, Ph); <sup>13</sup>C NMR (100.6 MHz, CDCl<sub>3</sub>)  $\delta$  46.7 (C-9*a*); 66.6 (C-4*a*); 67.9 (C-4); 74.9 (C-9*b*); 80.8 (C-6*a*); 101.6 (C-2); 125.8 (CH, Ph); 128.0 (CH, Ph); 128.1 (CH, Ph); 128.5 (CH, Ph); 128.9 (CH, Ph); 129.1 (CH, Ph); 130.4 (Cq, Ph); 135.7 (Cq, Ph); 157.3 (C-9); 163.7 (C-6). Elem. Anal. Found: C 67.32; H, 4.79; N 4.09; calcd for C<sub>20</sub>H<sub>17</sub>NO<sub>5</sub>·1/3H<sub>2</sub>O: C, 67.22; H, 4.98; N, 3.92.

**Isomer 10b** M.p. = 220.7 – 222.5 °C (dec.);  $[\alpha]_{D}^{25} = +184$  (c 0.3%; CH<sub>2</sub>Cl<sub>2</sub>); IR (nujol):  $\nu_{\max}$  1749 cm<sup>-1</sup>; <sup>1</sup>H NMR (400 MHz, CDCl<sub>3</sub>)  $\delta$  3.83 (1H, t,  $J = 10.4$  Hz, *H*-4<sub>ax</sub>); 4.12 (1H, dd,  $J = 3.2, 9.6$  Hz, *H*9*b*); 4.50 (1H, dd,  $J = 5.4, 11.0$  Hz, *H*4<sub>eq</sub>); 4.72 (1H, dt,  $J = 5.6, 10.0$  Hz, *H*4*a*); 4.98 (1H, d,  $J = 10.8$  Hz, *H*6*a*); 5.32 (1H, dd,  $J = 3.2, 10.8$  Hz, *H*9*a*); 5.65 (1H, s, *H*2); 7.38-7.48 (6H, m, Ph); 7.53-7.58 (2H, m, Ph); 7.89-7.93 (2H, m, Ph); <sup>13</sup>C NMR (100.6 MHz, CDCl<sub>3</sub>)  $\delta$  55.0 (C-6*a*); 65.3 (C-4*a*); 68.0 (C-4); 75.5 (C-9*b*); 78.5 (C-9*a*); 102.5 (C-2); 126.4 (CH, Ph); 126.7 (CH, Ph); 127.7 (CH, Ph); 128.4 (CH, Ph); 128.8 (CH, Ph); 129.6 (CH, Ph); 131.0 (Cq, Ph); 136.2 (Cq, Ph);

152.4 (C-7); 162.5 (C-6). Elem. Anal. found: C, 67.32; H, 4.79; N 4.09; calcd for  $C_{20}H_{17}NO_5 \cdot 1/3H_2O$ : C, 67.22; H, 4.98; N 3.92.

#### Method B

To a suspension of *N*-chlorosuccinimide (0.227 g; 1.70 mmol) in dichloromethane (3 mL) was added a solution of acetaldehyde oxime (0.127 g; 2.14 mmol), and pyridine (0.05 mL) in dichloromethane (2 mL). The mixture was kept under stirring till complete NCS dissolution. To this mixture was added lactone **1**.

#### 6.4.3.3 Synthesis of (2*R*,4*aR*,6*aR*,9*aR*,9*bS*)-9-methyl-2-phenyl-4,4*a*,9*a*,9*b*-tetrahydro[1,3]dioxino[4',5':5,6]pyrano[4,3-*d*]isoxazol-6(6*aH*)-one (**9c**) and (3*aR*,5*aR*,8*R*,9*aR*,9*bR*)-3-methyl-8-phenyl-5*a*,6,9*a*,9*b*-tetrahydro-[1,3]dioxino[4',5':5,6]pyrano[3,4-*d*]isoxazol-4(3*aH*)-one (**10c**)

A solution of lactone **1** (0.10 g; 0.431 mmol) in dry toluene (18 mL) was added to the acetaldehyde oxime generated "*in situ*" followed by dropwise addition of triethylamine (0.5 mL; 3.16 mmol) in dry toluene (5 mL), during 2h. The reaction mixture was stirred at rt for 15h. The solvents were removed in rotary evaporator, and the residue re-dissolved in dichloromethane and passed through a pad of celite. The filtrate was evaporated to give a solid consisting a 1.2 (**9c**):1 (**10c**) mixture of adducts. The crude product was recrystallized from ethanol to give two fractions: the first fraction contained pure isomer (**10c**) as white solid (0.035 g; 0.12 mmol; 28 %); the second fraction contained the other isomer **9c** which was not possible to purify from impurities (0.075g).

**Isomer 9c**  $^1H$  NMR (400 MHz,  $CDCl_3$ )<sup>a)</sup>  $\delta$  2.15 (3H, d,  $J=0.8$  Hz,  $CH_3$ ); 3.85-3.77 (m, 1H); 3.90 (1H, dd,  $J=7.6, 9.80$  Hz,  $H_{4a}$ ); 4.12 (1H, dd,  $J=7.3, 9.6$  Hz,  $H_{9b}$ ); 4.46-4.53 (m, 1H); 5.01 (1H, d,  $J=10.8$  Hz,  $H_{6a}$ ); 5.54 (1H, s,  $H_2$ ); 7.31-7.35 (3H, m, Ph); 7.37-7.42 (2H, m, Ph).

a) some peaks of isomer **9c**, taken from a spectrum containing both isomers (**9c** and **10c**)

**Isomer 10c** M.p. = 229.7 – 231.5 (dec.);  $[\alpha]_D^{25} = +33.6$  (c 0.75%;  $CH_2Cl_2$ ); IR (nujol):  $\nu_{max}$  1744  $cm^{-1}$ ;  $^1H$  NMR (400 MHz,  $CDCl_3$ )  $\delta$  2.11 (3H, d,  $J=0.8$  Hz,  $CH_3$ ); 3.82 (1H, t,  $J=10.6$  Hz,  $H_{4ax}$ ); 4.06 (1H, dd,  $J=3.4, 10.0$  Hz,  $H_{9b}$ ); 4.34 (1H, dd,  $J=0.8, 10.0$  Hz,  $H_{3a}$ ); 4.51 (1H, dd,  $J=5.6, 10.8$  Hz,  $H_{4ax}$ ); 4.62 (1H, dt,  $J=5.2, 10.0$  Hz,  $H_{4a}$ ); 5.09 (1H, dd,  $J=3.2, 10.8$  Hz,  $H_{9a}$ ); 5.62 (1H,

s, *H*<sub>2</sub>); 7.37-7.42 (3H, m, Ph); 7.50-7.54 (2H, m, Ph); <sup>13</sup>C NMR ( 100.6 MHz, CDCl<sub>3</sub>) δ 11.6 (CH<sub>3</sub>); 58.2 (C-6a); 65.3 (C-4a); 67.9 (C-4); 75.2 (C-9b); 76.7 (C-9a); 102.5 (C-2); 126.3 (CH, Ph); 128.4 (CH, Ph); 129.6 (CH, Ph); 136.1 (C<sub>q</sub>, Ph); 150.8 (C-3); 162.2 (C-4). Elem. Anal., found: C, 61.36; H, 5.54; N 4.89; calcd for C<sub>15</sub>H<sub>15</sub>NO<sub>5</sub> · 1/3H<sub>2</sub>O, C, 61.01; H, 5.35; N, 4.74.

## 6.5 Computational Methodology

All geometry optimizations were performed with Gaussian 09 [17], applying density functional theory [18], with the B3LYP functional [19] together with the 6-31G(d) basis set [20]. The geometry optimizations were conducted with a conductor-like polarizable continuum model using the integral equation formalism variant (IEF-PCM) [21].

In all geometry optimizations, we first searched for the transition state starting from a structure similar to the reactant model. This was generally obtained with un-dimensional scans along the particular reaction coordinate in which we were interested. Once a putative transition structure was located, it was fully optimized. The reactants and the products associated with it were determined after intrinsic reaction coordinate (IRC) calculations. In all cases, the geometry optimizations and the stationary points were obtained with standard Gaussian convergence criteria. The transition state structures were all verified by vibrational frequency calculations, having exactly one imaginary frequency with the correct transition vector, even using frozen atoms, which shows that the frozen atoms were almost free from steric strain. The ZPE and thermal and entropic energy corrections were calculated using the same method and basis set (T = 310.15 K, P = 1 bar).

The final electronic energies were calculated using the all-electron 6-311++G(3df,2pd) basis set and the functional M06-2X [22,23]. A conductor-like polarizable continuum model using the integral equation formalism variant (IEF-PCM), as implemented in Gaussian 09, with a dielectric constant of 2.4, 4.0, 33.0 was used to simulate the toluene, diethyl ether, methanol solvent, respectively [21].

All the activation and reaction energies provided in the text and figures refer to free energy differences calculated at the M06-2X/6-311++(3df,2pd) level detailed above, while the atomic charge distributions were calculated at the B3LYP level by employing a Mulliken population analysis, using the basis set 6-31G(d).

## 7. References

1. Casiraghi, G.; Zanardi, F.; Rassu, G.; Spanu, P., Stereoselective Approaches to Bioactive Carbohydrates and Alkaloids-With a Focus on Recent Syntheses Drawing from the Chiral Pool. *Chem. Rev.* **1995**, *95*(6), 1677-1716.
2. Sousa, C.E.A.; Mendes, R.R.; Costa, F.T.; Duarte, V.C.M.; G. Fortes, A.; Alves, M.J., Synthesis of Iminosugars from Tetroses. *Current Organic Synthesis*, **2014**, *11*, 182-203; and references cited herein.
3. Baker, S.R.; Clissold, D.W.; McKillop, A., Synthesis of leukotriene A4 methyl ester from D-glucose. *Tetrahedron Lett.* **1988**, *29*, 991-994.
4. Zimmermann, P.; Schmidt, R.R., Synthese von erythro-Sphingosinen über die Azidoderivate. *Liebigs Ann. Chem.* **1988**, 663-667.
5. (a) Alves, M.J.; Duarte, V.C.M.; Faustino, H.; Gil Fortes, A., Diastereo-controlled Diels-Alder cycloadditions of erythrose benzylidene-acetal 1,3-butadienes by 4-substituted-1,2,4-triazoline-3,5-dione: Evidence for the stereoelectronic effects on the dienes. *Tetrahedron: Asymmetry*, **2010**, *21*, 1817-1820; (b) Salgueiro, D.A.L.; Duarte, V.C.M.; Sousa, C.E.A.; Alves, M.J.; Gil Fortes, A., Diastereoselectivity in Diels-Alder Cycloadditions of Erythrose Benzylidene-acetal 1,3-Butadienes with Maleimides. *Synlett* **2012**, *23*, 1765-1768; Duarte, V.C.M.; (c) Faustino, H.; Alves, M.J.; Gil Fortes, A.; Micaelo, N., Asymmetric Diels-Alder Cycloadditions of D-Erythrose 1,3-Butadienes to Achiral t-Butyl 2H-Azirine 3-Carboxylate. *Tetrahedron: Asymmetry* **2013**, *24*, 1063-1068.
6. Pino-Gonzalez, M.S.; Oña, N., Synthesis of intermediates in the formation of hydroxy piperidines and 2-azido lactones from D-erythrose. *Tetrahedron: Asymmetry* **2008**, *19*, 721-729.
7. (a) Jasiński, R., Competition between the one-step and two-step, zwitterionic mechanisms in the [2+3] cycloaddition of gem-dinitroethene with (Z)-C,N-diphenylnitron: a DFT computational study. *Tetrahedron* **2013**, *69*, 927-932; (b) Jasiński, R.; Mróz, K., Kinetic aspects of [3+2] cycloaddition reactions between (E)-3,3,3-trichloro-1-nitroprop-1-ene and ketonitrones. *Reac. Kinet Mech. Cat.* **2015**, *116*, 35-41; (c) Jasiński, R.; Ziółkowska, M.; Demchuk, O.M.; Maziarka, A., *Regio*- and stereoselectivity of polar [2+3] cycloaddition reactions between (Z)-C-(3,4,5-trimethoxyphenyl)-N-methylnitron and selected (E)-2-substituted nitroethenes. *Centr. Eur. J. Chem.* **2014**, *12*(5), 586-593.
8. Kitagawa, O.; Fujiwara, H.; Taguchi, T., Radical [3+2]-cycloaddition reaction with alkenes using dimethyl 2-(iodomethyl)cyclopropane-1,1-dicarboxylate as a new homoallyl radical precursor. *Tetrahedron Letters* **2001**, *42*(11), 2165-2167.
9. (a) Domingo, L.R.; Saez, J.A., Understanding the Electronic Reorganization along the Nonpolar [3 + 2] Cycloaddition Reactions of Carbonyl Ylides. *J. Org. Chem.* **2011**, *76*(2), 373-379; (b) Młostoń, G.; Urbaniak, K.; Linden, A.; Heimgartner, H., Selenophen-2-yl-Substituted Thiocarbonyl Ylides – at the Borderline of Dipolar and Biradical Reactivity. *Helv. Chim. Acta* **2015**, *98*(4), 453-461.
10. Schoenebeck, F.; Ess, D.H.; Jones, G.O.; Hou, K.N., Reactivity and regioselectivity in 1, 3-dipolar cycloadditions of azides to strained alkynes and alkenes: a computational study. *J. Am. Chem. Soc.* **2009**, *131*, 8121-8133.



11. Dahl, R.S.; Finney, N.S., A surprising dipolar cycloaddition provides ready access to aminoglycosides. *J. Am. Chem. Soc.* **2004**, *126*, 27, 8356-7.
12. (a) Gold, B.; Dudley, G.B.; Alabugin, I.V., Moderating Strain without Sacrificing Reactivity: Design of Fast and Tunable Noncatalyzed Alkyne–Azide Cycloadditions via Stereoelectronically Controlled Transition State Stabilization. *J. Am. Chem. Soc.* **2013**, *135*, 1558-1569; (b) Gold, B.; Shevchenko, N.E.; Bonus, N.; Dudley, G.B.; Alabugin, I.V., Selective Transition State Stabilization via Hyperconjugative and Conjugative Assistance: Stereoelectronic Concept for Copper-Free Click Chemistry. *J. Org. Chem.* **2012**, *77*, 75-89; (c) Gold, B.; Batsomboon, P.; Dudley, G.B.; Alabugin, I.V., Alkynyl Crown Ethers as a Scaffold for Hyperconjugative Assistance in Noncatalyzed Azide–Alkyne Click Reactions: Ion Sensing through Enhanced Transition-State Stabilization. *J. Org. Chem.* **2014**, *79*, 6221-6232; (d) Aronoff, M.R.; Gold, B.; Raines, R.T., Rapid cycloaddition of a diazo group with an unstrained dipolarophile. *Tetrahedron Lett.* **2016**, *57*, 2347-2350; (e) Gold, B.; Aronoff, M.R.; Raines, R.T., 1,3-Dipolar Cycloaddition with Diazo Groups: Noncovalent Interactions Overwhelm Strain. *Org. Lett.* **2016**, *18*, 4466-4469.
13. Ju, Y.; Kumar, D.; Varma, R. S., Revisiting Nucleophilic Substitution Reactions: Microwave-Assisted Synthesis of Azides, Thiocyanates, and Sulfones in an Aqueous Medium. *J. Org. Chem.* **2006**, *71*, 6697-6700.
14. Gupta, P.; Dharuman, S.; Vankar Y. D., (3S,4R,5R)-3-(2-Hydroxyethyl)piperidine-3,4,5-triol as an isofagomine analogue: synthesis and glycosidase inhibition study. *Tetrahedron Asymmetry* **2010**, *21* (24), 2966–2972.
15. Liu, K-C; Shelton, B.R.; Howe, R.K., A particularly convenient preparation of benzohydroximinoyl chlorides (nitrile oxide precursors). *J. Org. Chem.* **1980**, *45*, 3916 – 3918.
16. Creary, X.; Tam, W.W.; Albizati, K.F.; Stevens, R.V. *Organic Syntheses* **1990**, Coll. Vol. 7, p. 438.
17. Frisch, M. J., Trucks, G. W.; Schlegel, H. B.; Scuseria, G. E.; Robb, M. A.; Cheeseman, J. R.; Scalmani, G.; Barone, V.; Mennucci, B.; Petersson, G. A.; Nakatsuji, H.; Caricato, M.; Li, X.; Hratchian, H. P.; Izmaylov, A. F.; Bloino, J.; Zheng, G.; Sonnenberg, J. L.; Hada, M.; Ehara, M.; Toyota, K.; Fukuda, R.; Hasegawa, J.; Ishida, M.; Nakajima, T.; Honda, Y.; Kitao, O.; Nakai, H.; Vreven, T.; Montgomery, J. A.; Jr, Peralta, J. E.; Ogliaro, F.; Bearpark, M. J.; Heyd, J.; Brothers, E. N.; Kudin, K. N.; Staroverov, V. N.; Kobayashi, R.; Normand, J.; Raghavachari, K.; Rendell, A. P.; Burant, J. C.; Iyengar, S. S.; Tomasi, J.; Cossi, M.; Rega, N.; Millam, N. J.; Klene, M.; Knox, J. E.; Cross, J. B.; Bakken, V.; Adamo, C.; Jaramillo, J.; Gomperts, R.; Stratmann, R. E.; Yazyev, O.; Austin, A. J.; Cammi, R.; Pomelli, C.; Ochterski, J. W.; Martin, R. L.; Morokuma, K.; Zakrzewski, V. G.; Voth, G. A.; Salvador, P.; Dannenberg, J. J.; Dapprich, S.; Daniels, A. D.; Farkas, Ö.; Foresman, J. B.; Ortiz, J. V.; Cioslowski, J.; and Fox, D. J. (2009) Gaussian 09. Gaussian, Inc., Wallingford, CT, USA.
18. Hohenberg, P., and Kohn, W., Inhomogeneous Electron Gas. *Phys. Rev.* **1964**, *136*, B864–B871.
19. (a) Becke, A. D., A new mixing of Hartree–Fock and local density-functional theories. *J. Chem. Phys.* **1993**, *98* (2), 1372-1377; (b) Lee, C. T.; Yang, W. T.; Parr, R. G., Development of the Colle-Salvetti correlation-energy formula into a functional of the electron density. *Phys. Rev. B: Condens. Matter Mater. Phys.* **1988**, *37* (2), 785-789. (c) Vosko, S. H.; Wilk, L.; Nusair, M., Accurate spin-dependent electron liquid correlation energies for local spin density calculations: a critical analysis. *Can. J. Phys.* **2011**, *58*, 1200–1211; (d) Stephens, P. J.; Devlin, F. J.; Chabalowski, C. F.; Frisch, M. J., Ab Initio Calculation of Vibrational Absorption

- and Circular Dichroism Spectra Using Density Functional Force Fields. *J. Phys. Chem.* **1994**, 98 (45), 11623-11627.
20. Rassolov, V. A.; Ratner, M. A.; Pople, J. A.; Redfern, P. C.; Curtiss, L., 6-31G\* basis set for third-row atoms. *J. Comput. Chem.* **2001**, 22 (9), 976-984.
21. Scalmani, G.; Frisch, M. J., Continuous surface charge polarizable continuum models of solvation. I. General formalism. *J. Chem. Phys.* **2010**, 132 (11), 114110.
22. Zhao, Y.; Truhlar, D. G. The M06 Suite of Density Functionals for Main Group Thermochemistry, Thermochemical Kinetics, Noncovalent Interactions, Excited States, and Transition Elements: Two New Functionals and Systematic Testing of Four M06-Class Functionals and 12 Other Functionals. *Theor Chem Account* **2008**, 120, 215–241.
23. Zhao, Y.; Truhlar, D. G., Density Functionals with Broad Applicability in Chemistry. *Acc. Chem. Res.* **2008**, 41, 157–167.

# 6

Synthesis of Pyrrolidine Derivatives and  
Tetrahydrofuran  $\alpha$ -Amino Acids from D-Erythrosyl  
Fused Triazole Lactones

*The results presented in this chapter will be published under the title:*

**Divergent Synthesis of Furanoid  $\alpha$ -Amino Acids from a D-Erythrosyl Derivative Under Three Different Protic Acids**

Cristina E. A. Sousa and Maria J. Alves

Submitted to *JOC*, 2019, Manuscript ID: jo-2019-030312.

## 1. Abstract

This is the first report on the synthesis of furanoid sugar  $\alpha$ -amino acids at the non-anomeric position. Besides, polihydroxyprolines can also be accessed from the same chemical intermediate. D-Erythrosyl triazoles are transformed into the respective fused aziridine either by photolysis or through a diazirine intermediate, unexpectedly obtained by  $\text{BiI}_3/\text{H}_2\text{O}$  treatment. The aziridines were transformed under HCl,  $\text{BiI}_3/\text{H}_2\text{O}$  and trifluoroacetic acid (TFA) into two types of SAA compounds. A mechanism has been proposed for both syntheses based on experimental evidence.

## 2. Introduction

Sugar amino acids (SAAs) are structurally hybrids of carbohydrates and amino acids, a somehow nature-like and yet unnatural kind of molecules bearing multifunctional groups anchored on a single ensemble.[1,2] SAAs represent an important class of molecules that can play an important role in drug design, namely with potential applications as glycomimetics and peptidomimetics.[3] Glycomimetic libraries have been built through SAAs derivatization and oligomerization of the amino acid moiety.[2] On the other hand, the furan rigidity makes SAAs ideal nonpeptidic scaffolds for incorporation into peptidomimetics in order to induce conformational restrictions and build enhanced metabolic stability in active peptides.[2,4] Besides, the multiple stereogenic centers of the molecules can be exploited for the creation of chemical diversity, namely giving access to hydrophilicity control through hydroxyl group protection in peptidomimetics.[1] SAAs have been classified according to the position of the amino acid moiety on the cyclic polyol.[2,4] The furanoid/pyranoid sugar  $\alpha$ -amino acids reported so far are spiro compounds in which a fused glycine occupies the anomeric position.[5]

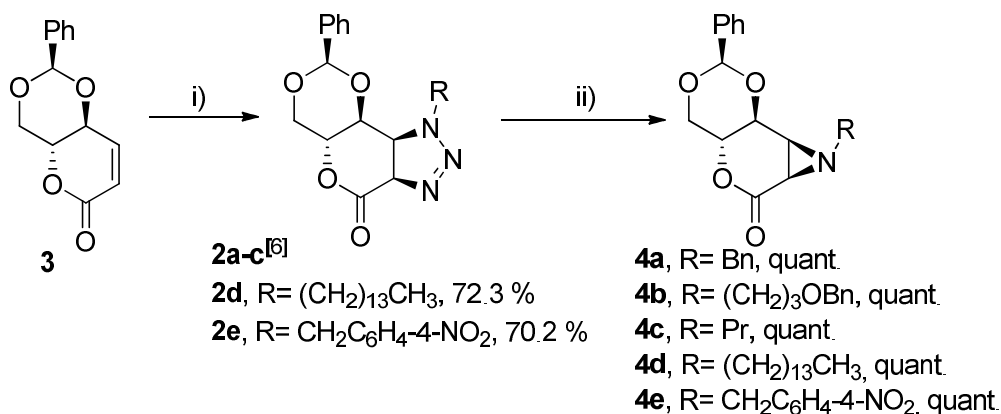
A new type of furanoid sugar  $\alpha$ -amino acid, **1**, has now been synthesized by a quite simple procedure, in excellent overall yield from D-erythrosyl fused 1,2,3-triazoles 1,5-lactones **2**, previously obtained in our laboratory from D-erythrosyl lactone **3** [6]. D-Erythrosyl fused-aziridine lactones **4** were first generated by nitrogen extrusion [7,8] under photolysis or synthesized by a complementary chemical process from diazirines **5**, unexpectedly generated by acid treatment of erythrosyl triazoles **2**[9].

In general, aziridines are constrained compounds of a high reactivity nature, likely to be excellent intermediates in syntheses. The D-Erythrosyl fused-aziridine **4** is reacted with three different protic acids:  $\text{BiI}_3/\text{H}_2\text{O}$ , TFA and HCl. Tetrahydrofuran amino acids **1** were obtained by a cascade of reactions initiated by reflux of aziridines **4** in water in the presence of  $\text{BiI}_3$ . A bicyclic structure related to compound **1**, **6**, was obtained by treatment of **4** with TFA at room temperature. Under hydrochloric acid treatment aziridines **4** initiate a different tandem sequence leading to prolines: (2*R*,3*R*,4*R*,5*R*)-1-alkyl-3,4-dihydroxy-5-(hydroxymethyl)pyrrolidine-2-carboxylic acids (**7**) were obtained in quantitative yields. Compounds **7** further evolve to its dehydration products **8** by prolonging HCl treatment. Compounds **7** are DMDP (2,5-dideoxy-2,5-imino-D-mannitol) type, known as a potent  $\beta$ -glucosidase inhibitor [10].

### 3. Results and Discussion

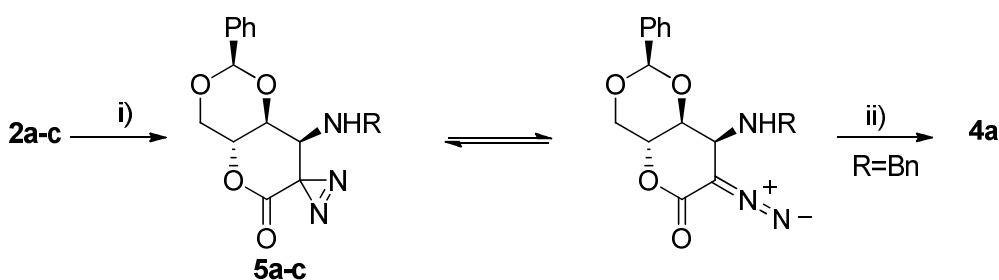
#### 3.1 Synthesis of aziridines **4a-e**

Aziridines are easily formed by a straightforward methodology from triazoles, either thermally or photochemically [7]. The thermo procedure was applied to the known triazole **2a** (R= Bn) by heating it at 150 °C in methyl orthoformate. No reaction was started after 24 h (**Scheme 1**). Though very stable under thermolysis conditions, compound **2a** suffer photolysis in less than 2 h under 254 nm UV light. Methanol was firstly used as a solvent to eventually open the aziridine ring once formed. Nevertheless, aziridine **4a** was obtained in 86 % yield after precipitation with ethanol. The process was optimized when DCM was used as solvent, giving **4a** in quantitative yield. Triazoles **2b,c** were also submitted to photolysis at 254 nm giving quantitative yields of the respective aziridines **4b,c**. Two new triazoles **2d,e** were successfully obtained applying the synthetic method previously developed in our laboratory [6], and then submitted to photolysis. Aziridines **4d,e** were isolated in quantitative yields.



**Scheme 1** – Synthesis of aziridines **4a-e** from triazoles **2a-e** having the D-erythrose core structure - **i)** methyl orthoformate (10 mL), alkyl azide (2 eq.), 100°C, N<sub>2</sub> atmosphere, 72 h; **ii)** CH<sub>2</sub>Cl<sub>2</sub>, 254 nm, 1 h 15 min – 9h.

In an attempt to cleave the acetal group under mild acidic conditions, a solution of compound **2a** was heated in water/acetonitrile in the presence of BiI<sub>3</sub> (0.1 eq.) [11]. Unexpectedly a diazirine compound **5a** was formed and the acetal unit kept. An equilibrium phenomenon described in the literature between diazirines and diazo compounds was detected [12] for compound **5a** (**Scheme 2**); a diazo stretching vibration was observed in the IR spectrum, and the carbon atom attached to the diazo group shows up at  $\delta = 58.2$  ppm in <sup>13</sup>C NMR spectrum. Upon reduction with triethylsilane in the presence of diruthenium tetraacetate, aziridine **4a** was formed in quantitative yield, possibly by substitution of the silane group at the  $\alpha$ -carbonyl position, by a displacement promoted by the vicinal nitrogen atom with aziridine closure [13].

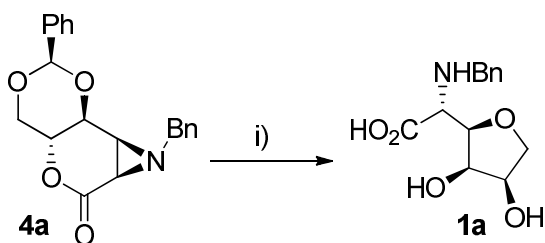


**Scheme 2** – Synthesis of aziridines **4a** from triazoles **2a**. **i)** BiI<sub>3</sub>/H<sub>2</sub>O-acetonitrile, 100°C, 2 h 30 min. **ii)** HSiEt<sub>3</sub> (1 eq.), Rh<sub>2</sub>(OAc)<sub>4</sub> (0.018 mmol), dry CH<sub>2</sub>Cl<sub>2</sub>, reflux, 25 h, quantitative yield.

### 3.2 Synthesis of tetrahydrofuran amino acids **1a-c**

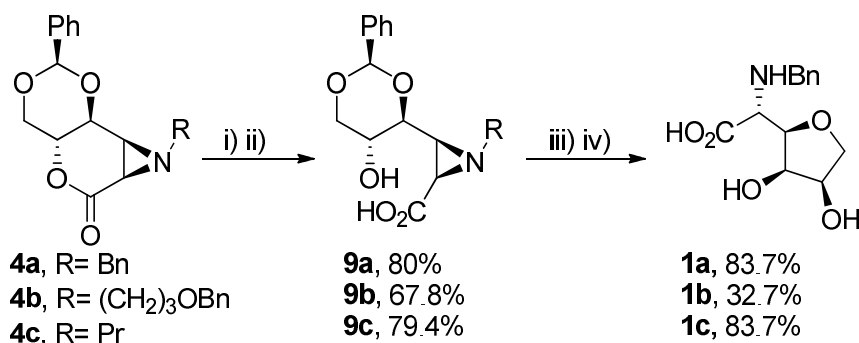
When a suspension of aziridine **4a** in water was heated at 100 °C in the presence of BiI<sub>3</sub> (10% mol) a mixture of products forms, with the disappearance of the starting material according to the

$^1\text{H}$  NMR spectra. New additions of  $\text{BiI}_3$  (2 x 10 % mol) prolonged for 5 hours led to the formation of a main product which was isolated in 32 % yield (**Scheme 3**).



**Scheme 3** – Synthesis of tetrahydrofuran amino acid **1a** from compound **4a**. **i)**  $\text{H}_2\text{O}$ ,  $\text{BiI}_3$  (3 portions of 10% mol),  $100\text{ }^\circ\text{C}$ , along the time.

Compound **1a** together with other analogues **1b,c** were further attained in much better yield from aziridines **9a-c**, previously obtained from **4a-c** by lactone ring-opening under  $\text{NaOH}$ . Tetrahydrofuran  $\alpha$ -amino acids **1a-c** were produced under reflux in water in the presence of  $\text{BiI}_3$  (10%) at a fairly good rate (2h-2h 30m) and yields from **9a-c** (**Scheme 4**).

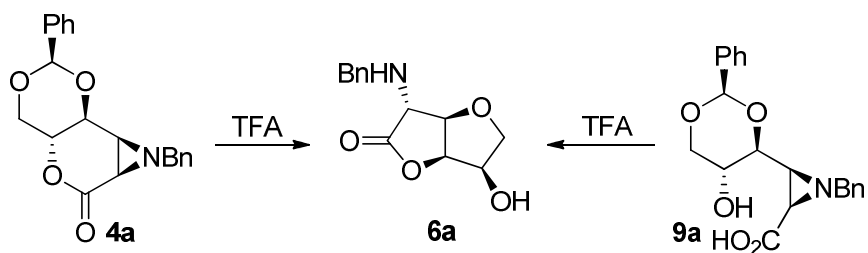


**Scheme 4** – Synthesis of aziridines **9a-c** by lactone ring opening **4a-c** and its transformation into amino acids **1a-c**. **i)**  $\text{NaOH}$  (1M, 15 mmol),  $\text{H}_2\text{O}$ : ACN (5:1 mL),  $40\text{ }^\circ\text{C}$ , 24 h; **ii)** Amberlite resin IR 120 (H $^+$ ); **iii)**  $\text{BiI}_3$  (10 mol %),  $\text{H}_2\text{O}$  (10-15 mL)  $115\text{ }^\circ\text{C}$ , 2 h - 2 h 30 m; **iv)** Dowex resin 1x3 (OH).

Trifluoroacetic acid (TFA) was also tested as a starter of the reaction. When compound **9a** was treated with TFA, a parent compound of amino acid **1a**, **6a**, was obtained in quantitative yield at room temperature in two days' time.

The very same product, lactone **6a**, could also be obtained in quantitative yield by treatment of the aziridine **4a** with TFA for a longer period of time, 15 days. The reaction was followed by successive  $^1\text{H}$  NMR analysis of the reaction mixture along the time, showing a very slow evolution.





**Scheme 5** – Synthesis of lactone **6a**, both from **9a** and **4a**, by reaction with TFA.

The structure of compounds **1** was elucidated by spectroscopic data and was excluded from other considered possibilities shown in **Figure 1**. The high field chemical shift of C-3 ( $\sim 80$  ppm) in the  $^{13}\text{C}$  NMR spectra of compounds **1a-c**, excluded pyrrolidines structures **I**, **II** and pipercolic acid **III** structure. The  $\text{C}_3\text{-H}$  correlation spectra could assign H-3 to a doublet of doublets with two vicinal H,  $J = 7.2\text{-}8.0$  Hz, and  $1.2\text{-}4.4$  Hz. This feature excludes the six-membered structures **III**, and **IV**. Structure **V** end up to be excluded because the exocyclic methylene group in compound **V** would be at  $\delta_{\text{c}} \sim 60$  ppm [13], and  $\delta_{\text{c}}$  of the endocyclic  $\text{CH}_2\text{O}$  unit is  $\sim 10$  ppm downfield, at  $\delta_{\text{c}} = 72.9$  ppm. Just as occur with the methylene, the methine protons do also agree with the methine units of a known compound related to compound **1**,  $3\alpha/3\beta$ -dihydroxytetrahydrofuran-2-hydroxycarboxamide, reported in the literature, with C-4 showing at  $\delta_{\text{c}} 72.7/72.4$ , and C-5 at  $\delta_{\text{c}} 78.7/78.3$  ppm [14].

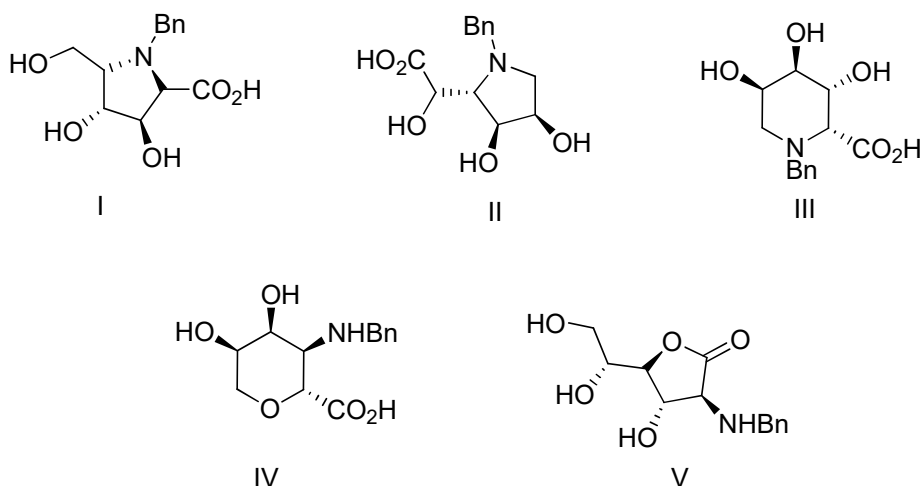
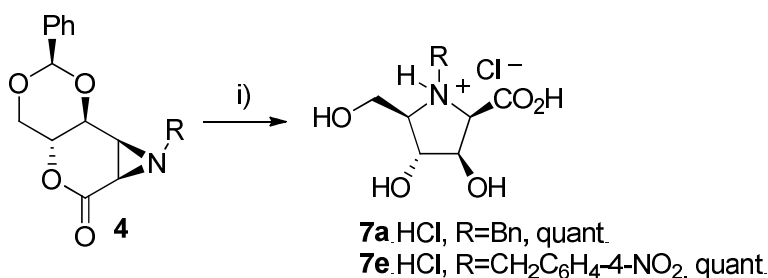


**Figure 1** – Other possible structures considered for compounds **1a**.

### 3.3 Synthesis of pyrrolidine-2-carboxylic acids **7a,e**, and **8a,e**

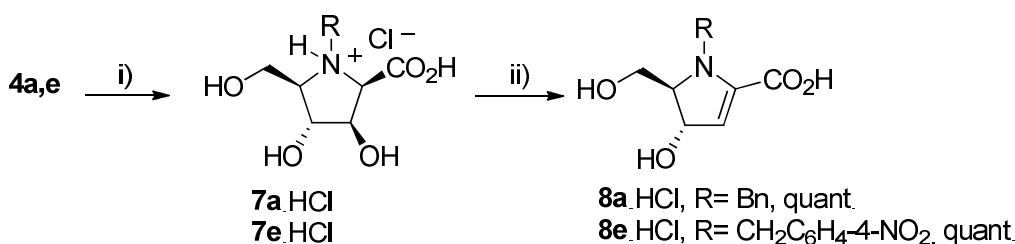
When compounds **4a,e** were suspended and stirred in HCl-dioxane 1M solution at room temperature new products **7a,e** were formed in quantitative yields after 20 h time. Compounds are solids and were isolated by simple filtration (**Scheme 6**).



**Scheme 6** – Synthesis of (2*R*,3*R*,4*R*,5*R*)-1-substituted-3,4-dihydroxy-5-(hydroxymethyl)pyrrolidine-2-carboxylic acid **7a,e** from the respective aziridines **4 - i)** **4a,e** 1M solution in dioxane, HCl (3.5 eq.), magnetic stirring, rt, ~20 h.

If the reaction's time is prolonged to 4 days in case **e** and to 17 days in case **a**, products **7a,e** do evolve to the respective dehydration products **8a,e** in quantitative yields (**Scheme 3**). Notably, the elimination process was detected to occur in the neutralized form **7a**, kept as a solid in the freezer for 1-year time.

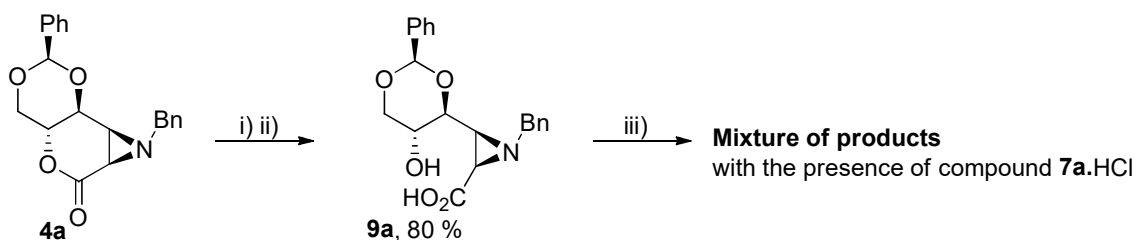
These new compounds **8a,e** are  $\alpha,\beta$ -unsaturated carboxylic acids, supposedly able to incorporate different nucleophiles, at the  $\beta$ -position, and eventually alter the stereochemistry of the carboxylic group attached to the pyrrolidine nucleus; they so are versatile intermediates in syntheses, which should be further explored in order to diversify the final proline compounds.



**Scheme 7** – Synthesis of (4*S*,5*R*)-1-benzyl-4-hydroxy-5-(hydroxymethyl)-4,5-dihydro-1*H*-pyrrole-2-carboxylic acids **8a.HCl**, **8e.HCl** directly from the respective aziridines **4a,e - i)** **2a,e** 1M solution in dioxane, HCl (3.5 eq.), magnetic stirring rt; **case a**, 20h; **case e** 18h; **ii)** continuing at rt; **case a**, 17 days; **case e**, 4 days.

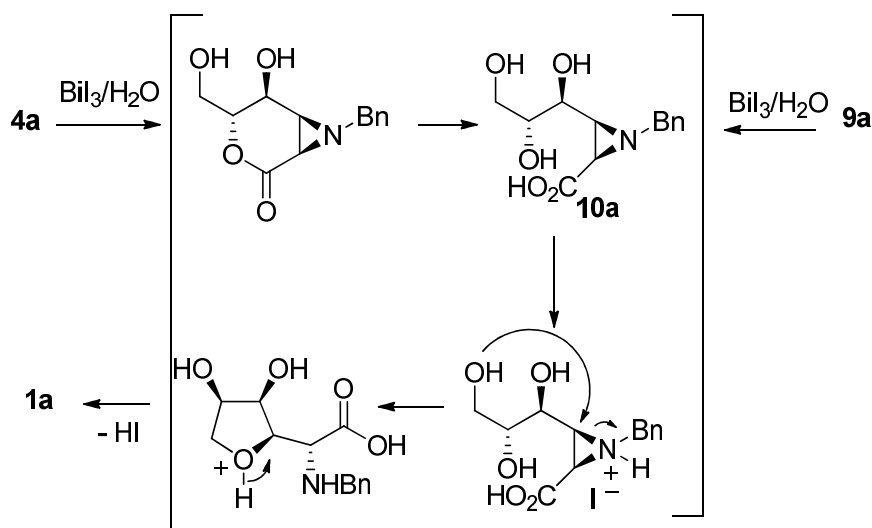
### 3.4 Reactions's Mechanisms

To judge about the first step of the cascade's reactions leading to compound **1**, its bicyclic isomer **6**, and to compound **7a.HCl**, both aziridines **4a**, and **9a** were treated under three different acids. The results are as follows: **1**) compound **1a** is formed in quantitative yield from **9a**, and in modest yield from **4a** under the same reaction's conditions (reflux in water in the presence of  $\text{BiI}_3$  catalysis); **2**) product **6a** formed in quantitative yields from either aziridines **9a** and **4a**, under TFA; notably reaction from **4a** is a much slower process (15 days *vs* 1 day); **3**) compound **7a.HCl** formed as a single product from reaction of aziridine **4a** with HCl; **4**) an undefined mixture of products, including a small amount of compound **7a.HCl** was formed by the treatment of aziridine **9a** with HCl.  $^1\text{H}$  NMR spectroscopy of aziridine **9a** /HCl reaction aliquots recorded along the 18 h necessary to consume aziridine **9a** showed the formation of several products at the same time (**Scheme 8**). Among the signals in each spectrum was found a doublet at  $\delta = 5.39$  ppm with  $J = 7.6$  Hz assigned to H-2, in accordance with the H-2 signal of an authentic sample of compound **7a.HCl**  $^1\text{H}$  NMR spectrum.



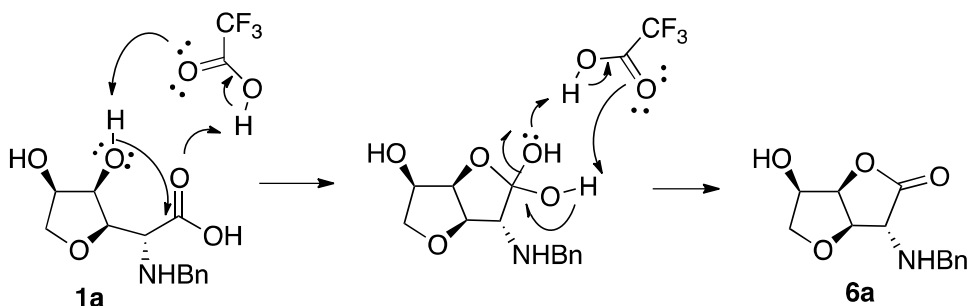
**Scheme 8** – Mixture of products obtained by treatment of aziridine **9a** with HCl: **i)** NaOH (1M, 15 mmol), H<sub>2</sub>O: ACN (5:1 mL), 40 °C, 24 h; **ii)** Amberlite resin IR 120 (H<sup>+</sup>); **iii)** 1M sol. in dioxane, HCl (3.5 eq.), magnetic stirring, rt, 18 h.

The hydrolysis of the acetal moiety in compounds **4a/9a** is presumed in every case at an early stage. Both aziridines **4a/9a** generate intermediate **10a** under  $\text{BiI}_3$  and TFA. Aziridine ring will open afterwards, possibly by a concomitant attack of the primary hydroxyl group onto the  $\beta$ -carbon atom relatively to the carbonyl, with the closing of a tetrahydrofuran ring, and formation of **1a**, as a single product (**Scheme 9**). In the case of TFA, compound **1a** once formed evolves to the bicyclic compound **6** (**Scheme 10**). No concurrent cleavage of the  $\text{C}\alpha$ -N bond in **10a** is observed, possibly because the  $\text{C}\alpha$  does not support an extra electron deficiency, besides the removing electron effect of the adjacent carboxylic group. A 6-membered structure (**IV**) would be formed by the attack of the primary alcohol function to this carbon, but structure **IV** was ruled out by spectroscopic analysis as shown ahead.



**Scheme 9**- Proposed mechanism for the synthesis of compound **1a** from aziridines **4a/9a** in  $\text{Bil}_3/\text{H}_2\text{O}$ .

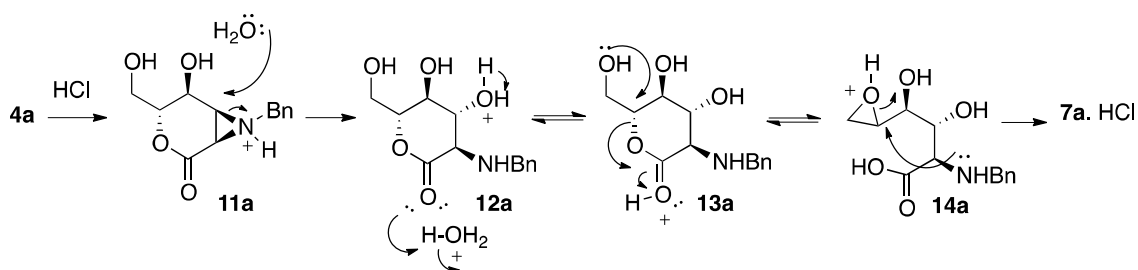
Under TFA, the intermediate **10**, in opposition to  $\text{Bil}_3$ /boiling water treatment, catalyse a second cyclization. This is in accordance with the literature which largely refers to the formation of bicyclic **6**-type structures, in cases a favored stereochemistry of the first formed 5-membered structures occur in the presence of TFA [14] (**Scheme 10**).



**Scheme 10**- Proposed mechanism for the synthesis of compound **6a** from **1a** in the presence of TFA.

A different mechanism is proposed for HCl. In opposition to the other acids, HCl gives a different outcome for the reactions starting with **4a** and **9a**: from **4a** is formed a single product **7a** (**Scheme 10**); from **9a** is formed a useless mixture of products. This means that the first step of the reaction's cascade should be the C-N bond cleavage, as shown in **Scheme 11** rather than the C-O cleavage in the lactone unit (compare with **Scheme 9**).  $\text{H}_2\text{O}$  nucleophilic attack on intermediate **11a** will give **12a**. The lactone C-O cleavage will occur later in the protonated intermediate **13a**, possibly with the assistance of an epoxide formation as known in the literature [15], and represented in structure

**14a.** Nitrogen atom will attack in the last step closing-up a proline structure, with the formation of compound **7a**.



**Scheme 11** - Proposed mechanism for the synthesis of compound **7a.HCl** from aziridine **4a** in HCl.

Looking back to Scheme 9, it seems likely that the protonated structure **11a** forms at the first instance in  $\text{BiI}_3/\text{H}_2\text{O}$  and in TFA medium. However, it seems that **11a** is not an intermediate in both reactions. Notably, the approach of TFA to the aziridine moiety in **11a** would be constrained because both species are bulky; so **11a** would remain unproductive. As the pair  $\text{BiI}_3/\text{H}_2\text{O}$  behaves similarly it seems that the same kind of impediment occurs with the transference of HI to the sugar molecule. In opposition, the activation of the carbonyl group does not suffer from such an entropic factor.

#### 4. Conclusion

This work shows the versatility of the 6-carbon atom erythrosyl fused aziridinolactone **4** as a chiral platform in the synthesis of SAA compounds. Different protic acids are capable to initiate diverse mechanism pathways with total selectivity, so that two different types of SAA products can be produced in very good overall yields, by simply changing the nature of the acid. Compounds **1** are of unknown type, although the unit can be found in macromolecules. The hydroxyprolines **7**, especially through their dehydrated counterparts **8** deserve a close look as Michael acceptors, in order to achieve the synthesis of new structures of an important type.

#### 5. Experimental Section

General.

Solvents were used as purchased except: dichloromethane and methanol, dried under CaH<sub>2</sub> and Mg/I<sub>2</sub>, respectively; tetrahydrofuran, and ether, dried under Na-benzophenone, and DMF and toluene distilled with elimination of the head distillation fractions. Petroleum ether 40–60 °C used in chromatography was submitted to distillation. D-Erythrose lactone **3** [6] and 1,2,3-triazolines **2a**, **b** [6], were obtained according to literature. All other reagents were purchased and used without further purification. Glassware was dried prior to use. Compounds were purified by dry flash chromatography using silica 60, <0.063 mm, and water pump vacuum or by flash-chromatography using silica 60 Å 230–400 mesh as stationary phases. TLC plates (silica gel 60 F254) were visualized either with a UV lamp or in a I<sub>2</sub> chamber.

### 5.1 Reaction of lactone **3** with alkyl azides

To a solution of lactone **3** (~0.10 g; ~0.4 mmol) in methyl orthoformate (10 mL) was added the alkyl azide (2 eq.). The reaction mixture was heated at 100°C under a nitrogen atmosphere for 72 h. The solvent was evaporated, and the resulting solid residue was recrystallized from ethanol. The title compounds were obtained as white solids *c.a.* ~72 %.

#### 5.1.1 Synthesis of (3*aR*,5*aR*,8*R*,9*aS*,9*bS*)-8-phenyl-1-tetradecyl-1,3*a*,5*a*,6,9*a*,9*b*-hexahydro-4*H*-[1,3]dioxino[4',5':5,6]pyrano[3,4-*d*][1,2,3]triazol-4-one (**2d**)

Lactone **3** (97 mg, 0.417 mmol); CH<sub>3</sub>(CH<sub>2</sub>)<sub>13</sub>N<sub>3</sub> (2 eq.); obtained product (0.138 g, 0.302 mmol, 72.3%). M.p. = 78 - 80°C; [α]<sub>D</sub><sup>25</sup> = - 140.0 ° (c 0.64 %, CH<sub>2</sub>Cl<sub>2</sub>); IR (nujol): ν<sub>max</sub> 2095.8, 1772.9 cm<sup>-1</sup>; <sup>1</sup>H NMR (400 MHz, CDCl<sub>3</sub>) δ 7.47-7.40 (m, 5H, Ph), 5.58 (s, 1H, 8-*H*), 5.41 (d, *J* = 13.2 Hz, 1H, 3*a*-*H*), 4.48 (dd, *J* = 10.9, 5.5 Hz, 1H, 6-*H*), 4.29 (td, *J* = 14.7, 5.5 Hz, 1H, 5*a*-*H*), 4.12-4.08 (m, 2H, 9*a*-*H* e 9*b*-*H*), 3.87 (ddd, *J* = 13.7, 7.0, 1.6 Hz, 1H, CH<sub>2</sub>), 3.80 (t, *J* = 10.5 Hz, 1H, 6-*H*), 3.66 (ddd, *J* = 8.5, 5.4, 3.3 Hz, 1H, CH<sub>2</sub>), 1.77-1.73 (m, 2H, CH<sub>2</sub>), 1.27-1.24 (m, 24H, CH<sub>2</sub>), 0.89 (t, *J* = 6.8 Hz, 3H, CH<sub>3</sub>); <sup>13</sup>C NMR (100.6 MHz, CDCl<sub>3</sub>) δ 161.9(C=O), 136.3, 129.6, 128.4, 126.0 (Ph), 102.3 (8-C), 80.2 (3*a*-C), 76.2 (9*a*-C), 67.9 (6-C), 65.6 (5*a*-C), 54.8 (9*b*-C), 50.7 (1', CH<sub>2</sub>), 31.9, 29.6, 29.6, 29.6, 29.5, 29.48, 29.3, 29.2, 29.13, 28.1, 26.7, 22.66 (CH<sub>2</sub>), 14.1 (CH<sub>3</sub>); HRMS (ESI-TOF), found for [C<sub>27</sub>H<sub>41</sub>N<sub>3</sub>O<sub>4</sub>+H<sup>+</sup>]: 472.3176; calcd: 472.3170.

#### 5.1.2 Synthesis of (3*aR*,5*aR*,8*R*,9*aS*,9*bS*)-1-(4-nitrobenzyl)-8-phenyl-1,3*a*,5*a*,6,9*a*,9*b*-hexahydro-4*H*-[1,3]dioxino[4',5':5,6]pyrano[3,4-*d*][1,2,3]triazol-4-one (**2e**)

Lactone **3** (100 mg, 0.430 mmol);  $\text{NO}_2\text{PHCH}_2\text{N}_3$  (2 eq.); obtained product (0.124 g, 0.302 mmol, 70.2%). M.p. = 148 - 151 °C;  $[\alpha]_{\text{D}}^{25} = -419.1^\circ$  (c 5%,  $\text{CH}_2\text{Cl}_2$ ); IR (nujol):  $\nu_{\text{max}}$  1755.6, 1517.9, 1344  $\text{cm}^{-1}$ ;  $^1\text{H}$  NMR (400 MHz,  $\text{CDCl}_3$ )  $\delta$  8.12 (d,  $J = 8.7$  Hz, 2H, Ar), 7.46 (m, 5H, Ph), 7.33 (d,  $J = 8.6$  Hz, 2H, Ar), 5.60 (s, 1H, 8-*H*), 5.43 (d,  $J = 12.8$  Hz, 1H, 3a-*H*), 5.30 (d,  $J = 15.2$  Hz, 1H,  $\text{CH}_2$ ), 4.86 (d,  $J = 15.2$  Hz, 1H,  $\text{CH}_2$ ), 4.52 (dd,  $J = 10.8, 5.2$  Hz, 1H, 6-*H*), 4.35 (ddd,  $J = 10, 5.2$  Hz, 1H, 5a-*H*), 4.16 (dd,  $J = 9.6, 3.6$  Hz, 1H, 9a-*H*), 3.87-3.79 (m, 2H, 6-*H* e 9b-*H*);  $^{13}\text{C}$  NMR (100.6 MHz,  $\text{CDCl}_3$ )  $\delta$  161.1 (C=O), 147.8 (Cq, Ar), 142.2 (Cq, Ar), 136.1 (Cq, Ar), 129.8 (CH, Ar), 129.6 (CH, Ar), 128.5 (CH, Ar), 125.9 (CH, Ar), 124.0 (CH, Ar), 102.3 (8-C), 81.1 (3a-C), 75.9 (9a-C), 67.8 (6-C), 65.8 (5a-C), 53.6 ( $\text{CH}_2$ ), 53.5 (9b-C); HRMS (ESI-TOF), found for  $[\text{C}_{20}\text{H}_{18}\text{N}_4\text{O}_6 + \text{H}^+]$ : 411.1291; calcd: 411.1299.

## 5.2 $\text{N}_2$ Extrusion from triazolones 2a-e

1,2,3-Triazoline **2a-e** (60 mg – 70 mg) was dissolved in  $\text{CH}_2\text{Cl}_2$  (8 mL) introduced in a quartz tub container, irradiated with 254 nm lamp for 1h 15 min – 9h. Evaporation of the reaction mixture gave the title aziridine **4a-e** as white solid/tick oil in quantitative yields.

### 5.2.1 Synthesis of (2*R*,4*aR*,6*aS*,7*aR*,7*bS*)-1-benzyl-2-phenyltetrahydro-4*H*-[1,3]dioxino(4',5',5,6)pyrano[3,4-b]aziridin-6(4*aH*)-one (4a)

Triazoline **2a** (70 mg, 0.195 mmol); 1 h 50 min. White solid; quantitative yield. M.p. = 135.8 – 136.9 °C;  $[\alpha]_{\text{D}}^{25} = +32.6^\circ$  (c 0.6 %,  $\text{CH}_2\text{Cl}_2$ ); IR (nujol):  $\nu_{\text{max}}$  1741.9  $\text{cm}^{-1}$ ;  $^1\text{H}$  NMR (400 MHz,  $\text{CD}_3\text{OD}$ )  $\delta$  7.44-7.28 (m, 10H, Ph), 5.69 (s, 1H, 2-*H*), 4.74 (dt,  $J = 9.6, 4.8$  Hz, 1H, 4a-*H*), 4.30 (dd,  $J = 10.0, 4.8$  Hz, 1H, 4-*H*), 4.20 (dd,  $J = 9.2, 1.6$  Hz, 1H, 7b-*H*), 3.82 (t,  $J = 10.4$  Hz, 1H, 4-*H*), 3.76 (d,  $J = 13.6$  Hz, 1H, 1'-*H*), 3.67 (d,  $J = 13.6$  Hz, 1H, 1'-*H*), 2.85 (dd,  $J = 6.4, 1.6$  Hz, 1H, 7a-*H*), 2.72 (d,  $J = 6.4$  Hz, 1H, 6a-*H*);  $^{13}\text{C}$  NMR (100.6 MHz,  $\text{CD}_3\text{OD}$ )  $\delta$  169.2 (6-C), 139.2 (Cq, Ph), 138.7 (Cq, Ph), 130.2 (CH, Ar), 129.4 (CH, Ar), 129.1 (CH, Ar), 129.0 (CH, Ar), 128.9 (CH, Ar), 128.4 (CH, Ar), 127.4 (CH, Ar), 127.2 (CH, Ar), 103.6 (2-C), 77.0 (7b-C), 69.1 (4-C), 68.3 (4a-C), 62.2 (1'-C), 42.8 (7a-C), 40.4 (6a-C); HRMS (ESI-TOF) found for  $[\text{C}_{20}\text{H}_{19}\text{NO}_4 + \text{H}^+]$ : 338.1390; calcd: 338.1387.

### 5.2.2 Synthesis of (2*R*,4*aR*,6*aS*,7*aR*,7*bS*)-1-(Propyl-3'-benzyloxy)-2-phenyltetrahydro-4*H*-[1,3]dioxino(4',5',5,6)pyrano[3,4-b]aziridin-6(4*aH*)-one (4b)

Triazoline **2b** (60 mg, 0.141 mmol); 1h 15 min; tick oil; quantitative yield.  $[\alpha]_{\text{D}}^{25} = + 4.4^\circ$  (c 0.25%,  $\text{CH}_2\text{Cl}_2$ ); IR (neat):  $\nu_{\text{max}}$  1749  $\text{cm}^{-1}$ ;  $^1\text{H}$  NMR (400 MHz,  $\text{CDCl}_3$ )  $\delta$  7.53-7.50 (m, 2H, *H<sub>A</sub>*), 7.41-7.36 (m, 3H, Ph), 7.33-7.26 (m, 5H, Ph), 5.58 (s, 1H, 2-*H*), 4.70 (dt,  $J = 9.6, 5.2$  Hz, 1H, 4a-*H*), 4.50 (s, 2H, 4'-*H*), 4.34 (dd,  $J = 10.0, 5.2$  Hz, 1H, 4-*H*), 3.99 (dd,  $J = 9.2, 1.6$  Hz, 1H, 7b-*H*), 3.74 (t,  $J = 10.6$  Hz, 1H, 4-*H*), 3.64 (dt,  $J = 15.2, 3.2$  Hz, 1H, 3'-*H*), 3.35 (d,  $J = 15.2$  Hz, 1H, 3'-*H*), 2.70-2.64 (m, 1H, 1'-*H*), 2.51-2.47 (m, 1H, 1'-*H*), 2.37 (dd,  $J = 6.4, 1.2$  Hz, 1H, 7a-*H*), 2.38 (d,  $J = 6.4$  Hz, 1H, 6a-*H*), 1.92 (dd,  $J = 12.8, 6.2$  Hz, 1H, 2'-*H*), 1.27 (t,  $J = 7.2$  Hz, 1H, 2'-*H*);  $^{13}\text{C}$  NMR (100.6 MHz,  $\text{CD}_3\text{OD}$ )  $\delta$  167.3 (6-C), 138.4 (Cq, Ph), 136.7 (Cq, Ph), 129.4 (CH, Ph), 128.4 (CH, Ph), 128.4 (CH, Ph), 127.7 (CH, Ph), 127.6 (CH, Ph), 126.2 (CH, Ph), 102.6 (2-C), 76.2 (7b-C), 72.9 (4'-C), 68.3 (4-C), 66.8 (3'-C), 66.6 (4a-C), 55.1 (1'-C), 41.3 (7a-C), 39.2 (6a-C), 29.6 (2'-C); HRMS (ESI-TOF) found for  $[\text{C}_{23}\text{H}_{25}\text{NO}_5 + \text{Na}]$ : 418.1608; calcd: 418.1625.

### 5.2.3 Synthesis of (2*R*,4*aR*,7*bS*)-2-phenyl-7-propyltetrahydro-4*H* [1,3]dioxino[4',5':5,6]pyrano[3,4-*b*]azirin-6(4*aH*)-one (4c)

Triazoline **2c** (70 mg, 0.241 mmol); 1h 57 m; tick oil; quantitative yield.  $[\alpha]_{\text{D}}^{25} = + 10.5^\circ$  (c 0.8%,  $\text{CH}_2\text{Cl}_2$ ); IR (neat):  $\nu_{\text{max}}$  1749  $\text{cm}^{-1}$ ;  $^1\text{H}$  NMR (400 MHz,  $\text{CDCl}_3$ )  $\delta$  7.52-7.44 (m, 2H, Ph), 7.42-7.34 (m, 2H, Ph), 5.55 (s, 1H, 2-*H*), 4.72 (dt,  $J = 10.2, 4.7$  Hz, 1H, 4a-*H*), 4.31 (dd,  $J = 10.0, 4.8$  Hz, 1H, 4-*H*), 3.96 (br d,  $J = 9.2$  Hz, 1H, 7b-*H*), 3.71 (t,  $J = 10.6$  Hz, 1H, 4-*H*), 2.47 (br d,  $J = 6.4$  Hz, 1H, 7a-*H*), 2.45-2.32 (m, 2H, 1'-*H*), 2.38 (d,  $J = 6.0$  Hz, 1H, 6a-*H*), 1.61 (q,  $J = 7.2$  Hz, 2H, 2'-*H*), 0.99 (t,  $J = 7.4$  Hz, 3H, 3'-*H*);  $^{13}\text{C}$  NMR (100.6 MHz,  $\text{CDCl}_3$ )  $\delta$  167.3 (6-C), 136.6 (Cq, Ph), 129.2 (CH, Ph), 128.2 (CH, Ph), 126.1 (CH, Ph), 102.4 (2-C), 76.0 (7b-C), 68.1 (4-C), 66.5 (4a-C), 60.3 (1'-C), 41.0 (7a-C), 39.1 (6a-C), 22.6 (2'-C), 11.4 (3'-C); HRMS (ESI-TOF) found for  $[\text{C}_{16}\text{H}_{19}\text{NO}_4 + \text{H}^+]$ : 290.1382; calcd: 290.1387.

### 5.2.4 Synthesis of (2*R*,4*aR*,7*bS*)-2-phenyl-7-tetradecyltetrahydro-4*H* [1,3]dioxino[4',5':5,6]pyrano[3,4-*b*]azirin-6(4*aH*)-one (4d)

Triazoline **2d** (70 mg, 0.158 mmol); 3h 30 m; tick oil; quantitative yield.  $[\alpha]_{\text{D}}^{25} = + 79.49^\circ$  (c 0.78 %,  $\text{CH}_2\text{Cl}_2$ ); IR (neat):  $\nu_{\text{max}}$  1745.4  $\text{cm}^{-1}$ ;  $^1\text{H}$  NMR (400 MHz,  $\text{CDCl}_3$ )  $\delta$  7.52-7.39 (m, 5H, Ph), 5.56 (s, 1H, 2-*H*), 4.73 (dt,  $J = 10.4, 4.9$  Hz, 1H, 4a-*H*), 4.33 (dd,  $J = 10.4, 4.9$  Hz, 1H, 4-*H*), 3.98 (dd,  $J = 9.3, 1.2$  Hz, 1H, 7b-*H*), 3.73 (t,  $J = 10.6$  Hz, 1H, 4-*H*), 2.50-2.45 (m, 2H,  $\text{CH}_2$  e 7a-*H*), 2.42-2.37 (m, 2H,  $\text{CH}_2$  e 6a-*H*), 1.61-1.57 (m, 2H,  $\text{CH}_2$ ), 1.43-1.40 (m, 2H,  $\text{CH}_2$ ), 1.26 (sl, 24H,  $\text{CH}_2$ ),



0.88 (t,  $J = 6.7$  Hz, 3H, CH<sub>3</sub>); <sup>13</sup>C NMR (100.6 MHz, CDCl<sub>3</sub>)  $\delta$  167.5 (6-C), 136.7 (Cq, Ph), 129.3 (CH, Ph), 128.3 (CH, Ph), 126.2 (CH, Ph), 102.5 (2-C), 76.2 (7b-C), 68.3 (4-C), 66.6 (4a-C), 58.8 (1', CH<sub>2</sub>), 41.3 (7a-C), 39.2 (6a-C), 31.9, 29.6, 29.6, 29.6, 29.5, 29.5, 29.4, 29.3, 27.0, 22.6 (CH<sub>2</sub>), 14.1 (CH<sub>3</sub>). HRMS (ESI-TOF) found for [C<sub>27</sub>H<sub>42</sub>NO<sub>4</sub>]: 444.3123; calcd: 444.3114.

### 5.2.5 Synthesis of (2*R*,4*aR*,7*bS*)-7-(4-nitrobenzyl)-2-phenyltetrahydro-4*H*-[1,3]dioxino[4',5':5,6]pyrano[3,4-*b*]azirin-6(4*aH*)-one (4e)

Triazoline **2e** (70 mg, 0.183 mmol); 9h; tick oil; quantitative yield.  $[\alpha]_{D^{25}} = +96.97^\circ$  (c 0.99 %, CH<sub>2</sub>Cl<sub>2</sub>); IR (neat):  $\nu_{\max}$  1750.6, 1513.8, 1341.2 cm<sup>-1</sup>; <sup>1</sup>H NMR (400 MHz, CDCl<sub>3</sub>)  $\delta$  8.21(d,  $J = 2.9$  Hz, 2H, Ar), 7.60(d,  $J = 8.8$  Hz, 2H, Ar), 7.52-7.39 (m, 5H, Ph), 5.60 (s, 1H, 2-*H*), 4.85 (ddt,  $J = 10.6, 4.8, 1.3$  Hz, 1H, 4*a-H*), 4.39 (dd,  $J = 10.4, 4.8$  Hz, 1H, 4-*H*), 4.09(d,  $J = 9.5$  Hz, 1H, 7*b-H*), 3.99 (d,  $J = 14.9$  Hz, 1H, 1'-*H*), 3.80(t,  $J = 10.6$  Hz, 1H, 4-*H*), 3.63 (d,  $J = 14.9$  Hz, 1H, 1'-*H*), 2.69 (br s, 2H, 7*a-H* e 6*a-H*); <sup>13</sup>C NMR (100.6 MHz, CDCl<sub>3</sub>)  $\delta$  166.2 (6-C), 147.3(Cq, Ar), 144.5(Cq, Ar), 136.4(Cq, Ar), 129.7(CH, Ar), 128.4(CH, Ar), 128.0(CH, Ar), 126.1(CH, Ar), 123.7(CH, Ar), 102.6 (2-C), 75.6 (7*b*-C), 68.2 (4-C), 66.8 (4*a*-C), 60.6 (1'-C), 41.5 (7*a*-C), 39.6 (6*a*-C); HRMS (ESI-TOF) found for [C<sub>20</sub>H<sub>18</sub>N<sub>2</sub>O<sub>6</sub> + H<sup>+</sup>]: 383.1243; calcd: 383.1238.

## 5.3 Synthesis of diazirines compounds

To a solution of 1,2,3-triazoline **2a-c** (70-110 mg, 0.166 - 0.300 mmol) in H<sub>2</sub>O/ACN (8:4 mL) heated for 20 min at 100-110 ° C, was added Bil<sub>3</sub> (20 mol%). The reaction mixture was kept under heating for 2 h 30 min. After this time the reaction mixture was allowed to reach room temperature, and activated basic resin added (Dowex 1x3, OH). The resin was filtered off, washed with H<sub>2</sub>O (2 x 5 mL), and the filtrate evaporated to give pure product, the diazirine compounds ( $\eta = 45.5$ -64.3%).

### 5.3.1 Synthesis of (2'*R*,4*a'R*,8'*S*,8*a'S*)-8'-(benzylamine)-2'-phenyl-8',8*a'*-dihydro-4'*H*-spiro[diazirine-3,7'-pyrano [3,2-*d*][1,3]dioxin]-6'(4*a'H*)-one (5a)

1,2,3-Triazoline **2a** (110 mg, 0.300mmol); compound **5a** (0.05 g, 0.137 mmol,  $\eta = 45.5\%$ ).  $[\alpha]_{D^{25}} = +24.7^\circ$  (c 0.55 %, CH<sub>2</sub>Cl<sub>2</sub>); IR (neat):  $\nu_{\max}$  3372, 2109, 1688 cm<sup>-1</sup>; <sup>1</sup>H NMR (400 MHz, CDCl<sub>3</sub>)  $\delta$

7.47-7.27 (m, 10H, Ph), 5.63 (s, 1H, 2-*H*), 4.85 (td,  $J = 10, 5.2$  Hz, 1H, 4a-*H*), 4.50 (dd,  $J = 10.8, 5.2$  Hz, 1H, 4-*H*), 4.25 (d,  $J = 4$  Hz, 1H, 8-*H*), 4.04 (dd,  $J = 9.6, 4.4$  Hz, 1H, 9-*H*), 3.99 (d,  $J = 13.2$  Hz, 1H, 1'-*H*), 3.90 (d,  $J = 13.2$  Hz, 1H, 1'-*H*), 3.85 (t,  $J = 10.6$  Hz, 1H, 4-*H*);  $^{13}\text{C}$  NMR (100.6 MHz,  $\text{CDCl}_3$ )  $\delta$  163.8 (6-C), 139.2 (Cq, Ar), 138.9 (Cq, Ar), 136.4 (CH, Ar), 129.5 (CH, Ar), 128.7 (CH, Ar), 128.4 (CH, Ar), 127.9 (CH, Ar), 127.5 (CH, Ar), 126.1 (CH, Ar), 101.9 (2-C), 75.6 (9-C), 68.3 (4-C), 65.6 (4a-C), 58.2 (7-C), 52.9 (8-C), 51.3 (1'-C). HRMS (ESI) found for  $[\text{C}_{20}\text{H}_{19}\text{N}_3\text{O}_4 + \text{H}^+]$ : 366.1437; calcd: 366.1448.

### 5.3.2 Synthesis of (2'R,4a'R,8'S,8a'S)-8'-(3-(benzyloxy)propylamine)-2'-phenyl-8',8a'-dihydro-4'H-spiro[diazirine-3,7'-pyrano[3,2-d][1,3]dioxin]-6'(4a'H)-one (5b)

1,2,3-Triazoline **2b** (70 mg, 0.166 mmol); compound **5b** (0.032 g, 0.076 mmol,  $\eta = 45.7\%$ ).  $[\alpha]_{\text{D}_{25}}^{25} = +102.48^\circ$  (c 0.51%,  $\text{CH}_2\text{Cl}_2$ ); IR (neat):  $\nu_{\text{max}}$  3326, 2108, 1689  $\text{cm}^{-1}$ ;  $^1\text{H}$  NMR (400 MHz,  $\text{CDCl}_3$ )  $\delta$  7.49-7.27 (m, 10H, HAr), 5.62 (s, 1H, 2-*H*), 4.75 (td,  $J = 10, 5.2$  Hz, 1H, 4a-*H*), 4.50-4.45 (m, 2H, 4'-*H*), 4.46 (dd,  $J = 10.8, 5.2$  Hz, 1H, 4-*H*), 4.17 (d,  $J = 4.4$  Hz, 1H, 8-*H*), 4.00 (dd,  $J = 9.6, 4.4$  Hz, 1H, 9-*H*), 3.82 (t,  $J = 10.6$  Hz, 1H, 4-*H*), 3.55 (dt,  $J = 11.6, 5.6$  Hz, 2H, 3'-*H*), 2.91-2.85 (m, 1H, 1'-*H*), 2.88-2.76 (m, 1H, 1'-*H*), 1.87-1.82 (m, 3H, 2'-*H*);  $^{13}\text{C}$  NMR (100.6 MHz,  $\text{CDCl}_3$ )  $\delta$  163.6 (6-C), 138.1 (Cq, Ar), 136.8 (CH, Ar), 129.5 (CH, Ar), 128.4 (CH, Ar), 127.7 (CH, Ar), 126.1 (CH, Ar), 101.8 (2-C), 75.2 (9-C), 73.0 (4'-C), 68.4 (3'-C), 68.2 (4-C), 65.4 (4a-C), 57.9 (7-C), 53.4 (8-C), 45.4 (1'-C), 29.7 (2'-C). HRMS (ESI) found for  $[\text{C}_{23}\text{H}_{26}\text{N}_3\text{O}_5 + \text{H}^+]$ : 424.1850; calcd: 424.1867.

### 5.3.3 Synthesis of (2'R,4a'R,8'S,8a'S)-2'-phenyl-8'-(propylamine)-8',8a'-dihydro-4'H-spiro[diazirine-3,7'-pyrano[3,2-d][1,3]dioxin]-6'(4a'H)-one (5c)

1,2,3-Triazoline **2c** (70 mg, 0.220 mmol); compound **5c** (0.045 g, 0.141 mmol,  $\eta = 64.3\%$ ).  $[\alpha]_{\text{D}_{25}}^{25} = +43.2^\circ$  (c 0.5%, ethyl acetate); IR (neat):  $\nu_{\text{max}}$  3335, 2107, 1692  $\text{cm}^{-1}$ ;  $^1\text{H}$  NMR (400 MHz,  $\text{CDCl}_3$ )  $\delta$  7.47-7.27 (m, 5H, Ar), 5.62 (s, 1H, 2-*H*), 4.81 (td,  $J = 10.2, 5.2$  Hz, 1H, 4a-*H*), 4.48 (dd,  $J = 10.8, 5.2$  Hz, 1H, 4-*H*), 4.17 (d,  $J = 4.4$  Hz, 1H, 8-*H*), 4.01 (dd,  $J = 9.6, 4$  Hz, 1H, 9-*H*), 3.82 (t,  $J = 10.6$  Hz, 1H, 4-*H*), 2.71-2.59 (m, 2H, 1'-*H*), 1.61-1.50 (m, 2H, 2'-*H*), 0.95 (t,  $J = 7.4$  Hz, 3H, 3'-*H*);  $^{13}\text{C}$  NMR (100.6 MHz,  $\text{CDCl}_3$ )  $\delta$  164.0 (6-C), 13.5 (Cq, Ar), 129.5 (CH, Ar), 128.4 (CH, Ar), 126.1 (CH, Ar), 125.5 (CH, Ar), 101.8 (2-C), 75.5 (9-C), 68.3 (4-C), 65.5 (4a-C), 58.0 (7-C), 53.9 (8-C), 49.4 (1'-C), 23.3 (2'-C), 11.8 (3'-C). HRMS (ESI) found for  $[\text{C}_{16}\text{H}_{19}\text{N}_3\text{O}_4 + \text{H}^+]$ : 318.1447; calcd: 318.1448.

## 5.4 Synthesis of (2*S*,3*R*)-1-substituted-3-((2*R*,4*S*,5*R*)-5-hydroxy-2-phenyl-1,3-dioxan-4-yl)aziridine-2-carboxylic acid (9a-c)

### 5.4.1 General procedure

A solution of (2*R*,4*aR*,6*aS*,7*aR*,7*bS*)-1-substituted-2-phenyltetrahydro-4*H*-[1,3]dioxino(4',5',5,6)pyrano[3,4-*b*]aziridin-6(4*aH*)-one **4a-c** (90 mg - 120 mg) in H<sub>2</sub>O/CH<sub>3</sub>CN (20/4 mL) under magnetic stirring at 40 °C was added NaOH (1M, 600 mL, 15 mmol). The reaction mixture was left stirring for 24 hand then allowed to reach room temperature. Activated acid resin [Amberlite resin IR 120 (H<sup>+</sup>)] was added for neutralization, washed with H<sub>2</sub>O (2 x 5 mL) and filtered off. Evaporation of the filtrate till dryness gave title products as oils (67.8 - 80%).

### 5.4.2 (2*S*,3*R*)-1-benzyl-3-((2*R*,4*S*,5*R*)-5-hydroxy-2-phenyl-1,3-dioxan-4-yl)aziridine-2-carboxylic acid (9a)

Compound **4a** (120 mg, 0.355 mmol),  $\eta = 80\%$ . IR:  $\nu_{\max}/\text{cm}^{-1}$  3362 (OH), 1633 (C=O);  $[\alpha]_{\text{D}}^{25} = +4.4^{\circ}$  (c 3 %, CH<sub>3</sub>CH<sub>2</sub>OH); <sup>1</sup>H NMR (400 MHz, D<sub>2</sub>O)  $\delta$  7.53-7.39 (m, 10H, *H<sub>A</sub>*), 5.57 (s, 1H, 3''-*H*), 4.26 (dd,  $J = 10.2, 3.8$  Hz, 1H, 5''-*H*), 3.79-3.76 (m, 2H, 1''-*H* + 6''-*H*), 3.73 (d,  $J = 13.6$  Hz, 1H, 1'-*H*), 3.72 (dd,  $J = 10.4, 6.4$  Hz, 1H, 5''-*H*), 3.57 (d,  $J = 13.2$  Hz, 1H, 1'-*H*); 2.41 (d,  $J = 7.2$  Hz, 1H, 2-H); 2.31 (t,  $J = 7.2$  Hz, 1H, 3-H); <sup>13</sup>C NMR (100.6 MHz, D<sub>2</sub>O)  $\delta$  175.6 (C=O), 137.4 (Cq, Ar), 136.0 (Cq, Ar), 129.1 (CH, Ar), 128.2 (CH, Ar), 128.1 (CH, Ar), 128.1 (CH, Ar), 127.1 (CH, Ar), 125.5 (CH, Ar), 100.3 (3''-C), 78.9 (1''-C), 69.7 (5''-C), 65.0 (6''-C), 61.6 (1'-C), 44.9 (3-C), 42.8 (2-C); HRMS (ESI-TOF) found for [C<sub>20</sub>H<sub>21</sub>NO<sub>5</sub> + H<sup>+</sup>]: 356.1489; calcd: 356.1493.

### 5.4.3 (2*S*,3*R*)-1-Propyl-3'-benzyloxy-3-((2*R*,4*S*,5*R*)-5-hydroxy-2-phenyl-1,3-dioxan-4-yl)aziridine-2-carboxylic acid (9b)

Compound **4b** (90 mg, 0.215 mmol),  $\eta = 67.8\%$ ; IR:  $\nu_{\max}/\text{cm}^{-1}$  3387 (OH), 1668 (C=O);  $[\alpha]_{\text{D}}^{25} = +23.5^{\circ}$  (c 0.5%, CH<sub>3</sub>CH<sub>2</sub>OH); <sup>1</sup>H NMR (400 MHz, D<sub>2</sub>O)  $\delta$  7.56 – 7.31 (m, 10H, *H<sub>A</sub>*), 5.50 (s, 1H, 1''-*H*), 4.53 (d,  $J = 2.3$  Hz, 2H, 5'-*H*), 4.24 (dd,  $J = 10.4, 4.8$  Hz, 1H, 5''-*H*), 3.77 (dt,  $J = 9.6, 4.7$  Hz, 1H, 6''-*H*), 3.70 (t,  $J = 10.0$  Hz, 1H, 1''-*H*), 3.69 (t,  $J = 8.8$  Hz, 1H, 5''-*H*), 3.63 (td,  $J = 6.4,$

1.6 Hz, 1H, 3'-*H*), 2.57 (dt,  $J = 13.4, 6.8$  Hz, 1H, 1'-*H*), 2.39 – 2.28 (m, 1H, 1'-*H*), 2.17 – 2.10 (m, 1H, 2'-*H*), 2.02 (dd,  $J = 15.0, 7.7$  Hz, 1H, 3'-*H*), 1.90 – 1.83 (m, 2H, 2'-*H*);  $^{13}\text{C}$  NMR (100.6 MHz,  $\text{D}_2\text{O}$ )  $\delta$  176.29 (C=O), 137.4 (Cq), 136.6 (Cq), 129.5 (CH, Ar), 128.7 (CH, Ar), 128.6 (CH, Ar), 128.3 (CH, Ar), 126.0 (CH, Ar), 100.7 (3''-C), 79.9 (1''-C), 72.6 (5'-C), 70.8 (5''-C), 68.2 (3'-C), 65.7 (6''-C), 55.8 (1'-C), 45.7 (3-C), 43.2 (2-C), 28.5 (2'-C); HRMS (ESI-TOF) found for  $[\text{C}_{23}\text{H}_{27}\text{NO}_6 + \text{H}^+]$ : 414.1911; calcd: 414.1911.

#### 5.4.4 (2*S*,3*R*)-1-Propyl-3-((2*R*,4*S*,5*R*)-5-hydroxy-2-phenyl-1,3-dioxan-4-yl)aziridine-2-carboxylic acid (**9c**)

Compound **4c** (107 mg, 0.369 mmol),  $\eta = 79.4\%$ . IR:  $\nu_{\text{max}}/\text{cm}^{-1}$  3409 (OH), 1665 (C=O);  $[\alpha]_{\text{D}}^{25} = +6.6^\circ$  (c 0.6 %,  $\text{CH}_3\text{CH}_2\text{OH}$ );  $^1\text{H}$  NMR (400 MHz,  $\text{D}_2\text{O}$ )  $\delta$  7.48 – 7.43 (m, 5H, *H<sub>a</sub>*), 5.54 (s, 1H, 3''-*H*), 4.27 (dd,  $J = 10.6, 5.0$  Hz, 1H, 5''-*H*), 3.85 (dt,  $J = 10, 4.8$  Hz, 1H, 6''-*H*), 3.75 (t,  $J = 8$  Hz, 1H, 1''-*H*), 3.70 (t,  $J = 10.8$  Hz, 1H, 5''-*H*), 2.55 (dt,  $J = 11.8, 7.0$  Hz, 1H, 1'-*H*), 2.21-2.14 (m, 2H, 1'-*H* and 2'-*H*), 2.04 (t,  $J = 7.2$  Hz, 1H, 3'-*H*), 1.58 (h,  $J = 7.4$  Hz, 2H, 2'-*H*), 0.90 (t,  $J = 7.5$  Hz, 3H, 3'-*H*);  $^{13}\text{C}$  NMR (100.6 MHz,  $\text{D}_2\text{O}$ )  $\delta$  176.0 (C=O), 136.1 (Cq, Ar), 129.0 (Cq, Ar), 128.1 (CH, Ar), 125.5 (CH, Ar), 100.2 (3''-C), 79.4 (1''-C), 70.3 (5''-C), 65.3 (6''-C), 60.6 (1'-C), 45.0 (3-C), 42.8 (2-C), 21.3 (2'-C), 10.7 (3'-C); HRMS (ESI-TOF) found for  $[\text{C}_{16}\text{H}_{21}\text{NO}_5 + \text{Na}^+]$ : 330.1308; calcd: 330.1312.

### 5.5 Synthesis of amino acids **1a-c**

#### 5.5.1 General procedure for method 1:

A solution of (2*S*,3*R*)-1-substituted-3-((2*R*,4*S*,5*R*)-5-hydroxy-2-phenyl-1,3-dioxan-4-yl)aziridine-2-carboxylic acid **9a-c** (65-100 mg, 0.169-0.282 mmol) in  $\text{H}_2\text{O}$  (10-15 mL) at 115 ° C temperature was added  $\text{BiI}_3$  (10 mol%). The reaction mixture was left for 2h-2h 30 m. After this time was allowed to reach room temperature, and activated basic resin (Dowex 1x3, OH). The resin was filtered off, washed with  $\text{H}_2\text{O}$  (2 x 5 mL), and the filtrate evaporated to yield a crude product, which purified by dry-flash chromatography (ethanol, 5%  $\text{NH}_3$  aq. sol.) to give pure products **1a-c** (32.7 - 83.7%).

#### 5.5.2 2-(Benzyl)-2-((3*R*,4*R*)-3,4-dihydroxytetrahydrofuran-2-yl)acetic acid (**5a**)

#### Method 1

Compound **9a** (100 mg, 0.282 mmol); H<sub>2</sub>O (15 mL); 2 h. Compound **1a**: Viscous oil;  $\eta = 83.7\%$ ;  $[\alpha]_{D}^{25} = +86.67^\circ$  (c 0.15 %, CH<sub>3</sub>CH<sub>2</sub>OH); IR (neat):  $\nu_{\max}$  3307, 1646 cm<sup>-1</sup>; <sup>1</sup>H NMR (400 MHz, CD<sub>3</sub>OD)  $\delta$  7.52 - 7.43 (m, 5H, *H<sub>a</sub>*), 4.63 (dd, *J* = 8, 1.2 Hz, 1H, 2a-*H*), 4.57 (dd, *J* = 7.8, 4.3 Hz, 1H, 3-*H*), 4.28 (d, *J* = 12.8 Hz, 1H, 1'-*H*), 4.23 (d, *J* = 12.0 Hz, 1H, 1'-*H*), 4.23-4.20 (m, 1H, 4-*H*), 3.81 (dd, *J* = 10.0, 1.5 Hz, 1H, 5-*H*), 3.72 (dd, *J* = 10.0, 3.2 Hz, 1H, 5-*H*), 3.64 (d, *J* = 1.4 Hz, 1H, 2-*H*); <sup>13</sup>C NMR (100.6 MHz, CD<sub>3</sub>OD)  $\delta$  172.0 (C=O), 133.5 (Cq, Ar), 131.0 (CH, Ar), 130.4 (CH, Ar), 130.2 (CH, Ar), 80.1 (2a-C), 73.4 (3-C), 72.9 (5-C), 72.2 (4-C), 62.5 (2-C), 52.6 (1'-C). HRMS (ESI-TOF) found for [C<sub>13</sub>H<sub>17</sub>NO<sub>5</sub> + H<sup>+</sup>]: 268.1175; calcd: 268.1180.

### Method 2

To a solution of (2*R*,4*aR*,6*aS*,7*aR*,7*bS*)-7-benzyl-2-phenyltetrahydro-4*H*[1,3]dioxino[4',5':5,6]pyrano[3,4-*b*]azirin-6(4*aH*)-one **4a** (31 mg, 0.092 mmol) in H<sub>2</sub>O/CH<sub>3</sub>CN (10:4 mL) heated at 100 ° C was added BiI<sub>3</sub> (30 mol %). The reaction mixture was left heating for 6h, allowed to reach room temperature, and activated basic resin (Dowex 1x3, OH) added. The resin was filtered off, washed with H<sub>2</sub>O (2 x 5 mL), and the filtrates combined and evaporated to yield product **1a** (32.6 %) as an oil.

### 5.5.3 2-(Propyl-3'-benzyloxy)-2-((3*R*,4*R*)-3,4-dihydroxytetrahydrofuran-2-yl)acetic acid (**1b**)

Compound **9b** (70mg, 0.169mmol); H<sub>2</sub>O (10 mL); 2 h. Viscous oil;  $\eta = 32.7\%$ ;  $[\alpha]_{D}^{25} = +80^\circ$  (c 0.15%, CH<sub>3</sub>CH<sub>2</sub>OH); IR (neat):  $\nu_{\max}$  3394, 1680 cm<sup>-1</sup>; <sup>1</sup>H NMR (400 MHz, CD<sub>3</sub>OD)  $\delta$  7.41 – 7.27 (m, 5H, *H<sub>a</sub>*), 4.62 (d, *J* = 11.7 Hz, 1H, 5'-*H*), 4.58 (dd, *J* = 7.8, 1.7 Hz, 1H, 2a-*H*), 4.55 (t, *J* = 3.5 Hz, 1H, 3-*H*), 4.53 (d, *J* = 11.7 Hz, 1H, 5'-*H*), 4.21 (ddd, *J* = 4.1, 3.4, 1.8 Hz, 1H, 4-*H*), 3.78 (dd, *J* = 10.0, 1.8 Hz, 1H, 5-*H*), 3.71 (dd, *J* = 10.0, 3.3 Hz, 1H, 5-*H*), 3.68 (dd, *J* = 6.3, 1.8 Hz, 1H, 3'-*H*), 3.67 (dd, *J* = 4.8, 2.4 Hz, 1H, 3'-*H*), 3.55 (d, *J* = 1.5 Hz, 1H, 2-*H*), 3.24 (t, *J* = 6.6 Hz, 2H, 1'-*H*), 2.05 – 1.97 (m, 2H, 2'-*H*). <sup>13</sup>C NMR (100,6 MHz, CD<sub>3</sub>OD)  $\delta$  172.5 (C=O), 139.4 (Cq, Ar), 129.4 (CH, Ar), 129.0 (CH, Ar), 128.9(CH, Ar), 128.7 (CH, Ar), 80.1 (2a-C), 74.3 (5'-C), 73.4 (3-C), 72.9 (5-C), 72.2 (4-C), 69.5 (3'-C), 63.2 (2-C), 48.3 (1'-C), 28.0 (2'-C); HRMS (ESI-TOF) found for [C<sub>16</sub>H<sub>23</sub>NO<sub>6</sub> + H<sup>+</sup>]: 326.1604; calcd: 326.1598.

### 5.5.4 2-(Propyl)-2-((3*R*,4*R*)-3,4-dihydroxytetrahydrofuran-2-yl)acetic acid (1c)

Compound **9c** (65 mg, 0.197 mmol); H<sub>2</sub>O (25 mL); 2h 30 min. Viscous oil;  $\eta$  = 83.7%;  $[\alpha]_{D}^{25} = +50^{\circ}$  (c 0.2%, CH<sub>3</sub>CH<sub>2</sub>OH); IR (neat):  $\nu_{\max}$  3412, 1632 cm<sup>-1</sup>; <sup>1</sup>H NMR (400 MHz, CD<sub>3</sub>OD)  $\delta$  4.57 (dd,  $J = 7.2, 4.4$  Hz, 1H, 2a-*H*), 4.38 (dd,  $J = 7.2, 2.2$  Hz, 1H, 3-*H*), 4.24 (h,  $J = 2.8$  Hz, 1H, 4-*H*), 3.91 (dd,  $J = 9.8, 4.2$  Hz, 1H, 5-*H*), 3.84 (dd,  $J = 9.8, 2.6$  Hz, 1H, 5-*H*), 3.29 (d,  $J = 2$  Hz, 1H, 2-*H*), 2.72 (dt,  $J = 11.4, 6.9$  Hz, 1H, 1'-*H*), 2.57 (dt,  $J = 11.6, 7.2$  Hz, 1H, 1'-*H*), 1.56 (h,  $J = 7.3$  Hz, 2H, 2'-*H*), 0.96 (t,  $J = 7.4$  Hz, 3H, 3'-*H*); <sup>13</sup>C NMR (100.6 MHz, CD<sub>3</sub>OD)  $\delta$  178.3 (C=O), 80.0 (2a-C), 72.6 (5-C), 72.0 (3-C), 70.5 (4-C), 61.5 (2-C), 49.6 (1'-C), 21.8 (2'-C), 10.9 (3'-C). HRMS (ESI-TOF) found for [C<sub>9</sub>H<sub>17</sub>NO<sub>5</sub> + H<sup>+</sup>]: 220.1182; calcd: 220.1180.

### 5.6 Synthesis of $\beta$ , $\delta$ -3-(benzylamino)-6-hydroxytetrahydrofuro[3,2-*b*]furan-2(3*H*)-one (6a)

#### Method 1

A solution of compound **9a** (30mg, 0.084 mmol) in H<sub>2</sub>O (6 mL) at rt was added TFA (120  $\mu$ L). The reaction mixture was left stirring for 2 days. Then solid NaHCO<sub>3</sub> (35 mg) and MeOH (5 mL) was added to the mixture, concentrated, and extracted with ethanol (5 mL). The solvent was removed in the rotary evaporator to give the pure product (tick oil; quantitative yield).  $[\alpha]_{D}^{25} = +17.5^{\circ}$  (c 0.4%, MeOH); IR (neat):  $\nu_{\max}$  3412, 1683.4 cm<sup>-1</sup>; <sup>1</sup>H NMR (400 MHz, D<sub>2</sub>O)  $\delta$  7.38-7.25 (m, 5H, H<sub>Ar</sub>), 4.35 (dd,  $J = 4.8, 5.6$  Hz, 1H, 6a-*H*), 4.26 (dd  $J = 2.4, 6$ Hz, 1H, 3a-*H*), 4.15 (q,  $J = 4.8$  Hz, 1H, 6-*H*), 3.87-3.82 (m, 1H, 5-*H*), 3.84 (d,  $J = 12.4$  Hz, 1H, 1'-*H*), 3.75 (dd,  $J = 9.2, 4.4$  Hz, 1H, 5-*H*), 3.63 (d,  $J = 12.4$  Hz, 1H, 1'-*H*), 3.37-3.15(m, 1H, 3-*H*); <sup>13</sup>C NMR (100.6 MHz, D<sub>2</sub>O)  $\delta$  161.3 (C=O), 140.5 (C<sub>qAr</sub>), 129.6 (CH, Ar), 129.5 (CH, Ar), 128.2 (CH, Ar), 81.8 (3a-C), 74.2 (6a-C), 73.4 (5-C), 72.6 (6-C), 63.4 (3-C), 53.3 (1'-C). HRMS (ESI) found for [C<sub>13</sub>H<sub>14</sub>NO<sub>4</sub> + H<sub>2</sub>O + H<sup>+</sup>]: 266.1022; calcd: 266.1033.

#### Method 2

To a solution of compound **4a** (47 mg, 0.139 mmol) in H<sub>2</sub>O (10 mL) was added TFA (300  $\mu$ L) at rt. The reaction mixture was left stirring for 15 days. Then solid NaHCO<sub>3</sub> (35 mg) and MeOH (5 mL) was added to the mixture, concentrated, and extracted with ethanol (5 mL). The solvent was removed in the rotary evaporator to give the pure product (tick oil; quantitative yield).

## 5.7 Synthesis of (2*R*,3*R*,4*R*,5*R*)-1-substituted-2-carboxy-3,4-dihydroxy-5-(hydroxymethyl)pyrrolidin-1-ia (7a.HCl, 7e.HCl)

### 5.7.1 *N*-benzyl substituted compound (7a.HCl)

#### Method 1 - from aziridinolactone 4a

To a solution of compound **4a** (28 mg, 0.830 mmol) in dioxane (2.70 mL) was added HCl 37% (295  $\mu$ L) at rt. The reaction mixture was maintained under magnetic stirring for 20 h. The solvent was removed in the rotary evaporator to give the pure product (tick oil; quantitative yield).  $[\alpha]_D^{25} = +96.6^\circ$  (c 0.2%, MeOH); IR (neat):  $\nu_{\max}$  3329.2, 1797.6  $\text{cm}^{-1}$ ;  $^1\text{H}$  NMR (400 MHz,  $\text{D}_2\text{O}$ )  $\delta$  7.49-7.44 (m, 5H, Ph), 5.39 (d,  $J = 7.6$  Hz, 1H, 2-*H*), 4.90 (dd  $J = 4.4, 6.8$  Hz, 1H, 4-*H*), 4.59 (d,  $J = 13.2$  Hz, 1H, 1'-*H*), 4.50 (dd,  $J = 6.8, 7.6$  Hz, 1H, 3-*H*), 4.44 (d,  $J = 13.2$  Hz, 1H, 1'-*H*), 4.12 (dd,  $J = 7.8, 3.4$  Hz, 1H, 5-*H*), 3.82 (dd,  $J = 12, 3.2$  Hz, 1H, 6-*H*), 3.76 (dd,  $J = 12.0, 3.6$  Hz, 1H, 6-*H*);  $^{13}\text{C}$  NMR (100 MHz,  $\text{D}_2\text{O}$ )<sup>a)</sup>  $\delta$  170.6 (C=O), 130.0 (Cq, Ph), 130.0 (CH, Ph), 129.8 (CH, Ph), 129.6 (CH, Ph), 129.4 (CH, Ph), 79.8 (4-C), 69.7 (5-C), 61.8 (6-C), 60.4 (3-C), 51.9 (2-C), 50.4 (1'-C); HRMS (ESI) found for  $[\text{C}_{13}\text{H}_{18}\text{ClNO}_5 + \text{H}^+]$ : 304.0946; calcd: 304.0952.

#### Method 2 - from aziridine 9a

i) The aziridine **9a** (29 mg; 0.082 mmol) was dissolved in dioxane (2.70 mL), and conc. HCl was added (295  $\mu$ L). The mixture was stirred for 18 h. Evaporation of the reaction mixture till dryness gave a mixture of compounds with no starting material present. The  $^1\text{H}$  NMR spectrum showed the presence of compound **7a.HCl** in the mixture<sup>a)</sup>. The reaction stands for a longer period being observed by RNM every day. No evolution was observed during this time. No purification to obtained **7a.HCl** pure was followed.

<sup>a)</sup>  $^1\text{H}$  MNR of the reaction mixture showed a signal that was assigned to H-2 of compound **7a.HCl**. The signal shows up at  $\delta = 5.43$  ppm, as a doublet with  $J = 7.6$  Hz.

### 5.7.2 *N*-(4-nitrobenzyl) compound (7e.HCl)

#### Method 1

A solution of compound **4e** (32 mg, 0.0837 mmol) in dioxane (2.705 mL) was added HCl 37% (295  $\mu$ L) at room temperature. The reaction mixture was maintained under magnetic stirring for 18 h. The mixture was evaporated till dryness in the rotary evaporator to give the pure product as

a tick oil in quantitative yield.  $[\alpha]_{\text{D}}^{25} = -177.5^{\circ}$  (c 0.4%, MeOH); ; IR (neat):  $\nu_{\text{max}}$  3326.3, 1798.1, 1524.1, 1349.3  $\text{cm}^{-1}$ ;  $^1\text{H}$  NMR (400 MHz,  $\text{D}_2\text{O}$ )  $\delta$  8.37-8.33 (m, 2H, Ar), 7.80-7.77 (m, 2H, Ar), 5.46 (dd  $J = 7.6$  Hz, 1H, 2-*H*), 4.93 (dd,  $J = 6.4, 4.4$  Hz, 1H, 4-*H*), 4.77 (d,  $J = 13.2$  Hz, 1H, 1'-*H*), 4.64 (d,  $J = 13.2$  Hz, 1H, 1'-*H*), 4.57 (dd,  $J = 7.4, 6.6$  Hz, 1H, 3-*H*), 4.21-4.10 (m, 1H, 5-*H*), 3.84 (dt,  $J = 13.2, 3.2$  Hz, 2H, 6-*H*);  $^{13}\text{C}$  NMR (100 MHz,  $\text{D}_2\text{O}$ )  $\delta$  170.6 (C=O), 148.5 (Cq, Ar), 137.0 (Cq, Ar), 131.0 (CH, Ar), 124.3 (CH, Ar), 79.8 (4-C), 69.8 (5-C), 61.9 (6-C), 60.9 (3-C), 52.1 (2-C), 49.4 (1'-C). HRMS (ESI) found for  $\text{C}_{13}\text{H}_{16}\text{N}_2\text{O}_6\text{Cl}$  ( $\text{M}+\text{H}^+-\text{H}_2\text{O}$ ): 331.0693; calcd: 331.0692 and found for  $[\text{C}_{13}\text{H}_{16}\text{N}_2\text{O}_7 + \text{H}^+]$ : 313.1026; calcd: 313.1030.

## 5.8 Dehydration of pyrrolidin-1-ia 7a.HCl, 7e.HCl

### 5.8.1 Synthesis of (2*R*,3*S*)-1-benzyl-5-carboxy-3-hydroxy-2-(hydroxymethyl)-2,3-dihydro-1*H*-pyrrol-1-ium (8a.HCl)

A solution of **4a** (28 mg, 0.830 mmol) in dioxane (2.705 mL) was added HCl 37% (295  $\mu\text{L}$ ) at room temperature. The reaction mixture was stirred for 17 days at room temperature. Tick oil; quantitative yield;  $[\alpha]_{\text{D}}^{25} = +10^{\circ}$  (c 0.2%, MeOH);  $^1\text{H}$  NMR (400 MHz,  $\text{D}_2\text{O}$ )  $\delta$  7.71 (s, 1H, 3-*H*), 7.48-7.740 (m, 5H, Ph), 5.29 (d,  $J = 3.2$  Hz, 1H, 4-*H*), 4.15 (s, 2H, 1'-*H*), 4.04 (ddd,  $J = 4.8, 5.6, 3.2$  Hz, 1H, 5-*H*), 3.72 (dd,  $J = 12.0, 4.0$  Hz, 1H, 6-*H*), 3.65 (dd,  $J = 12.0, 5.6$  Hz, 1H, 6-*H*);  $^{13}\text{C}$  NMR (100 MHz,  $\text{D}_2\text{O}$ )  $\delta$  170.6 (C=O), 147.6 (3-C), 132.5 (Cq, Ph), 129.8 ( $\text{CH}_{\text{Ar}}$ ), 129.1 ( $\text{CH}_{\text{Ar}}$ ), 128.7 ( $\text{CH}_{\text{Ar}}$ ), 129.8 (2-C), 82.7 (4-C), 70.9 (5-C), 61.7 (6-C), 43.0 (1'-C). HRMS (ESI) found for  $[\text{C}_{13}\text{H}_{16}\text{NO}_4\text{Cl} + \text{H}^+]$ : 286.0843; calcd: 286.0841.

### 5.8.2 Synthesis of (2*R*,3*S*)-1-benzyl-5-carboxy-3-hydroxy-2-(hydroxymethyl)-2,3-dihydro-1*H*-pyrrol-1-ium (8e.HCl)

A solution of **4e** (28 mg, 0.830 mmol) in dioxane (2.705 mL) was added HCl 37% (295  $\mu\text{L}$ ) at room temperature. The reaction mixture was stirred for 92 h at room temperature. Tick oil; quantitative yield;  $[\alpha]_{\text{D}}^{25} = -1,69^{\circ}$  (c 0.2%, MeOH); ; IR (neat):  $\nu_{\text{max}}$  3427.5, 1643.8, 1521.8, 1349.7



cm<sup>-1</sup>; <sup>1</sup>H NMR (400 MHz, D<sub>2</sub>O) δ 8.36-8.34 (m, 2H, Ar), 7.79 (d, *J* = 2.0 Hz, 1H, 3-*H*), 7.72-7.70 (m, 2H, Ar), 5.37 (dd, *J* = 4.4, 1.6 Hz, 1H, 4-*H*), 4.36 (s, 2H, 1'-*H*), 4.16 (dd, *J* = 14.4, 7.2 Hz, 1H, 6-*H*), 4.15- 4.11 (m, 1H, 5-*H*), 3.81-3.72 (m, 1H, 6-*H*); <sup>13</sup>C NMR (100 MHz, D<sub>2</sub>O) δ 171.0(C=O), 147.7 (3-C), 139.8 (Cq, Ar), 129.8 (CH, Ar), 124.2 (CH, Ar), 124.1 (2-C), 82.8 (4-C), 71.0 (5-C), 61.8 (6-C), 42.3 (1'-C). HRMS (ESI) found for [C<sub>13</sub>H<sub>15</sub>N<sub>2</sub>O<sub>6</sub>Cl + H<sup>+</sup>]: 331.0699; calcd: 331.0691.

## 6. References

1. Chakraborty, T. K.; Srinivasu, P.; Tapadar, S.; Mohan, B. K., Sugar amino acids in designing new molecules. *Glycoconjugate Journal* **2005**, vol. 22, no. 3, pp. 83–93.
2. Guang-Zong, T.; Xiao-Li, W.; Jing, H.; Xue-bin W.; Xiao-Qiang, G.; Jian, Y., Recent progress of sugar amino acids: Synthetic strategies and applications as glycomimetics and peptidomimetics. *Chin. Chem. Lett.* **2015**, 922-930.
3. Gruner, S. A. W.; Locardi, E.; Lohof, E., Kessler, H., Carbohydrate-Based Mimetics in Drug Design: Sugar Amino Acids and Carbohydrate Scaffolds. *Chem. Rev.* **2002**, 102, 491–514.
4. Y. Chapleur, Carbohydrate mimics : concepts and methods. Wiley-VCH, **1998**.
5. Risseuw, M. D. P.; Overhand, M.; Fleet, G. W. J.; Simone, M. I., A compendium of sugar amino acids (SAA): scaffolds, peptide- and glyco-mimetics. *Tetrahedron Asymmetry* **2007**, vol. 18, no. 17. pp. 2001–2010.
6. Sousa, Cristina E. A.; Ribeiro, António M. P.; Gil Fortes, António; Cerqueira, Nuno M. F. S. A. and Alves, Maria J., Total Facial Discrimination of 1,3-Dipolar Cycloadditions in a D-Erythrose 1,3-Dioxane Template: Computational Studies of a Concerted Mechanism. *J. Org. Chem.* **2017**, 82, 982–991.
7. M.J. Alves, T.L. Gilchrist, "Organic Azides: Syntheses and Applications", Ed. Stefan Bräse and Klaus Banert Chapter "Small Rings by Azide Chemistry", John Wiley & Sons, 167-190, **2009**. ISBN: 978-0-470-51998-1.
8. Singh, S. G.; D'hooghe, M.; De Kimpe, N., Synthesis and Reactivity of C-Heteroatom-Substituted Aziridines. *Chem. Rev.* **2007**, 107, 2080-2135
9. Huisgen, R. *Angew.*, 1,3-Dipolar Cycloadditions. Past and Future. *Chem. Int. Ed. Eng.* **1963**, 2, 565-632.
10. Asano, N.; Kato, A.; Miyauchi, M.; Kizu, H.; Kameda, Y.; Watson, A. A.; Nash, Robert J.; Fleet, George W. J., Nitrogen-Containing Furanose and Pyranose Analogues from Hyacinthus Orientalis. *J. Nat. Prod.* **1998**, 61, 625-628.
11. Bailey '07, Aaron D., "Green Chemistry Using Bismuth Salts Bismuth (III) Iodide Catalyzed Deprotection of Acetals and Ketals in H<sub>2</sub>O" (**2007**). Honors Projects, Paper 6.
12. Bogdanova, A.; Popik, V.V., Wavelength-Dependent Photochemistry of Diazo Meldrum's Acid and Its Spirocyclic Isomer, Diazirino Meldrum's Acid: Wolff Rearrangement versus Isomerization. *J. Am. Chem. Soc.*, **2003**, 125, 1456-1457.

13. Guptill, D.M.; Cohen, C.M.; Davies, H.M.L., Rhodium(II)-Catalyzed Stereoselective Synthesis of Allylsilanes. *Org. Lett.*, **2013**, *15*, 24, 6120-6123.
14. Pino-González, Soledad, M. and Noé Oña, Synthesis of intermediates in the formation of hydroxy piperidines and 2-azido lactones from D-erythrose. *Tetrahedron: Asymmetry*, **2008**, *19*(6):721–29.
15. Malle, Birgitte M.; Inge Lundt; Tanja, M. Wrodnigg, Regioselective intramolecular ring closure of 2-amino-6-bromo-2,6-dideoxyhexono-1,4-lactones to 5- or 6-membered iminuronic acid analogues: synthesis of 1-deoxymannojirimycin and 2,5-dideoxy-2,5-imino-D-glucitol. *Organic and Biomolecular Chemistry*, **2008**, *6*(10):1779–86.

# 7

Synthesis of Indolizidines from D-Erythrosyl 1,3  
Butadienes

*The results presented in this chapter will be published under the title:*

**Diels-Alder Cycloaddition of a D-Erythrose-1,3-Butadiene to Azo-dienophiles. Transformation of Cycloadducts into (3*S*,4*S*,4a*S*,5*S*,6*R*)-Octahydropyrrolo[1,2-*b*]pyridazine-3,4,5,6-tetraol. Computational Studies on Selectivity.**

Cristina E. A. Sousa, Daniela A. L. Salgueiro, Nuno M. F. S. A. Cerqueira and Maria J. Alves

In submission process.

## 1. Introduction

Glucosyl-type dienes are excellent partners in Diels–Alder cycloadditions, showing high diastereoselectivity to a range of cyclic or acyclic carba- [1] and aza- [2,3], and azo-dienophiles [4]. In particular, 1,3-butadienes bearing a D-erythrose benzylidene-acetal diene **1** have been used in our laboratory in  $4\pi + 2\pi$  cycloadditions with azo [5], aza [6], and carba-dienophiles [7].

Cycloadducts from azo-dienophiles may be considered interesting chiral blocks in the synthesis of aza-indolizidines, which would be attained in a couple of steps. On the basis that swainsonine molecule bearing groups at position 6 seems to have a good impact on activity against mannosidase[8]. So, it was reasoned that a nitrogen atom at this position would make it easier from the synthetic point of view to obtain 6-substituent azo-indolizidines.

In a previous work, D-erythrosyl dienes **1** were reacted with PTAD giving a 1(*R*):5(*S*) mixture of cycloadducts. A sole product, in *S*-configuration, was obtained with the diene **1** bearing the alcohol function protected (**Figure 1**) [5]. However, the cycloaddition of **1** with 2*H*azirine-3-carboxylic methyl ester, had furnished a mixture of diastereomers in which the *R* structure was the major product[6]. Reaction with maleimides were low yielding and less selective [7]. Would it be possible to modulate the cycloaddition selectivity by changing the ester disposition around the C=C bond in the azo-dienophile? Would the *trans* esters disposition in DEAD and DBAD lead to the *R* configuration in the cycloadduct? In the end, the answer to this question resulted to be no! Cycloadducts incorporating DEAD and DBAD gave the very same stereoselectivity as PTAD with the formation of the *S*-stereoisomer.

This paper describes the cycloadditions of DEAD and DBAD to the diene **1**, and its transformation into the aza-indolizidine nucleus. The stereochemistry assignments for the cycloadducts could only be solved after a sequence of FGT leading to aza-indolizidines done for cycloadducts obtained from DEAD and DBAD in parallel with the PTAD cycloadducts **2a,b** [5]. (**Figure 1**) PTAD cycloadducts are known to be *S*-configuration by X-ray crystallography. At the end of the work, it was found that the same aza-indolizidines was formed in all and every case.

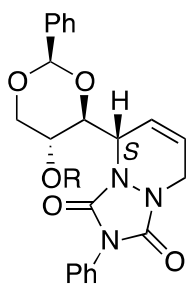
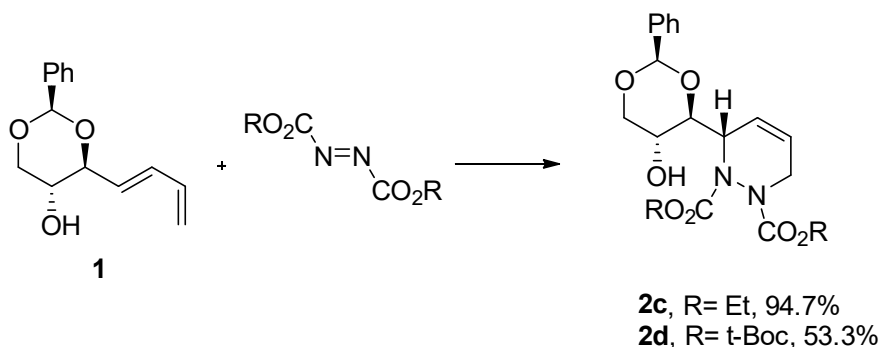


**Figure 1** – Assigned of stereochemistry at C-1 of cycloadduct **2a,b** obtained from diene **1** and PTAD. (**2a** R= H, **2b** R= Me)

## 2. Results and Discussion

### 2.1 Synthesis of Cycloadducts

Diene **1** was reacted with DEAD and DBAD at low temperature for several hours, reproducing the procedure of diene **1** with PTAD [5]. Cycloaddition to DBAD was done for the extra volume of the ester groups. The yield is high with DEAD, but moderate in DBAD. The stereochemistry at the new stereogenic center was found to be *S* in both cases, and the same as PTAD. This was demonstrated by a comparison of final products, obtained after functional group manipulation of cycloadducts from the three azo-dienophile source (DEAD, DBAD, PTAD).



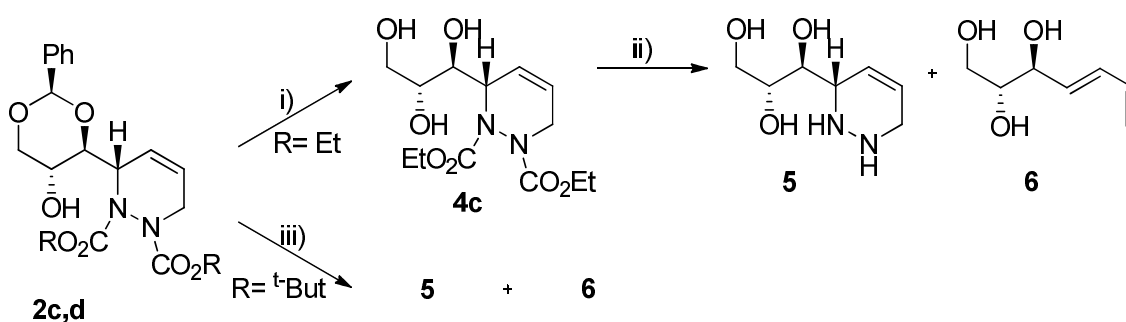
**Scheme 1** – Synthesis of **2c,d** cycloadducts obtained from D-erythrose-4-yl-1,3-butadiene **1** and DEAD or DBAD. Reaction conditions: THF, N<sub>2</sub>, - 47 °C, DEAD (1.0 eq.)/ DBAD (1.1 eq.), 4h. Compound **2c**, 94.7 %; **2d**, 53.3 %.

### 2.2 Functional Group Transformation of Cycloadducts 2 Leading to Aza-indolizidine 3

Reflux of compound **2c** in water (10): acetonitrile (3) mixture in the presence of BiI<sub>3</sub> (20 %) for 3 h, furnished compound **4c** in 99.6 % yield, as a pure product. Compound **4c** was found stable under the acid hydrolysis conditions referred above, but **4c** reacted in dioxane - aq. NaOH 1M after

24 h at room temperature giving the deprotected compound **5**, together with the *retro*-Diels-Alder product **6**. Compound **5** was isolated after chromatography in 21 %, together with **6** (12 %). The amount of compound **6** rose markedly during the course chromatographic purification in silica.

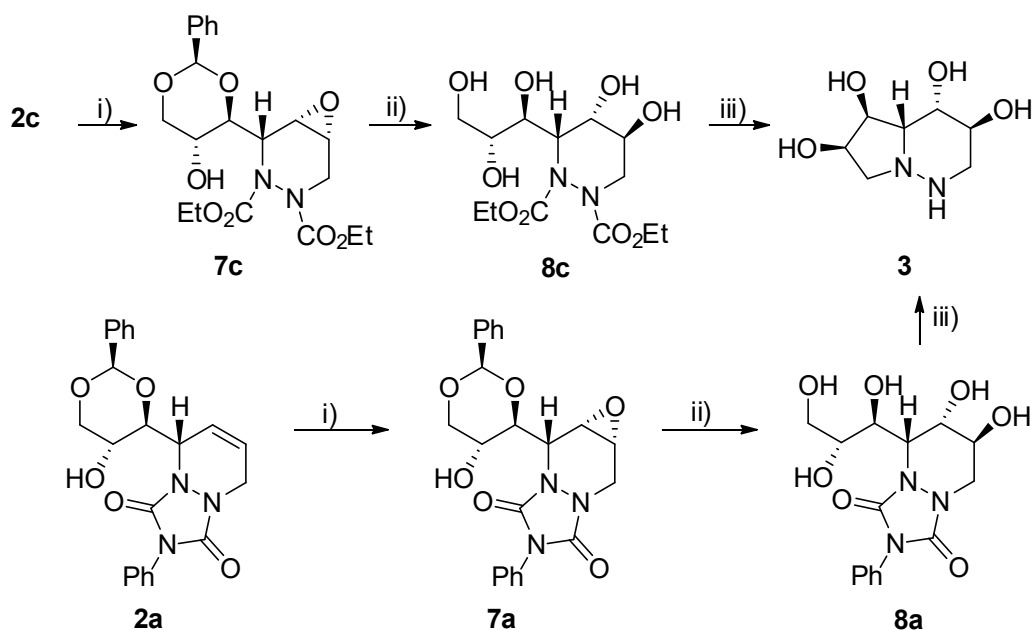
Hydrolysis of cycloadduct **2d** in refluxing H<sub>2</sub>O: acetonitrile in the presence of Bil<sub>3</sub> (25 %) gave product **5** in 25 % yield after chromatography. Prolonging the reaction time, compound **6** was the only product isolated. By monitoring the course of hydrolysis of compound **2d** by <sup>1</sup>H NMR spectroscopy it has become clear that the *retro*-Diels-Alder product **6** is generated as soon as compound **4c** appears in solution.



**Scheme 2** – Functional group transformation of cycloadducts **2c,d**.

Reaction conditions: i) a) Bil<sub>3</sub> (20 %), H<sub>2</sub>O/ACN (10:3), reflux, 3h; b) resina Dowex 50x (OH), η=99.6 %; ii) NaOH 1M, dioxane, 24 h, rt., compound **5** (20.6 %), compound **6** (12.4%); iii) a) Bil<sub>3</sub>(25 %), H<sub>2</sub>O/ACN (2:1), reflux, 13 h: 30 min; b) resina Dowex 50x (OH), compound **5**: η=25 %.

To avoid *retro*-Diels-Alder during hydrolysis a previous manipulation of the C=C in cycloadduct is needed. So, an epoxide was generated in the presence of trifluoromethylacetone/Oxone and NaHCO<sub>3</sub>. The reaction was found to be stereoselective, giving compound **7c** in 51 % yield. Treatment of epoxide **7c** with conc. H<sub>2</sub>SO<sub>4</sub> followed by reflux for 6 h furnished diol **8c** in 59 % yield. Compound **8c** upon reflux in hydrazine monohydrate during 6 h led to the removal of urethane groups and the aminocyclization was promoted, with the formation of aza-indolizidine **3** (96 % yield), and 29 % overall yield from **2c**.



**Scheme 3** – Synthesis of aza-indolizidine **3**.

Reaction conditions: i) a) ACN / H<sub>2</sub>O (15:9 mL), 0 °C, trifluoroacetone (27 eq.), solid NaHCO<sub>3</sub> (22 eq.), Oxone (30 eq.); b) rt., 22 h, **2a** η = 87.1 %, **2c** η = 51.1 %. ii) water, conc. H<sub>2</sub>SO<sub>4</sub> (0.012 eq.), reflux, 6 h; b) aqueous NaHCO<sub>3</sub>, **7a** η = 62.0%, **7c** η = 59.3%. iii) NH<sub>2</sub>NH<sub>2</sub>·H<sub>2</sub>O (12 eq.), reflux, 6 - 18h, **8a** η = 88.2 %, **8c** η = 96.1 %.

The same sequence of reactions with the PTAD cycloadduct **2a** [5] led to the same product **3**: 1) formation of the epoxide derivative **7a**, 2) epoxide ring-opening with formation of diol **8a**, 3) treatment of **8a** with hydrazine and formation of the aza-indolizidine **3** in 42 % overall yield from **2a**.

In conclusion, the approaches of PTAD/DEAD/DBAD to 1,3-butadiene **1** occur by the same face of the diene, leading to the *S* configuration at the new stereogenic center.

### 3. Computational results

Computer mechanistic studies began due to the initial difficulty in understanding the diastereochemistry of cycloadducts when using DEAD or DBAD.

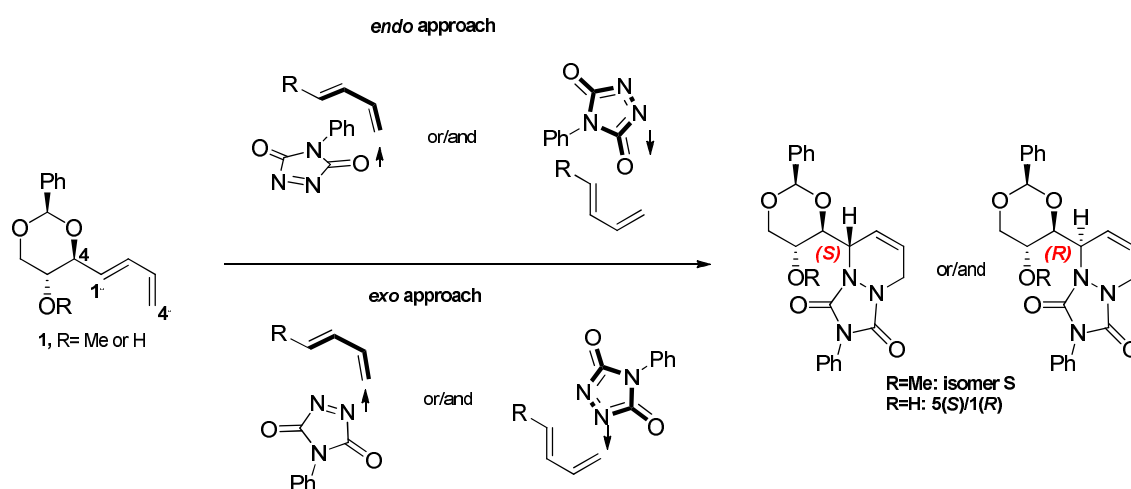
In these studies, we analyzed the *si* and *re* face reactivities between diene **1** and different dienophiles: PTAD, DEAD, and DBAD. And the possible explanation for diastereoselectivity in these Diels-Alder cycloadditions.



In order to make it simpler, it was first analyzed the reaction with PTAD, and then the mechanism with DEAD and DBAD.

### 3.1 Diels-Alder cycloaddition mechanisms between diene **1** and PTAD

The Diels-Alder cycloaddition between diene **1** and PTAD was studied by the *endo* and *exo* approaches, and in either approach for the *R* and *S* isomers (Scheme 4). Experimentally only the *S* isomer is obtained in case the diene bears a R = Me, and a mixture of both diastereomers *S*(5): *R*(1) when R = H.



**Scheme 4** – The four theoretical approaches between D-erythrosyl diene **1** and PTAD

In all cases studied, the free activation energy and free reaction energy reveals that the favored approach is *endo* (Table 1).

**Table 1:** Reaction energies ( $\Delta$ ) and activation energies ( $\Delta^\ddagger$ ) for the *endo* and *exo* approaches between diene **1** and PTAD

	Isomer	ENDO		EXO	
		<i>S</i>	<i>R</i>	<i>S</i>	<i>R</i>
R=Me	$\Delta^\ddagger$ (kcal.mol <sup>-1</sup> )	1.2	15.3	17.1	23.2
	$\Delta$ (kcal.mol <sup>-1</sup> )	-51.1	-36.4	-39.1	-38.4
R=H	$\Delta^\ddagger$ (kcal.mol <sup>-1</sup> )	9.3	8.9	17.4	17.1
	$\Delta$ (kcal.mol <sup>-1</sup> )	-25.5	-36.0	-34.7	-35.4

When diene **1** possesses an OMe group at C-5, the dienophile choose to attack the diene by the opposite face to the OMe group. The four possible orientations were studied, the two *endo* (*si* and *re*) and the two *exo* (*si* and *re*): the *endo* approaches are energetically favoured; the *endo* approach by the *si* face give the *S* isomer, the *endo* approach by the *re* face give the *R* isomer. Interestingly the *R* product would result in a non-usual diene configuration: 1,2-*s-cis* configuration; this would avoid the bulky effect of the methoxy group at C-5 with the incoming PTAD, as shown in the respective TS (Figure 2).

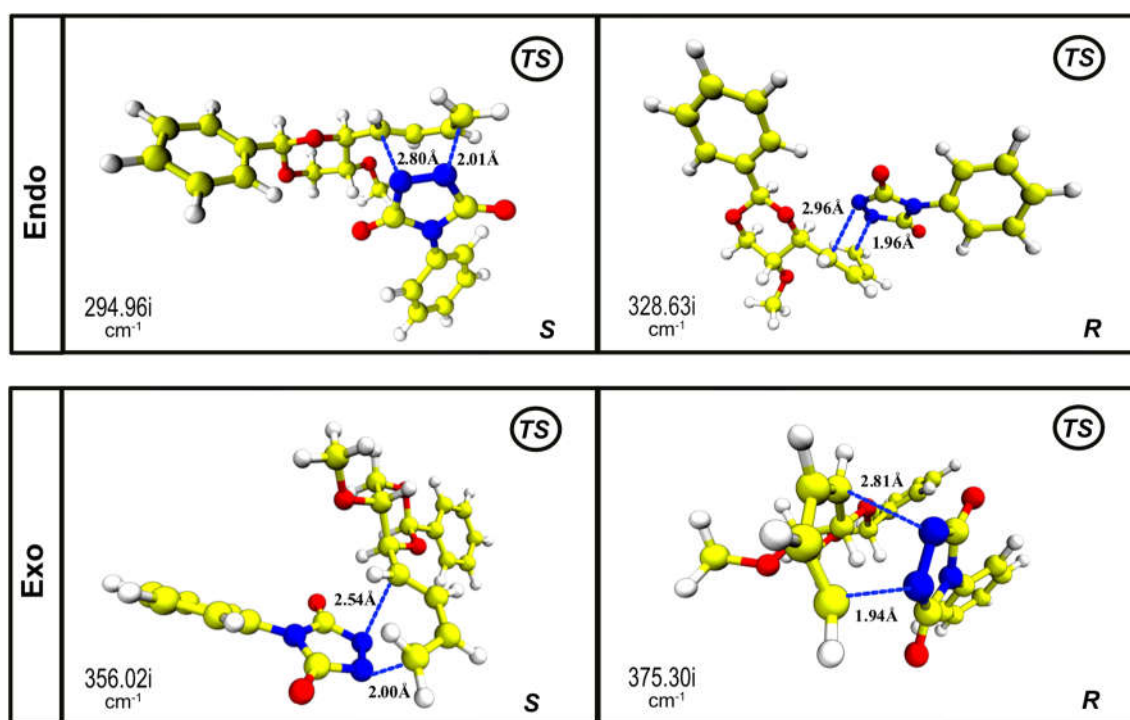
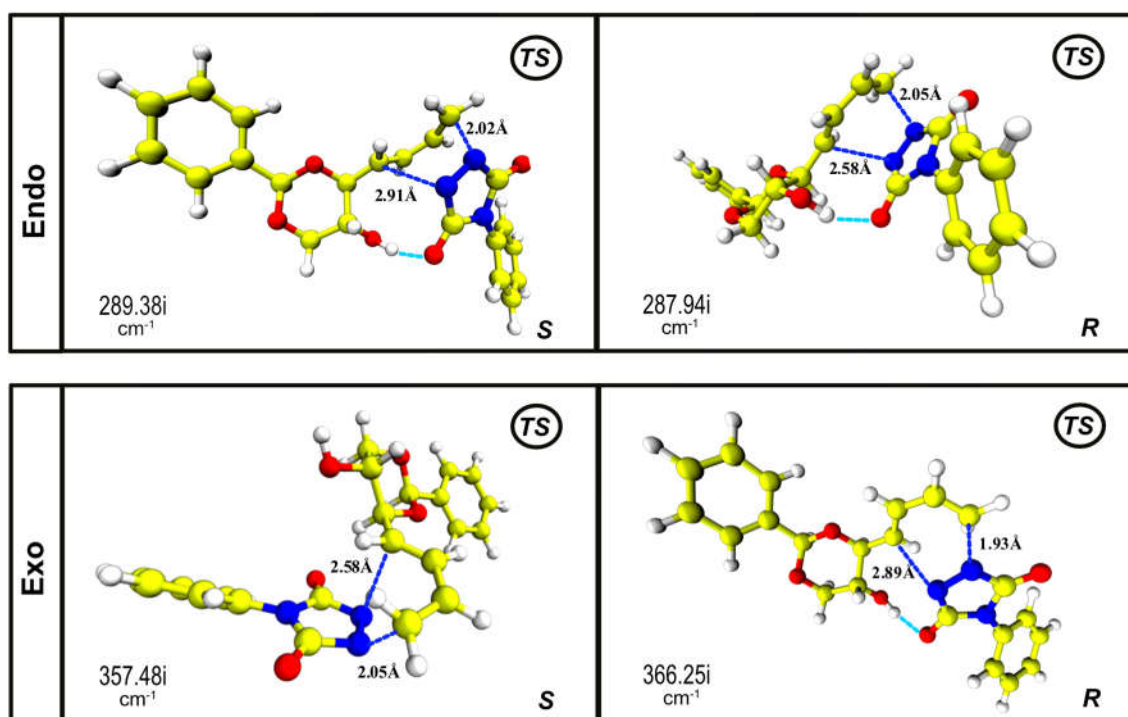


Figure 2 – Possible transition states of Diels-Alder cycloaddition between PTAD with diene **1** (R=Me)

The formation of isomer *S* involves a transition state with the imaginary frequency of 294.96i cm<sup>-1</sup> (Figure 2). The TS structure reveals a decrease in distance between C1'-N (2.80 Å) and C4'-N (2.01 Å) relatively to reactants: C1'-N (3.14 Å) and C4'-N (2.90 Å). At the end of the reaction, the new bonds are established forming a 6-member heterocycle with C1'-N length 1.48 Å and C4'-N length 1.46 Å. The reaction is almost spontaneous, with the free activation energy of 1.2 kcal.mol<sup>-1</sup>, and is a very exergonic process in -51.1 kcal.mol<sup>-1</sup>.

In the case of reaction with diene **1** (R=H) the energies are very similar for the two *endo* approaches, and for the two *exo* approaches, but differences between them. The *endo* approach is more favorable from the thermodynamic point of view (Table 1), which means that this should be the approach underlying the synthesis of the isomeric mixture *S*(5): *R*(1) observed

experimentally. All the mechanisms studied are concerted and desynchronized. The hydrogen bond that is established between the incoming PTAD carbonyl and the OH in the diene make the PTAD to access by the bottom face of the diene, which is opposite to the case where the diene bear an OMe at C-5. The formation of isomer *S* involves the transition state with the imaginary frequency the 289.38i cm<sup>-1</sup> (**Figure 3**). This structure reveals a decrease in distance between the following pair of atoms in the TS and in reactants; C1'-N (2.91 Å) and C4'-N (2.02 Å) in TS, and C1'-N (3.06 Å) and C4'-N (2.95 Å) in reactants. The hydrogen bond between OH group and the carbonyl group is 1.86 Å in TS, against 1.92 Å in reactants. In the cycloadduct C1'-N and C4'-N bond lengths are the same (1.49 Å), and the hydrogen bond is 2.85 Å. This process requires the free activation energy of 9.3 kcal.mol<sup>-1</sup> and is an exoenergonic process in -25.5 kcal.mol<sup>-1</sup>.



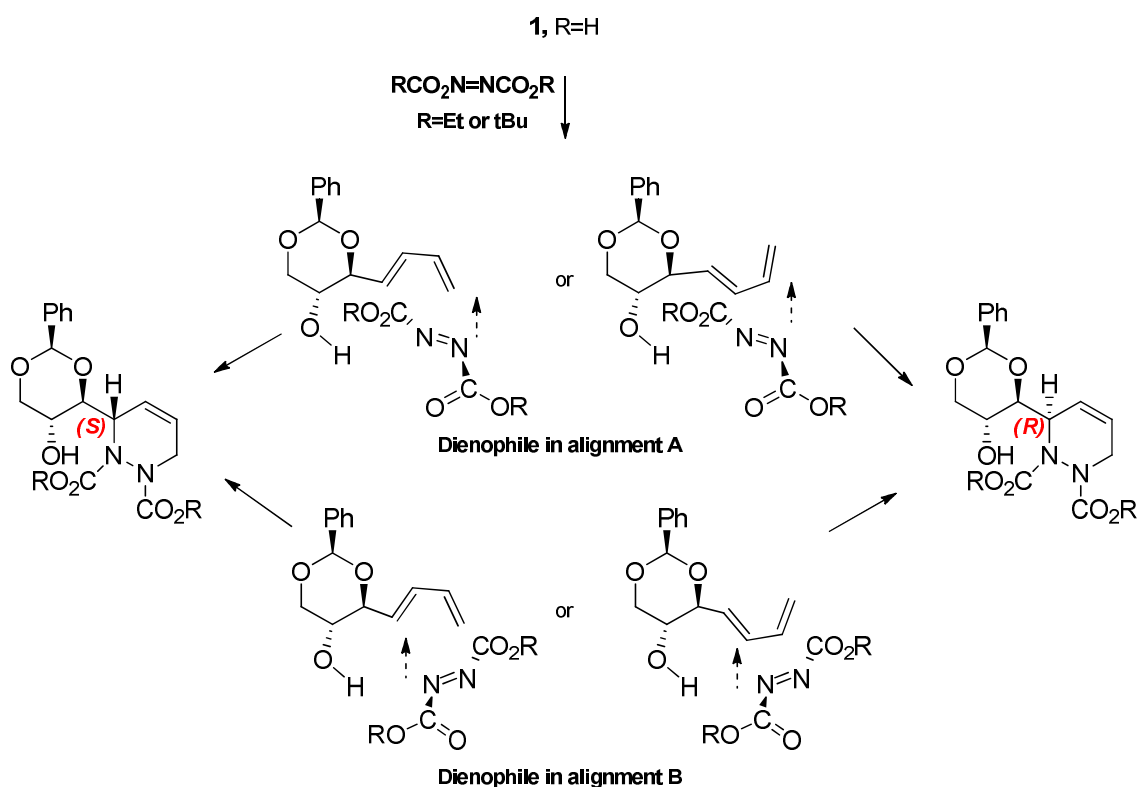
**Figure 3** – The four possible transition states of Diels-Alder cycloaddition between PTAD and diene **1** (R=H)

On the other hand, the formation of isomer *R* involves the transition state with the imaginary frequency the 287.94i cm<sup>-1</sup> (**Figure 3**). There is a shorter distance between C1'-N (2.58 Å), C4'-N (2.05 Å) in TS, compared to the distance in the reactants C1'-N (2.90 Å), C4'-N (2.03 Å). A hydrogen bond formed between reactants, and in TS, it has the same value: 2.03 Å. In the reaction product, the bond lengths between C1'-N and C4'-N are respectively 1.47 Å, 1.46 Å. In the product, the hydrogen bond is shortened, 1.99 Å than in TS (2.03 Å). This mechanism requires a free activation energy of 8.9 kcal.mol<sup>-1</sup> and is highly exergonic in -36.0 kcal.mol<sup>-1</sup>.

The main difference between the *endo* approaches to give the *S* isomer and the *R* isomer is the hydrogen bond length in TS structures: 1.86 Å (*S*) versus 2.03 Å (*R*), and in the product: 2.85 Å (*S*) versus 1.99 Å (*R*). From the thermodynamic point of view the isomer *R* is more favorable, but as the synthetic process occurs at -78°C, the thermodynamic difference is not relevant to define the pathway process.

### 3.2 Diels-Alder cycloaddition mechanisms with DEAD or DBAD

The Diels-Alder cycloaddition's mechanistic studies between diene **1** (R=H) and dienophiles DEAD or DBAD, followed the four types of approaches possible (Scheme 5). The processes are concerted and desynchronized, and the dienophile attacks by the same side of the hydroxyl group, which is due to a hydrogen bond formation. In one case the attack still occurs by the same side, but no hydrogen bond formation is observed (see Scheme 5, alignment B to give the *S* isomer, in dienophile R= *t*Bu).



**Scheme 5** – The four theoretical approaches between D-erythrosl diene **1** (R=H) and DEAD or DBAD

Taking a look at **Table 2** containing the energies for the reactions in study it was clear that alignment **A** with the formation of isomer *S*, is preferred from the kinetic point of view. Since the reactions occur experimentally at - 47 ° C, the kinetic control is certainly more relevant.

The dienophile approaches in alignment **A** are desynchronized with the C1'-N bond being established in the first place, leading to the *S* product. The dihedral angle between H-4-C4-C1'-H-1' within the diene in TS is around  $\sim -126^\circ$ , either for DEAD and for DBAD interactions.

**Table 2:** Reaction energies ( $\Delta$ ) and activation energies ( $\Delta^\ddagger$ ) for the four approaches between diene **1** (R=H) and DEAD or DBAD

Dienophile	Isomer	From Alignment A		From Alignment B	
		<i>S</i>	<i>R</i>	<i>S</i>	<i>R</i>
DEAD	$\Delta^\ddagger$ (kcal.mol <sup>-1</sup> )	20.6	25.8	24.7	24.4
	$\Delta$ (kcal.mol <sup>-1</sup> )	-18.2	-31.6	-28.5	-23.2
DBAD	$\Delta^\ddagger$ (kcal.mol <sup>-1</sup> )	18.5	25.5	25.6	24.9
	$\Delta$ (kcal.mol <sup>-1</sup> )	-34.0	-31.0	-32.8	-23.1

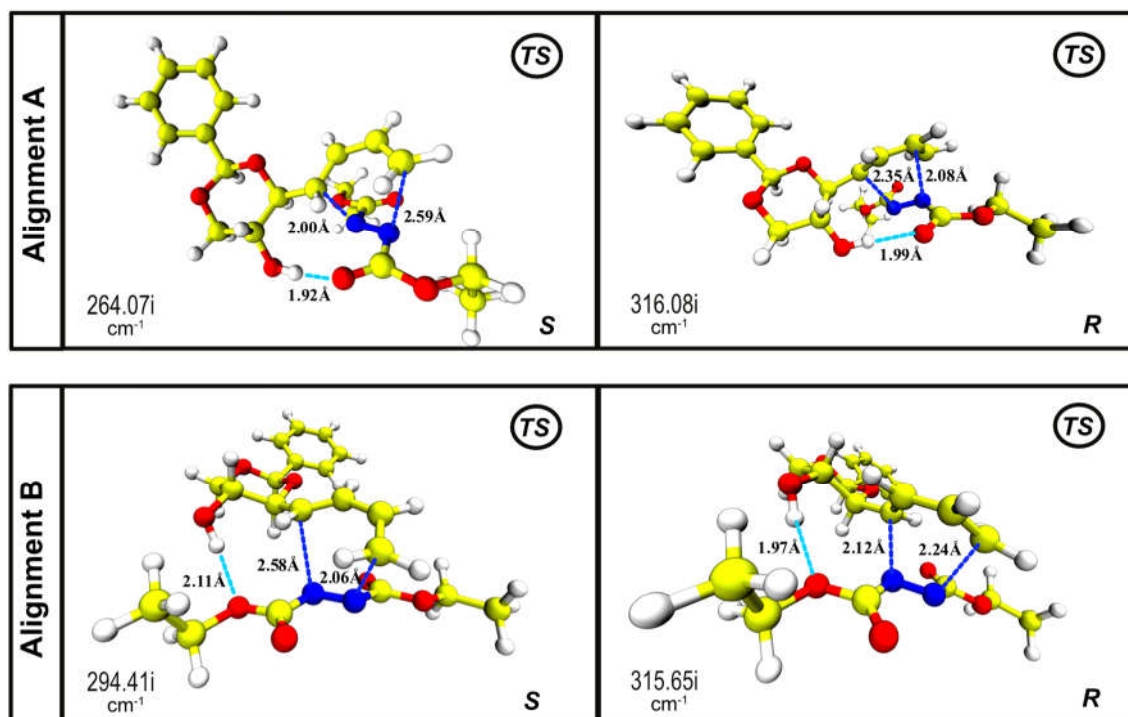


**Figure 4** – The four possible transition states of Diels-Alder cycloaddition between DEAD and diene **1** (R=H)

For DEAD dienophile, the TS is characterized by one imaginary frequency ( $264.07i\text{ cm}^{-1}$ ). At the TS structure the attack angle of one nitrogen atom to C-1' is  $95.40^\circ$  and the other nitrogen to C-4' is  $92.57^\circ$ . The distances in TS between C1'-N ( $2.00\text{ \AA}$ ) and C4'-N ( $2.59\text{ \AA}$ ) are shorter than in reactants C1'-N ( $4.08\text{ \AA}$ ) and C4'-N ( $3.53\text{ \AA}$ ), and the hydrogen bond between OH group and the carbonyl in the urethane group are in TS,  $1.92\text{ \AA}$ , against  $2.00\text{ \AA}$  in reactants. This shows that the mechanisms are concerted and desynchronized starting by C-1 terminal.

In the product, the bonds between C1'-N and C4'-N are  $1.48\text{ \AA}$  and  $1.47\text{ \AA}$ , respectively; and the hydrogen bond become longer ( $2.30\text{ \AA}$ ). This mechanism requires a free activation energy of  $20.6\text{ kcal.mol}^{-1}$  and is exergonic in  $-18.2\text{ kcal.mol}^{-1}$ .

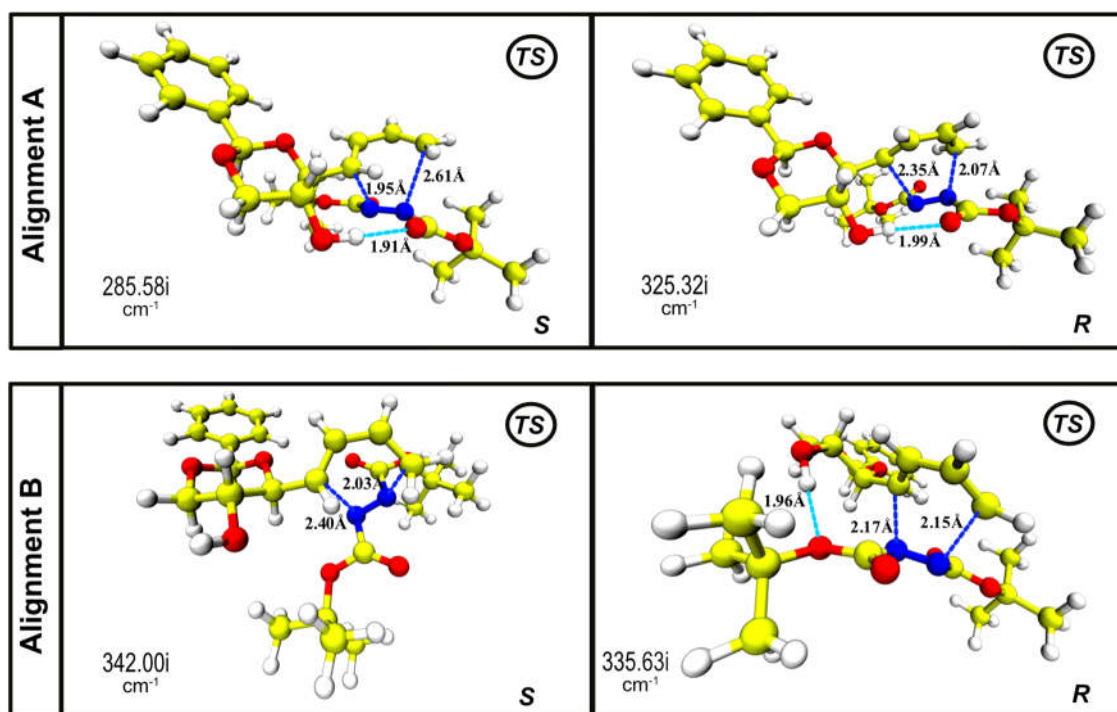


Figure 5 – The four possible transition states of Diels-Alder cycloaddition between DBAD and diene 1 (R=H)

With the dienophile DBAD, the TS is characterized by one imaginary frequency ( $285.58i\text{ cm}^{-1}$ ). At the TS structure the attack angle of one nitrogen atom to C-1' is  $96.40^\circ$  and the other nitrogen to C-4' is  $92.59^\circ$ . The distances in TS between C1'-N ( $1.95\text{ \AA}$ ) and C4'-N ( $2.61\text{ \AA}$ ), against C1'-N ( $4.38\text{ \AA}$ ) and C4'-N ( $4.05\text{ \AA}$ ) in reactants, and the hydrogen bond between OH group and the carbonyl a urethane group are in TS,  $1.91\text{ \AA}$ , against  $1.89\text{ \AA}$  in reactants.

In the end, the bonds between C1'-N and C4'-N are formed with 1.48 Å and 1.47 Å lengths, respectively; and the hydrogen bond is longer, 2.71 Å. This mechanism requires a free activation energy of 18.5 kcal.mol<sup>-1</sup> and is exergonic in -34.0 kcal.mol<sup>-1</sup>.

#### 4. Conclusion

The present work shows that Diels-Alder cycloadditions of studied azodienophiles (PTAD, DEAD, DBAD) add to D-erythrosyl dienes by the *si* face leading to the *S* stereochemistry at the new stereogenic centre. The *S* cycloadducts formed were submitted to FGT leading to the aza-indolizidine (3).

Computational mechanistic studies were run for the all the possible approaches of reagents: they are all concerted and desynchronized processes, although with different energy gaps. As the reactions occur at very low temperature, the kinetic control is relevant, but the thermodynamic difference is not relevant to define the pathway process. Analyzing the kinetic profiles of the reactions between diene (R=H) and PTAD, it was found that the energies required for the formation of the *R* and of the *S* isomer are sensible the same. However, the experimental results showed a preference for the *S* isomer, in 5 (*S*): 1 (*R*). Reaction of diene (R=Me) with PTAD gave a unique product in the *S* configuration. This effect is due to the absence of the hydrogen bond and the blocking effect of the methyl group towards the azodienophile approach.

#### 5. Experimental

##### 5.1 General

Solvents were used as purchased except: dichloromethane, tetrahydrofuran; dichloromethane was dried under CaH<sub>2</sub> and THF was dried under Na-benzophenone. D-Erythrose benzylidene acetal was obtained according to lit. [9,10], PTAD cycloadduct was obtained as described [5].

All other reagents were purchased and used without further purification. Glassware was dried prior to use. Compounds were purified by dry flash chromatography using silica 60, <0.063 mm and water pump vacuum or by flash-chromatography using silica 60Å 230–400 mesh as stationary phases. TLC plates (silica gel 60 F<sub>254</sub>) were visualized either at a UV lamp or in I<sub>2</sub> chamber.

## 5.2 Diels-Alder Cycloaddition of (2*R*,4*S*,5*R*)-4-((*E*)-buta-1,3-dien-1-yl)-2-phenyl-1,3-dioxan-5-ol to dialkyl azocarboxylates

### 5.2.1 Synthesis of Diethyl 3-((2*R*,4*S*,5*R*)-5-hydroxy-2-phenyl-1,3-dioxan-4-yl)pyridazine-1,2(3*H*,6*H*)-dicarboxylate

To a stirred solution of D-erythrose benzylidene-acetal diene (**1**) (400 mg, 1.72 mmol) in dry tetrahydrofuran (20 mL) kept under nitrogen atmosphere, immersed in liquid N<sub>2</sub>/ethyl acetate (-47 ° C) was added diethyl azodicarboxylate (DEAD, 40% in toluene, 1.04 eq., 660.2 μL, 1.79 mmol) dropwise. The reaction mixture was allowed to slowly reach room temperature for 4h. The solvent was evaporated to give a pasty material that was submitted to dry flash chromatography (silica, ethyl acetate: petroleum ether, polarity gradient), giving the product as a tick colourless oil **2c** (661 g, 1.63 mmol, 94.7 %). <sup>1</sup>H NMR showed a mixture of a major and minor rotamers in 71.6:28.4 ratio, at rt. At 50 °C the rotamers ratio: 70: 30.

[α]<sub>D</sub><sup>25</sup> = -66.67° (c 0.48 %, DCM); IR (neat): ν<sub>max</sub> 3451.3, 1779.1, 1695.4 cm<sup>-1</sup>; <sup>1</sup>H NMR (400 MHz, CDCl<sub>3</sub>) δ 7.47 – 7.39 (m, 2H), 7.39 – 7.33 (m, 3H), 6.13 (ddt, *J* = 10.4, 4.4, 2.2 Hz, 1H, H-4), 5.87 (ddd, *J* = 10.4, 3.0, 1.8 Hz, 1H, H-5), 5.47 (s, 1H, H-2'), 4.87 (sl, 1H, H-3), 4.36 – 4.15 (m, 6H, H-6, H-6', 2 x OCH<sub>2</sub>), 3.945-3.901 (m, 2H, H-6, H-5'), 3.73 (t, *J* = 9.0 Hz, 1H, H-4'), 3.58 (m, 1H, H-6'), 1.33-1.27 (m, 6H, CH<sub>3</sub>)<sup>a)</sup>. <sup>13</sup>C NMR (101 MHz, CDCl<sub>3</sub>) δ 156.3, 156.2, 155.4, 154.6 (C=O), 137.6, 137.4 (Cq, Ph), 128.9, 128.8, 128.13, 128.11, 125.9 (CH, Ph), 125.9, 125.2 (C-4), 124.2, 123.7 (C-5), 123.3 (CH, Ph), 100.6, 100.5 (C-2'), 81.3, 81.2 (C-4'), 71.1, 70.7 (C-6'), 65.4, 65.2 (C-5'), 63.4, 63.2, 62.8, 62.1 (OCH<sub>2</sub>), 57.6 (C-3), 42.9, 42.1 (C-6), 14.4, 14.3, 14.25 (CH<sub>3</sub>)<sup>b)</sup>. HRMS (ESI): calcd: 407.1813 [C<sub>20</sub>H<sub>27</sub>N<sub>2</sub>O<sub>7</sub>]<sup>+</sup>, found: 407.1813

- a) refers to the major rotamer
- b) refers to both rotamers

Some signals of the minor rotamer in the <sup>1</sup>H NMR spectrum: δ 6.07 (ddt, *J* = 10.5, 4.4, 2.2 Hz, 1H, H-4), 5.94 – 5.90 (dm, *J* = 10.8 Hz, 1H, H-5), 3.80 (t, *J* = 8.5 Hz, 1H, H-6').

### 5.2.2 Synthesis of Di-*tert*-butyl 3-((2*R*,4*S*,5*R*)-5-hydroxy-2-phenyl-1,3-dioxan-4-yl)-3,6-dihydropyridazine-1,2-dicarboxylate

To a stirred solution of D-erythrose benzylidene-acetal diene (**1**) (600 mg, 2.58 mmol) in dry tetrahydrofuran (25 mL) kept under nitrogen atmosphere, immersed in liquid N<sub>2</sub>/ethyl acetate (-47 ° C) was added dropwise di-*tert*-butyl azodicarboxylate (DBAD, 1.1 eq., 654 mg). The reaction mixture was allowed to slowly reach room temperature for 4h. The solvent was evaporated to give



a pasty material that was submitted to dry flash chromatography (silica, diethyl ether/ petroleum ether, polarity gradient). The product was isolated as oil **2d** (636 mg, 1.38mmol, 53.3 %).  $^1\text{H}$  NMR in  $\text{CDCl}_3$  showed a 2 (A):1 (B) mixture of rotamers.

$[\alpha]_{\text{D}}^{25} = -50.77^\circ$  (c 0.65 %, DCM); IR (neat):  $\nu_{\text{max}}$  3415.8, 1706.1  $\text{cm}^{-1}$ ;  $^1\text{H}$  NMR (400 MHz,  $\text{CDCl}_3$ )  $\delta$  7.49-7.47 (m, 2H, Ph), 7.38-7.36 (m, 3H, Ph), 6.12 (ddt,  $J = 10.5, 4.5, 2.3$  Hz, < 1H, H-4, **A**), 6.10 – 6.04 (m, < 1H, H-4, **B**), 5.91 (ddt,  $J = 10.4, 4.7, 1.8$  Hz, < 1H, H-5, **B**), 5.88 – 5.82 (m, < 1H, H-5, **A**), 5.49 (s, < 1H, H-2', **B**), 5.47(s, < 1H, H-2', **A**), 4.38-4.32 (m, 1H, H-6', **A+B**), 4.31-4.24 (m, <1H, H-6, **B**), 4.23-4.17 (m, < 1H, H-6, **A**), 4.06 (td,  $J=9.9, 4.9$  Hz, < 1H, H-5', **B**), 3.96–3.90 (m, > 1H, H-3 (**A+B**), H-5' (**B**)), 3.87-3.71 (m, 1H, H-6, **A+B**), 3.74 (t,  $J = 8.8$  Hz, < 1H, H-4', **B**), 3.65 (dd,  $J = 8.8, 9.2$  Hz, < 1H, H-4', **A**), 3.65 – 3.56 (m, 1H, H-6', **A+B**), 1.52 – 1.49 (m, 18H,  $\text{CH}_3$ ).  $^{13}\text{C}$  NMR (101 MHz,  $\text{CDCl}_3$ )  $\delta$  155.10, 153.99 (C=O), 137.8, 137.5 (Cq, Ph), 128.9, 128.8, 128.2, 128.16, 128.1 (CH, Ph), 126.01, 126.0, 125.9 (CH, Ph, + C-4), 124.8 (C-4), 123.70 (br, C-5), 100.7, 100.6 (C-2'), 83.2, 82.9, 82.7, 82.5 (Cq, Boc), 81.4, 81.1 (C-4'), 70.84, 70.8 (C-6'), 66.2 (C-5), 65.4 (br, C-3), 62.5 (C-5'), 43.0, 41.6 (C-6), 28.2, 28.1, 28.06 ( $\text{CH}_3$ ). HRMS (ESI): calcd: 463.2439 $[\text{C}_{24}\text{H}_{35}\text{N}_2\text{O}_7]^+$ , found: 463.2439

### 5.3 Synthesis of indolizidine compound: (5*S*,6*R*)-octahydropyrrolo[1,2-*b*]pyridazine-3,4,5,6-tetraol **3**

#### 5.3.1 Method A: From Diethyl-2-((2*R*,4*S*,5*R*)-5-hydroxy-2-phenyl-1,3-dioxan-4-yl)-7-oxa-3,4-diazabicyclo[4.1.0]heptane-3,4-dicarboxylate

##### i) Epoxidation of the double bound

To a stirred solution of the cycloadduct **2c** (230 mg, 0.57 mmol) in ACN /  $\text{H}_2\text{O}$  (15:9 mL) at 0 °C was added  $\text{CF}_3\text{COCH}_3$  (1373  $\mu\text{L}$ ), followed by solid  $\text{NaHCO}_3$  (1.044 g, 12.42 mmol) and Oxone (5.14g, 16.72 mmol). The reaction mixture was allowed to slowly reach room temperature. After 22h to the reaction mixture was added  $\text{H}_2\text{O}$  (10 mL) and extracted with DCM (3 x 30 mL). The organic phase was concentrated and the crude material purified by dry flash chromatography (silica, ethyl acetate / petroleum ether 1:1). The pure product **7c** was isolated as a translucent oil (123 mg, 0.29mmol, 51.1 %).  $^1\text{H}$  NMR in  $\text{CDCl}_3$  solution show the presence of at least 3 rotamers.  $[\alpha]_{\text{D}}^{25} = -62.98^\circ$  (c 1.81 %, DCM ); IR (neat):  $\nu_{\text{max}}$  3453.5, 1718.8, 1699.3  $\text{cm}^{-1}$ ;  $^1\text{H}$  NMR (400 MHz,  $\text{CDCl}_3$ )  $\delta$  7.47 - 7.44 (m, 2H), 7.37 - 7.27 (m, 3H), 5.53, 5.50, 5.48 (s, 1H, H-2'), 5.01 (m,

< 1H, H-3), 4.78 (d,  $J = 7.6$  Hz, < 1H, H-3), 4.38-4.15 (m, 8H, 2x H-6', 2 x CH<sub>2</sub>), 4.07 (dd,  $J = 14.4$ , 4.8Hz, < 1H, H-6), 4.02 (dd,  $J = 14.4$ , 4.8 Hz, < 1H, H-6), 3.94-3.91 (m, 2H, H-5', H-4'), 3.82 (d,  $J = 14.4$  Hz, < 1H, H-6), 3.69-3.60 (m, < 2H, H-6, H-6'), 3.57-3.54 (m, 1H, H-4 or H-5), 3.45-3.41 (m, 1H, H-4 or H-5), 1.35-1.25 (m, 6H, CH<sub>3</sub>). <sup>13</sup>C NMR (101 MHz, CDCl<sub>3</sub>)  $\delta$  156.7, 156.5, 156.2, 156.1, 156.0 (C=O), 137.4, 137.3, 137.2 (Cq, Ph), 129.1, 129.0, 128.3, 128.2, 128.1, 126.0, 125.9, 125.9 (CH, Ph), 100.7, 100.6 (C-2'), 79.7, 78.8, 78.3 (C-4'), 71.1, 71.0, 70.9, 70.7 (C-6'), 65.7, 65.2 (C5'), 64.8, 64.7, 64.1, 63.7, 63.4, 63.3, 63.2, 62.8, 62.5, 62.2 (CH<sub>2</sub>), 58.4, 56.6, 56.1 (C-3), 49.7, 49.6, 49.4, 48.2, 48.1, 48.1 (C-5 + C-4), 41.1, 40.4, 40.1, 39.6 (C-6), 14.4, 14.3, 14.29, 14.1 (CH<sub>3</sub>). HRMS (ESI): calcd: 445.1581 for [C<sub>20</sub>H<sub>26</sub> N<sub>2</sub>O<sub>8</sub>Na], found: 445.1585.

### ii) Acetal Cleavage

A solution of the epoxide **7c** (40 mg, 0.091mmol) in water (8 mL) was added conc. H<sub>2</sub>SO<sub>4</sub> (84  $\mu$ L). The reaction mixture was refluxed for 6 h, treated with aqueous. sat. NaHCO<sub>3</sub>, and extracted with ethyl acetate (8 x 10 mL). The combined organic fractions were dried over MgSO<sub>4</sub>, concentrated in the rotary evaporator, giving the product as a thick clourless oil, compound **8c** (20 mg, 0.054 mmol, 59.3%). <sup>1</sup>H NMR showed a 1: 1 ratio of isomers A and B in solution CDCl<sub>3</sub>.

$[\alpha]_D^{25} = -33.33^\circ$  (c 0.78 %, ethyl acetate); IR (neat):  $\nu_{\max}$  3498.5, 1658.1 cm<sup>-1</sup>; <sup>1</sup>H NMR (400 MHz, D<sub>2</sub>O)  $\delta$  4.97 (quint,  $J = 6.8$  Hz, 1H, H-3, **A+B**), 4.40-4.18 (m, 7H, H-1', H-4, H-5, CH<sub>2</sub>CH<sub>3</sub>, **A+B**), 4.17 (dd,  $J = 13.4$ , 5.6 Hz,  $\frac{1}{2}$  H, H-6, **A**), 4.08 (dd,  $J = 13.2$ , 5.4 Hz,  $\frac{1}{2}$  H, H-6, **B**), 3.90 (ddd,  $J = 6.0$ , 4.8, 3.2 Hz,  $\frac{1}{2}$  H, H-2', **A**), 3.85 (ddd,  $J = 6.3$ , 4.9, 3.2 Hz,  $\frac{1}{2}$  H, H-2', **B**), 3.79 (ddd,  $J = 12.3$ , 3.0, 2.3 Hz, 1H, H-3', **A+B**), 3.67 (ddd,  $J = 12.4$ , 4.8, 1.4 Hz, 1H, H-3', **A+B**), 3.38 (dd,  $J = 13.1$ , 3.5 Hz,  $\frac{1}{2}$  H, H-6, **A**), 3.24 (dd,  $J = 13.2$ , 5.1 Hz,  $\frac{1}{2}$  H, H-6, **B**), 1.36 – 1.25 (m, 6H, CH<sub>2</sub>CH<sub>3</sub>, **A+B**). <sup>13</sup>C NMR (101 MHz, D<sub>2</sub>O)  $\delta$  157.8, 157.6, 157.0, 156.5 (C=O), 84.4, 84.4 (C-2'), 75.6, 75.4 (C-4), 70.4, 70.10 (C-1'), 65.3 (CH<sub>2</sub>), 64.4, 64.6 (C-5), 64.1, 63.8, 63.6, 63.0 (CH<sub>2</sub>), 61.5, 61.4 (C-3'), 59.1 (C-3), 47.0, 46.0 (C-6), 13.8, 13.7, 13.6, 13.6, 13.3 (CH<sub>3</sub>). HRMS (ESI): calcd: 335.1449 [M+H-H<sub>2</sub>O<sup>+</sup>; C<sub>13</sub>H<sub>23</sub> N<sub>2</sub>O<sub>8</sub><sup>+</sup>], found: 335.1461.

### iii) Aminocyclization

Diethyl 4,5-dihydroxy-3-((1*S*,2*R*)-1,2,3-trihydroxypropyl)tetrahydropyridazine-1,2-dicarboxylate **8c** (200 mg, 0.57 mmol) was added the hydrazine monohydrate (3.0 mL, 6.18 mmol). The reaction mixture was refluxed for 6 h, concentrated in the rotary evaporator and purified by dry flash

chromatography (silica, ethanol/ ammonia 5%). The pure product was obtained as an oil, compound **3** (104 mg, 0.546 mmol, approximately 96.1 %).  $[\alpha]_{\text{D}}^{25} = +14.96^\circ$  (c 0.78 %, MeOH); IR (neat):  $\nu_{\text{max}}$  3321.3  $\text{cm}^{-1}$ ;  $^1\text{H}$  RMN (400 MHz,  $\text{D}_2\text{O}$ )  $\delta$  4.35 (t,  $J = 5.4$  Hz, 1H, H-7), 4.09 (ddd,  $J = 3.5, 5.4$  Hz, 1H, H-8), 3.97 (t,  $J = 5.3$  Hz, 1H, H-5), 3.89 (ddd,  $J = 3.6, 5.2$  Hz, 1H, H-4), 3.78 (dd,  $J = 3.4, 12.2$  Hz, 1H, H-9), 3.68 (dd,  $J = 5.2, 12.4$  Hz, 1H, H-9), 3.56 (t,  $J = 5.2$  Hz, 1H, H-8), 3.09 (dd,  $J = 3.4, 14.2$  Hz, 1H, H-3), 2.71 (dd,  $J = 5.2, 14$  Hz, 1H, H-3).  $^{13}\text{C}$  NMR (101 MHz,  $\text{D}_2\text{O}$ )  $\delta$  83.1 (C-8), 77.2 (C-5), 72.6 (C-7), 64.3 (C-4), 61.8 (C-9), 56.3 (C-6), 48.3 (C-3). HRMS (ESI): calculado: 191.1026 [ $\text{C}_7\text{H}_{14}\text{N}_2\text{O}_4\text{H}^+$ ], found: 191.1036.

### 5.3.2 Method B: From (1*S*,2*S*,8*a**R*)-2-((2*R*,4*S*,5*R*)-5-hydroxy-2-phenyl-1,3-dioxan-4-yl)-5-phenyltetrahydro-4*H*-oxireno[2,3-*d*][1,2,4]triazolo[1,2-*a*]pyridazine-4,6(5*H*)-dione

#### i) Epoxidation of the double bound

A solution of the cycloadduct **2a** (356 mg, 0.874 mmol) in ACN /  $\text{H}_2\text{O}$  (15 : 9 mL) with magnetic stirring at  $t = 0^\circ\text{C}$  was added the  $\text{CF}_3\text{COCH}_3$  (1755  $\mu\text{L}$ ) followed by the  $\text{NaHCO}_3$  (1.335g x 2) and Oxone (6.574g x 2) during 20 min. The reaction mixture is allowed to reach room temperature. After 22 h the reaction  $\text{H}_2\text{O}$  was added (10 mL), and the mixture extracted with DCM (3 x 30 mL). The organic layers were combined, dried over  $\text{MgSO}_4$ , filtered, concentrated, and purified by dry flash chromatography (silica, petroleum ether/ether, followed by petroleum ether/ethyl acetate, polarity gradient). The pure product **7a** was isolated as thick transparent oil (322 mg, 0.761mmol; 87.1 %).

$[\alpha]_{\text{D}}^{25} = -185.5$  (c 0.11 %, DCM); IR (neat):  $\nu_{\text{max}}$  3436, 1766, 1700  $\text{cm}^{-1}$ ;  $^1\text{H}$  NMR (400 MHz,  $\text{CDCl}_3$ ),  $\delta$  7.47 – 7.39 (10H, m, H-Ph), 5.44 (1H, s, H-2'), 5.10 (1H, dd,  $J = 2.0, 4.0$  Hz, H-2), 4.31 (1H, d,  $J = 14$  Hz, H-8), 4.26 (1H, dd,  $J = 5.6, 10.8$  Hz, H-6'), 4.13 (1H, dd,  $J = 3.6, 13.6$  Hz, H-4'), 3.90 (1H, dt,  $J = 5.2, 14.4$  Hz, H-5'), 3.87 (1H, dd,  $J = 2.0, 14.0$  Hz, H-8), 3.75 (1H, dd,  $J = 2.0, 4.4$  Hz, H-1a), 3.55 (d,  $J = 10.8$  Hz, H-6'), 3.52 (1H, dd,  $J = 2.0, 4.4$  Hz, H-8a);  $^{13}\text{C}$  NMR (100 MHz,  $\text{CDCl}_3$ ),  $\delta$  150.8 (C=O), 150.6 (C=O), 136.9 (Cq, Ph), 130.9 (Cq, Ph), 129.2 (C-H, Ph), 128.4 (C-H, Ph), 125.8 (C-H, Ph), 125.7 (C-H, Ph), 101.0 (C-2'), 81.2 (C-4'), 71.1 (C-6'), 62.7 (C-5'), 53.4 (C-2), 48.8 (C-1a), 47.9 (C-8a), 40.9 (C-8) ppm. HRMS (ESI): calcd: 424.1503 [ $\text{M}+\text{H}^+$ ;  $\text{C}_{22}\text{H}_{22}\text{N}_3\text{O}_6^+$ ], found: 424.1505.

**ii) Acetal Cleavage**

A solution of the epoxide **7a** (64 mg, 0.151mmol) in H<sub>2</sub>O (12 mL) was added conc. H<sub>2</sub>SO<sub>4</sub> (122  $\mu$ L). The reaction mixture was refluxed for 6h, treated with sat. NaHCO<sub>3</sub> and was extracted with ethyl acetate (8 x 10 mL). The combined organic fractions were dried over MgSO<sub>4</sub>, filtered and concentrated in the rotary evaporator, to give the product as a thick transparent oil **8a** (33 mg, 0.093 mmol, 62%).

$[\alpha]_D^{25} = -72^\circ$  (c 0.5 %, MeOH); IR (neat):  $\nu_{\max}$  3442.5, 1647.3 cm<sup>-1</sup>; <sup>1</sup>H NMR (400 MHz, D<sub>2</sub>O)  $\delta$  7.67-7.57 (m, 3H, Ph); 7.50-7.45 (m, 2H, Ph), 4.97 (dd,  $J = 7.6, 6.4$  Hz, 1H, H-5), 4.54 (dd,  $J = 7.6, 6.0$  Hz, 1H, H-6), 4.53 (dd,  $J = 6.0, 5.2$  Hz, H-2'), 4.37 (td,  $J = 6.4, 4.0$  Hz, 1H, H-7), 4.16-4.09 (m, 2H, H-8 e H-1'), 3.83 (dd,  $J = 12.4, 3.2$  Hz, 1H, H-3'), 3.75-3.70 (m, 2H, H-3' + H-8). <sup>13</sup>C NMR (100 MHz, D<sub>2</sub>O)  $\delta$  151.8, 151.7 (C=O), 129.9 (Cq-Ph), 129.83, 129.81, 127.0 (CH-Ph), 84.5 (C-1'), 75.8 (C-6), 70.4 (C-2'), 64.5 (C-7), 60.9 (C-3'), 56.3 (C-5), 44.2 (C-8). HRMS (ESI): calcd: 358.1010[M+H-H<sub>2</sub>O<sup>+</sup>; C<sub>15</sub>H<sub>17</sub>N<sub>3</sub>NaO<sub>6</sub><sup>+</sup>], found: 358.1015.

**iii) Aminocyclization**

A solution of compound **8a** (42 mg; 0.119 mmol) in NH<sub>2</sub>NH<sub>2</sub>. H<sub>2</sub>O (3 mL) was refluxed for 18h, evaporated to dryness to give an oil after evaporation. The crude oil was submitted to flash chromatography (silica, ethanol, ammonia 5%) giving compound **3** in 88.2 % yield (20 mg; 0.105 mmol).

**5.4 Synthesis of (1*S*,2*R*)-1-((*S*)-1,2,3,6-tetrahydropyridazin-3-yl)propane-1,2,3-triol (5)****Method 1- From DEAD Cycloadduct****i) Acetal cleavage: synthesis of Diethyl 3-((1*S*,2*R*)-1,2,3-trihydroxypropyl)pyridazine-1,2(3*H*,6*H*)-dicarboxylate (4c)**

A solution of the adduct **2c** (100 mg, 0.246 mmol) in H<sub>2</sub>O/ACN (10:3 mL) was added the BiI<sub>3</sub> (30 mg, 20%). The reaction mixture was putting in reflux during 3h. After that the reaction mixture is treated with resina dowex 50x (OH). The solution was concentrated, giving the product **4c**, as a translucent oil (78 mg, 0.245mmol, 99.6%).

$[\alpha]_D^{25} = -122.9^\circ$  (c 3.5 %, ethyl acetate); IR (neat):  $\nu_{\max}$  3429.9, 2983.4, 2937, 1710.2 cm<sup>-1</sup>; <sup>1</sup>H RMN (400 MHz, D<sub>2</sub>O)  $\delta$  6.07 (dddd,  $J = 10.6, 4.3, 3.1, 1.7$  Hz, 2H, H-4), 5.99 (ddd,  $J = 10.2,$

4.6, 2.8 Hz, 2H, *H*5), 4.92 (ddd, *J* = 6.1, 4.5, 1.7 Hz, 1H, *H*3), 4.87 (ddd, *J* = 6.9, 4.2, 1.4 Hz, 1H, *H*3), 4.49 (ddd, *J* = 18.0, 2.9, 1.2 Hz, 1H, *H*6), 4.41 (dd, *J* = 18.0, 2.8 Hz, 1H, *H*6), 4.26 (dd, *J* = 14.2, 7.1 Hz, 4H, OCH<sub>2</sub>), 4.19 (dt, *J* = 10.8, 3.6 Hz, 4H, OCH<sub>2</sub>), 3.95 – 3.81 (m, 6H, 6-*H*, *H*3' and *H*2'), 3.78 (td, *J* = 7.0, 2.6 Hz, 2H, *H*-1'), 3.67 (ddd, *J* = 11.6, 7.1, 4.5 Hz, 2H, *H*-3'), 1.31 (q, *J* = 7.0 Hz, 12H, CH<sub>3</sub>). <sup>13</sup>C NMR (101 MHz, D<sub>2</sub>O) δ 156.8, 156.7, 156.7, 156.6 (C=O), 125.4, 125.3 (C-4), 122.2, 121.9 (C-5), 73.9, 73.5 (C-2'), 72.2 (C-1'), 64.1, 63.7, 63.6 (OCH<sub>2</sub>), 62.4, 62.2 (C-3'), 54.5, 55.1 (C-3), 43.3, 42.3 (C-6), 13.8, 13.7, 13.6 (CH<sub>3</sub>). HRMS (ESI): calcd: 269.1108 [M+Na-CO<sub>2</sub>Et<sup>+</sup>; C<sub>13</sub>H<sub>18</sub>N<sub>2</sub>NaO<sub>5</sub><sup>+</sup>], found: 269.1103.

**ii. Urethane cleavage: Synthesis of (1*S*,2*R*)-1-(1,2,3,6-tetrahydropyridazin-3-yl)propane-1,2,3-triol (5)**

A solution of compound **4c** (59 mg, 0.185 mmol) in dioxane (10 mL) was added the NaOH (1M, 1 mL). The reaction mixture was stirring at rt. for 24 h. After that, the reaction mixture is resin Amberlite resin IR 120 (H+). The solution was concentrated, giving the oily product as a mixture of compounds **5** and **6** in 2:1 ratio; compound **5** (20.6 %), compound **6** (12.4%) by 1H NMR. <sup>a)</sup>

a) The characterization of compounds **5** and **6** is bellow in method 2.

**Method 2- From DBAD Cycloadduct**

**Synthesis of (1*S*,2*R*)-1-(1,2,3,6-tetrahydropyridazin-3-yl)propane-1,2,3-triol (5)<sup>a)</sup>**

A solution of the adduct **2d** (159 mg, 0.344mmol) in H<sub>2</sub>O/ACN (24:12 mL) was added the BiI<sub>3</sub> (52 mg, 25%). The reaction mixture was putting in reflux during 13:30 h. After that, the reaction mixture was concentrated under vacuum; the residue obtained was solubilized in water and neutralized with basic resin (Dowex 1X2 50-100 mesh). The solution was filtered through glass fiber paper and the filtrated was concentrated under reduce pressure. The residue was purified by silica gel dry flash chromatography eluting with ethanol/ ammonia 5%. The pure compound was obtained as oil (0.015 g; 0.086 mmol, 25.0 %). A mixture of the title compound **5** with (2*R*,3*S*,*E*)-hepta-4,6-diene-1,2,3-triol (**6**) come out of the column successively.

**Compound 5<sup>a)</sup>**: [α]<sub>D</sub><sup>25</sup> = - 61.5° (c 0.13 %, H<sub>2</sub>O); IR (neat): ν<sub>max</sub> 3353.8 cm<sup>-1</sup>; <sup>1</sup>H NMR (400 MHz, D<sub>2</sub>O) δ 6.14 (ddd, *J* = 10.8, 4.4, 3.5 Hz, 1H, *H*4), 5.97 (ddd, *J* = 10.8, 4, 2.2 Hz, 1H, *H*5), 3.83 (dd, *J* = 11.8, 2.6 Hz, 2H, *H*3'), 3.74-3.70(m, 1H, *H*1') 3.70-3.61(m, 3H, *H*3, *H*2', *H*3'), 3.37 (ddd, *J* = 17.6, 5, 2.6 Hz, 1H, *H*6), (ddd, *J* = 17.6, 5.3, 3.1 Hz, 1H, *H*6). <sup>13</sup>C NMR (101 MHz, D<sub>2</sub>O) δ

128.5 (C-4), 123.3 (C-5), 72.3 (C-1'), 71.6 (C-2'), 62.7 (C-3'), 53.6 (C-3), 44.2 (C-6). HRMS (ESI): calcd for  $[C_7H_{15}N_2O_3]^+$ : 175.1083, found: 175.1074.

<sup>a</sup>An important note is that compound **5** is not stable enough to be used as an intermediate, because it decomposes on silica, and in contact with Dowex resin preventing its isolation in a reasonable yield.

**Compound 6:** <sup>1</sup>H NMR (400 MHz, D<sub>2</sub>O)  $\delta$  6.46 (dt,  $J$  = 5.2, 8.4 Hz, 1H, H-6) 6.37 (dd,  $J$  = 5.2, 7.6 Hz, 1H, H-5) 5.81 (dd,  $J$  = 3.6, 7.6 Hz, 1H, H-4) 5.33 (d,  $J$  = 8.4 Hz, 1H, H-7), 5.20 (d,  $J$  = 5.2 Hz, 1H, H-7) 4.19 (t,  $J$  = 3.2 Hz, 1H, H-3), 3.73-3.71 (m, 1H, H-2), 3.57 (dd,  $J$  = 6.4, 4.0 Hz, 1H, H-1). <sup>13</sup>C NMR (100 MHz, D<sub>2</sub>O)  $\delta$  136.3 (C-6), 133.9 (C-5), 131.2 (C-4), 118.5 (C-7), 74.3 (C-2), 72.4 (C-3), 62.4 (C-1).

### 5.5 Computational Methodology

All geometry optimizations were performed with Gaussian 09 [11], applying density functional theory [12], with the B3LYP functional [13] together with the 6-31G(d) basis set [14]. The geometry optimizations were conducted with a conductor-like polarizable continuum model using the integral equation formalism variant (IEF-PCM) [15].

In all geometry optimizations, we first searched for the transition state starting from a structure similar to the reactant model. This was generally obtained with uni-dimensional scans along the particular reaction coordinate in which we were interested. Once a putative transition structure was located, it was fully optimized. The reactants and the products associated with it were determined after intrinsic reaction coordinate (IRC) calculations. In all cases, the geometry optimizations and the stationary points were obtained with standard Gaussian convergence criteria. The transition state structures were all verified by vibrational frequency calculations, having exactly one imaginary frequency with the correct transition vector, even using frozen atoms, which shows that the frozen atoms were almost free from steric strain. The ZPE and thermal and entropic energy corrections were calculated using the same method and basis set ( $T = 310.15$  K,  $P = 1$  bar).

The final electronic energies were calculated using the all-electron 6-311++G(3df,2pd) basis set and the functional B3LYP. A conductor-like polarizable continuum model using the integral equation

formalism variant (IEF-PCM), as implemented in Gaussian 09, with a dielectric constant of 2.3741 and 7.4257 was used to simulate the Toluene and THF, respectively [15].

All the activation and reaction energies provided in the text and figures refer to free energy differences calculated at the B3LYP/6-311++(3df,2pd) level detailed above, while the atomic charge distributions were calculated at the B3LYP level by employing a Mulliken population analysis, using the basis set 6-31G(d).

## 6. References

1. Larsen, D. S.; Stoodley, R. J., Asymmetric Diels–Alder reactions. Part 3. Influence of butadiene structure upon the diastereofacial reactivity of (E)-1-(2',3',4',6'-tetra-O-acetyl- $\beta$ -D-glucopyranosyloxy)buta-1,3-dienes. *J. Chem. Soc., Perkin Trans. I* **1989**, 1841–1852.
2. 76Aspinall, I. H.; Cowley, P. M.; Stoodley, R. J., Enhanced discrimination by aza dienophiles over their olefinic counterparts for the diastereotopic faces of methyl (E,E)-5-(2',3',4',6'-tetra-O-acetyl- $\beta$ -D-glucopyranosyloxy)penta-2,4-dienoate. *Tetrahedron Lett.* **1994**, 3397–3400.
3. Aspinall, I. H.; Cowley, P. M.; Mitchell, G.; Stoodley, R. J., Asymmetric synthesis of (3S)-2,3,4,5-tetrahydropyridazine-3-carboxylic acid. *J. Chem. Soc., Chem. Commun.* **1993**, 1179–1180.
4. Mukhopadhyay, A.; Ali, S. M.; Husain, M.; Suryawanshi, S. N.; Bhakuni, D. S., Diels-Alder reaction of generated 2-methoxycarbonyl-quinone with D-glucose based dienes: A new approach to forskolin. *Tetrahedron Lett.* **1989**, *30*, 1853–1856.
5. M.J. Alves, Vera C. M. Duarte, H. Faustino, A. Gil, Diastereo-controlled Diels–Alder cycloadditions of erythrose benzylidene-acetal 1,3-butadienes by 4-substituted-1,2,4-triazoline-3,5-dione: Evidence for the stereoelectronic effects on the dienes. *Tetrahedron Asymmetry*, **2010**, *21*, 1817-1820.
6. Duarte, V. C. M.; Faustino, H.; Alves, M. J.; Gil Fortes, A.; Micaelo, Nuno, Asymmetric Diels–Alder cycloadditions of D-erythrose 1,3-butadienes to achiral t-butyl 2H-azirine 3-carboxylate. *Tetrahedron-Asymmetry*, **2013**, *24*, 1063-1068.
7. Salgueiro, D.A.L.; Duarte, V.C.M.; Sousa, C.E.A.; Alves, M.J.; Gil Fortes, A., Asymmetric Diels–Alder cycloadditions of D-erythrose 1,3-butadienes to achiral t-butyl 2H-azirine 3-carboxylate. *Synlett* **2012**, *23*, 1765-1768.
8. Fujita, T.; Nagasawa, H.; Uto, Y.; Hashimoto, T.; Asakawa, Y.; & Hori, H., Synthesis of the new mannosidase inhibitors, diversity-oriented 5-substituted swainsonine analogues, via stereoselective Mannich reaction. *Organic Letters*, **2004**, *5*(5), 827–830.
9. Baker, S.R.; Clissold, D.W.; McKillop, A., Synthesis of leukotriene A4 methyl ester from D-glucose. *Tetrahedron Lett.* **1988**, *29*, 991–994.
10. Zimmermann, P.; Schmidt, R.R., Synthese von erythro-Sphingosinen über die Azidoderivate. *Liebigs Ann. Chem.* **1988**, 663–667.

11. Frisch, M. J., Trucks, G. W.; Schlegel, H. B.; Scuseria, G. E.; Robb, M. A.; Cheeseman, J. R.; Scalmani, G.; Barone, V.; Mennucci, B.; Petersson, G. A.; Nakatsuji, H.; Caricato, M.; Li, X.; Hratchian, H. P.; Izmaylov, A. F.; Bloino, J.; Zheng, G.; Sonnenberg, J. L.; Hada, M.; Ehara, M.; Toyota, K.; Fukuda, R.; Hasegawa, J.; Ishida, M.; Nakajima, T.; Honda, Y.; Kitao, O.; Nakai, H.; Vreven, T.; Montgomery, J. A., Jr, Peralta, J. E.; Ogliaro, F.; Bearpark, M. J.; Heyd, J.; Brothers, E. N.; Kudin, K. N.; Staroverov, V. N.; Kobayashi, R.; Normand, J.; Raghavachari, K.; Rendell, A. P.; Burant, J. C.; Iyengar, S. S.; Tomasi, J.; Cossi, M.; Rega, N.; Millam, N. J.; Klene, M.; Knox, J. E.; Cross, J. B.; Bakken, V.; Adamo, C.; Jaramillo, J.; Gomperts, R.; Stratmann, R. E.; Yazyev, O.; Austin, A. J.; Cammi, R.; Pomelli, C.; Ochterski, J. W.; Martin, R. L.; Morokuma, K.; Zakrzewski, V. G.; Voth, G. A.; Salvador, P.; Dannenberg, J. J.; Dapprich, S.; Daniels, A. D.; Farkas, Ö.; Foresman, J. B.; Ortiz, J. V.; Cioslowski, J.; and Fox, D. J. (2009) Gaussian 09. Gaussian, Inc., Wallingford, CT, USA.
12. Hohenberg, P., and Kohn, W., Inhomogeneous Electron Gas. *Phys. Rev.* **1964**, *136*, B864–B871.
13. (a) Becke, A. D., A new mixing of Hartree–Fock and local density-functional theories. *J. Chem. Phys.* **1993**, *98* (2), 1372-1377; (b) Lee, C. T.; Yang, W. T.; Parr, R. G., Development of the Colle-Salvetti correlation-energy formula into a functional of the electron density. *Phys. Rev. B: Condens. Matter Mater. Phys.* **1988**, *37* (2), 785-789. (c) Vosko, S. H.; Wilk, L.; Nusair, M., Accurate spin-dependent electron liquid correlation energies for local spin density calculations: a critical analysis. *Can. J. Phys.* **2011**, *58*, 1200–1211; (d) Stephens, P. J.; Devlin, F. J.; Chabalowski, C. F.; Frisch, M. J., Ab Initio Calculation of Vibrational Absorption and Circular Dichroism Spectra Using Density Functional Force Fields. *J. Phys. Chem.* **1994**, *98* (45), 11623–11627.
14. Rassolov, V. A.; Ratner, M. A.; Pople, J. A.; Redfern, P. C.; Curtiss, L., 6-31G\* basis set for third-row atoms. *J. Comput. Chem.* **2001**, *22* (9), 976-984.
15. Scalmani, G.; Frisch, M. J., Continuous surface charge polarizable continuum models of solvation. I. General formalism. *J. Chem. Phys.* **2010**, *132* (11), 114110.



# Section C: Work Perspectives

8

Conclusion

## 1. Final Remarks

The focus of this thesis has been the synthesis of iminosugars with potential biological activity by a common starting compound: 2,4-benzylidene-D-erythrose, achieved by diverse synthetic routes.

The highlights of the obtained results are summarized next:

### Chapter 4

In this chapter was reported the development of a very simple and high yielding strategy for the synthesis of (3*S*,4*R*)-dihydroxy L-homoprolines. Trivial reagents have been employed, the reactions follow a cascade mechanism, with no needs of products purification, being completely selective processes. Computational studies reveal that the synthetic mechanism.

### Chapter 5

The main highlight of this chapter is the introduction of a new D-erythrose-1,3-dioxane lactone, shown to be a highly selective model in 1,3-dipolar cycloadditions. The computational results showed that the *stereo*-selectivity is due to the steric effect of a hydrogen atom in the fused constrained structure. The *regio*-selectivity for alkyl azides and diazo compounds is explained from kinetic and thermodynamic points of view and is connected to a lower distortion of the 1,3-dipole molecules during the reactions.

### Chapter 6

This chapter shows the versatility of the 6-carbon atom erythrosyl fused aziridinolactone as a chiral platform in the synthesis of SAA compounds. The reactivity of aziridines with three different acids:  $\text{BiI}_3$  /  $\text{H}_2\text{O}$ , TFA, and HCl, allows diverse mechanism pathways with total selectivity, so that two different types of SAA products can be produced in very good overall yields, by simply changing the nature of the acid.

## Chapter 7

This chapter describes the cycloadditions of PTAD, DEAD, and DBAD to erythrosyl butadiene, and its transformation into aza-indolizidine. The stereochemistry at the new stereogenic center was found to be *S*, in every cases, but stereochemistry could only be discovered at the end of the FGT process leading to the aza-indolizidine.

Computational mechanistic studies confirm the preference for the approach of reagents by the *si* face of the diene in every case. The processes are concerted and desynchronized, although with different energy profiles.

### 2. Perspectives

In this thesis is presented the synthesis of several types of compounds that fall into class A and E defined in Chapter 2 for GM II.

The results of this thesis will include in the future biological evaluation tests in various glycosidases, especially GM II, and in cancer cells. The results to be obtained will define the impact of the work on health. Molecular modeling will also be applied to predict the best analogues and direct their synthesis. The computational studies will allow in the future to accelerate the synthesis of other analogues.

From the synthetic point of view two new chiral platforms, based on D-erythrose was disclosed and will continue to be useful tools for new synthetic purposes on sugar chemistry.

## Annexes

Supporting Information of chapter 5:

Figure 1

1. X-ray data of compound 7a

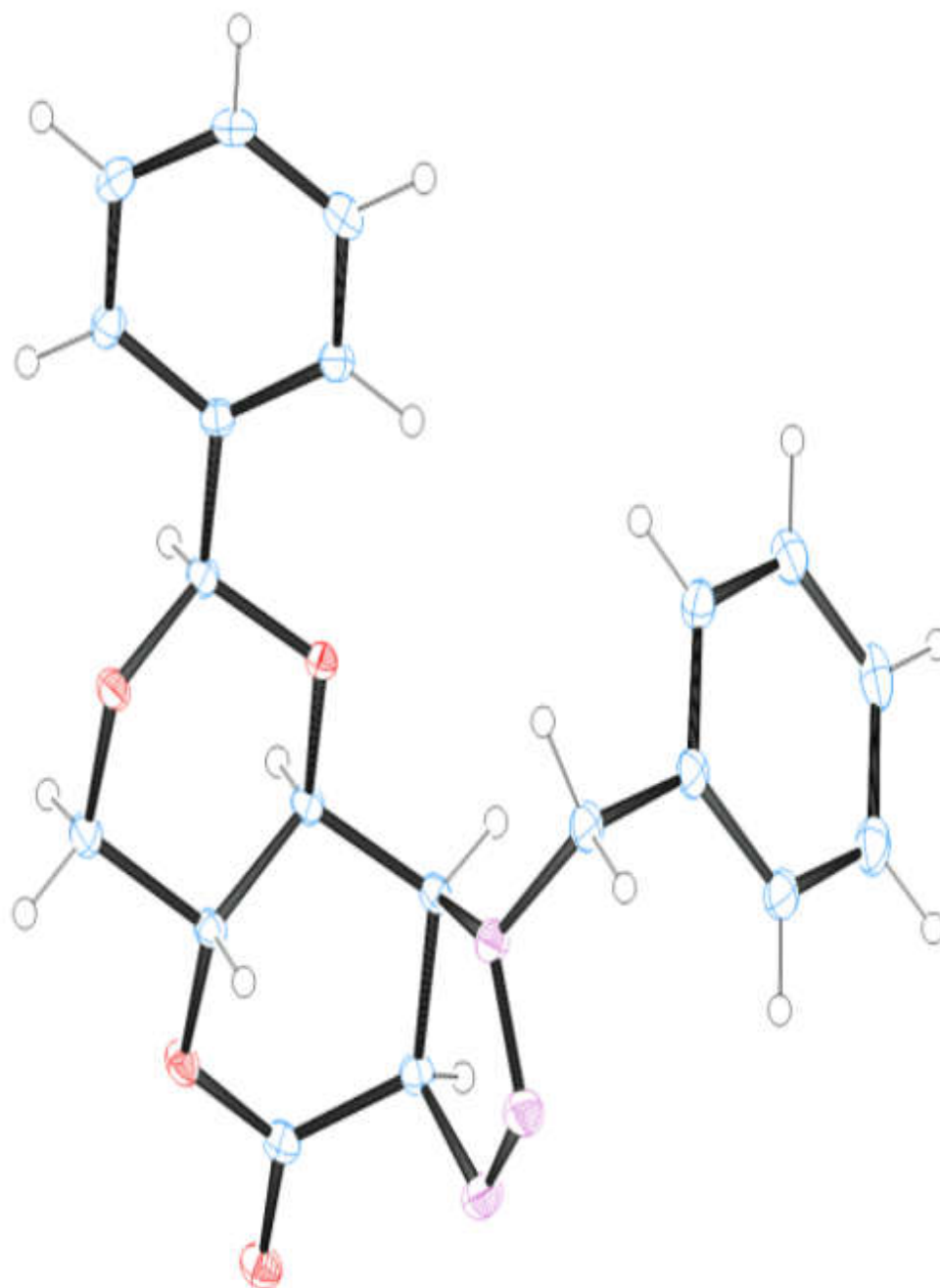


Figure 1: ORTEP structure of compound 7a (30% ellipsoid contour probability).

## Annexes

**Table SI-2: Evaluation of the type of mechanism of the cycloadditions according to the frontier molecular orbitals (FMO) concepts.**

1,3-dipole Molecule	Cyclisation pathway	Molecular Orbitals Energies (eV)				Energy Gap (eV)**		FMO type of mechanism
		1,3-dipole		Lactone		HD-LL*	LD-HL*	
		Homo	Lumo	Homo	Lumo			
Alkyl Azide	Pathway A	-0.25180	-0.13794	-0.26378	-0.10578	<b>0.14602</b>	<b>0.12584</b>	Type II
R=n-Pr	Pathway B	-0.25132	-0.10598	-0.26425	-0.09191	<b>0.15941</b>	<b>0.15827</b>	Type II
Alkyl Azide	Pathway A	-0.23923	-0.09295	-0.25115	-0.07720	<b>0.16203</b>	<b>0.1582</b>	Type II
R= Bn	Pathway B	-0.24994	-0.10978	-0.26427	-0.09167	<b>0.15827</b>	<b>0.15449</b>	Type II
Alkyl Azide	Pathway A	-0.25305	-0.11173	-0.26404	-0.09246	<b>0.16059</b>	<b>0.15231</b>	Type II
R= (CH <sub>2</sub> ) <sub>3</sub> -OBn	Pathway B	-0.24921	-0.10749	-0.26428	-0.09265	<b>0.15656</b>	<b>0.15679</b>	Type II
Nitrile Oxides	Pathway A	-0.25770	-0.09280	-0.26617	-0.08889	<b>0.16881</b>	<b>0.17337</b>	Type II
R=Me	Pathway B	-0.25604	-0.08838	-0.26467	-0.08821	<b>0.16783</b>	<b>0.17629</b>	Type II
Nitrile Oxides	Pathway A	-0.24421	-0.10668	-0.26651	-0.08922	<b>0.15499</b>	<b>0.15983</b>	Type II
R=Ph	Pathway B	-0.24376	-0.10091	-0.26472	-0.08798	<b>0.15578</b>	<b>0.16381</b>	Type II
Nitrile Oxides	Pathway A	-0.26016	-0.11999	-0.26398	-0.08945	0.17071	<b>0.14399</b>	Type II-III
R=2,6-Cl-C <sub>6</sub> H <sub>3</sub>	Pathway B	-0.25866	-0.11929	-0.26454	-0.08720	0.17146	<b>0.14525</b>	Type II-III
Diazo compound	Pathway A	-0.20976	-0.08237	-0.26363	-0.09591	<b>0.11385</b>	0.18126	Type I
	Pathway B	-0.20774	-0.08806	-0.26427	-0.09335	<b>0.11439</b>	0.17621	Type I

Note: Theoretical Level used in these calculations was B3LYP/6-311++G(3df,2pd).

\* HD-LL stands for the coupling of the HOMO from the dipole molecule and the LUMO from the lactone.

\* LD-HL stands for the coupling of the LUMO from the dipole molecule and the HOMO from the lactone.

\*\* The most favourable transition between the HOMO and LUMO of the dipole and lactone molecules are highlighted in bold, according to the FMO theory.

Table SI-3: Evaluation of the effect of the distortion and interaction between the reactant and the transition state of the cycloadditions.

1,3-Dipole (substituite)	Pathway	Distortion Energy (R/TS) (kcal/mol)			Interaction Energy (kcal/mol)			Ea
		1,3-Dipole	Lactone	Total	Reactants	TS	Total	
Alkyl Azide	Pathway A	20.6	6.2	26.8	-2.5	-8.5	-6.0	18.9
R=n-Pr	Pathway B	22.9	7.8	30.7	-1.9	-7.5	-5.6	25.0
		76.8	18.9					
Alkyl Azide	Pathway A	21.9	8.2	30.1	-1.1	-8.8	-7.6	22.5
R= Bn	Pathway B	22.7	7.6	30.3	-2.5	-7.4	-4.9	25.4
		72.7						
Alkyl Azide	Pathway A	20.4	8.0	28.5	-2.3	-7.6	-5.3	23.2
R= (CH <sub>2</sub> ) <sub>3</sub> -OBn	Pathway B	23.0	8.7	31.7	-1.5	-8.0	-6.5	25.1
		71.8						
Nitrile Oxides	Pathway A	18.1	5.8	23.9	-2.4	-7.8	-5.4	18.5
R=Me	Pathway B	18.6	5.1	23.7	-4.7	-8.4	-3.7	20.0
		75.7						
Nitrile Oxides	Pathway A	20.3	6.5	26.8	-1.8	-8.1	-6.2	20.5
R=Ph	Pathway B	19.5	6.1	25.6	-4.1	-8.5	-4.4	21.2
		75.7						
Nitrile Oxides	Pathway A	20.7	6.0	26.7	-1.3	-7.2	-5.9	20.8
R=2,6-Cl-C <sub>6</sub> H <sub>3</sub>	Pathway B	20.1	5.2	25.2	-2.5	-7.0	-4.5	20.7
		77.4						
Diazo compound	Pathway A	17.0	8.6	25.6	-1.6	-8.8	-7.1	18.4
	Pathway B	20.0	7.8	27.9	-2.5	-8.2	-5.8	22.1

Note: Theoretical Level used in these calculations was B3LYP/6-311++G(3df,2pd).

*“Todo obstáculo em seu caminho será pequeno, se sua vontade de vencer for grande. Seja esse obstáculo, um sentimento, um problema, uma situação ou uma fase.”*

**Hudson Pessini.**